

Titre: Décomposition directe du NO sur des catalyseurs de type pérovskite
Title: Direct decomposition of NO on perovskite catalysts

Auteur: Carmen Gabriela Tofan
Author: Carmen Gabriela Tofan

Date: 2001

Type: Mémoire ou thèse / Dissertation or Thesis

Référence: Tofan, C. G. (2001). Décomposition directe du NO sur des catalyseurs de type pérovskite [Thèse de doctorat, École Polytechnique de Montréal]. PolyPublie.
Citation: <https://publications.polymtl.ca/7076/>

Document en libre accès dans PolyPublie

Open Access document in PolyPublie

URL de PolyPublie: <https://publications.polymtl.ca/7076/>
PolyPublie URL:

Directeurs de recherche: Danilo Klvana, & Jamal Chaouki
Advisors:

Programme: Non spécifié
Program:

INFORMATION TO USERS

This manuscript has been reproduced from the microfilm master. UMI films the text directly from the original or copy submitted. Thus, some thesis and dissertation copies are in typewriter face, while others may be from any type of computer printer.

The quality of this reproduction is dependent upon the quality of the copy submitted. Broken or indistinct print, colored or poor quality illustrations and photographs, print bleedthrough, substandard margins, and improper alignment can adversely affect reproduction.

In the unlikely event that the author did not send UMI a complete manuscript and there are missing pages, these will be noted. Also, if unauthorized copyright material had to be removed, a note will indicate the deletion.

Oversize materials (e.g., maps, drawings, charts) are reproduced by sectioning the original, beginning at the upper left-hand corner and continuing from left to right in equal sections with small overlaps.

ProQuest Information and Learning
300 North Zeeb Road, Ann Arbor, MI 48106-1346 USA
800-521-0600

UMI[®]

UNIVERSITÉ DE MONTRÉAL

**DÉCOMPOSITION DIRECTE DU NO SUR DES CATALYSEURS DE TYPE
PÉROVSKITE**

CARMEN GABRIELA TOFAN

DÉPARTEMENT DE GENIE CHIMIQUE

ÉCOLE POLYTECHNIQUE DE MONTRÉAL

**THÈSE PRÉSENTÉE EN VUE DE L'OBTENTION
DU DIPLÔME DE PHILOSOPHIAE DOCTOR (Ph.D.)**

(GÉNIE CHIMIQUE)

AOÛT 2001



National Library
of Canada

Acquisitions and
Bibliographic Services

395 Wellington Street
Ottawa ON K1A 0N4
Canada

Bibliothèque nationale
du Canada

Acquisitions et
services bibliographiques

395, rue Wellington
Ottawa ON K1A 0N4
Canada

Your file Votre référence

Our file Notre référence

The author has granted a non-exclusive licence allowing the National Library of Canada to reproduce, loan, distribute or sell copies of this thesis in microform, paper or electronic formats.

L'auteur a accordé une licence non exclusive permettant à la Bibliothèque nationale du Canada de reproduire, prêter, distribuer ou vendre des copies de cette thèse sous la forme de microfiche/film, de reproduction sur papier ou sur format électronique.

The author retains ownership of the copyright in this thesis. Neither the thesis nor substantial extracts from it may be printed or otherwise reproduced without the author's permission.

L'auteur conserve la propriété du droit d'auteur qui protège cette thèse. Ni la thèse ni des extraits substantiels de celle-ci ne doivent être imprimés ou autrement reproduits sans son autorisation.

0-612-71321-0

Canada

UNIVERSITÉ DE MONTRÉAL

ÉCOLE POLYTECHNIQUE DE MONTRÉAL

Cette thèse intitulée:

DÉCOMPOSITION DIRECTE DU NO SUR DES CATALYSEURS DE TYPE
PÉROVSKITE

présentée par: TOFAN Carmen Gabriela
en vue de l'obtention du diplôme de : Philosophiae Doctor
a été dûment acceptée par le jury d'examen constitué de:

M. LEGROS Robert, Ph.D., président

M. KLVANA Danilo, Ph.D., membre et directeur de recherche

M. CHAOUKI Jamal, Ph.D., membre et codirecteur de recherche

M. TATIBOUËT Jean-Michel, Ph.D., membre

M. SAVADOGO Oumarou, Ph.D., membre

REMERCIEMENTS

Ce projet a été réalisé au laboratoire de cinétique du département de génie chimique de l'École Polytechnique de Montréal.

Je tiens à exprimer mes sincères remerciements à mon directeur de recherche, professeur Danilo Klvana, pour m'avoir acceptée comme étudiante et, par le fait même, d'avoir eu confiance en mes capacités, pour ses conseils prodigues, pour sa disponibilité, sa patience et son support. J'aimerais également offrir ma gratitude au professeur Jamal Chaouki, mon codirecteur, pour ses conseils, particulièrement au début du projet.

Mes plus sincères remerciements vont également à Dr. Jitka Kirchnerova. Sa grande disponibilité, la rigueur de ses conseils, ainsi que sa compréhension et ses encouragements m'ont beaucoup aidée tout au long de mes travaux de recherche.

Je tiens aussi à exprimer toute ma sympathie à Jean Huard et Robert Delisle pour l'aide qu'ils m'ont apportée au laboratoire.

Enfin, que toutes les personnes qui ont contribué à l'élaboration de ce travail trouvent ici l'expression de ma sincère gratitude.

RÉSUMÉ

Les oxydes d'azote sont générés principalement par la combustion à hautes températures. Leur élimination est un des plus grands défis dans la protection de l'environnement. La catalyse est appelée à jouer un rôle important dans ce domaine. Le développement d'un catalyseur et la mise au point d'un procédé de décomposition catalytique du NO représenterait un avancement important dans la lutte contre la pollution atmosphérique. Malgré un effort soutenu, à date, aucun catalyseur approprié n'a pas été trouvé. Les oxydes mixtes de type pérovskite représentent un des groupes des matériaux étudiés en vue de la décomposition catalytique du NO. Comparée à d'autres matériaux, la structure de type pérovskite permet d'obtenir une très large variation des caractéristiques physiques et catalytiques. La désorption facile d'oxygène et la bonne stabilité thermique font partie de ces caractéristiques importantes pour la catalyse.

L'objectif des études qui font l'objet de cette thèse était d'évaluer les performances des pérovskites pour la décomposition directe du NO sur un large éventail de conditions expérimentales et de cerner les effets des divers paramètres réactionnels afin de contribuer à la compréhension de cette réaction très complexe.

Plusieurs nouvelles compositions $La_{1-x}Sr_xB_{1-y}B''_yO_{3-\delta}$ ont été synthétisées spécifiquement pour ces études. Les pérovskites ont été réparties dans trois groupes, le premier basé sur le cobalt comme principal élément actif, le second basé sur le nickel et le manganèse, et le troisième ayant le cuivre comme élément actif. Des échantillons sous forme de poudres avec des surfaces spécifiques comprises entre 9 et 22 m^2/g ont été préparés par une méthode utilisant comme précurseur une suspension homogène et réactive, obtenue à partir de l'hydroxyde de lanthane et d'une solution des nitrates des autres métaux, mélangés en proportions stoichiométriques. Cette suspension est séchée par cryodessication et ensuite calcinée, sous des conditions contrôlées, dans l'air.

La réaction de décomposition du NO a été étudiée dans un réacteur à écoulement piston avec 1 g de catalyseur dilué avec 7 mL de la pierre ponce dans un large éventail de conditions expérimentales: débits entre 10 et 200 mL/min, 1 à 10 %NO, températures entre 723 et 923 K. La chromatographie en phase gazeuse a été utilisée pour suivre la conversion du NO en N₂, et le FTIR a servi pour détecter la présence du protoxyde d'azote dans les effluents.

La première étude a été faite en l'absence de l'oxygène ajoutée à l'alimentation. La majorité des pérovskites étudiées dans cette étude ont montré une meilleure activité que les différents constituants sous forme oxyde ou les autres catalyseurs ayant une structure de type pérovskite, mais testées précédemment dans d'autres laboratoires. Malgré le fait que les activités de tous les pérovskites évaluées sont du même ordre de grandeur, on a pu observer des différences en fonction de leur composition. Bien qu'importante, la surface spécifique n'est pas le facteur principal qui détermine l'activité catalytique. Les aspects structuraux de la surface catalytique, influencent la formation des sites spécifiques favorisant la décomposition du NO, semblent être de loin les plus importants. La décomposition du NO a été trouvée plus complexe que ce que l'on admet généralement. L'analyse des données cinétiques suggère une forte adsorption de l'oxyde nitrique, probablement menant à des réactions d'oxydation concurrentes. Ces réactions inhibent la décomposition du NO et peuvent être en partie responsables du fort effet inhibiteur de l'oxygène. Parmi plusieurs modèles cinétiques testés, la meilleure représentation des données expérimentales a été obtenue avec un nouveau modèle dans lequel l'oxygène joue un rôle non seulement d'inhibiteur, mais aussi de réactif. L'oxygène pourrait être impliqué dans la formation de quelques espèces intermédiaires qui pourraient à leur tour jouer un rôle dans la réaction de décomposition du NO. Il a été également montré qu'il y a un changement de mécanisme autour de 853 K. Ce changement est probablement associé à la disponibilité des différentes espèces d'oxygène qui évolue avec la température.

Trois différentes pérovskites qui ont montré les meilleures activités aux températures élevées, $\text{La}_{0.87}\text{Sr}_{0.13}\text{Mn}_{0.2}\text{Ni}_{0.8}\text{O}_{3.5}$ (LSMN-28), $\text{La}_{0.8}\text{Sr}_{0.2}\text{Cu}_{0.15}\text{Fe}_{0.8}\text{O}_{3.5}$ (LSCuF) et $\text{La}_{0.66}\text{Sr}_{0.34}\text{Ni}_{0.3}\text{Co}_{0.7}\text{O}_{3.5}$ (LSNC), appartenant chacune à un groupe précédemment mentionné, ont été choisies pour une étude cinétique complète. On a constaté que l'effet inhibiteur de l'oxygène est relativement faible à basse température (723-800 K). Par contre, il est particulièrement fort aux températures élevées et change avec la composition de la pérovskite et le temps de contact. Parmi les trois pérovskites étudiées, LSMN-28 est la moins affectée par l'oxygène, tandis que la LSNC subit la plus forte inhibition par l'oxygène. À des températures élevées (873-923 K) un modèle simple faisant intervenir l'effet inhibiteur de l'oxygène décrit bien les données expérimentales. Cependant, le mécanisme semble être plus complexe et ne peut pas être basé sur une désorption contrôlante de l'oxygène.

Par une étude complémentaire on a constaté que l'effet inhibiteur de l'eau sur l'activité catalytique de trois pérovskites (LSMN-28, LSNC et LSCuF) dans la décomposition du NO est faible, tandis que celui de l'anhydride carbonique est plutôt fort, mais dans la majorité de cas il reste plus faible que l'effet de l'oxygène. Dans le domaine de température 873-923 K les deux effets inhibiteurs (de l'eau et d'anhydride carbonique) augmentent avec la température, c.-à-d. sont activés. Des paramètres cinétiques reflétant les effets inhibiteurs ont été déterminés. L'ajout du méthane dans un rapport de quatre à une alimentation de NO/He augmente la conversion de l'oxyde nitrique en azote de deux à quatre fois, selon la concentration initiale et la température. L'effet de CH_4 sur la conversion du NO en N_2 dépend moins de la composition de la pérovskite que les effets inhibiteurs de O_2 , CO_2 et H_2O .

Malgré une certaine amélioration par rapport aux catalyseurs de type pérovskites testées dans d'autres laboratoires, on a constaté que l'activité des pérovskites pour la décomposition du NO qui font l'objet de cette recherche reste encore trop basse pour des applications pratiques.

La contribution originale de cette thèse, menée avec plusieurs pérovskites dont les performances pour la décomposition du NO ont été évaluées dans un large éventail de conditions opératoires, est la suivante :

- Les résultats montrent clairement que l'activité des pérovskites est insuffisante pour des applications pratiques.
- Les résultats ayant cerné les effets des divers paramètres opératoires sur la réaction de décomposition du NO révèlent une grande complexité de la réaction tout en dégageant des pistes qui permettront d'élucider le mécanisme de décomposition du NO en présence d'une surface catalytique.

ABSTRACT

Nitrogen oxides originate mainly from high temperature combustion used for heat and energy generation. Their removal is one of the greatest challenges in environment protection. Catalysis plays an important role in this area. Development of a practical catalyst and process for NO decomposition would be a major advance in pollution control technology. In spite of a long effort, no suitable catalyst has been developed. Perovskite-type oxides represent one of the approaches to design NO decomposition catalysts. The perovskite structure provides a wide range of possibilities to tailor physical and catalytic characteristic properties, because it can accommodate a large number of metallic ions. Some perovskites are characterized by easy and reversible oxygen desorption. Most of the perovskites are relatively stable at high temperatures.

The objective of the studies comprising this thesis was to evaluate the performance of several specific perovskites in direct decomposition of nitric oxide under a wide range of experimental conditions and to determine the effect of various reaction parameters in order to contribute to a better understanding of this elusive reaction.

Several new multi-metal compositions were formulated specifically for this study. Three groups of compositions were included, one based on cobalt as principal active element, the second based on nickel and manganese, and the third including copper as an active element. Fine powders with specific surface areas ranging between 9 and 22 m²/g were prepared from highly homogenous reactive precursor slurry processed by a spray-freezing/freeze-drying based method and subsequently calcined in air under controlled conditions. The precursor slurry was obtained by admixing aqueous suspension of in-situ formed lanthanum hydroxide in a solution of metal nitrates.

The NO decomposition was studied at a steady state in plug flow reactor with 1 g catalyst diluted by 7 mL pumice over a wide range of experimental conditions: flowrates

between 10 and 200 mL/min, 1 to 10 % NO, temperatures from 723 to 923 K. Gas chromatography was used to monitor NO conversion to nitrogen, and FTIR served to detect the presence of nitrous oxide in the effluents.

The first part of the study was carried out in absence of oxygen added to the feed. Majority of the perovskites studied in this work exhibit better activity than the individual component oxides or other perovskite catalysts tested previously in other laboratories. Although the activities of the studied perovskites fall in the same order of magnitude, some dependence of the catalytic activity on the catalyst composition and on its corresponding physical and chemical characteristics was observed. The decomposition was found more complex than generally admitted. While important, high specific surface area is not the key factor in determining the activity. Structural aspects of catalyst surface determining specific sites favoring fast decomposition of NO seem to be by far the most important. Kinetic analysis of the data suggests a strong adsorption of nitric oxide, possibly leading to competing oxidation reactions, inhibiting the decomposition, which may in part be responsible for the strong inhibiting effect of oxygen. Among several kinetic models tested to fit the conversion data obtained in the absence of oxygen in the feed, the best fit was obtained with a model involving oxygen not only as inhibitor, but also as reactant. This type of model was proposed in none of previous studies on NO decomposition. While seemingly controversial, it could be explained by the participation of oxygen in formation of some intermediate surface oxygen species that might participate in NO decomposition reaction. There is also evidence for a change of mechanism around 853 K, which is probably related to the availability of different types of oxygen species evolving with increasing temperature.

Three perovskite compositions that exhibited the best activities at high temperatures, $\text{La}_{0.87}\text{Sr}_{0.13}\text{Mn}_{0.2}\text{Ni}_{0.8}\text{O}_{3-\delta}$ (LSMN-28), $\text{La}_{0.8}\text{Sr}_{0.2}\text{Cu}_{0.15}\text{Fe}_{0.85}\text{O}_{3-\delta}$ (LSCuF) and $\text{La}_{0.66}\text{Sr}_{0.34}\text{Ni}_{0.3}\text{Co}_{0.7}\text{O}_{3-\delta}$ (LSNC), were chosen as representative for a complete kinetic study. Oxygen added to the feed reduces the nitric oxide conversion, but the degree of

this inhibition depends on temperature and varies with composition and contact time. Over LSNC the inhibition is the strongest, regardless the temperature. At low temperatures (723-800 K) the inhibiting effect of oxygen is relatively weak. It rapidly increases with temperature between about 800 and 873 K, where it is strongest. Finally, the strong inhibition of oxygen decreases between 873 and 923 K. Of the three perovskites, LSMN-28 is the least affected by oxygen. Although at high temperatures (873-923 K) a simple model describes well the data, the reaction mechanism is far more complex than simply involving slow oxygen desorption.

In a complementary study, the effects of water, carbon dioxide and methane on the nitric oxide decomposition were determined. Both water and carbon dioxide inhibit the decomposition. However, the inhibiting effect of water is considerably weaker than that of carbon dioxide. In majority of cases the inhibition by CO_2 is weaker than the inhibition by oxygen. Between 873 and 923 K the inhibiting effects of carbon dioxide and water increase with temperature, i.e. are activated. Kinetic parameters of all inhibiting effects were determined. Addition of methane in a ratio NO/CH_4 of four to a feed of NO/He increases the conversion of nitric oxide to nitrogen two to four times, depending on the initial NO concentration and on temperature. The effect of added CH_4 seems to be less influenced by the catalyst composition than the inhibition effects of O_2 , CO_2 and H_2O .

In spite of some improvement, in comparison with perovskites tested in other laboratories, the activity in NO decomposition of the studied perovskites remains much too low to be considered for practical applications.

The original contribution of the work of this thesis, in which performance of several perovskites was evaluated in the decomposition of nitric oxide under a wide range of experimental conditions, is the following :

- The results show clearly that the catalytic activity of the tested perovskites is inadequate for practical applications.
- Covering a wide range of operational parameters, the results demonstrate the great complexity of the reaction, but indicate some useful information, which can help to elucidate the mechanism of nitric oxide decomposition in the presence of a catalytic surface.

TABLE DES MATIÈRES

REMERCIEMENTS	iv
RÉSUMÉ	v
ABSTRACT	ix
TABLE DES MATIÈRES	xiii
LISTE DES TABLEAUX.....	xvii
LISTE DES FIGURES	xix
LISTE DES SIGLES ET ABRÉVIATIONS.....	xxv
LISTE DES ANNEXES.....	xxvii
CHAPITRE I : LES OXYDES D'AZOTE ET LEUR ÉLIMINATION.....	1
1.1 Les oxydes d'azote.....	1
1.1.1 Sources et formes d'oxydes d'azote	1
1.1.2 Mécanismes de formation de NO _x	3
1.1.3 Effet de NO _x sur la santé et l'environnement.....	4
1.1.4 Contrôle de NO _x	7
1.2 Décomposition catalytique de NO _x	8
1.2.1 Considérations thermodynamiques.....	9
1.2.2 Principaux systèmes catalytiques.....	9
1.2.2.1 Oxydes simples.....	10
1.2.2.2 Zéolites.....	13
1.2.2.3 Pérovskites.....	17
1.2.2.4 Cinétique et mécanisme.....	20
1.3 Conclusions tirées de la revue de la littérature.....	23
1.4 Principaux objectifs.....	24
1.5 Méthodologie.....	25
1.6 Structure de la thèse.....	26

CHAPITRE II : DIRECT DECOMPOSITION OF NITRIC OXIDE OVER PEROVSKITE-TYPE CATALYSTS, PART I : ACTIVITY WHEN NO OXYGEN IS ADDED TO THE FEED.....	28
2.1 Contexte	29
2.2 Abstract	31
2.3 Introduction	31
2.4 Experimental	34
2.4.1 Catalyst preparation	34
2.4.2 Catalyst characterization.....	36
2.4.3 Catalytic activity determination.....	36
2.5 Results	37
2.5.1 Catalyst design, preparation and characteristics	37
2.5.2 Catalytic performance.....	39
2.5.2.1 Empty reactor and catalyst diluent (pumice).....	39
2.5.2.2 Activity of perovskite compositions.....	40
2.5.2.3 Kinetic analysis of conversion data.....	43
2.5.2.4 Kinetic model.....	48
2.6 Discussion.....	51
2.7 Summary and conclusions	54
2.8 Acknowledgments.....	55
2.9 References	56
CHAPITRE III : DIRECT DECOMPOSITION OF NITRIC OXIDE OVER PEROVSKITE – TYPE CATALYSTS, PART II : EFFECT OF OXYGEN IN THE FEED ON THE ACTIVITY OF THREE SELECTED COMPOSITIONS.....	59
3.1 Contexte	60
3.2 Abstract	61
3.3 Introduction	61
3.4 Experimental	64

3.4.1 Preparation and characterization of catalysts.....	64
3.4.2 Determination of kinetic data.....	65
3.5 Results and discussion.....	66
3.5.1 Catalyst performance in the absence of oxygen in the feed.....	66
3.5.2 Effect of oxygen on the activity	69
3.5.3 Kinetics and mechanism of NO decomposition.....	81
3.5.3.1 Low temperature range.....	82
3.5.3.2 High temperature range (873 – 923 K).....	83
3.6 Summary and conclusions	89
3.7 Acknowledgement.....	91
3.8 References	91

CHAPITRE IV : DECOMPOSITION OF NITRIC OXIDE OVER PEROVSKITE OXIDE CATALYSTS : EFFECT OF CO₂, H₂O AND CH₄	93
4.1 Contexte	94
4.2 Abstract	95
4.3 Introduction	95
4.4 Experimental.....	98
4.5 Results and discussion.....	99
4.5.1 Perovskites characteristics and their activity in NO decomposition.....	99
4.5.2 Effect of carbon dioxide	101
4.5.3 Effect of water	108
4.5.4 Effect of CH ₄ on NO decomposition	113
4.6. Summary and conclusions	118
4.7 Acknowledgement.....	118
4.8 References	119
DISCUSSION GÉNÉRALE	121
CONCLUSIONS ET RECOMMANDATIONS	129

BIBLIOGRAPHIE.....	134
ANNEXES.....	159

LISTE DES TABLEAUX

Tableau 1.1 Sources d'émissions des NO _x	2
Tableau 1.2 Paramètres thermodynamiques pour NO, l'énergie libre et la constante d'équilibre pour la réaction de décomposition du NO.....	9
Table 2.1 Compositions and characteristics of perovskite catalysts studied in direct nitric oxide decomposition.....	35
Table 2.2 Selected activity data for nitric oxide decomposition over several perovskite catalysts.....	42
Table 2.3 Apparent kinetic parameters of the pseudo-first order rate model for nitric oxide decomposition over several perovskite catalysts.....	48
Table 2.4 Results of the search for the best fitting kinetic model (773 K and 923 K).....	50
Table 3.1 Results of the search for the best fitting model for data obtained in the absence of oxygen added to the feed.....	68
Table 3.2 Effect of oxygen added to the feed on the NO conversion to nitrogen over three perovskites.....	76
Table 3.3 Ratios of kinetic constants k_{II}/k_I of model III (Table 3.1) for three perovskites at four temperatures.....	82
Table 3.4 Parameters for the kinetic model: $r = k_{NO} \cdot P_{NO} / (1 + K \cdot P_{O_2})$	88

Table 4.1 Composition of exhaust gases from mobile and stationary sources.....	96
Table 4.2 Parameters for the kinetic model: $r = k_{NO} \cdot P_{NO} / (1 + K \cdot P_{O_2})$, where $k_{NO} = A \cdot e^{(-E_{app}/RT)}$	101
Table 4.3 Apparent activation energies and preexponential factors for the constants representing inhibition by CO_2 and H_2O of NO direct decomposition ($r = k_{NO} \cdot P_{NO} / (1 + K \cdot P_{O_2} + k_{inh_j} P_j)$) over three perovskite catalysts.....	108
Tableau A1.1 Caractéristiques physiques du monoxyde, dioxyde, trioxyde, tetraoxyde et protoxyde d'azote.....	159
Table A3.1 Comparison of Available Methods for Preparation of Perovskite Powders.....	169
Table A3.2 Selected Perovskites Prepared By a New Method (Kirchnerova and Klvana, 1999).....	170
Table A3.3 Apparent Kinetic Parameters of the Pseudo-First Order Rate Model for Nitric Oxide Decomposition over Several Perovskite Catalysts.....	180

LISTE DES FIGURES

Figure 1.1	Structure cubique idéale d'une pérovskite ABO_3.....	17
Figure 2.1	XRD patterns of three selected perovskite compositions.....	38
Figure 2.2	Conversion of nitric oxide to nitrogen over some new perovskite catalysts; 1 g catalyst, 50 ml/min total flowrate, 5 % nitric oxide in helium.....	40
Figure 2.3	Conversion of nitric oxide to nitrogen over different nickel - manganese (LSMN) perovskite catalysts; 1 g catalyst, 50 ml/min total flowrate, 5 % nitric oxide in helium.....	41
Figure 2.4	Arrhenius plots for integrated pseudo-first order kinetic parameters derived from conversions at different conditions for 1 g of LSNC catalyst.....	44
Figure 2.5	Arrhenius plots for integrated pseudo-first order kinetic parameters derived from conversions at different conditions for 1 g of LSMN-28 catalyst.....	45
Figure 2.6	Arrhenius plots for integrated pseudo-first order kinetic parameters derived from conversions at different conditions for 1 g of LSCuF catalyst.....	46
Figure 3.1	Conversion to nitrogen of 2 % nitric oxide in helium over LSMN-28, LSNC and LSCuF perovskites (1 g) as a function of temperature; open symbols: 15 ml/min; full symbols: 75 ml/min.....	67

Figure 3.2 Conversion to nitrogen of 2 % nitric oxide in helium over 1 g LSCuF without (full symbols) and with (open symbols) oxygen added to the feed as a function of temperature.....	70
Figure 3.3 Relative activity (x_{NO+O_2}/x_{NO}) of LSCuF perovskite in the decomposition of 2 % NO as a function of temperature; effect of flowrate and of O₂ concentration.....	71
Figure 3.4 Conversion to nitrogen of 2 % nitric oxide in helium over 1 g LSMN-28 without (full symbols) and with (open symbols) oxygen added to the feed as a function of temperature.....	72
Figure 3.5 Conversion to nitrogen of 2 % nitric oxide in helium over 1 g LSNC without (full symbols) and with (open symbols) oxygen added to the feed as a function of temperature.....	73
Figure 3.6 Relative activity (x_{NO+O_2}/x_{NO}) of LSMN-28 (full symbols) and of LSNC (open symbols) perovskites in the decomposition of 2 % NO as a function of temperature; effect of flowrate and of O₂ concentration.....	74
Figure 3.7 Influence of O₂ concentration in the feed on the conversion of nitric oxide over LSMN-28 perovskite at 873 K (open symbols) and 923 K (full symbols).....	78
Figure 3.8 Influence of O₂ concentration in the feed on the conversion of nitric oxide over LSNC perovskite at 873 K (open symbols) and 923 K (full symbols).....	79

Figure 3.9 Influence of O ₂ concentration in the feed on the conversion of nitric oxide over LSCuF perovskite at 873 K (open symbols) and 923 K (full symbols).....	80
Figure 3.10 Predicted versus experimental conversion of nitric oxide to nitrogen over LSCuF perovskite ($r = k_{NO} \cdot P_{NO} / (1 + K \cdot P_{O_2})$); parameters given in Table 3.2 used in calculations; open symbols correspond to data obtained in the presence of oxygen added to the feed.....	84
Figure 3.11 Predicted versus experimental conversion of nitric oxide to nitrogen over LSMN-28 perovskite ($r = k_{NO} \cdot P_{NO} / (1 + K \cdot P_{O_2})$); parameters given in Table 3.2 used in calculations; open symbols correspond to data obtained in the presence of oxygen added to the feed.....	85
Figure 3.12 Predicted versus experimental conversion of nitric oxide to nitrogen over LSNC perovskite ($r = k_{NO} \cdot P_{NO} / (1 + K \cdot P_{O_2})$); parameters given in Table 3.2 used in calculations; open symbols correspond to data obtained in the presence of oxygen added to the feed.....	86
Figure 3.13 Arrhenius plot for k_{NO} (dotted line) and for K (full line) of the kinetic model $r = k_{NO} \cdot P_{NO} / (1 + K \cdot P_{O_2})$	87
Figure 4.1 Conversion of 5% NO to nitrogen over LSMN-28, LSNC and LSCuF perovskites (1 g) as a function of temperature; open symbols: 50 ml/min; full symbols: 100 ml/min.....	100
Figure 4.2 Effect of added CO ₂ on direct NO decomposition to nitrogen over 1 g LSMN-28 perovskite at different flowrates and NO partial pressures at 873 K (open symbols) and 923 K (full symbols).....	102

Figure 4.3 Effect of added CO ₂ on direct NO decomposition to nitrogen over 1 g LSNC perovskite at different flowrates and NO partial pressures at 873 K (open symbols) and 923 K (full symbols).....	103
Figure 4.4 Effect of added CO ₂ on direct NO decomposition to nitrogen over 1 g LSCuF perovskite at different flowrates and NO partial pressures at 873 K (open symbols) and 923 K (full symbols).....	104
Figure 4.5 Arrhenius plots for the inhibition constants $k_{inh\ CO_2}$ (full lines) and $k_{inh\ H_2O}$ (dotted lines) of the kinetic models representing the inhibition of nitric oxide decomposition by CO ₂ and H ₂ O over three perovskite catalysts.....	107
Figure 4.6 Effect of oxygen, carbon dioxide and water on direct NO decomposition to nitrogen over 1 g LSMN-28 perovskite; total flowrate 100 ml/min.....	109
Figure 4.7 Relative activity of LSMN-28 (full symbols) and of LSNC (open symbols) perovskites in the direct decomposition of 2 or 5 %NO to nitrogen in the presence of water as a function of temperature.....	111
Figure 4.8 Relative activity of LSCuF perovskite in the direct decomposition of 2 or 5 %NO to nitrogen in the presence of water as a function of temperature.....	112
Figure 4.9 Effect of temperature on NO reduction by methane, NO/CH ₄ = 4, (open symbols) and NO decomposition (full symbols) over LSMN-28 catalyst; total flowrate 100 ml/min.....	114

Figure 4.10 Effect of temperature on NO reduction by methane, $\text{NO/CH}_4 = 4$, (open symbols) and NO decomposition (full symbols) over LSNC catalyst; total flowrate 100 ml/min.....115

Figure 4.11 Oxidation of 2.6 % methane to carbon dioxide by oxygen and by nitric oxide over 0.5 g of $\text{La}_{0.8}\text{Sr}_{0.2}\text{Cu}_{0.15}\text{Fe}_{0.85}\text{O}_3$ perovskite powder ($< 10 \mu\text{m}$); plug-flow reactor, steady state conversions, feed flow 200 ml/min. The lines are calculated using following pseudo-first order constants:
air: $E_{\text{app}} = 97 \text{ kJ/mol}$, $\ln A = 20.05 \mu\text{mol/g}\cdot\text{s}\cdot\text{bar}$;
5.2 % O_2/N_2 : $E_{\text{app}} = 97 \text{ kJ/mol}$, $\ln A = 19.75 \mu\text{mol/g}\cdot\text{s}\cdot\text{bar}$;
10 % NO: $E_{\text{app}} = 76 \text{ kJ/mol}$, $\ln A = 14.65 \mu\text{mol/g}\cdot\text{s}\cdot\text{bar}$117

Figure A2.1 Montage expérimental
1- débitmètres massiques; 2- humidificateur; 3- contrôleur de débit;
4- manomètre; 5- réacteur; 6- écran métallique; 7- éléments chauffants;
8- isolant; 9- agitateur; 10- thermocouples; 11- contrôleur de température
12- dessicant; 13- spectromètre; 14- gaz chromatographe.....162

Figure A3.1 Effect of water, of carbon dioxide and of oxygen on the decomposition of nitric oxide over 1 g of $\text{La}_{0.8}\text{Sr}_{0.2}\text{Cu}_{0.15}\text{Fe}_{0.85}\text{O}_3$ perovskite powder ($< 10 \mu\text{m}$) diluted by 7 mL of precalcined inert pumice particles (350-416 μm); plug-flow reactor, steady state conversions.....181

Figure A3.2 Oxidation of 2.6 vol % methane to carbon dioxide by oxygen and by nitric oxide over 0.5 g of $\text{La}_{0.8}\text{Sr}_{0.2}\text{Cu}_{0.15}\text{Fe}_{0.85}\text{O}_3$ perovskite powder ($< 10 \mu\text{m}$) diluted by 10 mL of precalcined inert pumice particles (350–416 μm); plug-flow reactor, steady state conversions, feed flow 200 mL/min.

The lines are calculated using following pseudo-first order constants:

air: $E_{\text{app}} = 97 \text{ kJ/mol}$, $\ln A = 20.05 \mu\text{mol/g}\cdot\text{s}\cdot\text{bar}$;

5.2 vol % O_2/N_2 : $E_{\text{app}} = 97 \text{ kJ/mol}$, $\ln A = 19.75 \mu\text{mol/g}\cdot\text{s}\cdot\text{bar}$;

10 vol % NO: $E_{\text{app}} = 76 \text{ kJ/mol}$, $\ln A = 14.65 \mu\text{mol/g}\cdot\text{s}\cdot\text{bar}$183

LISTE DES SIGLES ET ABRÉVIATIONS

a :	paramètre pseudocubique de la structure pérovskite (nm)
A :	facteur préexponentiel
AFC :	alkaline fuel cells
BET :	Brunauer Emmet Taylor
c_{NO} :	concentration du NO (mol/m ³)
δ :	déficit en oxygène pour la structure pérovskite
D_e :	diffusivité effective (m ² /s)
E :	énergie d'activation (J/mol)
E_{app} :	énergie apparente d'activation (J/mol)
F_i :	débit molaire du composé i (μmol/s)
F_{tot} :	débit gazeux total (mL/min)
FTIR :	Fourier Transform Infrared
ΔG°_r :	énergie libre de Gibbs (J/mol)
ΔH_{ad} :	enthalpie d'adsorption (J/mol)
ΔH_r :	chaleur de réaction (J/mol)
h :	coefficient de transfert de chaleur (W/cm ² s)
k :	constante cinétique
k_c :	coefficient de transfert de masse (m/s)
K_i :	constante d'équilibre d'adsorption du composé i
K_p :	constante d'équilibre de réaction
λ :	conductibilité thermique (J/m s K)
LH :	Langmuir-Hinshelwood
m :	ordre cinétique de réaction par rapport à O ₂
n :	ordre cinétique de réaction par rapport à NO
NO_x :	NO + NO ₂
ppm :	partie par million
P_i :	pression partielle du composé i (bar)

r :	vitesse de la réaction
r_i :	rayon ionique de l'élément i (nm)
R :	constante des gaz parfaits (8,314 J/mol K)
R₀ :	rayon de la particule (m)
R₁ :	rayon des pores (m)
ρ_b :	densité du lit catalytique (kg/m ³)
ρ_p :	densité apparente de la pérovskite (kg/m ³)
ΔS_{ad} :	entropie d'adsorption (J/mol K)
SCR :	selective catalytic reduction
SOFC :	solid oxide fuel cells
SSA :	surface spécifique d'un catalyseur (m ² /g)
t :	facteur de tolérance pour la structure pérovskite
T :	température (K)
T_s :	température de surface (K)
UV :	ultraviolet
W :	masse du catalyseur (g)
x :	conversion du NO en N ₂ (%)
x :	degré de substitution de A par A' dans une structure pérovskite $A_{1-x}A'_x B_{1-y-z}B'_y B''_z O_{3-\delta}$
XPS :	X-ray photoemission spectroscopy
XRD :	X-ray diffratometry
y :	degré de substitution de B par B' dans une structure pérovskite $A_{1-x}A'_x B_{1-y-z}B'_y B''_z O_{3-\delta}$
z :	degré de substitution de B par B'' dans une structure pérovskite $A_{1-x}A'_x B_{1-y-z}B'_y B''_z O_{3-\delta}$

LISTE DES ANNEXES

Annexe 1 Caractéristiques physiques d'oxydes d'azote.....	159
Annexe 2 Montage expérimental.....	160
Annexe 3 Perovskites in environmental and related catalysis : their potentiel and limitations.....	163
Annexe 4 Évaluation des modèles cinétiques.....	198
Annexe 5 Calcul d'un réacteur hypothétique pour la décomposition du NO.....	201

CHAPITRE I

LES OXYDES D'AZOTE ET LEUR ÉLIMINATION

1.1 Les oxydes d'azote

La composition chimique de l'atmosphère a un rôle important dans la cinétique des échanges atmosphériques, dans l'absorption de l'énergie solaire et dans le rejet d'énergie vers l'espace. Cette composition a évolué beaucoup au cours des temps.

Actuellement la pollution atmosphérique suscite une attention particulière. Elle est accusée d'être à l'origine de graves problèmes, telles la formation de photooxydants (smog dans les grandes agglomérations), le caractère acide des précipitations, la destruction de la couche d'ozone et le réchauffement de la planète lié à l'effet de serre.

On considère comme polluant toute substance ajoutée au milieu en concentration suffisante pour produire un effet mesurable sur l'homme, la végétation, les animaux ou les matériaux de construction. Les polluants peuvent être classés en deux catégories :

- les polluants primaires, émis directement par des sources identifiables;
- les polluants secondaires, produits dans l'atmosphère par interaction entre les polluants primaires ou réaction entre les polluants et les constituants normaux de l'atmosphère.

1.1.1 Sources et formes d'oxydes d'azote

Les oxydes d'azote sont reconnus depuis longtemps comme des importants polluants atmosphériques (Hightower et van Leisburg, 1975). Le monoxyde d'azote (NO) et le dioxyde d'azote (NO₂) sont généralement étudiés simultanément et exprimés sous la forme de NO_x. Leur durée de vie dans l'atmosphère est comprise entre un et sept jours pour le monoxyde d'azote et le dioxyde d'azote et 170 ans pour le protoxyde d'azote

(N₂O). Selon la vitesse du vent, les NO_x peuvent parcourir jusqu'à 500 km avant de se désintégrer pour atteindre environ 1/3 de leur concentration d'origine.

Les apports artificiels les plus importants de NO_x proviennent de l'emploi de combustibles fossiles : ils sont émis par des sources mobiles (véhicules, chemins de fer, avions, navires) ou des sources fixes (production d'électricité, chauffage à l'aide de combustibles, procédés industriels, incinération). Quelques-unes de ces sources et les caractéristiques de leurs effluents sont présentées au Tableau 1.1.

Le NO est le plus abondant des dérivés nitrés émis dans l'atmosphère. Il représente environ 95 % des émissions de NO_x. Le NO est aussi émis naturellement par l'activité bactérienne des sols. Une fois dans l'atmosphère le NO est oxydé à base température, formant le NO₂. Le N₂O apparaît également dans les processus microbiens de nitrification et de dénitrification dont l'action est amplifiée par l'emploi de plus en plus intensif d'engrais nitrés et ammoniacaux. Il est également engendré dans les combustions (Hulgaard et Dam-Johansen, 1993) ou dans certaines processus chimiques comme la production de l'acide adipique. N₂O représente moins de 5 % du total des émissions d'oxydes d'azote. Quelques caractéristiques physiques des oxydes d'azote : NO, NO₂, N₂O₃, N₂O₄ et N₂O sont présentées dans l'ANNEXE 1.

Tableau 1.1 Sources d'émissions des NO_x

Source	T, K	[NO _x], %	[O ₂], %	Autres composants
Mobile				
moteur diesel ^a	473 - 673	0.002 - 0.07	4 - 10	CO _x , H ₂ O, HC, particules, SO _x
moteur à essence ^b	573 - 1173	0.01 - 0.4	0.2 - 2	CO ₂ (10-13.5 %), H ₂ O(10-12 %), HC(0.5-1 %), SO _x (0.0015-0.006 %)
Stationnaire				
centrale électrique ^a	473 - 723	0.04 - 0.1	4 - 10	CO _x (5-7 %), H ₂ O(10-15 %), SO _x (0.001-0.3 %)

a-Kung et Kung, 1996; b-Degobert, 1992

Dans un rapport d'Environnement Canada (1998) on mentionne que les émissions canadiennes de NO_x ont atteint en 1995 quelque 2000 kilotonnes (situation stable par rapport à 1980). Au Canada, les émissions de NO_x sont associées au secteur des transports principalement (60 %), à la combustion industrielle et non industrielle de combustibles (28 %) et à la production d'électricité (12 %). En 1995 ces émissions représentaient 9 % des émissions totales en Amérique du Nord. Selon les prévisions établies pour le Canada jusqu'à 2010, les émissions de NO_x demeureront stables.

1.1.2 Mécanismes de formation de NO_x

La recherche fondamentale sur les mécanismes de formation et de destruction de NO_x a trouvé souvent son stimulant dans la nécessité pratique. Les brouillards oxydants qui tourmentent les grandes villes avaient donné l'impulsion à la recherche des mécanismes responsables des émissions de NO par la combustion. Le trou dans la couche d'ozone stratosphérique a déclenché l'effort de recherche sur la cinétique des émissions de N_2O . L'émission de NO_x par la combustion est la résultante d'un ensemble de phénomènes chimiques (réactions en phase gazeuse et réactions hétérogènes se déroulant à l'interface d'une phase solide et d'une phase gazeuse) qui, à leur tour, subissent l'influence de certains phénomènes physiques (diffusion, gradients et fluctuations des concentrations des réactifs et de la température, induits par la turbulence). On considère qu'il y a quatre mécanismes de formation du NO : NO thermique, NO précoce, NO du combustible et NO par l'intermédiaire du N_2O (Warnatz et al., 1996).

La formation de NO thermique (mécanisme de Zeldovich) est due à la dissociation thermique de l'azote et de l'oxygène présents dans l'air de combustion, suivie d'une réaction entre les radicaux formés. La formation de NO thermique augmente de façon exponentielle avec la température et à environ 2000 K on peut considérer que c'est le mécanisme dominant.

NO précoce (mécanisme de Fenimore) est formé suite aux réactions entre les radicaux CH et l'azote de l'air. Le mécanisme NO précoce peut être considéré comme un cas particulier du mécanisme NO du combustible, l'azote moléculaire se comportant comme un azote du combustible en présence de radicaux CH.

NO du combustible est un mécanisme qui postule la formation du NO à partir des espèces azotées organiques présentes dans certains combustibles fossiles (pyridines et pyroles dans le charbon, structures porphyriniques dans les fractions lourdes des huiles résiduelles). Lors de la combustion de ces combustibles lourds, ces azotes organiques primaires se libèrent dans la phase gazeuse sous forme de molécules relativement petites, appartenant au groupe des cyanures (principalement HCN) et des amines légères, qui conduisent par la suite à la formation du NO.

Finalement, le NO peut se former à partir du N₂O. Le protoxyde d'azote se forme par réaction entre les atomes d'oxygène et l'azote moléculaire. Il réagit par la suite avec un autre atome d'oxygène, produisant du NO.

1.1.3 Effet de NO_x sur la santé et l'environnement

Les émissions d'oxydes d'azote sont des facteurs importants dans la détérioration de la santé humaine, la formation de l'ozone troposphérique, la destruction de l'ozone stratosphérique et l'acidification de l'environnement.

Le monoxyde d'azote est en lui-même peu toxique. Les effets soupçonnés concernent sa fixation sur l'hémoglobine (qui limite la fixation de l'oxygène) et des modifications légères du type emphysème. Ces effets n'interviennent qu'au-dessus de 15 à 20 ppm. L'effet essentiel du NO tient à son rôle de précurseur du NO₂. Le dioxyde d'azote peut pénétrer profondément dans le système pulmonaire. Il agit au niveau des alvéoles pulmonaires et amène des altérations de leurs structures, des inhibitions des défenses

pulmonaires et un effet cytotoxique sur les macrophages alvéolaires. Le dioxyde d'azote peut amener la mort de cellules spécifiques au sein du poumon et altérer la régulation des fonctions pulmonaires. Les symptômes de l'action toxique du NO₂ sont l'insomnie, la toux, la respiration haletante et une altération des muqueuses (Degobert, 1992). De récentes études épidémiologiques (Burnett et al., 1998) montrent que le mélange des polluants atmosphériques courants, comme le dioxyde d'azote, le dioxyde de soufre (SO₂), l'oxyde de carbone (CO) et l'ozone (O₃), est associé à la mortalité prématuée et à une gamme d'autres problèmes dans le domaine de la santé. Le risque afférent à ce mélange, dont le NO₂ constitue une composante importante, est sensiblement plus grand que le risque lié à un seul polluant.

Outre ses effets sur la santé humaine, la pollution atmosphérique intervient dans la physiologie des végétaux et dans les phénomènes de corrosion qui affectent les matériaux constitutifs des constructions humaines. Les polluants atmosphériques d'origine anthropogène sont accusés d'être responsables de l'acidification des lacs, du phénomène des précipitations acides et de la mort des forêts.

NO joue un rôle important dans les réactions photochimiques qui ont lieu dans la troposphère et dans la stratosphère. Il réagit avec l'ozone, le formaldéhyde, les hydroperoxydes organiques et les nitrates de peroxyacyle. Les réactions sont rapides et génèrent encore d'oxydes d'azote et de nitrates organiques.

La concentration normale moyenne d'ozone dans l'atmosphère est environ 10⁻¹⁰ %vol. Le maintien de la couche d'ozone stratosphérique, créée par la dissociation photochimique de l'oxygène, dépend de l'équilibre entre les réactions de formation et de destruction de l'ozone, catalysées par les traces des gaz azotés, chlorés ou hydrogénés. Cette couche filtre le rayonnement UV-B (280-320 µm) qui, sans cela, entraînerait une multiplication des cancers cutanés et des mutations biologiques. Le N₂O est un polluant peu actif dans la troposphère par suite de sa faible réactivité. Mais c'est un facteur actif

d'attaque de la couche d'ozone stratosphérique. Sous l'effet du rayonnement UV le protoxyde d'azote est oxydé en NO et ce dernier attaque la molécule d'ozone. De plus, le N₂O est un gaz à effet de serre et participe au réchauffement global de l'atmosphère terrestre.

Dans la basse atmosphère (troposphère) les NO_x réagissent pour former du brouillard photochimique oxydant (smog urbain) dont l'ozone est un important constituant. Les dommages causés par l'ozone sur l'environnement se manifestent par la détérioration du feuillage, le ralentissement de la croissance des arbres sensibles de plusieurs essences ou l'augmentation de leur sensibilité aux maladies.

Les NO_x peuvent aussi affecter d'une manière directe les plantes et les animaux. Ils peuvent provoquer le blanchissement des tissus végétaux, leur mort, la perte de feuilles et peuvent réduire leur vitesse de croissance. Une exposition à 0,5 ppm NO₂ pendant 10 à 20 jours peut arrêter la croissance des certaines espèces végétales.

En présence de l'oxygène, le NO est rapidement oxydé en NO₂ qui, étant soluble dans l'eau, est impliqué dans les précipitations acides. Celles-ci affectent les écosystèmes terrestres, ainsi que les écosystèmes aquatiques et contribuent à la détérioration des constructions.

Les émissions annuelles d'oxydes d'azote touchent clairement l'environnement et la santé humaine. Leur réduction sera favorable à la santé de la population locale et des habitants de régions situées en aval des sources d'émissions, permettra d'abaisser les niveaux ambients d'ozone troposphérique et aidera à prévenir l'acidification des écosystèmes fragiles.

1.1.4 Contrôle de NO_x

Il existe deux approches envisageables pour le contrôle des émissions de NO_x : le contrôle primaire et le contrôle secondaire. Le contrôle primaire englobe toutes les technologies mises au point pour réduire la formation de NO_x, tandis que le contrôle secondaire correspond aux technologies d'élimination d'oxydes d'azote déjà formés. Dans beaucoup de cas un contrôle efficace doit envisager les deux approches en même temps.

Le contrôle primaire doit conduire à la minimisation de la formation de NO_x. Ainsi, on peut envisager l'utilisation de combustibles à faible teneur en azote, comme le gaz naturel à la place du charbon, un meilleur design de fournaises et brûleurs et un contrôle plus précis du rapport combustible/air (Gard, 1994; Kuehn, 1994). Une autre façon de minimiser la formation du NO sera de travailler à plus basses températures. Cela impliquera l'utilisation de mélanges pauvres en combustible. Cependant, l'utilisation de tels mélanges nécessite l'emploi de catalyseurs, car dans ce cas la combustion classique par flamme est instable. Un avantage de la combustion catalytique des mélanges pauvres est qu'elle permet l'abaissement de la température de combustion, donc la minimisation de la formation de NO_x. D'ailleurs, la combustion catalytique peut être considérée comme la technologie la plus efficace parmi les méthodes de contrôle primaire (Trimm, 1983, Prasad et al., 1984, Pfefferle et Pfefferle, 1987, Warnatz et al., 1996, Ciambelli et al., 2000, Sekizawa et al., 2000).

On divise les méthodes d'élimination de NO_x déjà formés en deux catégories : les méthodes humides et les méthodes sèches. Les méthodes humides les plus communes prévoient l'oxydation en phase gazeuse ou en phase liquide du NO (insoluble dans l'eau) en NO₂ (soluble en eau) à l'aide des réactifs tels que ClO₂, KMnO₄, O₃, H₂O₂, NaOCl, suivie de l'absorption du NO₂ dans des solutions alcalines (Chironna et Altshuler, 1999). Ces méthodes sont utilisées pour des effluents à forte teneur en NO_x, tels que ceux

provenant des installations à acide nitrique. Généralement ces méthodes sont chères à mettre en œuvre (surtout celles appliquant l'oxydation stœchiométrique du NO).

Les méthodes sèches ont à la base le principe de la réduction, sélective ou non, catalytique ou non, de NO_x . Dans le cas des méthodes sélectives un agent réducteur est injecté dans la zone post combustion où il va réagir préférentiellement avec NO ou NO_2 . Dans le cas des méthodes non sélectives l'agent réducteur réagit avec l'oxygène avant de réduire les NO_x . La réduction sélective catalytique est la mesure de contrôle secondaire la plus efficace démontrée commercialement, mais assez chère à installer (Pârvulescu et al., 1998 a). Les catalyseurs utilisés sont à base de vanadium et de titane et l'agent réducteur est l'ammoniac ou l'urée. L'application la plus connue de la réduction catalytique non sélective est le convertisseur catalytique trois-voies (Degobert, 1992) qui élimine simultanément le CO, les NO_x et les hydrocarbures imbrûlés par des réactions d'oxydoréduction. Cependant pour réussir à éliminer simultanément les polluants, le contrôle de la richesse du mélange d'admission est essentiel.

1.2 Décomposition catalytique de NO_x

La décomposition catalytique directe est, en théorie, la plus attractive solution pour l'élimination de NO_x . Cette réaction ne nécessite pas d'autres réactifs et produirait seulement de l'azote et de l'oxygène. L'utilisation de différents agents de réduction (hydrocarbures, H_2 , NH_3 , CO) amène toujours un risque supplémentaire de pollution, car des réactions secondaires peuvent produire des composés oxygénés, CO, CO_2 , N_2O , NH_3 , cyanates ou isocyanates. Ce risque serait complètement écarté si on mettrait au point une technologie basée sur la décomposition directe du NO.

1.2.1 Considérations thermodynamiques

Les paramètres thermodynamiques (S° , ΔH°_f) pour le monoxyde d'azote, l'énergie libre de Gibbs (ΔG°) et la constante d'équilibre (K_p) pour la réaction de décomposition du NO en azote et oxygène ($\text{NO} \rightarrow \frac{1}{2} \text{N}_2 + \frac{1}{2} \text{O}_2$) sont présentés dans le Tableau 1.2 (Pârvulescu et al., 1998 a).

Tableau 1.2 Paramètres thermodynamiques pour NO, l'énergie libre et la constante d'équilibre pour la réaction de décomposition du NO

Température K	S° J/mol.K	ΔH°_f kJ/mol	$-\Delta G^\circ$ kJ/mol	K_p
298	210,71	90,40	86,71	$1,88 \times 10^{15}$
300	210,92	90,40	86,67	$1,23 \times 10^{15}$
400	219,50	90,44	85,42	$1,43 \times 10^{11}$
500	226,24	90,48	84,16	$6,20 \times 10^8$
600	231,89	90,48	82,90	$1,65 \times 10^7$
700	236,75	90,48	81,65	$1,24 \times 10^6$
800	241,10	90,52	80,39	$1,77 \times 10^5$
900	244,99	90,52	79,14	$3,92 \times 10^4$
1000	248,55	90,56	77,84	$1,16 \times 10^4$

La molécule de NO est thermodynamiquement instable même à 1000 K et 1 atm. Cependant son énergie de dissociation est très élevée (641,56 kJ/mol) et la vitesse de décomposition est très, très lente. Aucune décomposition (thermique) n'a pu être observée à 825 K (Pârvulescu et al., 1998 a). Cela amène à la nécessité de trouver des catalyseurs très efficaces pour réaliser cette décomposition.

1.2.2 Principaux systèmes catalytiques

Pour la décomposition du NO il est difficile de trouver un catalyseur efficace (actif, sélectif et durable). Il doit fonctionner dans des conditions très spécifiques : large domaine de températures, vitesses spatiales élevées, faibles concentrations de NO_x ,

concentrations élevées pour d'autres composants de l'effluent à traiter (O_2 , CO_2 , H_2O). Ces conditions peuvent aussi changer beaucoup pendant le fonctionnement.

L'étude de la décomposition catalytique a débuté il y a presque cent ans, mais elle est devenue plus poussée dans les années '60 quand le problème de la pollution automobile a commencé à se poser. Un grand nombre de matériaux a été testé, en commençant par les métaux nobles (Pt) et les oxydes simples. Plus tard les oxydes mixtes avec une structure pérovskite et les zéolithes ont été inclus dans l'étude de la décomposition du NO. À date les plus actifs matériaux sont les zéolithes. Dans les sous-chapitres suivants on passe en revue les oxydes simples, les pérovskites et les zéolithes en analysant l'état actuel de connaissances concernant la décomposition catalytique directe du NO.

1.2.2.1 Oxydes simples

Les premières études concernant la décomposition du NO sur des oxydes de métaux de transition et de métaux alcalino-terreux datent dès années '30, mais la recherche est devenue plus soutenue dès les années soixante (Fraser et Daniels, 1958, Yur'eva et al., 1965). Depuis, plusieurs types d'oxydes simples ont été testés afin d'évaluer leur activité (Shelef et al., 1969, Winter, 1971, Amirnazmi et al., 1973, Meubus, 1977, Golodets, 1983).

L'adsorption du NO sur différents oxydes tel que de chrome (Otto et Shelef, 1969), de fer (Otto et Shelef, 1970), de nickel, de cuivre (Gandhi et Shelef, 1972, 1973) et de cobalt (Yao et Shelef, 1974) a été étudiée en détail pour déterminer les interactions entre NO et la surface catalytique. La vitesse relative de chimisorption décroît dans l'ordre : $Co_3O_4 > Fe_3O_4 > Cr_2O_3 > NiO$.

Winter (1971) a publié une étude sur l'activité catalytique d'une quarantaine d'oxydes métalliques et a fait une première proposition concernant le mécanisme de

décomposition du NO. Les énergies d'activation apparentes déterminées dans cette étude sont comprises entre 38 kJ/mol (CuO) et 172 kJ/mol (ZnO). Amirnazmi et al., (1973) ont étudié les oxydes de fer, de cobalt, de nickel, de cuivre et de zirconium. Ils ont constaté que le Co_3O_4 est plus actif que le CuO. En 1975 Hightower et van Leirsburg ont fait une mise au point sur les catalyseurs testés pour la décomposition directe du NO, la cinétique et le mécanisme de réaction. Selon ces auteurs la plupart des matériaux sont actifs dans l'état réduit. L'oxygène produit reste fortement lié à la surface, diminuant ainsi l'activité.

Les oxydes de métaux alcalino-terreux (MgO, CaO, SrO) ont été étudiés pour la première fois par Schwab et al. (1933), ensuite par Fraser et Daniels (1958) et par Winter (1971). Mais c'est Meubus (1977) qui a publié une étude plus détaillée sur la décomposition du NO sur BaO, SrO et CaO, en absence et en présence de l'oxygène. Il trouve que, à 17 mL/min, le plus performant est BaO, sur lequel le rendement de la décomposition est de 60 % à 1123 K, suivi par SrO (35 %) et CaO (25 %). Sur BaO l'oxygène n'a pas d'effet inhibiteur pour un mélange 0,5 %NO, 3 %O₂ et He formant la balance.

Quoique l'activité par unité de surface pour la plupart des oxydes simples est très faible, on observe dans les dernières années des nouvelles recherches sur des systèmes catalytiques déjà étudiés auparavant. On peut mentionner ici les oxydes de terres rares (Zhang et al., 1994 a, 1995 a, Vannice et al., 1996), les oxydes de manganèse (Yamashita et Vannice, 1996, 1997) et l'oxyde de baryum (Xie et al., 1997, Mestl et al., 1997 a, b, 1998). Toutes ces études récentes essayent d'offrir une meilleure compréhension du mécanisme de décomposition du NO. Xie et al. (1997) et Mestl et al. (1997 a, b, 1998) ont trouvé qu'un catalyseur à base de BaO/MgO (avec au moins 11 %Ba) est très actif dans la décomposition du NO. La vitesse de réaction sur BaO/MgO (14 %mol Ba) est 2,5 $\mu\text{mol N}_2/\text{g.s}$ à 973 K, ce qui est une performance exceptionnelle pour un catalyseur de type oxyde. Une vitesse de même ordre on trouve avec Cu-ZSM-

5 à 773 K (Li et Hall, 1991). Cependant, il faut mentionner que le catalyseur BaO/MgO présente cette activité maximale dans un domaine très restreint de températures (moins de 10 degrés) et seulement entre 903 et 973 K, dépendement de la concentration du NO dans les effluents à traiter. En dehors de ces limites, les vitesses diminuent beaucoup (plus que 10 fois). De ce point de vue son comportement semble similaire aux zéolithes. Contrairement à Winter (1971), Zhang et al. (1994 a) n'observent pas de décomposition directe du NO sur MgO, ni sur MgO dopé au Li. Ils observent cependant une certaine activité sur La_2O_3 , mais beaucoup plus faible que dans le cas de la réduction du NO par CH_4 . La décomposition directe a été étudiée pour un mélange 4,04 %NO dans He, $\text{GHSV}=2200 \text{ h}^{-1}$, entre 773 et 973 K. Bien que la vitesse de réaction est faible ($1,6 \cdot 10^{-3} \text{ } \mu\text{mol/g.s}$), ils vont continuer les études sur quelques oxydes de terres-rares (La_2O_3 , $\text{Sr/La}_2\text{O}_3$, Ce_2O_3 , Nd_2O_3 , Sm_2O_3 , $\text{Sr/Sm}_2\text{O}_3$, Tm_2O_3 , Lu_2O_3) à pression atmosphérique, pour un mélange initial 2 %NO dans He et un débit de 40 mL/min ou 4 %NO et 5 mL/min, entre 773 et 973 K (Zhang et al., 1995 a). Ils constatent que la décomposition peut être observée pour la majorité des matériaux à partir de 773 K (exception Ce_2O_3 et Tm_2O_3). Parmi les oxydes dernièrement testés on trouve aussi les oxydes de manganèse (Yamashita et Vannice, 1996, 1997). Mn_2O_3 est plus actif que Mn_3O_4 dans la décomposition catalytique du NO, mais toujours moins actif que le Co_3O_4 . De plus on n'observe pas une activité importante en bas de 773 K.

Le Co_3O_4 est considéré comme étant le meilleur catalyseur parmi les oxydes simples étudiés (Hightower et van Leirsburg, 1975). Le dopage de celui-ci par l'argent augmente encore cette activité (Hamada et al., 1990). Néanmoins, il faut assurer un rapport optimal Ag/Co. Les meilleurs résultats ont été obtenus pour un rapport 1/20. En plus, le dopage du Co_3O_4 par Ag diminue l'effet inhibiteur de l'oxygène. Malheureusement, Ag/ Co_3O_4 est peu résistant à l'empoisonnement au soufre. Le dopage du Co_3O_4 avec des métaux alcalins, particulièrement Na, semble aussi bénéfique (Park et al., 1998).

1.2.2.2 Zéolithes

Les zéolithes sont des silice-alumines cristallisées qui présentent un réseau de pores et des cavités dont les dimensions sont comprises entre 0,3 et 1,0 nm. On connaît plus de 100 types de structures différentes, dont nombreuses sans équivalents naturels. Chaque structure est caractérisée par certaines dimensions des pores et une orientation particulière des canaux. Les plus connues dans la catalyse sont la zéolithe Y (l'anologue synthétique de la faujasite), la ZSM-5 (sans équivalent naturel) et la mordenite.

La découverte que les zéolithes échangées au cuivre sont très actives pour la décomposition directe du NO (Iwamoto et al., 1981) a relancé la recherche dans ce domaine. Certaines zéolithes ont montré une activité nettement supérieure par rapport aux autres catalyseurs déjà évalués pour la réaction de décomposition du NO. En 1991, Iwamoto avait même supposé l'application industrielle de la Cu-ZSM-5 dans les prochains années. L'intérêt pour l'utilisation des zéolithes échangées aux métaux de transition (en particulier le cuivre) dans le domaine d'élimination de NO_x a donc augmenté (Li et Hall, 1990, 1991, Hall et Valyon, 1992, Shelef, 1995, Iwamoto, 1996, Bell, 1997).

Les premières études sur les zéolithes ont été faites sur la zéolithe de type Y (Iwamoto et al., 1981). Pour un mélange de 4 %NO dans He avec un débit total 19,6 mL/min et 3,56 g catalyseur ils obtiennent à 773 K une sélectivité de 49,2 % en N₂ pour une conversion presque totale du NO (99,0 %). La conversion augmente avec la température entre 573 et 823 K. En comparant les performances de la Cu-Na-Y avec celles du CuO-SiO₂, ils suggèrent que la principale différence entre la zéolithe Cu-Na-Y et le CuO-SiO₂ réside dans le fait que l'oxygène est beaucoup moins fortement lié à la surface dans le cas de la zéolithe-Y que dans le cas de CuO-SiO₂. Par conséquent, l'oxygène peut se désorber à des températures plus basses dans le cas des zéolithes.

Une étape importante dans le domaine des structures de type zéolithe est la découverte de la Cu-ZSM-5, qui démontre à date la plus grande activité pour la décomposition directe du NO. Les études de Iwamoto et al. (1986) sur la faujasite, la zéolithe-Y, la mordenite et la ZSM, indiquent la supériorité de ZSM pour la décomposition du NO (au même taux d'échange du cuivre) : ZSM >> zéolithe-Y \cong mordenite >> faujasite. Li et Hall (1991) et Valyon et Hall (1993 a, b) ont constaté aussi la supériorité de la Cu-ZSM-5 par rapport à la Cu-Y. Les raisons pour lesquelles la Cu-ZSM-5 est meilleure par rapport aux autres zéolithes ne sont pas bien connues. Plusieurs suppositions ont été faites. Valyon et Hall (1993 a) ont suggéré que les espèces intermédiaires pourraient être différentes pour la ZSM-5 et pour la Cu-Y. Centi et Perathoner (1995) ont montré que la covalence de la liaison métal-structure zéolithe décroît dans l'ordre : ZSM-5 > mordenite > faujasite. On peut aussi supposer que la structure et la porosité de ZSM-5 sont très importantes pour assurer et maintenir une grande dispersion du cuivre et pour permettre une plus grande accessibilité des réactifs (NO_x) vers les sites actifs. Cette structure joue probablement un rôle dans la stabilité de certains intermédiaires durant la réaction.

Li et Hall (1990) ont rapporté la conversion complète du NO en N_2 et O_2 sur une composition Cu-ZSM-5 avec un taux d'échange de 140 %. Leurs conditions expérimentales étaient : température 773 K, 4 % NO dans He, le débit total de 11 mL/min et W = 0,75 g catalyseur. Ils ont mis en évidence l'effet inhibiteur de l'oxygène et de la vapeur d'eau (2 %). L'activité catalytique a été retrouvée après l'élimination de l'oxygène (respectivement H_2O) de l'effluent et une augmentation de la température a été suggérée pour compenser l'effet dû à l' O_2 et H_2O . Le CO_2 ne semble pas influencer l'activité catalytique. L'effet de l'oxygène dépend de la structure de la zéolithe, du taux d'échange du cuivre et du rapport $\text{P}_{\text{O}_2}/\text{P}_{\text{NO}}$ (Iwamoto, 1991). L'effet de l'oxygène est moindre pour les zéolithes suréchangées au cuivre (Iwamoto et al., 1991 b, c). Les zéolithes suréchangées sont plus actives et sont plus facile à obtenir dans le cas de la Cu-ZSM-5 que de la Cu-Y (Iwamoto et al., 1991 a, Campa et al., 1993). On a rapporté une

activité maximale pour un taux d'échange de 500 % (Pirone et al., 1996). Headon et al., 1996 ont mis en évidence l'effet promoteur de l'oxygène sur la décomposition de NO_x à des températures plus basses que 573 K et l'effet inhibiteur de celui-ci pour des températures supérieures à 623 K.

Les ZSM-5 double-échangées avec Cu et des métaux alcalins ou métaux de transition ont une meilleure activité que certaines Cu-ZSM-5 suréchangées pour la décomposition du NO aux températures supérieures à 723 K (Kagawa et al., 1991) et en présence de l'oxygène (Zhang et al., 1994 b). La présence d'un deuxième métal semble augmenter la stabilité du cuivre comme site actif. La Mg-Cu-ZSM-5 est plus active que la Cu-ZSM-5, en absence ou en présence de l'oxygène, les cations Mg^{2+} stabilisant les cations Cu^{2+} . La vapeur d'eau (20 %mol) provoque la désactivation de la Cu-ZSM-5 à 773 K et la déalumination aux températures plus élevées que 873 K. La présence du Mg^{2+} diminue cet effet (Zhang et al., 1994 b). Le même rôle joue le cérium dans Ce/Cu-ZSM-5 (Zhang et al., 1995 b). De plus le Ce (III) empêche la formation de la phase CuO à l'intérieur des canaux de la zéolithe et donc sa désactivation (Zhang et Flytzani-Stephanopoulos, 1996). L'échange avec du Ni n'augmente pas l'activité des Cu-ZSM-5 suréchangées. On observe même une légère diminution de l'activité. Par contre, pour les zéolithes souséchangées on remarque une légère augmentation de l'activité. Cela pourrait indiquer, que dans le cas des zéolithes souséchangées la présence du nickel détermine les ions de cuivre à occuper les sites actifs ou à s'associer et former des sites actifs (Curtin et al., 1997). Le Sm semble avoir pour effet d'augmenter la dispersion du cuivre, ce qui expliquerait la meilleure activité de la Cu-Sm-ZSM-5 pour la décomposition du NO comparativement à l'activité de la Cu-ZSM-5 (Pârvulescu et al., 1998 b).

Parmi d'autres zéolithes étudiées pour la décomposition du NO on peut mentionner aussi Au-Na-Y (Salama et al., 1994), Ni-ZSM-5 et Fe-ZSM-5 (Varga et al., 1995). Pour la Co-ZSM-5 on a constaté une stabilité plus élevée en présence de la vapeur d'eau que

dans le cas de la Cu-ZSM-5 (Armor et Farris, 1994). Cette zéolithe à base du Co est considérée de plus en plus comme un catalyseur pour la réduction sélective du NO (Bell, 1997). En ce qui concerne la formation de l'azote, à basse température (< 473 K), la Co-NaZSM-5 est 2-3 fois plus active que la Cu-NaZSM-5. Co-NaZSM-5 est très peu active dans la décomposition du NO pour des températures plus grandes que 633 K, mais pour la décomposition du NO₂ son activité est comparable à celle du Cu-NaZSM-5 (Chang et McCarty, 1997). Après une réduction à 773 K avec CO, la Cu-HZSM-5 (Cu/H = 1,5) est très active même à 573 K pour la décomposition. Après une réduction dans H₂, le catalyseur devient très actif à 773 K (Halasz et al., 1997).

La Cu-ZSM-5 suréchangée est le meilleur matériel connu actuellement pour la décomposition directe du NO. Cependant les zéolithes présentent leur maximum d'activité généralement entre 773 et 873 K. En dehors de ces limites leur activité devient trop faible pour des applications pratiques. Malgré leurs bonnes performances, les zéolithes n'ont pas une bonne stabilité thermique. De plus elles sont rapidement empoisonnées par les oxydes du soufre particulièrement, mais probablement aussi par les composés à base d'arsène et de phosphore. En présence du SO₂ le catalyseur perd parfois complètement son activité entre 673 et 923 K (Iwamoto et al., 1991 c). L'effet de l'empoisonnement par SO₂ est réversible. Cependant la régénération du catalyseur nécessite un traitement à haute température. La vapeur d'eau représente un autre problème qui pourrait empêcher l'application pratique de la Cu-ZSM-5. Aux températures élevées, elle peut produire la déalumination du matériau. En présence des agents réducteurs, on a observé la formation du HCN sur Cu-ZSM-5 ce qui rend peu probable l'utilisation de ce système catalytique pour les effluents des moteurs Diesel (Radtke et al., 1995). L'activité des zéolithes augmente avec le taux du cuivre, mais l'obtention de zéolithes avec des taux d'échange élevées coûte assez cher.

1.2.2.3 Pérovskites

Les oxydes mixtes de type pérovskite ont une structure semblable au CaTiO_3 , le minéral qui a donné son nom à ce groupe de composés. Il a été découvert en 1839 par Rose et a été dédié au minéralogiste russe L. A. von Perovski. Les pérovskites sont habituellement représentées par la formule ABO_3 . Les sites A ($r_A > 0,09 \text{ nm}$), considérés généralement inactifs, sont constitués principalement des métaux alcalins, alcalino-terreux ou des lanthanoides. Les sites B ($r_B > 0,05 \text{ nm}$) désignent principalement les métaux de transition de type 3d, 4d ou 5d. Il a été observé que pour former une structure de type pérovskite ABO_3 les atomes A et B doivent satisfaire la relation de Goldschmidt :

$$0,75 < (r_A + r_O) / 2^{0.5} (r_B + r_O) < 1,0$$

r_O étant le rayon ionique de l'ion O^{2-} .

La structure idéale des pérovskites est cubique (fig. 1.1), A étant entouré par 12 ions O^{2-} , B par 6 ions O^{2-} . Chaque ion O^{2-} est entouré par 4 ions A et 2 ions B.

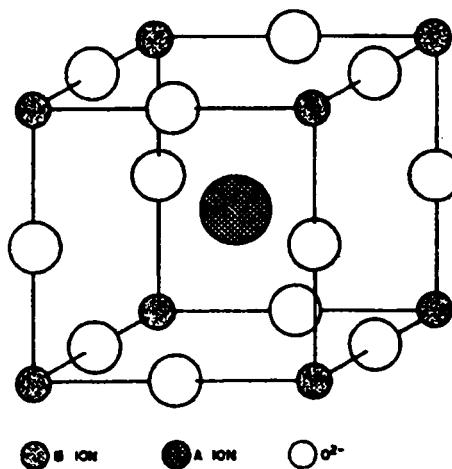


Figure 1.1 Structure cubique idéale d'une pérovskite ABO_3

En substituant en partie la composition des sites A ou B ($A_{1-x}A'_xB_{1-y}B'_yO_3$), sans changer la structure cristalline de base, on provoque l'apparition des défauts dans le réseau et on peut obtenir des propriétés catalytiques nouvelles. Une des caractéristiques très intéressantes de cette structure est qu'elle permet la stabilisation des métaux en B (Co, Fe, Mn, Cu, Ni, Ti) dans différents états d'oxydation non usuels.

Malgré le fait que quelques pérovskites ont été testées comme catalyseurs dans les années 1950 (Paravano, 1952, 1953), pour la catalyse ils ont vraiment attiré l'attention des chercheurs dans les années 1970. Meadowcroft (1970) a étudié l'activité de la $La_{0.8}Sr_{0.2}CoO_3$ comme électrode d'oxygène et Libby (1971) a suggéré l'utilisation des pérovskites à base de cobalt et terres-rares comme catalyseurs d'oxydation pour l'épuration des gaz d'échappement des automobiles. Avec le temps l'intérêt pour les pérovskites comme catalyseurs a vite augmenté (Voorhoeve et al., 1975, Tejaca et al., 1989). Plus de détails sur le potentiel d'application des pérovskites sont présentés à l'ANNEXE 3.

Voorhoeve et al. (1975) en étudiant la décomposition du NO sur des manganates substitués en A et/ou B indiquent que ces pérovskites sont peu actives pour la décomposition directe à la différence de la réduction du NO par CO ou H_2 où leurs performances sont très bonnes.

Quelques années plus tard, suite à la découverte de la superconductivité aux températures élevées de la $YBa_2Cu_3O_{7-\delta}$, l'intérêt pour les pérovskites augmente à nouveau. Arakawa et Adachi (1989) montrent qu'entre 500 et 800 K, NO s'adsorbe et se désorbe reversiblement sur $YBa_2Cu_3O_{7-\delta}$, sans qu'une décomposition importante en éléments ait lieu. La décomposition est possible aux températures plus élevées (Shimada et al., 1988), mais l'activité diminue aux alentours de 1073 K à cause du frittage. Par contre, $YBa_2Cu_3O_7/MgO$ a été trouvé plus actif qu'un catalyseur commercial à base de platine à 1073 K (3 %NO dans He, $F_{tot} = 20$ mL/min, $W = 0,5-2,5$

g catalyseur). Des cuprates superconducteurs ont été étudiés aussi par Halasz et al. (1993) dans des conditions des concentrations des réactifs et des temps de contact proches des situations pratiques. Toutes les pérovskites testées ont été trouvées inactives dans le cas de la décomposition directe du NO pour des températures en dessous de 973 K. Les matériaux qu'ils ont utilisés avaient cependant des surfaces spécifiques très petites (0,1 à 1,0 m²/g). Yasuda et al. (1990, 1993) ont étudié la décomposition du NO sur des cuprates substitués ayant une structure de type K_2NiF_4 ($La_{2-x}Sr_xCu_{1-y}B'_yO_4$; B' = Al, Zr; x = 0–1,0; y = 0–0,2). Ils ont constaté que l'activité catalytique maximale est obtenue pour x = 0,4–0,5. La plus grande activité a été observée pour $La_{1,5}Sr_{0,5}CuO_4$. Elle est trois fois plus grande que l'activité de $La_{0,8}Sr_{0,2}CoO_3$, qui représente la pérovskite la plus active parmi celles étudiées par Teraoka. Une étude plus systématique de plusieurs pérovskites faite par Teraoka et al. (1993) indique que l'activité catalytique pour la décomposition directe du NO peut être variée de manière significative en fonction des métaux qu'on sélectionne dans le site B et de leurs proportions relatives. Ainsi, ils trouvent que $La_{0,8}Sr_{0,2}Co_{0,8}B'_{0,2}O_3$ et $La_{0,4}Sr_{0,6}Mn_{0,8}B'_{0,2}O_3$ (B' = Fe, Co, Ni) manifestent une activité importante et stable entre 973 et 1073 K dans les conditions suivantes : NO (0,1–1,0 %vol.)–O₂ (0–9 %vol.)–He (balance); W = 0,1–1,0 g catalyseur; W/F_{tot} = 0,25–4,0 g.s/mL. Les surfaces spécifiques des catalyseurs testés ont été généralement en dessous de 10 m²/g. Les travaux de Teraoka et al. (1993) ont confirmé que la substitution du La par Sr provoque une augmentation importante de l'activité. Les manganates nonsubstitués ne sont pas de bons catalyseurs, mais leur performance peut être améliorée par substitution partielle du Mn par du nickel, du fer ou du cobalt. Zhao et al. (1996) qui ont étudié les pérovskites de type ABO₃ et A₂BO₄ à base de nickel ont démontré aussi que la substitution du La par Sr rendent les catalyseurs plus actifs.

Tout récemment Uchida et al. (1998) ont testé une pérovskite de type $SrTi_{1-x}Fe_xO_3$ (x = 0–1) et ont trouvé qu'à 1073 K la $SrTi_{0,8}Fe_{0,2}O_3$ est deux fois plus active que $La_{0,8}Sr_{0,2}CoO_3$ en absence d'oxygène (1 %vol. NO dans He, F_{tot}=100 mL/min,

$W/F_{tot}=3,0$ g.s/mL) et cinq fois plus active en présence de 10 %vol. O_2 . Ils suggèrent que cette combinaison Ti-Fe favorise la désorption rapide de l'oxygène.

Beaucoup d'effort a été consacré aux méthodes de préparation dans le but d'augmenter la surface spécifique du matériau final. On a réussi ainsi à passer des surfaces plus petites que 1 m^2/g (Voorhoeve et al., 1975) aux surfaces d'au moins 10–15 m^2/g . Certainement la surface spécifique est influencée par la nature des métaux qu'on va retrouver dans le matériau final, mais la méthode de préparation joue un rôle important concernant l'homogénéité du précurseur avant l'étape de calcination. La meilleure méthode semble être la cryodessiccation (Tejuca et al., 1989, Kirchnerova et Klvana, 1999). Elle permet la formation d'une relativement grande surface spécifique et préserve une répartition idéale des constituants, telle qu'elle existe dans la solution initiale. Plus d'informations sur les différentes méthodes de préparation sont données dans l'ANNEXE 3.

Les pérovskites, de même que les oxydes simples, sont susceptibles à l'empoisonnement au soufre. Cependant il a été démontré pour quelques compositions qu'elles peuvent tolérer des faibles concentrations des composés soufrés (Kvana et al., 1997 a, b).

Malgré les efforts employés jusqu'à présent on n'a pas trouvé une composition de type pérovskite qui posséderait une activité suffisante pour une utilisation pratique dans le domaine de la décomposition directe du NO (Zhao et al., 1996, Lombardo et Ulla, 1998).

1.2.2.4 Cinétique et mécanisme

En ce qui concerne le mécanisme de décomposition du NO les étapes suivantes doivent être considérées dans tous les cas :

- l'adsorption;

- le couplage de deux espèces contenant l'azote;
- la décomposition de l'intermédiaire avec la formation de N₂;
- la désorption des produits.

Chacune de ces étapes peut être l'étape déterminante de vitesse.

La molécule de l'oxyde nitrique est un radical π^* ($\sigma_{1s}^2 \sigma_{1s}^{*2} \sigma_{2s}^2 \sigma_{2s}^{*2} \pi_{2p}^4 \pi_{2p}^{*1}$), qui en présence d'un site actif peut soit accepter un électron et former l'ion NO⁻, soit céder un électron et former NO⁺. La formation de l'ion NO⁻ a pour effet la diminution de la force de liaison N-O, ce qui facilite la rupture de la molécule.

Une première proposition concernant le mécanisme a été faite par Winter (1971) pour des oxydes simples. Il suppose l'existence de paires de sites actifs qui contiennent des électrons piégés (sites R₂). L'adsorption d'une première molécule de NO a lieu sur un site (formation de NO⁻). Elle est suivie de l'adsorption d'une deuxième molécule sur le site voisine (site F). Teraoka et al. (1993) supposent aussi l'existence des paires de sites actifs sur les pérovskites, mais formés dans ce cas par de lacunes d'oxygène. Sur les zéolithes Hall et Valyon (1992), Iwamoto (1994), Komatsu et al. (1994) ont supposé l'existence de paires d'ions Cu²⁺ comme sites actifs, tandis que Shelef (1992, 1995) considère la possibilité des sites uniques Cu²⁺.

Le couplage en vue de la formation de la liaison N-N peut se réaliser suite aux interactions entre les molécules de NO adsorbées sur deux sites voisins, suite au déplacement de deux molécules de NO adsorbées sur des sites individuels l'une vers l'autre ou par l'adsorption de deux molécules de NO sur le même site.

La décomposition de l'intermédiaire peut avoir lieu avec la formation de l'azote moléculaire ou avec la formation du N₂O qui reste adsorbé et va se décomposer par la suite, en libérant la molécule de N₂. L'oxygène moléculaire sera formé à partir des

atomes d'oxygène adsorbé à la surface ou par couplage entre les atomes d'oxygène adsorbés et l'oxygène mobile (cas des pérovskites).

Pour tous les trois systèmes (oxydes, zéolithes, pérovskites) on a considéré d'abord que la décomposition du NO se réalise suivant un cycle redox sur des paires de sites actifs. Le NO agit comme oxydant et l'oxygène qui se désorbe agit comme réducteur pour le site actif du catalyseur. On a conclu que l'effet inhibiteur de l'oxygène est dû à sa désorption lente. L'étape déterminante de vitesse a été considérée le couplage suite à l'adsorption de la deuxième molécule de NO (Amirnazmi, 1973, Teraoka et al., 1993, Yamashita et Vannice, 1996).

Shelef (1992, 1995) a fait une autre proposition de mécanisme qui ne suppose pas un cycle redox pendant la décomposition du NO. Sur chaque site actif (Cu^{2+}) deux molécules de NO peuvent s'adsorber en formant une structure Cu^{2+} -gem-dinitrosyle, un dimère qui va se décomposer en azote et oxygène moléculaire. Ce mécanisme est appuyé par les études expérimentales de Kucherov et al., (1994). Ils n'ont pas détecté la présence des ions Cu^+ . D'ailleurs même Valyon et Hall (1993 b) acceptent cette hypothèse mais pour des conditions particulières : températures plus basses que 573 K ou conversions du NO en N_2 inférieures à 40 %, quand le NO peut agir comme son propre agent réducteur. Dans la récente étude sur BaO/MgO , Xie et al.(1997) présentent des données qui semblent soutenir l'hypothèse d'un mécanisme qui n'est pas basé sur un cycle redox. Par spectroscopie Raman, Xie et al. (1997) ont mis en évidence la formation d'un intermédiaire $Ba-NO_2$ qui peut conduire à une structure de type dimère sur le centre actif. Le dimère se décompose par la suite en azote et oxygène moléculaire. Récemment, Huang et al. (2000) ont étudié la décomposition du NO sur La_2O_3 et ont mis en évidence quelques espèces qui contiennent une liaison N-N. Parmi celles-ci $(N_2O_2)^2-$ a pu être détectée à 800 K et les auteurs supposent qu'elle pourrait être l'intermédiaire actif pendant la décomposition du NO. La formation des nitrites et nitrates sur la surface catalytique pourrait expliquer l'effet inhibiteur de l'oxygène. Sur le $YBa_2Cu_3O_7$,

Lin et al. (1993) ont mis en évidence la formation des ions nitrate à basse température (< 540 K) et des ions nitrites à haute température (>820 K).

Le mécanisme reste toujours controversé. Le problème le plus étudié, mais qui n'est toujours pas résolu avec certitude concerne la nature du site actif et l'étape limitante de vitesse.

Des cinétiques allant d'ordre zéro à deux pour le NO ont été proposées. On présente seulement quelques équations cinétiques proposées pour la décomposition du NO sur oxydes, zéolithes et pérovskites :

$$r = \frac{kP_{NO}}{1 + K_{O_2}P_{O_2}} \quad (\text{Winter, 1971, Amirkazmi et al., 1973})$$

$$r = \frac{kP_{NO}}{1 + K_{O_2}P_{O_2}^{1/2}} \quad (\text{Li et Hall, 1991})$$

$$r = \frac{kK_{NO}P_{NO}^2}{1 + K_{NO}P_{NO} + K_{O_2}P_{O_2}} \quad (\text{Teraoka et al., 1993})$$

$$r = \frac{kK_{NO}^2P_{NO}^2}{(1 + K_{NO}P_{NO} + K_{O_2}^{1/2}P_{O_2}^{1/2})^2} \quad (\text{Vannice et al., 1996, Yamashita et Vannice, 1996})$$

Les énergies d'activation déterminées pour la réaction de décomposition du NO sur les oxydes et les zéolithes sont généralement comprises entre 38 et 172 kJ/mol (Winter, 1971, Meibus, 1977, Li et Hall, 1991, Yamashita et Vannice, 1996, Huang et al., 1998).

1.3 Conclusions tirées de la revue de la littérature

La décomposition catalytique serait la voie la plus souhaitable pour l'élimination économique des oxydes d'azote. Malgré tous les efforts faits et la diversité des matériaux testés, on n'a pas réussi jusqu'à date à mettre au point un catalyseur ayant une activité suffisante pour des applications pratiques.

La plupart des études expérimentales ont été faites à des débits très faibles, généralement à moins de 30 mL/min (temps de contact élevés) et à des températures élevées (>973 K) pour les oxydes simples et les quelques pérovskites ABO_3 testées. L'effet de l'oxygène a été mis en évidence et quantifié dans la plus part des cas, mais très peu d'études ont été faites en présence du CO_2 ou H_2O .

Pour des températures inférieures à 873 K les plus actifs catalyseurs, à date, sont les zéolithes suréchangées au cuivre, Cu-ZSM-5. Cependant, les zéolithes gardent leur activité dans un domaine étroit de températures.

Quand on regarde la stabilité thermique, la stabilité en présence de l'eau et possiblement la résistance à l'empoisonnement, les pérovskites commencent à susciter l'attention. Les propriétés physiques et catalytiques des pérovskites peuvent être influencées par les choix de métaux en A et B. On peut ainsi augmenter le déficit en oxygène de cette structure, on peut augmenter leur stabilité thermique et on peut stabiliser des métaux qui forment des faibles liaisons avec l'oxygène. Cependant, ce système catalytique a été le moins étudié comparativement aux deux autres.

Le mécanisme de réaction n'est pas, non plus, complètement élucidé sur aucune classe de catalyseurs testés. Sur tous les matériaux il reste encore beaucoup de travail à faire pour clarifier la nature des sites actifs, la nature des espèces intermédiaires et leur rôle, l'étape limitante de la vitesse de réaction, le domaine de températures dans lequel un mécanisme proposé reste valable, etc.

1.4 Principaux objectifs

Au département de génie chimique de l'École Polytechnique de Montréal ont a mené plusieurs études sur les matériaux de type pérovskite dans les domaines de la combustion catalytique et d'électrocatalyse. On a développé aussi une nouvelle

méthode de préparation de ces matériaux basée sur la cryodessiccation qui permet d'obtenir des surfaces spécifiques assez importantes et une bonne homogénéité structurale du matériau final. On a considéré ainsi intéressant d'évaluer le potentiel des pérovskites dans la décomposition directe du NO.

L'objectif général du projet est de déterminer la possibilité de développer un procédé catalytique permettant la décomposition directe du NO présent dans les effluents gazeux de combustion à l'aide de catalyseurs de type pérovskite.

Pour atteindre cet objectif on se propose de formuler et préparer des catalyseurs avec la structure pérovskite, en essayant le mieux possible de respecter les exigences pour un bon catalyseur de décomposition du NO. Par la suite on va évaluer, pour les meilleures compositions, leurs performances en présence d'oxygène et d'autres produits de combustion (CO₂, H₂O).

1.5 Méthodologie

Pour atteindre les objectifs fixés, la méthodologie suivante a été appliquée :

-Recherche bibliographique.

Périodiquement sont compilées et analysées les informations disponibles au sujet des mécanismes de formation et des sources de NO_x, des effets de NO_x sur l'environnement, des techniques pour réduire les émissions de NO_x, de la décomposition catalytique de NO_x.

-Formulation et préparation de catalyseurs.

La formulation de différentes compositions A_{1-x}A'_xB_{1-y}B'_yO_{3-δ} est basée sur les principales exigences pour un catalyseur de décomposition du NO, mais elle doit tenir compte de la contrainte que la structure de type pérovskite exige en ce qui concerne les

rayons ioniques pour les différents métaux constitutifs. Dans le site A/A' on utilise le lanthane (La) et le strontium (Sr), en essayant de garder un rapport La : Sr = 2 : 1 quand cela est possible. Dans le site B/B' on essaye plusieurs combinaisons Ni-Co, Mn-Ni, Cu-Fe, Al, Ti.

La méthode de préparation, qui a été développée au département de génie chimique de l'École Polytechnique par Dr. J. Kirchnerova et Prof. D. Klvana, est basée sur la cryodessiccation.

La structure de type pérovskite est confirmée par diffraction de rayons X. La surface spécifique de chaque catalyseur est déterminée à l'aide de la méthode BET (Brunauer, Emmett et Teller). Pour certaines compositions on utilise aussi la porosymétrie à mercure.

-Évaluation de l'activité catalytique.

L'activité catalytique est suivie par des analyses à l'aide de la chromatographie G-L et évaluée par calcul de la conversion du NO en N₂ pour chaque catalyseur testé. Le montage expérimental est décrit en ANNEXE 2.

-Détermination des modèles cinétiques

L'analyse des données est faite par régression linéaire multiple à l'aide du logiciel Excel (ANNEXE 4).

1.6 Structure de la thèse

Dans ce document (Chapitre I) on passe d'abord en revue la pollution atmosphérique due aux oxydes d'azote. On fait un bref rappel sur leurs formes, les mécanismes de formation et leur effet sur la santé et l'environnement (pluies acides et acidification des lacs et cours d'eau, dégénérescence de végétaux et mort de forêts, corrosion de

matériaux de constructions). Les méthodes de contrôle d'émissions de NO_x sont par la suite présentées. Une revue bibliographique sur les principaux systèmes catalytiques étudiés pour la décomposition directe du NO y est intégrée. Trois articles sont ensuite présentés.

Le premier article, Chapitre II, traite la décomposition catalytique du NO en absence de l'oxygène. On présente les critères de choix de catalyseurs, on analyse leurs performances et on propose un modèle cinétique qui reflète les données expérimentales.

Le second article, Chapitre III, présente l'étude cinétique de la décomposition du NO en présence de l'oxygène sur trois pérovskites sélectionnées suite aux premières expérimentations.

Le troisième article, Chapitre IV, se rapporte aux influences du CO_2 , H_2O , $\text{O}_2 + \text{H}_2\text{O}$ et CH_4 sur la décomposition du NO. L'étude a été toujours faite sur les trois pérovskites sélectionnées précédemment.

Étant donné qu'on a choisi comme forme de présentation des résultats celle des articles intégrés dans le corps de la thèse, une Discussion générale est introduite après le quatrième chapitre. Dans cette partie et dans les annexes on trouve des explications sur le choix des modèles, leur évaluation, ainsi que d'autres données complémentaires qui faciliteront la compréhension de la thèse. Une proposition de mécanisme de décomposition du NO en N_2 est également présentée dans la partie Discussion générale.

La partie Conclusion et Recommandation reprend les principales contributions de ce travail, ainsi que les suggestions pour de futures recherches.

CHAPITRE II
DIRECT DECOMPOSITION OF NITRIC OXIDE OVER PEROVSKITE-TYPE
CATALYSTS, PART I : ACTIVITY WHEN NO OXYGEN IS ADDED TO THE
FEED

Reference :

C. Tofan, D. Klvana* et J. Kirchnerova (2001) Direct Decomposition of Nitric Oxide over Perovskite-Type Catalysts, Part I : Activity when no Oxygen is Added to the Feed, *Applied Catalysis A : General* (in print).

Keywords :

Perovskite Catalysts; Catalytic Nitric Oxide Decomposition

* Author for correspondence, e-mail address : danilo.klvana@courriel.polymtl.ca

2.1 Contexte*

Ce chapitre présente sous forme d'un article la première partie de l'étude de la décomposition directe du NO sur des catalyseurs de type pérovskite $\text{La}_{1-x}\text{Sr}_x\text{M}_{1-y}\text{M}'_y\text{O}_{3-\delta}$. Des considérations sur les choix des compositions ainsi que des résultats préliminaires ont déjà été publiés (Klvana et al., 1999 b).

Les échantillons de catalyseurs utilisés ont été préparés par la méthode basée sur la technique de cryodessication. Cela a permis d'obtenir des pérovskites ayant une surface spécifique comprise entre 9 et 22 m^2/g . Les conditions réactionnelles utilisées lors de l'étude sont considérablement plus étendues par rapport à d'autres études : débits entre 10 et 200 mL/min , concentration du NO entre 1 et 10 %, températures entre 723 et 923 K. La réaction a lieu dans un réacteur à écoulement piston sur 1 g de catalyseur dilué avec de la pierre ponce. L'étude est réalisée en absence d'oxygène ajouté dans l'alimentation.

Les catalyseurs étudiés se sont révélés plus actifs que les pérovskites $\text{La}_{1-x}\text{Sr}_x\text{MO}_{3-\delta}$ évaluées antérieurement dans d'autres laboratoires, mais ils restent cependant moins actifs que les zéolithes Cu-ZSM-5 à 773 K. Cette étude a permis de tirer quelques conclusions intéressantes concernant la relation entre la composition et l'activité des pérovskites testées. La pérovskite $\text{La}_{0.8}\text{Sr}_{0.2}\text{Cu}_{0.15}\text{Fe}_{0.85}\text{O}_{3-\delta}$ est la plus active à base température; à haute température c'est la pérovskite $\text{La}_{0.87}\text{Sr}_{0.13}\text{Mn}_{0.2}\text{Ni}_{0.8}\text{O}_{3-\delta}$.

L'analyse des données cinétiques indique que la réaction est inhibée par l'oxygène et aussi par le NO. De plus elle met en évidence un changement du mécanisme réactionnel entre 823 et 870 K, dépendamment de la composition des pérovskites. Finalement l'analyse montre que l'oxygène peut jouer aussi un rôle de réactif. Dans ce cas, on

* ce texte n'est pas inclus dans l'article

suppose qu'il participe à la formation d'intermédiaires, probablement de type dimère, N_2O_3 ou N_2O_4 .

Une analyse cinétique complète fait l'objet du chapitre suivant.

2.2 Abstract

The direct decomposition of nitric oxide over several $\text{La}_{1-x}\text{Sr}_x\text{M}_{1-y}\text{M}'_y\text{O}_{3.6}$ ($\text{M} = \text{Co, Ni, Cu}$) perovskites, having specific surface area between 9 to 22 m^2/g , was studied at a steady state in a plug-flow reactor with 1 g catalyst and flowrates between 10 and 200 ml/min of 1 to 10 % NO in helium, at temperatures from 723 to 923 K. No oxygen was added to the feed. The studied perovskites exhibit an activity better than most of other metal oxides, including previously studied perovskites, but at 773 K are much less active than the best copper zeolites. Analysis of the collected data suggests inhibition by both nitric oxide and oxygen formed by decomposition and a change of kinetics at temperatures between 820 and 870 K, depending on the catalyst composition. Oxygen inhibition appears to be very strong at high temperatures (> 800 K), but comparatively weak at low temperatures. Several kinetic models were tested. For the low temperature range, for majority of the studied perovskites, the best fit was obtained with a model in which oxygen is an inhibitor, but also reactant. This suggests that some surface oxygen species plays a role of an active site. For higher temperature range (823 to 923 K) two limiting values of the apparent activation energies may be derived, with the difference of about 40 kJ/mol .

2.3 Introduction

Nitrogen oxides, mostly originating in high temperature combustion processes, have for years been recognized as serious pollutants. Their removal from all sources remains a great challenge, in spite of all progress made over the years [1]. Development of direct catalytic decomposition of nitric oxide to nitrogen and oxygen at mild temperatures in the presence of oxygen is the most desirable. Direct decomposition would in principle be the simplest, the most efficient and the least expensive solution to their abatement. With respect to its molecular elements, nitric oxide is at low temperature thermodynamically unstable [2]. However, its decomposition is not only extremely

slow, but it is, especially in the presence of oxygen, further complicated by a series of fast competing reactions producing toxic nitrogen dioxide, or nitrous oxide which is not toxic, but plays a role in ozone depletion.

Catalytic decomposition of nitric oxide has been studied for nearly a century. In the late sixties and early seventies this area of research was very intensive [3, 4] and dozens of materials were evaluated. Platinum and high surface area cobalt oxide (Co_3O_4) were found the most active, but still about three to four orders of magnitude less than required for practical use. Deemed impractical, direct catalytic decomposition gave way to the development of the three-way and selective reduction catalytic processes [1,5]. Nevertheless, the discovery of new materials initially considered as promising, in particular of copper exchanged zeolites [6-8] and of silver doped cobalt oxide [9,10] has revived the interest in this important reaction and other suitable materials were also searched from the family of perovskites [11-16]. Due to their relatively high catalytic activity, copper exchanged zeolites have been a focus of most of the recent work [5,17], but other materials including perovskites [18,19], supported noble metals [20,21], or several simple oxides previously shown impractical have received attention [22-24]. While some progress in the understanding of this elusive reaction has been made, no practical catalyst was found and it seems unlikely in a near future. However, because of their implications in other catalytic nitric oxide removal systems, studies of direct nitric oxide decomposition continue to be worthwhile.

Available data and information suggest that solid-state properties such as electron conductivity and oxygen mobility, as well as surface morphology influence the activity, but the relative importance of individual characteristics is not well understood. Due to their structure, which can accommodate a large number of ions and defects and thus permits a wide variety of physical and catalytic properties, perovskite-type oxides may serve as a model to evaluate the importance of individual factors.

The catalytic properties of perovskite-type oxides have been studied extensively [25,26]. Numerous transition metal based, oxygen nonstoichiometric perovskites ($\text{La}_{1-x}\text{Sr}_x\text{M}_{1-y}\text{M}'_y\text{O}_{3-\delta}$), which exhibit fast electron transfer, high oxygen mobility and facile oxygen desorption are also highly active in many oxygen-involving reactions [26-30]. In the early work on nitric oxide decomposition, mostly carried out at relatively high flowrates, the cobalt, and especially manganese-based perovskites were found inactive [31], in contrast to their high activities in carbon monoxide or hydrocarbon oxidation reactions. Later studies, at low flowrates, of other perovskite compositions indicated some improvement in activity, which was considered as promising [11-15]. Teraoka et al. [13] demonstrated that the performance of poorly active manganites could be enhanced by partial substitution with other transition metal ions, particularly with nickel. Yasuda et al. [14], showed that in a series of substituted $\text{La}_{2-x}\text{A}'_x\text{Cu}_{1-y}\text{B}'_y\text{O}_{4-\delta}$ cuprates the catalytic activity improved with increasing δ and that oxygen desorption, while inhibiting, is not the rate-determining step over these catalysts. Halasz et al. [16] evaluated highly sintered cuprates under conditions resembling those required for automotive exhaust pollution control (0.1 % NO and high space velocities) and found all of them inactive up to 973 K. They also concluded, contrary to other studies [13-15,18], that under their experimental conditions oxygen vacancies have no effect on the activity.

Our previous work has shown that nickel and cobalt based perovskites are excellent catalysts for a variety of oxygen involving reactions [29,30,32], and a new efficient method for their preparation was developed [33]. It was of interest to evaluate the activity of such materials also in the nitric oxide decomposition.

This first part of our study concerns the direct nitric oxide decomposition in the absence of oxygen added to the feed over several perovskites and covers a wide range of flowrates and temperatures. In an attempt to elucidate the importance of various physical properties in the reaction, eleven different $\text{La}_{1-x}\text{Sr}_x\text{M}_{1-y}\text{M}'_y\text{O}_{3-\delta}$ compositions containing cobalt, nickel or copper as the principal active component M were included.

In these compositions the strontium substitution x and the complementary metal M' were selected in a way to vary the nominal oxygen nonstoichiometry δ between 0 – 0.3. For the second part of this work on the NO decomposition, published separately and treating the effect of oxygen added to the feed on the activity and the overall kinetics, we have selected three representative perovskites.

2.4 Experimental

2.4.1 Catalyst preparation

Compositions of perovskite powders used in this study are indicated in Table 2.1. Except LSMN-46 sample, they were prepared by a new method, which is based on spray-freezing/freeze-drying of reactive precursor slurry [33,34]. This precursor slurry was obtained by suspending under vigorous stirring lanthanum hydroxide paste, prepared by wetting pure lanthanum oxide (Molycorp Inc.) with a solution of strontium nitrate, in a solution of metal nitrates. The components were mixed in required ratios. The least amount of water necessary to dissolve all nitrates and to give a fluid, but sufficiently stable for further processing, suspension was used. The suspension was quickly frozen by spraying or by direct pouring in liquid nitrogen. The frozen material was then separated from the nitrogen and dried under vacuum on a commercial freeze-drier (Labconco Lyph.Lock4.5). The dry precursor mixture was crushed, when needed, and calcined in air under controlled conditions, typically 12 h at 863 K followed 4 h at 923 K. Some of the samples were additionally aged 5 h at 973 K. Alumina or magnesia crucibles were used to hold the powders during calcination.

Table 2.1 Compositions and characteristics of perovskite catalysts studied in direct nitric oxide decomposition

COMPOSITION	I. D.	δ^*	SSA m ² /g
$\text{La}_{0.66}\text{Sr}_{0.34}\text{Ni}_{0.3}\text{Co}_{0.7}\text{O}_{3-\delta}$	LSNC	0.17	9.0
$\text{La}_{0.66}\text{Sr}_{0.34}\text{Ni}_{0.29}\text{Co}_{0.69}\text{Fe}_{0.02}\text{O}_{3-\delta}$	LSNCF	0.17	10.5
$\text{La}_{0.6}\text{Sr}_{0.34}\text{Ag}_{0.06}\text{Ni}_{0.4}\text{Co}_{0.6}\text{O}_{3-\delta}$	LSANC	0.23	10.0
$\text{La}_{0.4}\text{Sr}_{0.6}\text{Mn}_{0.4}\text{Ni}_{0.6}\text{O}_{3-\delta}$	LSMN-46	< 0.3	16.0
$\text{La}_{0.7}\text{Sr}_{0.3}\text{Mn}_{0.3}\text{Ni}_{0.7}\text{O}_{3-\delta}$	LSMN-37	0.15	9.8
$\text{La}_{0.87}\text{Sr}_{0.13}\text{Mn}_{0.2}\text{Ni}_{0.8}\text{O}_{3-\delta}$	LSMN-28	> 0.065	12.7
$\text{La}_{0.95}\text{Sr}_{0.05}\text{Mn}_{0.13}\text{Ni}_{0.87}\text{O}_{3-\delta}$	LSMN-19	> 0.025	10.5
$\text{La}_{0.8}\text{Sr}_{0.2}\text{Cu}_{0.15}\text{Fe}_{0.85}\text{O}_{3-\delta}$	LSCuF	< 0.175	10.1
$\text{La}_{0.8}\text{Sr}_{0.2}\text{Cu}_{0.15}\text{Al}_{0.85}\text{O}_{3-\delta}$	LSCuA	0.175	21.8
$\text{La}_{0.66}\text{Sr}_{0.34}\text{Ti}_{0.66}\text{Cu}_{0.34}\text{O}_{3-\delta}$	LSCuT	0.01	1.1
$\text{La}_2\text{CuO}_4/\text{CuO/LaFeO}_3$	LFCu	-	8.6

*: estimate based on Sr (and Cu when applicable) substitution

Generally, at least 20 g of powder was prepared in a single batch. No intermittent milling was used during the preparation. For the preparation of LSCuT sample anatase (commercial titanium dioxide with SSA = 10 m²/g) was used as a titanium precursor. In the case of LSCuF and LSCuA iron or aluminium hydroxide was first precipitated from nitrate solution by using ammonia solution and washed to remove soluble salts. The washed precipitate (hydroxide) was then mixed with other components and the resulting slurry processed as already described. Sample LSMN-46 was prepared by spray-freezing/freeze-drying 1 M (all metal) metal nitrates solution [30]. Before use all samples were lightly milled to obtain fine powder with particle size smaller than 10 μm .

2.4.2 Catalyst characterization

Formation of perovskite phase was confirmed by X-ray powder diffractometry (XRD) using a Philips X'Pert diffractometer with Cu-K_α radiation.

Specific surface area of each sample was determined on a Micromeritics Flow Sorb II 2300 apparatus by using a single-point BET method with a 30 % N₂/70 % He gas mixture as the adsorbate.

2.4.3 Catalytic activity determination

The nitric oxide decomposition was carried out in a stainless steel U-shape plug-flow reactor under a wide range of conditions: temperature between 723 and 923 K, nitric oxide concentration between 1.0 and 10.0 % in helium, catalyst weight 1.0 or 1.5 g, total flow rate 10 to 200 ml/min, contact time W/F_{NO} (0.25–4.9 g.s/μmol). Two certified mixtures of nitric oxide in helium were used, 2 and 10 %. Other concentrations were obtained by an on line dilution with helium. The reactor had 0.7 cm inner diameter, 10 ml reaction zone and 30 cm overall length. The catalyst powder (< 10 μm) was diluted by 7 ml of inert pumice particles 350–416 μm large, precalcined 12 h at 923 K. The catalyst diluent was used to provide a quasi-isothermicity of the reactor bed and to ensure good permeability. Two K-type thermocouples inserted in the reactor with the tips touching the catalytic bed at the inlet and outlet were used to monitor the temperature. The reactant gas flowrates were controlled with MKS and Brooks mass flow-meters. Before starting the measurement, the reactor was purged several hours at 773 K by pure helium to remove air and adsorbed impurities. FTIR spectrometer (Bomem Inc) was used to detect impurities. Catalytic activity was measured at temperatures between 723 and 923 K in steps of 50 degrees. The gas composition was analyzed before and after the reaction by an on line gas chromatography using 5 Å molecular sieve column kept at 373 K, with the carrier gas (helium) velocity of 30

ml/min. Due to the severe tailing of the nitric oxide peak only nitrogen was determined quantitatively. In parallel the presence of nitrous oxide was monitored by FTIR spectrometer. All experimental data were taken after at least 1 h on stream at each temperature when the catalytic reaction reached a steady state. Because of a possible gas phase reaction between remaining nitric oxide and produced oxygen, catalytic performance was evaluated in terms of the conversion of nitric oxide to nitrogen: $x (\%) = 100 \cdot 2 \cdot [N_2]_{out} / [NO]_{in}$.

2.5 Results

2.5.1 Catalyst design, preparation and characteristics

The composition and some physical characteristics of the eleven catalysts evaluated in this study and represented by a formula $La_{1-x}Sr_xM_{1-y-z}M'yM''zO_{3-\delta}$ are given in Table 2.1. In these compositions, cobalt, nickel or copper were considered as the principal source of active sites and the complementary M ions (M' and M'') were selected in a way to assure a good stability of the perovskite structure to at least 1000 K. In this respect, the substitution of strontium (x), which to a large degree controls the nominal oxygen nonstoichiometry, has been taken into account.

In most cases, nearly pure perovskite phase was obtained by low temperature calcination indicated in the previous section. Figure 2.1 shows the XRD patterns of three perovskites. The position of the main peaks illustrates the wide range of the crystal unit size. For example, for LSCuA and LSCuF the pseudocubic a parameter was 0.3805 nm and 0.3897 nm respectively. At the mentioned relatively low calcination temperatures, SSA between 9 and 22 m²/g was typically obtained. Pure perovskite phase was obtained also in the case of LSCuT, having the largest $a = 0.3915$ nm, but only after calcination 12 h at 1248 K. Consequently, the SSA of this sample was only 1.1 m²/g. In contrast, the nominal composition corresponding to a targeted $LaFe_{0.34}Cu_{0.66}O_{3-\delta}$ ($\delta < 0.33$)

perovskite, sample LFCu, resulted in a three-component (phase) mixture of La_2CuO_4 , LaFeO_3 , and CuO . Evidently, the proportion of copper in this composition is much too high for the formation of a stable perovskite phase, although the tolerance factor based on the available ionic radius data is about 0.89, i.e. still in the range of generally accepted limit. The main reason is apparently the inability of the system to accommodate such a large number of oxygen vacancies; only a small fraction of copper and iron ions may assume valence higher than two and three respectively. Attempt to substitute silver for lanthanum into the perovskite structure at the level of six atomic percent was not fully successful. Part of this element precipitated as a metal.

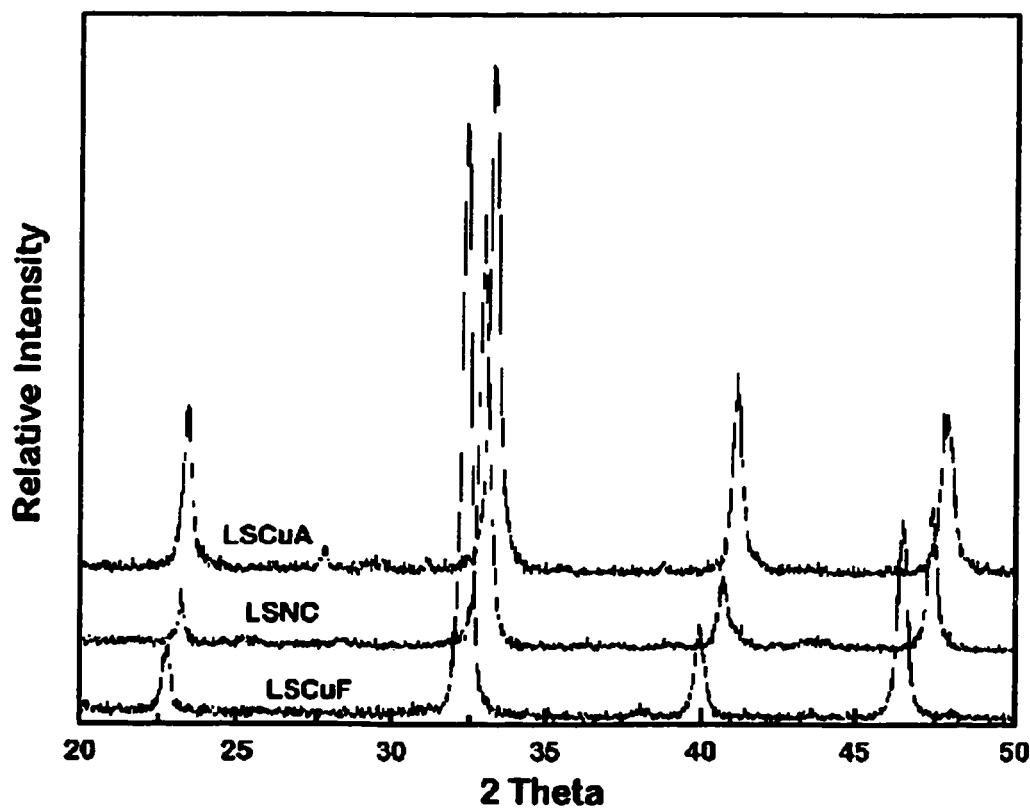


Figure 2.1 XRD patterns of three selected perovskite compositions

Electrical conductivity (ionic and electronic) of the samples was not measured in this work. However, it is well known that in $\text{ABO}_{3-\delta}$ perovskites, oxygen ion conductivity increases with the oxygen nonstoichiometry δ , which can to a large degree be controlled by A-site substitution, x , by divalent cation (Sr^{2+}) [35]. Thus, LSCuT and LFCu are expected to be poor O^{2-} conductors. On the other hand, electronic conductivity of perovskite oxides depends primarily on the B-site cation and is generally much higher than that of the corresponding transition metal oxides, increasing in the order $\text{Ti} \ll \text{Cr} < \text{Fe} < \text{Mn} < \text{Cu} < \text{Co-Ni}$ [36]. Thus, in our series of catalysts, LSCuA can be considered as the least conducting, because of its low concentration of a B-site transition metal (Cu), followed by LSCuT. On the other hand, LSNC has been shown previously as the best conductor in a group of several perovskite compositions, which included LSMN-46 and LSNCF [30].

2.5.2 Catalytic performance

2.5.2.1 Empty reactor and catalyst diluent (pumice)

No measurable conversion to nitrogen was observed in an empty reactor up to the highest temperature (923 K) with 50 ml/min of 5% NO in helium. In the reactor filled with 10 ml (7.5 g) of pumice particles having SSA of $4.6 \text{ m}^2/\text{g}$, again no measurable conversion was observed up to 923 K when using high flowrates, but with 15 ml/min, weak catalytic activity was detected. Specifically, for 5 % nitric oxide in helium, conversions varied from 1.3 % at 773 K to 1.5 % at 923 K, whereas for 2 % NO conversions between 5.9 % at 773 K and 7.4 % at 923 K were observed. At 50 ml/min of 2 % NO conversions between 0.5 to 0.7 % were detected. Therefore for use as a diluent of the catalyst, the volume of pumice was reduced to 7 ml, the amount needed for a uniform dispersion of the catalyst powder. Appropriate corrections for the weak activity of pumice were made when needed.

2.5.2.2 Activity of perovskite compositions

All materials, except LSCuT, showed measurable catalytic activity (conversion) starting at 723 K, even at flowrates 100 ml/min of 5% NO, and the activity increased monotonically with increasing temperature. For the case of 5% NO flowing at 50 ml/min the conversion data are presented in Figures 2.2 and 2.3.

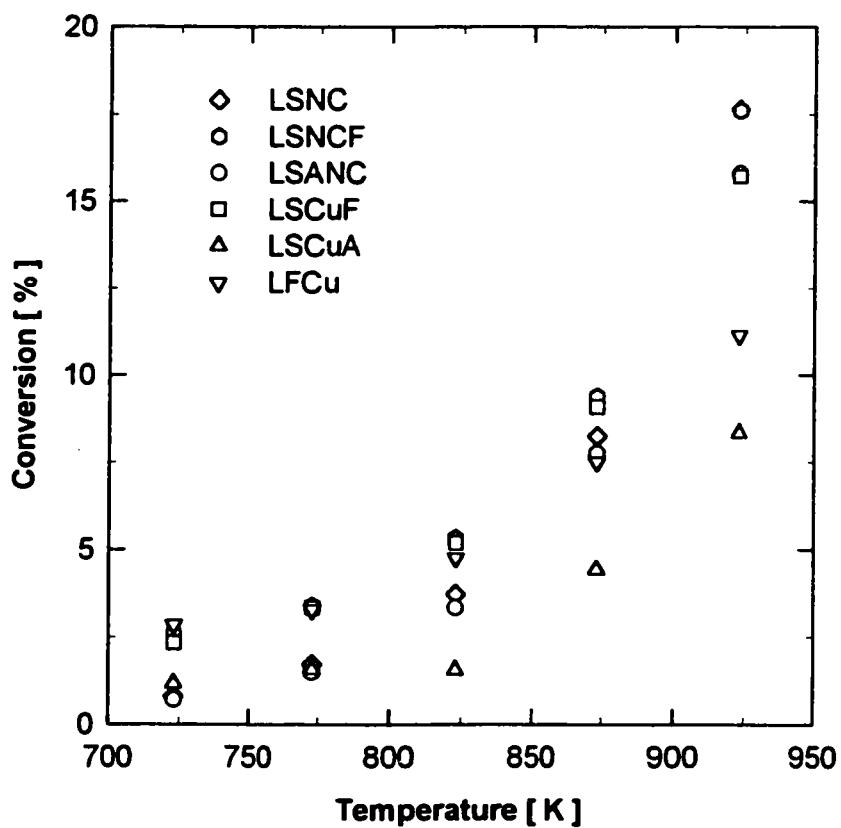


Figure 2.2 Conversion of nitric oxide to nitrogen over some new perovskite catalysts; 1 g catalyst, 50 ml/min total flowrate, 5 % nitric oxide in helium.

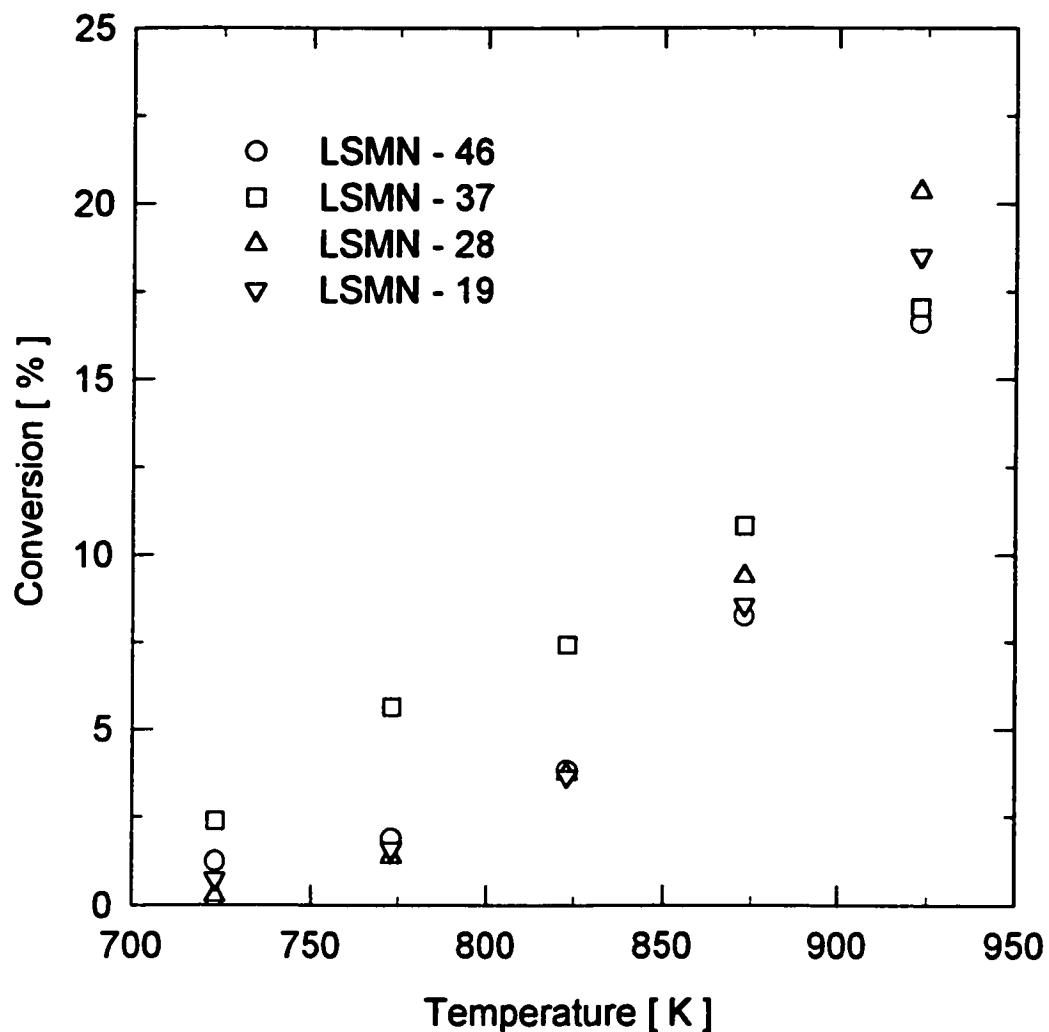


Figure 2.3 Conversion of nitric oxide to nitrogen over different nickel – manganese (LSMN) perovskite catalysts; 1 g catalyst, 50 ml/min total flowrate, 5 % nitric oxide in helium.

For other conditions, conversions at 773 K and 923 K selected as the most representative are presented in Table 2.2.

Table 2.2 Selected activity data for nitric oxide decomposition over several perovskite catalysts

Catalyst	X ₇₇₃ %	X ₉₂₃ %	k ₁₋₇₇₃ μmol/g s bar	k ₁₋₉₂₃ μmol/g s bar
$F_{\text{tot}} = 100 \text{ ml/min, 5 \% NO (W/F}_{\text{NO}} = 0.27 \text{ g s /μmol)}$				
LSNC	0.9	12.3	0.7	10.0
LSNCF	0.7	10.4	0.6	9.1
LSANC	0.8	11.4	0.6	8.9
LSMN-46	0.9	11.7	0.7	9.4
LSMN-37	1.4	8.0	1.0	6.5
LSMN-28	0.8	14.3	0.6	11.4
LSMN-19	1.0	12.7	0.8	10.3
LSCuF	1.9	10.9	1.4	8.6
LSCuA	0.7	5.0	0.5	4.0
LSCuT	0.1	0.3	0.1	0.2
LFCu	0.9	5.9	0.7	4.6
$F_{\text{tot}} = 75 \text{ ml/min, 2 \% NO (W/F}_{\text{NO}} = 0.92 \text{ g s /μmol)}$				
LSNC	2.0	12.6	1.1	7.4
LSANC	0.8	13.6	0.4	7.8
LSMN-46	1.7	14.4	0.9	8.6
LSMN-28	1.1	17.0	0.6	10.1
LSMN-19	0.8	14.5	0.4	8.7
LSCuF	3.6	13.6	1.9	7.9
LSCuA	1.4	6.5	0.8	3.8
LSCuT	0.9	1.2	0.5	0.6
$F_{\text{tot}} = 15 \text{ ml/min, 2 \% NO (W/F}_{\text{NO}} = 4.84 \text{ g s /μmol)}$				
LSNC	13.1	38.6	1.4	5.1
LSANC	7.4	36.2	0.8	4.6
LSMN-46	15.6	44.8	1.7	6.2
LSMN-28	5.4	38.9	0.6	5.1
LSMN-19	8.7	35.3	0.9	4.5
LSCuF	24.2	45.8	2.9	6.4
LSCuA	17.2	27.8	2.0	3.4
LSCuT	17.3	17.6	1.9	2.0

With all materials the experiments were carried out over several days, overnight the catalyst being left to cool to ambient temperature under a flow of helium. Over the period of actual experiments lasting at least 30 h no diminution of activity of any of the catalysts was observed. Over none of the catalysts significant quantity of nitrous oxide in the effluent gases was observed. Typically, at higher conversions the detected amount of nitrous oxide (N_2O) barely exceeded few ppm present as impurity in nitric oxide, i.e. selectivity to nitrous oxide less than 1 %.

Oxygen as a product of NO decomposition was detected in the effluents over all catalysts, except LSCuA and LSCuT, when the conversion of nitric oxide to nitrogen reached about 5 %, in spite of its possible gas phase reaction with the unreacted nitric oxide. The detected amount of oxygen increased steadily with conversion. Over LSCuA, presence of oxygen was detected only in the case of low flowrate and above 873 K, when the conversion reached about 20 %. Over LSCuT, no oxygen was detected at any condition, the highest conversion reached being 17.6 %.

2.5.2.3 Kinetic analysis of conversion data

To make sure that the observed conversion data were not influenced by mass or heat transfer, the potential effects of the external and internal mass and heat transport were evaluated mathematically by using Mears and Wiez-Prater criteria [37]. As expected, the slow reaction, accompanied by only a weak thermal change, was found free of diffusion control at all experimental conditions.

Due to their integral mode, the collected conversion data were first analysed in terms of deviations from the simple first order model. The integrated apparent pseudo-first order kinetic constants for 773 and 923 K, k_{1-773} and k_{1-923} respectively, are collected in Table 2.2. Complete sets of these kinetic constants (k_1) are shown as Arrhenius plots in

Figures 2.4-2.6 for LSMN-28, LSNC and LSCuF respectively. Similarly complex plots were obtained for the remaining catalysts.

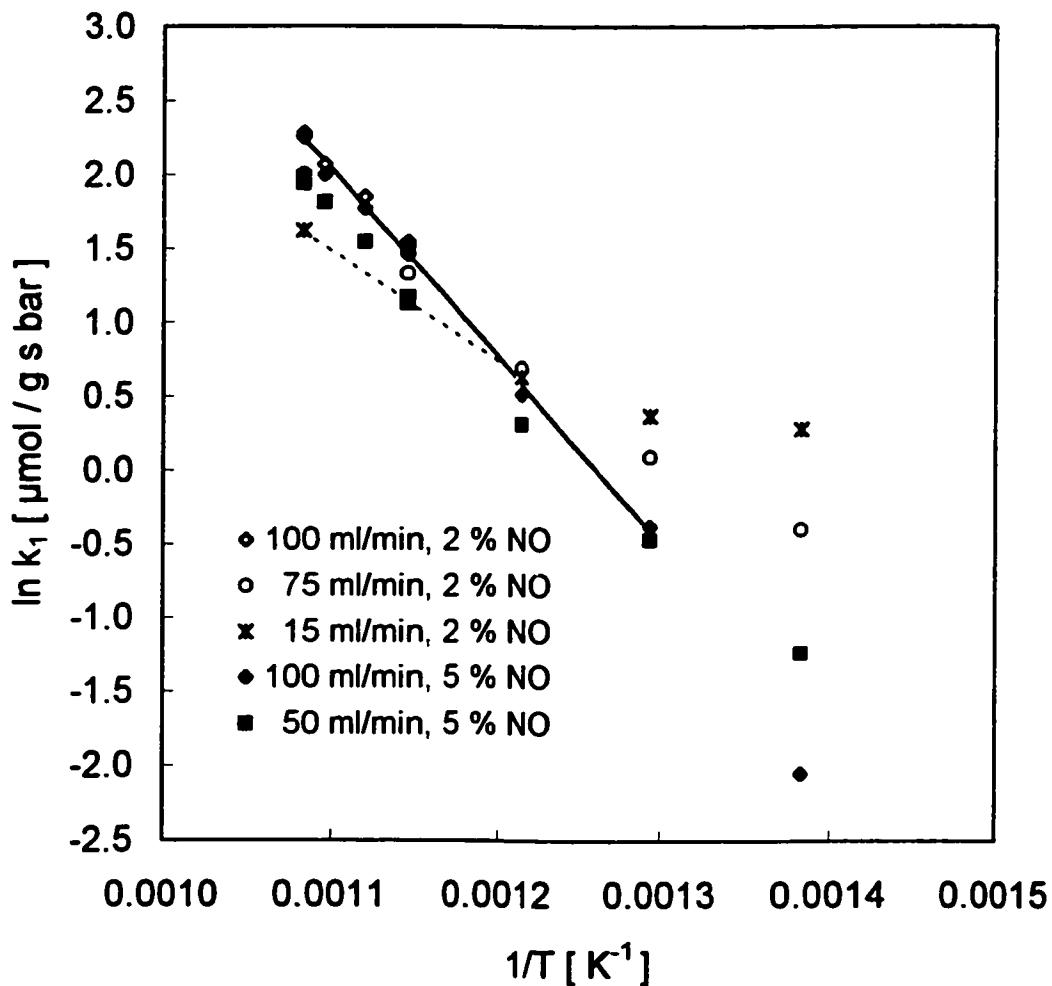


Figure 2.4: Arrhenius plots for integrated pseudo-first order kinetic parameters derived from conversions at different conditions for 1 g of LSNC catalyst.

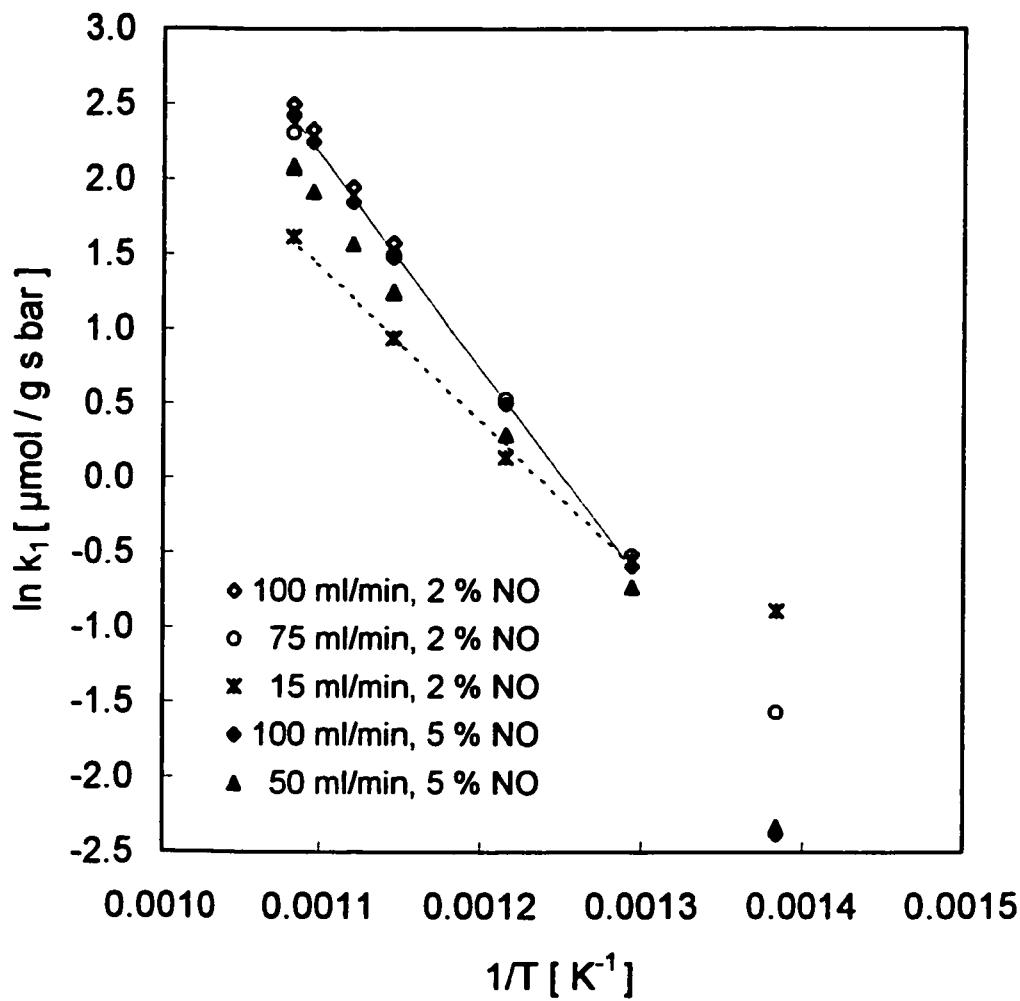


Figure 2.5 Arrhenius plots for integrated pseudo-first order kinetic parameters derived from conversions at different conditions for 1 g of LSMN-28 catalyst.

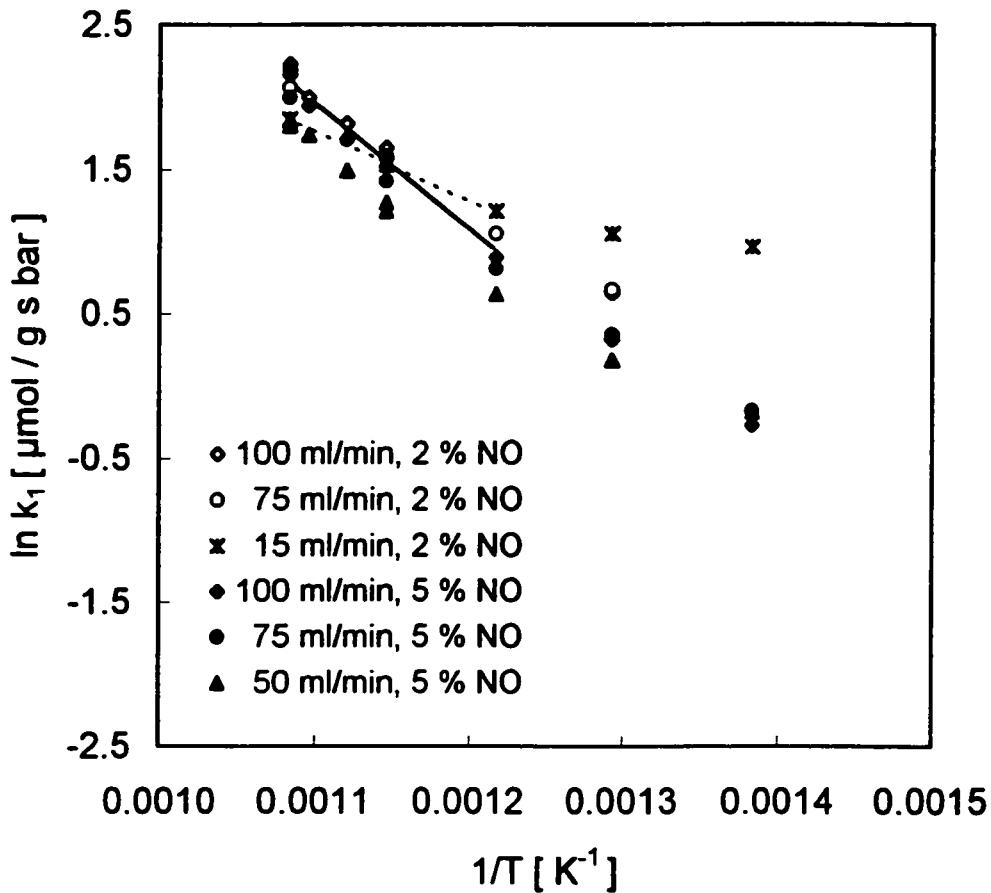


Figure 2.6 Arrhenius plots for integrated pseudo-first order kinetic parameters derived from conversions at different conditions for 1 g of LSCuF catalyst.

As evident, the first order model is by far inadequate. For each individual catalyst the deviations from the first order model at a given temperature depend on flowrate and NO concentration. We can draw attention to several important aspects. First, the dependence on the reciprocal temperature of the apparent activities ($\ln k_1$) is not linear

over the whole range and this dependence on temperature varies with experimental conditions. In addition, the temperature at which the change (of kinetics) occurs depends also on the catalyst. For example, in the low temperature region (723 to about 823 K) the highest k_1 values were calculated from data obtained at low flowrate. In contrast, at high temperatures (from about 823 K) the k_1 calculated from data at low flowrates, are, in most cases, significantly lower than those derived from conversions at high flowrates. Knowing that on most materials oxygen has a strong inhibiting effect [4,8,27,38], the dependence of k_1 on flowrate observed at high temperatures suggests a strong inhibition by generated oxygen. This is also reflected in the apparent activation energies, E_{app} , derived for the two limiting cases and collected in Table 2.3. Furthermore, higher values of apparent k_1 parameter obtained from conversion data for lower nitric oxide concentration (2 %) as compared to those for higher concentration (5 %) suggest inhibition by nitric oxide, which in some cases, for example LSCuF, seems stronger than that of oxygen. On the other hand, the dependence on flowrate of low temperature k_1 indicates that in this temperature range the effect of oxygen on the NO decomposition is different from that at high temperatures.

Exception to the described behavior was LSCuT perovskite. Its activity was extremely dependent on flowrate, but relatively independent of temperature. At high flowrates (100 ml/min) the activity was more than ten times lower than that of other perovskites, but it was comparable at low flowrate (15 ml/min).

Table 2.3 Apparent kinetic parameters of the pseudo-first order rate model for nitric oxide decomposition over several perovskite catalysts

CATALYST	E_{app}^a kJ/mol	E_{app}^b kJ/mol	k_{I-723}^c μmol/g s bar	k_{I-923}^d μmol/g s bar	k_{I-723}^c μmol/m ² s bar	k_{I-923}^d μmol/m ² s bar
LSNC	60	105	1.32	9.8	0.15	1.10
LSNCF	55 ^e	108	2.25 ^e	9.1	0.21	0.87
LSANC	79	109	0.68	8.9	0.07	0.89
LSMN-46	65	108	1.50	9.4	0.09	0.59
LSMN-37	45 ^f	87	2.36 ^f	6.5	0.24	0.66
LSMN-28	94	119	0.41	11.3	0.03	0.89
LSMN-19	65	103	0.79	10.3	0.08	0.98
LSCuF	40	75	2.61	8.8	0.26	0.87
LSCuA	28	82	1.93	4.0	0.09	0.19
LSCuT	0.6	40	1.95	0.2	1.77	0.18
LFCu	56 ^g	76	1.00 ^g	4.6	0.12	0.53

^a : apparent activation energy derived by regression from high temperature k_I values (dashed line in Fig.2.4-2.6) obtained from conversion data for 15 ml/min, 2 % NO, 1g catalyst

^b : apparent activation energy derived by regression from high temperature k_I values (full line in Fig.2.4-2.6) obtained from conversion data for 100 ml/min, 5 % NO, 1g catalyst,

^c : the highest apparent first order kinetic parameter at 723 K (from data for 15 ml/min, 2 % NO, 1 g catalyst)

^d : the highest apparent first order kinetic parameter at 923 K (from data for 100 ml/min, 5 % NO, 1g catalyst)

^e : for 5 % NO, 50 ml/min, 1.5 g catalyst

^f : for 5 % NO, 30 ml/min, 1 g catalyst

^g : for 5 % NO, 50 ml/min, 1 g catalyst

2.5.2.4 Kinetic model

To rationalize the diversity of the experimental data, attempt was made to deduce kinetic model(s) that would take the observed effects of flowrate and NO concentration (as well as generated oxygen) into account. This was done by fitting at each individual temperature the collected experimental conversion data by linear regression analysis to integrated forms of several kinetic equations. In these equations the P_{O_2} , which depends on experimental conditions, was assumed to correspond to P_{N_2} produced by NO

decomposition ($P_{O_2} = P_{NO}^m / (1 + K_{O_2} P_{O_2}^m)$). The tested models (see Table 2.4) included all Langmuir-Hinshelwood type models (II and III) previously proposed for other catalytic systems [4,8,22,23,38,39]:

$$r = k_{NO} P_{NO} / (1 + K_{O_2} P_{O_2}^m), \quad m = \frac{1}{2}, 1 \quad \text{II}$$

$$r = k_{NO} P_{NO}^n / (1 + K_{NO} P_{NO}^n + K_{O_2} P_{O_2}^m), \quad n = 1, 2; m = \frac{1}{2}, 1, 2 \quad \text{III}$$

or for perovskites [40] :

$$r = k_{NO} P_{NO}^2 / (K_{NO} P_{NO} + K_{O_2} P_{O_2}) \quad \text{III.5}$$

For low temperature data, most of the models II or III failed to provide a satisfactory fit. Majority of them produced negative parameters. Model III.5 resulted in some improvement in most cases, but the fit was the best only for LSANC, LSMN-37 and LSMN-19.

Several new empirical models, in which the produced oxygen is considered both reactant and inhibitor, were therefore also tested (type IV):

$$r = k_{NO} P_{NO}^n P_{O_2}^m / (k_I P_{NO}^n + k_{II} P_{O_2}^m), \quad n = 1, 2; m = \frac{1}{2}, 1, 2 \quad \text{IV}$$

Model IV with $n = 1$ and $m = 1/2$ provided the best fit for the remaining seven catalysts.

At high temperatures, it was again models IV that provided a very good fit for most of the catalysts, but with higher exponents (order) of P_{O_2} . Nevertheless, models II, particularly that with $m = 1$, fitted the data also reasonably well, with the exception of LSMN-28 and of LSCuT. Actually, this latter model, previously proposed for several oxides and platinum [38,39], provided the best fit for LSANC, LSMN-37, and LSCuF.

Table 2.4 Results of the search for the best fitting kinetic model (773 K and 923 K)

Catalyst	$k_{NO}P_{NO}/(1+k_{O_2}P_{O_2}^m)$	Rate model, $r =$												
		$n=1$	$n=2$	$n=1$	$n=2$	$n=1$	$n=2$	$n=1$	$n=2$	$n=1$	$n=2$			
1	$m=\frac{1}{2}$ II.1	$m=1$ II.2	$m=\frac{1}{2}$ III.1	$m=1$ III.2	$m=\frac{1}{2}$ III.3	$m=1$ III.4	$m=\frac{1}{2}$ III.5*	$m=1$ III.6	$m=\frac{1}{2}$ IV.1	$m=1$ IV.2	$m=\frac{1}{2}$ IV.3	$m=1$ IV.4	$m=\frac{1}{2}$ IV.5	$m=1$ IV.6
$T = 773 \text{ K}$														
LSNC	+	++	-	++	-	-	-	-	++	-	++	-	-	
LSNCF	+	++	-	++	-	-	-	-	++	-	++	-	-	
LSANC	+	++	-	++	-	-	-	-	++	-	++	-	-	
LSMN-46	+	++	-	++	-	-	-	-	++	-	++	-	-	
LSMN-37	+	++	-	++	-	-	-	-	++	-	++	-	-	
LSMN-28	+	++	-	++	-	-	-	-	++	-	++	-	-	
LSMN-19	+	++	-	++	-	-	-	-	++	-	++	-	-	
LSCuF	+	++	-	++	-	-	-	-	++	-	++	-	-	
LSCuA														
LSCuT														
LFCu														
$T = 923 \text{ K}$														
LSNC	+	++	-	++	-	-	-	-	++	-	++	-	-	
LSNCF	+	++	-	++	-	-	-	-	++	-	++	-	-	
LSANC	+	++	-	++	-	-	-	-	++	-	++	-	-	
LSMN-46	+	++	-	++	-	-	-	-	++	-	++	-	-	
LSMN-37	+	++	-	++	-	-	-	-	++	-	++	-	-	
LSMN-28	+	++	-	++	-	-	-	-	++	-	++	-	-	
LSMN-19	+	++	-	++	-	-	-	-	++	-	++	-	-	
LSCuF	+	++	-	++	-	-	-	-	++	-	++	-	-	
LSCuA														
LSCuT														
LFCu														

* $K_{NO}P_{NO} + K_{O_2}P_{O_2} \gg 1$; + reasonable fit; ++ poor fit; +++ excellent fit; - one of the parameters negative

2.6 Discussion

The results of this study, covering much wider range of experimental conditions, in particular flowrates, than any other reported in literature, highlight the complexity of surface reactions involved in the catalytic decomposition of nitric oxide. By their range and variation, they help to understand the diverse and often contradictory literature results and conclusions based upon them.

Globally, the obtained upper limit values of E_{app} (Table 2.3), which may be considered as approaching those free of inhibition effect, seem to correlate well with the available literature data for perovskite compounds and for other transition metal oxides [4, 23]. For example, for Co_3O_4 apparent activation energy between 94 kJ/mol [39] and 118 kJ/mol [4, 23] has been reported. Winter had obtained 109, 67, and 38 kJ/mol for NiO , Fe_2O_3 and CuO respectively [38]. Yet, it is interesting that the copper containing perovskites of higher activity exhibit activation energies lower than those reported found for Cu-ZSM5 [8] or for $\text{La}_{1.5}\text{Sr}_{0.5}\text{CuO}_{4.8}$ [14].

Although it is customary to compare the activities in terms of rates, in this work use of pseudo-first order kinetic constants was more convenient. Based on available conversion or rate data [4,8,10,12,22], typically for 2 or 4 % nitric oxide, the values of calculated pseudo-first order kinetic constants for the known active catalysts range at 773 K from 0.5 $\mu\text{mol/g}\cdot\text{s}\cdot\text{bar}$ for copper monoxide to 300 $\mu\text{mol/g}\cdot\text{s}\cdot\text{bar}$ for copper exchanged ZSM-5 zeolites, with values of 2 $\mu\text{mol/g}\cdot\text{s}\cdot\text{bar}$ for Co_3O_4 and 0.5 %Pt/ Al_2O_3 and 14 $\mu\text{mol/g}\cdot\text{s}\cdot\text{bar}$ for Ag/ Co_3O_4 . Activities of other simple transition metal oxides (Mn_2O_3 , NiO , Fe_2O_3) are lower than that of CuO and compare to that of La_2O_3 [23]. In the case of perovskites, the available activity data at 773 K (conversion obtained for 0.5 g, 3 % NO and 30 ml/min) are limited to $\text{YBa}_2\text{Cu}_3\text{O}_{7-\delta}$ / MgO and to $\text{La}_{0.85}\text{Sr}_{0.15}\text{CoO}_3$ [12,27], giving 1 and 0.7 $\mu\text{mol/g}\cdot\text{s}\cdot\text{bar}$ respectively, which compares well with the data

of this study (k_{1-773} in Table 2.2). In fact, some of the new compositions, in particular LSCuF and LSMN-37, show significantly better activity. For all other perovskites the literature activity data are available only for higher temperatures, typically between 973 and 1073 K, and for low flowrates. For example, Teraoka et al., [13, 40] obtained conversions between 47 % and 3 % for $\text{La}_{0.8}\text{Sr}_{0.2}\text{Co}_{0.8}\text{Fe}_{0.2}\text{O}_3$ and $\text{La}_{0.8}\text{Sr}_{0.2}\text{Co}_{0.8}\text{Cr}_{0.2}\text{O}_3$ respectively when using 1 g catalyst and 15 ml/min, 1 % NO. Clearly, the activities of the present materials are superior, probably approaching that of platinum and of Co_3O_4 . Although at 773 K the activities of the perovskites are rather low in comparison with $\text{Ag}/\text{Co}_3\text{O}_4$, and especially in comparison with Cu-ZSM-5, at 923 K, the difference is less important. In fact, at the higher temperatures the perovskites of this study are possibly more active than $\text{Ag}/\text{Co}_3\text{O}_4$. Most importantly, perovskites are far more active than their individual oxide components having similar SSA. This must be due to their structure characterized by octahedral metal ion coordination with oxygen and determining, depending on the composition, other important physical characteristics such as higher electronic and ion (O^{2-}) conductivity.

With respect to composition, the catalysts of this study may be divided in three groups: first consisting of perovskites containing cobalt, second regrouping the perovskites based on nickel and manganese, and third assembling the copper containing materials. Within the group of cobalt containing perovskites relatively little effect of doping (substitution by a minor amount) with iron or silver is observed, but there is some indication that the overall performance of LSNCF is slightly improved, similarly as was previously found in the case of methane combustion [30, 32]. The group of the four nickel-manganese perovskites exhibits activities that are very similar to those of nickel-cobalt perovskites, but subtle variations with composition are observed. For example, LSMN-37 is measurably more active at low temperatures, whereas at high temperatures, it is the least active of the group. In contrast, LSMN-28 composition is actually the least active at low temperatures, but the most active at high temperatures. However, there appears no direct clear-cut correlation between these observed activities and the Sr

and/or Mn substitution, or the nominal degree of nonstoichiometry δ . The group of copper containing materials covers the widest range of different physical, physico-chemical and even structural properties such as SSA (ranging from 22 to $1.1\text{ m}^2/\text{g}$), electronic and oxygen ion conductivity and crystal unit size. Interestingly, this group includes the overall best performing composition (LSCuF) as well as the two least performing compositions (LSCuT and LSCuA). In general, these copper containing compositions exhibit relatively high activity at low temperatures, but rather poor activity at high temperatures. Activity of these, copper containing, perovskites is also characterized by lower apparent activation energies (Table 2.3). By comparing the activities and the physical properties such as SSA, crystal size, and possibly electronic and ionic conductivity of the individual compositions of this group, we may assume that electronic conductivity plays an important, although not necessarily predominant, role in enhancing the activity, particularly at high temperatures. As already explained, LSCuT and LSCuA presumably exhibit significantly lower electronic conductivity than LSCuF and LFCu or the other compositions of this study and are the two least performing perovskites. On the other hand, oxygen nonstoichiometry δ has evidently much less effect. Halasz et al. [16] concluded also that for a series of highly sintered copper containing oxides δ had little effect on the activity under high flow-rates. SSA appears to play a less important role than generally assumed, particularly when its values exceed approximately $10\text{ m}^2/\text{g}$. Most likely, in this particular case the number of specific active sites is not necessarily increasing linearly with SSA. However, some critical value well above $1\text{ m}^2/\text{g}$ at which sufficiently large number of active sites is created is certainly needed. Similar situation was also observed in the case of catalytic combustion [30, 33]. The behavior of LSCuT as the NO decomposition catalyst is the most interesting. In spite of its comparatively poor performance at high flowrates over the whole temperature range, at low flowrates and low temperatures, LSCuT actually exhibited an activity that was among the better ones of this work. Furthermore, the fact that no oxygen was detected over this catalyst, even at conditions of high conversions under

which large quantities of oxygen were detected over the other materials (except LSCuA), suggests that the nitric oxide decomposition over this catalyst actually involves the disproportionation, i.e. formation of N₂ and NO₂.

While the suggestion that oxygen could to some degree play a role of a reactant may appear controversial, such possibility could be explained in terms of the formation of an intermediate involving some specific surface bound oxygen. Formation of oxygen involving intermediate has already been proposed for the case of Cu-ZSM5 zeolites [41] and was also documented by Raman spectroscopy for barium oxide [42]. In fact, it is surprising that such a possibility has not yet been discussed more widely, although it is generally accepted in the case of selective nitric oxide reduction [43].

2.7 Summary and conclusions

This study, extending over a wide range of flowrates and temperatures, illustrates the complexity of surface reactions involved in the catalytic decomposition of nitric oxide. Indirectly, it provides an understanding to the results appearing in literature, which are often contradictory. Although the activities in this reaction of the new perovskites fall short of demands for practical applications, they are substantially higher than those of the individual component oxides, suggesting that the perovskite structure favors to some degree the reaction. Nevertheless, the activity depends on the composition and its corresponding physical and chemical characteristics. Both electronic and oxygen ion conductivity play some role in the activity of the perovskite catalysts. Cations which can be oxidized to higher but unstable oxidation state particularly copper, nickel and possibly cobalt are likely to serve as a source of active sites for nitric oxide adsorption which can take place via a specific surface oxygen species. Structural aspects of the catalyst surface seem to play the crucial role.

While very important, high specific surface area is not the key factor in determining the activity. It is the actual number of sites favoring fast decomposition that is required, but not necessarily present on materials having large SSA. In spite of moderate specific surface areas several of the new perovskite compositions exhibit activities up to an order of magnitude higher than corresponding high specific surface areas single transition metal oxides.

Kinetic analysis suggests that depending on temperature, the decomposition of nitric oxide follows at least two different reaction mechanisms. In addition, the results provide some evidence about the possible dual role of oxygen in the mechanism:

- it acts, at limited concentrations maintaining specific surface species, as a reactant, probably by participating in the continuous formation of an intermediate, possibly dimmer species [N₂O₄ or even N₂O₃]
- it acts as an inhibitor by blocking the renewal of appropriate active sites. This could in part be by oxidizing a specific –NO₂ species to nitrite or nitrate desorbing as NO or NO₂.

Nevertheless, at low temperatures the implication of oxygen in the NO decomposition differs significantly from that at high temperatures.

2.8 Acknowledgments

This work has mainly been supported by Natural Sciences and Engineering Research Council of Canada.

2.9 References

- [1] V.I. Pârvulescu, P. Grange, B. Delmon, *Catal. Today*, 46 (1998) 233.
- [2] O. Kubaschewski, C.B. Alcock, P.J. Spencer, "Materials Thermochemistry", 6th Ed., Pergamon Press, Oxford, 1993.
- [3] M. Shelef, K. Otto, H. Gandhi, *Atmos. Environ.*, 3(2) (1969) 107.
- [4] J. W. Hightower, D. A. van Leirsburg, in "The Catalytic Chemistry of Nitrogen Oxides", R. L. Klimisch and J. G. Larson, Eds., Plenum Press, New York, 1975, p.63.
- [5] M. Shelef, *Chem. Rev.*, 95 (1995) 209.
- [6] M. Iwamoto, S. Yokoo, K. Sakai, S. Kagawa, *J. Chem. Soc. Faraday Trans. I*, 77 (1981) 1629.
- [7] M. Iwamoto, *Stud. Surf. Sci. Catal.*, (Chem. Microporous Cryst.), 60 (1991) 327.
- [8] Y. Li, W. K. Hall, *J. Catal.*, 129 (1991) 202.
- [9] H. Hamada, Y. Kintaichi, M. Sasaki, T. Ito, *Chem. Lett.*, 7 (1990) 1069.
- [10] M. Iwamoto, H. Hamada, *Catal. Today*, 10(1) (1991) 57.
- [11] K. Tabata, *J. Mater. Sci. Lett.*, 7(2) (1988) 147.
- [12] H. Shimada, S. Miyama, H. Kuroda, *Chem. Lett.*, (1988) 1797.
- [13] T. Teraoka, H. Fukuda, S. Kagawa, *Chem. Lett.*, (1990) 1.
- [14] H. Yasuda, N. Mizuno, M. Misono, *J. Chem. Soc., Chem. Commun.*, (1990) 1094.
- [15] K. Ladavos, P. J. Pomonis, *J. Chem. Soc., Faraday Trans.*, 87(19) (1991) 3291.
- [16] I. Halasz, A. Brenner, M. Shelef, K.Y.S. Ng, *Catal. Lett.*, 11(3-6) (1991) 327.
- [17] A. T. Bell, *Catal. Today*, 38 (1997) 151.
- [18] Zhao, Z., Yang, X., and Wu, Y., *Appl. Catal., B: Environmental*, 8(3) (1996) 281.
- [19] R. Bontchev, K. Cheshkova, D. Mehandjiev, J. Darriet, *React. Kinet. Catal. Lett.*, 63(1) (1996) 121.
- [20] A. Ogata, A. Obuchi, K. Mizuno, A. Ohi, H. Ohucki, *J. Catal.*, 144(2) (1993) 452.
- [21] S. S. C. Chuang, C-D. Tan, *J. Phys. Chem., B*, 101(15) (1997) 3000.
- [22] X. Zhang, A. B. Walters, M. A. Vannice, *J. Catal.*, 155 (1995) 290.

- [23] T. Yamashita, M. A. Vannice, A., *J. Catal.*, 163 (1996) 158.
- [24] S. Xie, G. Mestl, M. P. Rosynek, J. H. Lunsford, *J. Am. Chem. Soc.*, 119 (1997) 10186.
- [25] R. J. H. Voorhoeve, in "Advanced Materials in Catalysis", J. J. Burton and R. L. Garten Eds., Academic Press, New York, 1977, p.129.
- [26] L. G. Tejuca, J. L. G. Fierro, J. M. D. Tascon, in "Advances in Catalysis", Vol. 36, D.D. Eley, H.Pines and P.B. Weisz, Eds., Academic Press, New York, 1989, p. 237.
- [27] K. Tabata, M. Misono, *Catal. Today*, 8 (1990) 249.
- [28] L. G. Tejuca, J. L. G. Fierro, Eds., "Properties and Applications of Perovskite-Type Oxides", Marcel Dekker, New York, 1993.
- [29] J. Kirchnerova, D. Klvana, *Int. J. Hydrogen Energy*, 19(6) (1994) 501.
- [30] J. Kirchnerova, D. Klvana, J. Vaillancourt, J. Chaouki, *Catal. Lett.*, 21(1&2) (1993) 77.
- [31] R. J. H. Voorhoeve, J. P. Remeika, L. E. Trimble, in "The Catalytic Chemistry of Nitrogen Oxides ", R. L. Klimisch, and J. G. Larson, Eds., Plenum Press, New York, 1975, p.215.
- [32] D. Klvana, J. Vaillancourt, J. Kirchnerova, J. Chaouki, *Appl. Catal., A: General*, 109 (1994) 181.
- [33] J. Kirchnerova, D. Klvana, *Solid State Ionics*, 123 (1999) 307.
- [34] C. Tofan, PhD Thesis, Ecole Polytechnique de Montreal, Montreal, August 2001.
- [35] R. M. Dell and A. Hooper, in "Solid Electrolytes – General Principles, Characterization, Materials, Applications", P. Hagenmuler, W. van Gool, Eds., Academic Press, New York, 1978, p. 291.
- [36] F. S. Galasso, "Structure, Properties and Preparation of Perovskite-Type Compounds", Pergamon, Oxford, 1969.
- [37] H.S. Fogler, "Elements of Chemical Reaction Engineering", Prentice Hall, Englewood Cliffs, N J, 1991.

- [38] E. R. S. Winter, *J. Catal.*, 22 (1971) 158.
- [39] A. Amirnazmi, J. E. Benson, M. Boudart, *J. Catal.*, 30 (1973) 55.
- [40] Y. Teraoka, T. Harada, H. Furukawa, S. Kagawa, S., *Stud. Surf. Sci. Catal.*, 75 (1993) 2649.
- [41] J. Valyon, K. W. Hall, *J. Phys. Chem.*, 97 (1993) 1204.
- [42] G. Mestl, M. P. Rosynek, J. H. Lunsford, J.H., *J. Phys. Chem. B*, 101 (1997) 9329.
- [43] H. H. Kung, "Transition Metal oxides: Surface Chemistry and Catalysis", *Studies in Surface Science and catalysis*, Vol. 45, Elsevier, New York, 1989, p.164.

CHAPITRE III

DIRECT DECOMPOSITION OF NITRIC OXIDE OVER PEROVSKITE - TYPE CATALYSTS, PART II : EFFECT OF OXYGEN IN THE FEED ON THE ACTIVITY OF THREE SELECTED COMPOSITIONS

Reference :

C. Tofan, D. Klvana* et J. Kirchnerova (2001) Direct Decomposition of Nitric Oxide over Perovskite - Type Catalysts, Part II : Effect of Oxygen in the Feed on the Activity of Three Selected Compositions, *Applied Catalysis A : General* (in print).

Keywords :

Perovskite Catalysts; Catalytic Nitric Oxide Decomposition; Kinetics; Oxygen Inhibition

* Author for correspondence, e-mail address : danilo.klvana@courriel.polymtl.ca

3.1 Contexte*

Dans le chapitre précédent trois groupes de pérovskite du type $\text{La}_{1-x}\text{Sr}_x\text{M}_{1-y}\text{M}'_y\text{O}_{3-\delta}$ ont été analysés en ce qui concerne leur activité pour la décomposition du NO en éléments en absence d'oxygène ajouté dans l'alimentation. Le premier groupe était formé par des pérovskites contenant du cobalt, le second par celles contenant du nickel et du manganèse et le troisième par des pérovskites contenant du cuivre.

L'oxygène étant généralement présent dans les effluents de combustion, l'étude de son influence sur la décomposition du NO s'avérait nécessaire. Bien que l'effet inhibiteur de l'oxygène pour cette réaction est relativement bien cerné dans le cas des oxydes simples et des zéolithes, il existe très peu d'informations qui seraient issues d'une analyse cinétique complète dans le cas des pérovskites.

Pour compléter l'étude, on a donc choisi une composition catalytique représentative pour chaque groupe de pérovskites précédemment testées et on a tenté de quantifier l'effet de l'oxygène rajouté à l'alimentation sur la décomposition du NO. L'analyse cinétique des données pour cette réaction avec des équations cinétiques et leurs paramètres associés, sous forme d'un article, font l'objet du présent chapitre.

* ce texte n'est pas inclus dans l'article

3.2 Abstract

Direct decomposition of nitric oxide over three selected perovskites, both in the absence and the presence of oxygen added to the reaction gas mixture, was investigated at a steady state under a wide range of experimental conditions in a plug-flow reactor with 1 g catalyst. Temperatures between 723 and 923 K were covered. The catalysts ($\text{La}_{0.87}\text{Sr}_{0.13}\text{Mn}_{0.2}\text{Ni}_{0.8}\text{O}_{3-\delta}$, $\text{La}_{0.66}\text{Sr}_{0.34}\text{Ni}_{0.3}\text{Co}_{0.7}\text{O}_{3-\delta}$, and $\text{La}_{0.8}\text{Sr}_{0.2}\text{Cu}_{0.15}\text{Fe}_{0.85}\text{O}_{3-\delta}$) were prepared with specific surface area of 12.7, 9.0 and 10.1 m^2/g respectively. When no oxygen was added to the feed, these perovskites showed an improved activity in comparison with other literature known materials, except Cu-ZSM-5 zeolites. Oxygen has an inhibiting effect, which depends strongly on temperature and varies with flowrate (contact time) and composition. It is relatively weak at lower temperatures and higher contact times and increases between about 773 and 873 K. Between 873 and 923 K, where the oxygen inhibition decreases with temperature, the rate of decomposition can be best expressed by a simple model: $r = k_{\text{NO}} \cdot P_{\text{NO}} / (1 + K \cdot P_{\text{O}_2})$. For the low temperature range, the NO decomposition is best described by a model, in which oxygen is an inhibitor but also reactant. Overall data analysis permits to assume that oxygen takes part in the formation of an intermediate giving dinitrogen and that inhibition by oxygen is caused by its parallel participation in the formation of surface nitrates.

3.3 Introduction

Nitric oxide, precursor of toxic NO_2 , is one of the most serious atmospheric pollutants. It is responsible for the smog in the urban areas, for acidic depositions and for stratospheric ozone depletion. Since it is an inherent part of all high temperature fossil fuel combustion processes on which we rely for energy, control of NO emissions and eventually their complete removal is an ever-increasing challenge. Number of approaches has been taken and different methods of abatement were developed. Theoretically, the thermodynamically favored direct decomposition to nitrogen and

oxygen [1] would seem the best way to eliminate nitric oxide, but the reaction is very slow, requiring a highly active catalyst.

Catalytic direct NO decomposition has been studied since the beginning of this century. Despite numerous experimental and theoretical studies of nitric oxide decomposition over a variety of materials [2-18], those concerning its kinetics are relatively rare and the mechanism of this reaction is far from being well understood. It is well known, however, that on all materials, the NO decomposition is inhibited by added oxygen, and the degree of inhibition varies with catalyst and/or temperature. Winter described the kinetics of nitric oxide decomposition over a dozen of metal oxides by a simple model $r = k_{NO} \cdot P_{NO} / (1 + K \cdot P_{O_2})$ [3]. Amirnazmi et al. [4] derived the same model for supported platinum and several transition metal oxides. In both cases the model related to temperatures above 873 K. Over several perovskites, at temperatures above 973 K, Teraoka et al. [9] observed inhibition not only by oxygen, but also by nitric oxide itself and proposed a kinetic equation, which took the two effects into account: $r = k_{NO} \cdot P_{NO}^2 / (K_{NO} \cdot P_{NO} + K_{O_2} \cdot P_{O_2})$. Recently, in the case of La_2O_3 , studied at somehow lower temperatures than those in the work by Winter, Vannice et al., [5], also observed inhibition by both nitric oxide and oxygen and proposed a more complex LH type model: $r = k \cdot L \cdot K_{NO}^2 \cdot P_{NO}^2 / (1 + K_{NO} \cdot P_{NO} + K_{O_2} \cdot P_{O_2}^{1/2})^2$. Similar model was later proposed also for nitric oxide decomposition over Mn_2O_3 [6]. Both lanthana and Mn_2O_3 are nearly an order of magnitude less active than perovskites of this study, or than high SSA Co_3O_4 . Over Cu-ZSM-5 zeolites, exhibiting the highest activity around 800 K, the kinetics, studied at temperatures between 723 and 823 K, was described by a model mathematically very similar to that of Winter or Amirnazmi et al.: $r = k_{NO} \cdot P_{NO} / (1 + K \cdot P_{O_2}^{1/2})$ [13].

The deduced kinetic models have often served as a guideline to propose a plausible mechanism, which continues to be actively debated. The main speculation concerns the

nature of the actual active site and the form of the intermediate species. Until about ten years ago, it was generally accepted that the decomposition proceeds via some redox-type mechanism characterized by an adsorption of NO molecule on a reduced surface site, oxidized in the process of adsorption and accompanied by an electron transfer to form $[NO]_{ad}$, and then regenerated by oxygen desorption. In this scheme, the actual adsorption site is a pair of oxygen vacancies with trapped electrons. Such mechanism was initially proposed even for Cu-ZSM-5 zeolites [13]. In the case of zeolites, the redox mechanism was later contested on the grounds of thermodynamics [15] and it was admitted that in these materials, where the oxygen mobility is restricted, some specific surface adsorbed oxygen species may actually participate in the formation of an intermediate such as $-NO_2$ [16]. Similarly, in the case of barium oxide supported on magnesia it was shown [17,18] that under a narrow range of restricted experimental conditions, where the activity dramatically increases, surface oxygen, most likely peroxide ion, takes apparently part in the formation of an intermediate.

Perovskite oxides, represented by $La_{1-x}Sr_xM_{1-y}M'_yO_{3-\delta}$, where M and M' are catalytically active transition metals (Co, Mn, Cu, Ni, Fe), represent a convenient model system for the study of various properties influencing catalytic activity and were for some time even considered as promising catalysts [14]. In comparison with simple oxides, perovskite oxides offer several advantages. Structure of perovskites may accommodate variety of ions of different, even unusual, valences and defects, often leading to high electronic conductivity and high oxygen mobility. In general, perovskites are also more stable thermally than the individual transition metal oxides.

Our previous study of NO decomposition over several new perovskites, most of which were prepared with a relatively high specific surface area (SSA) ranging between 9 – 22 m^2/g concerned the effect of different metal ions in the perovskite composition on the activity when no oxygen was added to the feed [19]. The studied perovskite compositions included cobalt, nickel or copper as the principal active element M. Based

on the observed conversions between 723 and 923 K in the absence of oxygen added to the feed, most of these perovskites were found more active than any other reported in literature. Furthermore, analysis of the experimental conversions suggested that oxygen, in spite of having an inhibiting effect, might also be involved as a reactant, i.e. take part in the formation of the reaction intermediate. A change of kinetics at about 823 K, accompanied by a different dependence on a flowrate (contact time) in a high and a low temperature region, was also evident. Among the studied perovskites $\text{La}_{0.87}\text{Sr}_{0.13}\text{Mn}_{0.2}\text{Ni}_{0.8}\text{O}_{3-\delta}$ (LSMN-28) and $\text{La}_{0.66}\text{Sr}_{0.34}\text{Ni}_{0.3}\text{Co}_{0.7}\text{O}_{3-\delta}$ (LSNC) exhibited the best activity at high temperatures (823 - 923 K), whereas $\text{La}_{0.8}\text{Sr}_{0.2}\text{Cu}_{0.15}\text{Fe}_{0.85}\text{O}_{3-\delta}$ (LSCuF) was the most active at low temperatures (723 - 800 K). Although the activities of these catalysts are for practical applications insufficient, with the intention to obtain a better understanding of this complex reaction system, a global kinetic study including evaluation under different conditions of the effect of oxygen added to the feed was undertaken for the three representative perovskite compositions. The results are presented in this paper.

3.4 Experimental

3.4.1 Preparation and characterization of catalysts

The catalysts were prepared from highly homogeneous reactive slurry of precursor components, mixed in strictly stoichiometric proportions. This precursor slurry, obtained by suspending lanthanum hydroxide in a solution of metal nitrates, was frozen and dried under vacuum on a commercial laboratory freeze-drier. The dry precursor mixtures were calcined in air under controlled conditions, typically 12 h at 863 K, followed by 4 h at 923 K. A complete description of catalyst preparation can be found elsewhere [19,20].

Formation of the perovskite phase was confirmed by X-ray powder diffraction using a Philips X'Pert diffractometer with Cu-K_α radiation. The powders were nearly phase pure. Specific surface area (SSA) was determined by a single-point BET method using a Micromeritics Flow-Sorb II 2300 apparatus with nitrogen as the adsorbate (30 % nitrogen in helium). The SSA of the studied perovskites was 12.7, 9.0 and 10.1 m²/g respectively for LSMN-28, LSNC and LSCuF. The particle size of the powders was less than 10 μm.

3.4.2 Determination of kinetic data

For each of the catalysts the experimental kinetic data were obtained at ambient pressure by using an integral plug-flow U-type reactor consisting of a stainless steel tube, having 0.7 cm internal diameter. Conditions were very similar to those presented in the previous paper [19]: temperature (723-923 K), reaction gas: NO (1.0-5.0 %)-O₂ (0-10.0 %)-He (balance), 1 g of catalyst, total flow rate (15-100 ml/min). The catalyst powder was diluted by 7 ml of inert pumice particles (350-416 μm diameter) precalcined 12 h at 923 K to provide a quasi-isothermicity of the reaction bed and to ensure good permeability. The temperature was monitored by two K-type thermocouples inserted at the inlet and outlet of the catalytic bed. The reactant gas flow rates were controlled with MKS and Brooks 580 mass flow controllers. The product gases were analyzed by a gas chromatograph equipped with 5 Å molecular sieve column kept at 373 K with the carrier gas (helium) velocity of 30 ml/min. The concentration of nitrous oxide in the effluents, monitored by a FTIR spectrometer, was insignificant with respect to that present as impurity in nitric oxide. Before starting the evaluation, the reactor was purged several hours at 773 K by pure helium to remove air and adsorbed impurities. The tests were carried out over several days. Between two experiments the catalyst was cooled down to ambient temperature under a flow of helium. In a reaction run the experimental data were taken after at least 1 h on stream at each temperature, when the catalytic reaction practically reached steady-state conditions. Because of the gas phase reaction in the exit

lines between the reactor and gas chromatograph column of undecomposed NO with O₂ the NO decomposition activity was evaluated in terms of the NO conversion into N₂: $x_{N_2} = 2 \cdot 100 \cdot [N_2]_{out} / [NO]_{in}$. About 50 ppmv N₂ was the limit of detection, while concentrations above 100 ppmv were quantified with the uncertainty of 30 ppmv. Thus, for 2 % NO in the feed the uncertainty was lower than $\pm 10\%$ for conversions $> 3\%$.

All conversion data were collected under the conditions free of transport phenomena control as verified mathematically using Mears and Wiez-Prater criteria [21]. For a so slow reaction (over a fine powder), accompanied by only a weak thermal change, this was a priory expected.

3.5 Results and Discussion

3.5.1 Catalyst Performance in the Absence of Oxygen in the Feed

In principle, the use of an integral reactor and high conversion data for a kinetic study allows discerning, to some degree, the effects of products on the reaction without their explicit addition to the feed.

Figure 3.1, where the conversions of nitric oxide to nitrogen are plotted as a function of temperature gives an example of the activities of the three selected perovskites at two different flowrates, when no oxygen was added to the feed. Previous analysis of complete conversion data indicated large deviations from a simple first order model depending strongly on flowrate and temperature [19] and a search for a suitable kinetic model lead to the results summarized in Table 3.1. A multiple regression analysis was used for fitting at each individual temperature the collected data to the integrated forms of kinetic equations in which P_{O₂} = P_{O₂-produced} was assumed to correspond to P_{N₂} produced by NO decomposition. From a large number of tested models, only those giving acceptable fit are included in the table. As indicated, no model was valid over the

whole temperature range and for individual compositions the change from one model to another occurred at different temperatures. Most interestingly, the best fitting models involved oxygen as an inhibitor, but also a reactant.

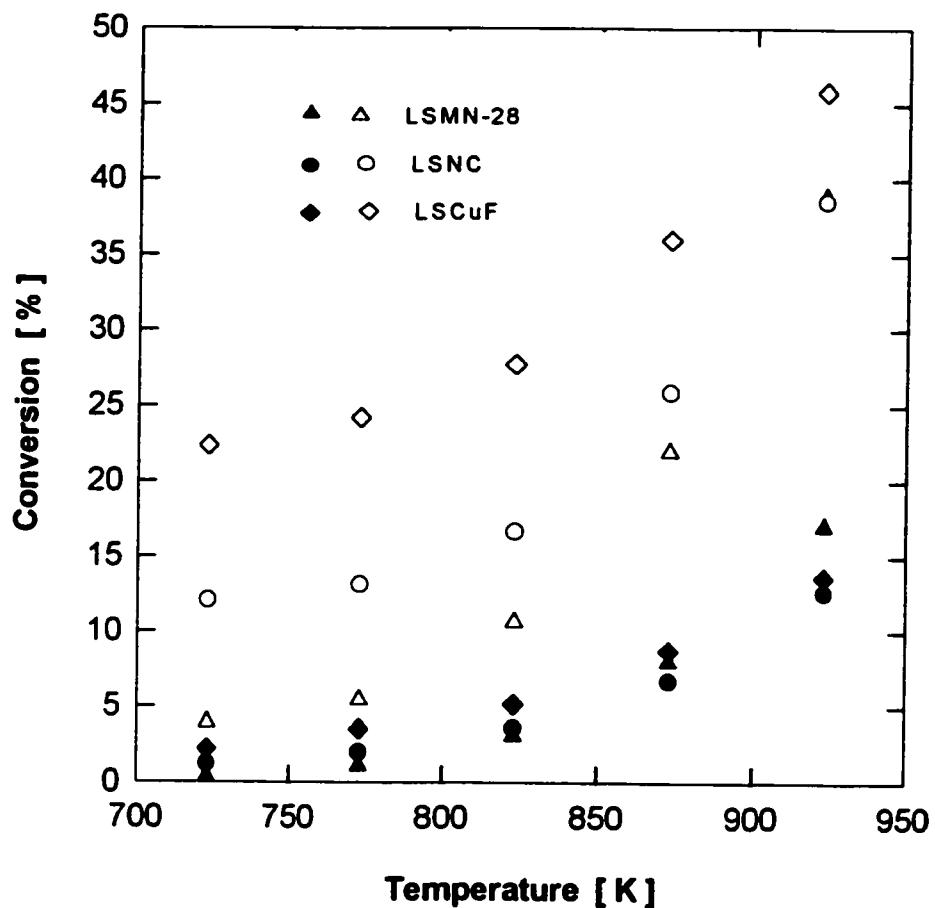


Figure 3.1 Conversion to nitrogen of 2 % nitric oxide in helium over LSMN-28, LSNC and LSCuF perovskites (1 g) as a function of temperature; open symbols: 15 ml/min; full symbols: 75 ml/min.

Table 3.1 Results of the search for the best fitting model for data obtained in the absence of oxygen added to the feed.

Temp. K	Model			
	I	II	III	IV
	$\frac{k_{NO}P_{NO}}{1+K_{O2}P_{O2}}$	$\frac{k_{NO}P_{NO}^2}{K_{NO}P_{NO} + K_{O2}P_{O2}}$	$\frac{k_{NO}P_{NO}P_{O2}^{1/2}}{k_I P_{NO} + k_{II} P_{O2}^{1/2}}$	$\frac{k_{NO}P_{NO}P_{O2}}{k_I P_{NO} + k_{II} P_{O2}}$
LSMN-28 (La_{0.87}Sr_{0.13}Mn_{0.2}Ni_{0.8}O_{3-δ})				
723	-	++	+++	-
773	-	++	+++	-
823	++	-	-	+++
873	++	-	-	+++
893	++	-	+	+++
913	++	-	+	+++
923	+	-	-	+++
LSNC (La_{0.66}Sr_{0.34}Ni_{0.3}Co_{0.7}O_{3-δ})				
723	-	++	+++	-
773	-	++	+++	-
823	-	++	+++	-
873	++	-	-	+++
893	++	-	+	+++
913	++	-	-	+++
923	++	-	-	+++
LSCuF (La_{0.8}Sr_{0.2}Cu_{0.15}Fe_{0.85}O_{3-δ})				
723	-	++	+++	-
773	-	++	+++	-
823	-	++	+++	-
873	-	++	+++	-
893	+++	-	++	++
913	+++	-	++	++
923	+++	-	-	(+++)

+ poor fit; ++ reasonable fit; +++ excellent fit; - one of the parameters negative

3.5.2 Effect of Oxygen on the Activity

To allow a direct quantitative evaluation of the actual effect of oxygen, especially its inhibition, activity of each catalyst was evaluated as a function of the added oxygen concentration at several different flowrates. At temperatures between 723 and about 823 K, where the conversions are relatively low, the effect of oxygen could have been determined only for lower flowrates and for restricted oxygen concentrations. At any temperature, the observed inhibition by oxygen was strictly reversible. When removing oxygen from the feed, the initial activity was always restored.

In the case of LSCuF, which at lower temperatures was considerably more active than the other two catalysts and reasonable conversions were observed, effect of higher oxygen concentrations could have been determined with a good precision over the whole range of temperatures. The results are shown in Figure 3.2. Clearly, addition of oxygen to the feed in concentrations significantly higher (about an order of magnitude) than those produced by NO decomposition, which varied between about 0.03 and 0.5 % as the temperature changed from 723 to 923 K, has a marked inhibition effect that is particularly strong at 873 K. The degree of this oxygen inhibition and its variation with temperature can be appreciated even better in Figure 3.3 representing the relative activity (ratio of NO conversion to nitrogen in the presence of added oxygen to that when no oxygen was added, i.e. reference conversion) as a function of temperature. Between 723 and 773 K the oxygen inhibition slowly decreases, but above 773 K the inhibition is getting stronger with temperature. Between 823 and 873 K the effect of temperature is really dramatic, suggesting an activated process. Finally, between 873 and 923 K the oxygen inhibition decreases again with temperature.

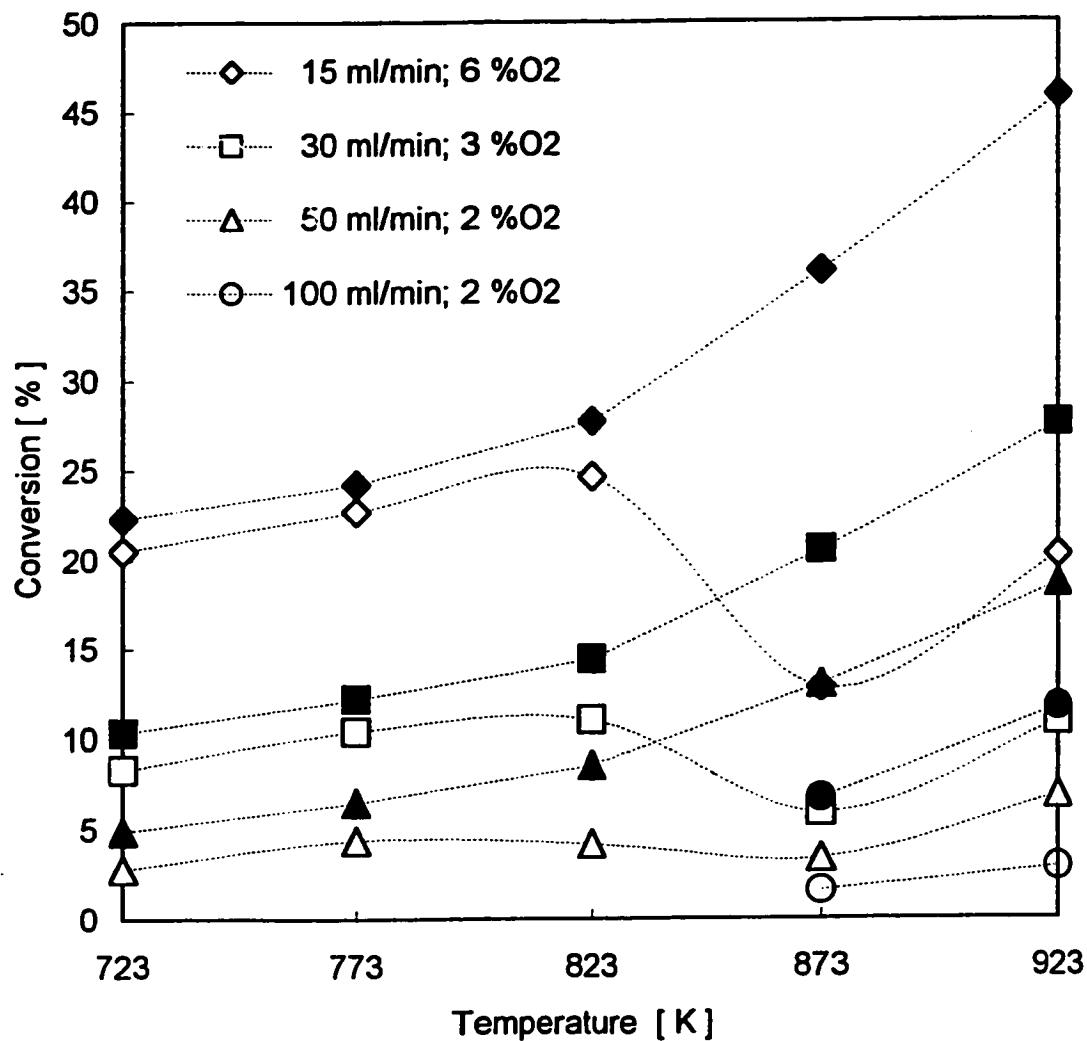


Figure 3.2 Conversion to nitrogen of 2 % nitric oxide in helium over 1 g LSCuF without (full symbols) and with (open symbols) oxygen added to the feed as a function of temperature

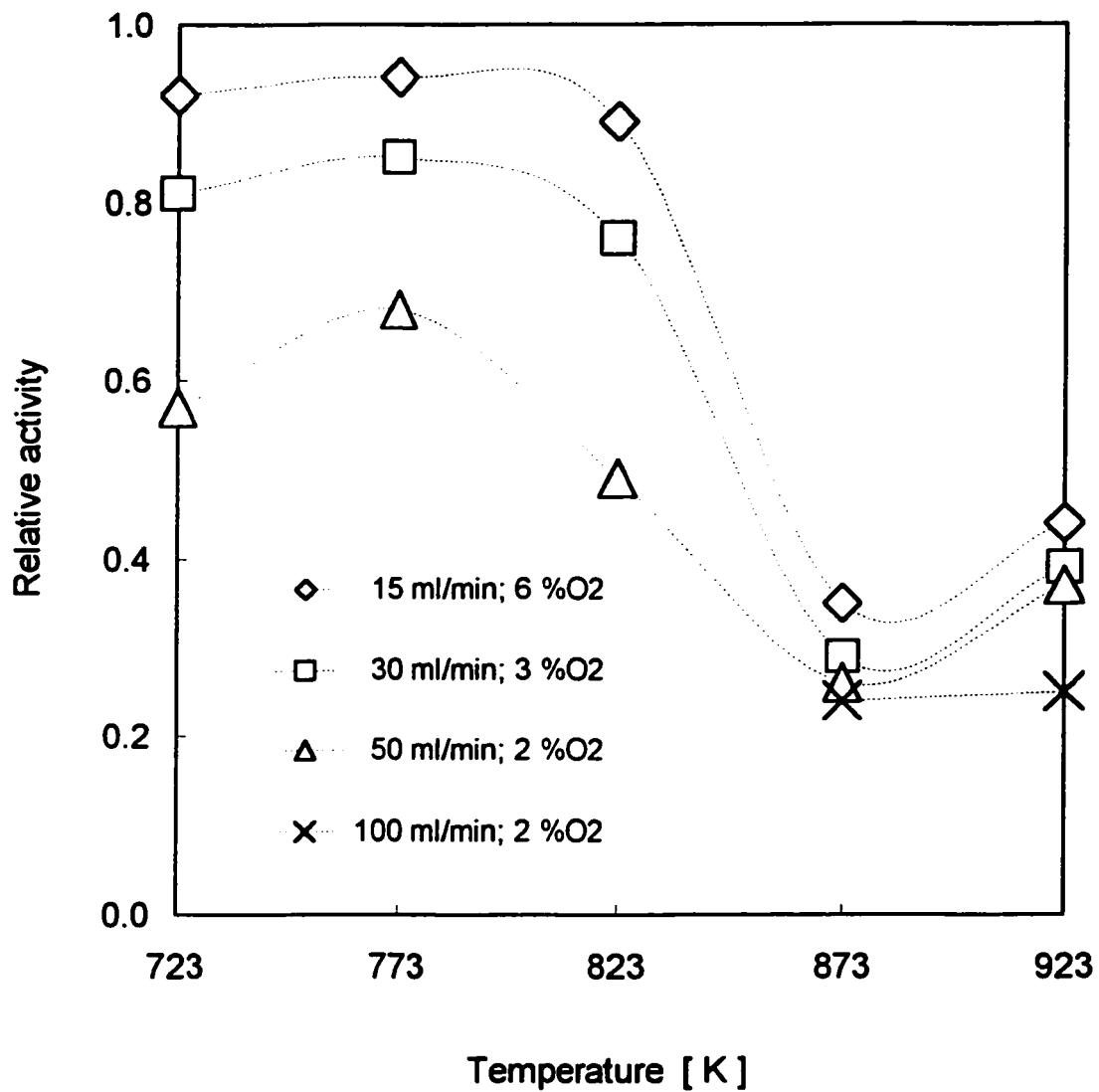


Figure 3. 3 Relative activity (x_{NO+O_2}/x_{NO}) of LSCuF perovskite in the decomposition of 2 % NO as a function of temperature; effect of flowrate and of O₂ concentration.

For the case of LSMN-28 and LSNC, over which the low temperature conversions were very low, evaluation of the effect of added oxygen had to be limited to rather low concentrations. Figures 3.4 and 3.5 show for LSMN-28 and LSNC respectively the change in conversions when low concentrations of oxygen are added to the feed, whereas Figure 3.6 provides a direct comparison in terms of relative activities for the two catalysts.

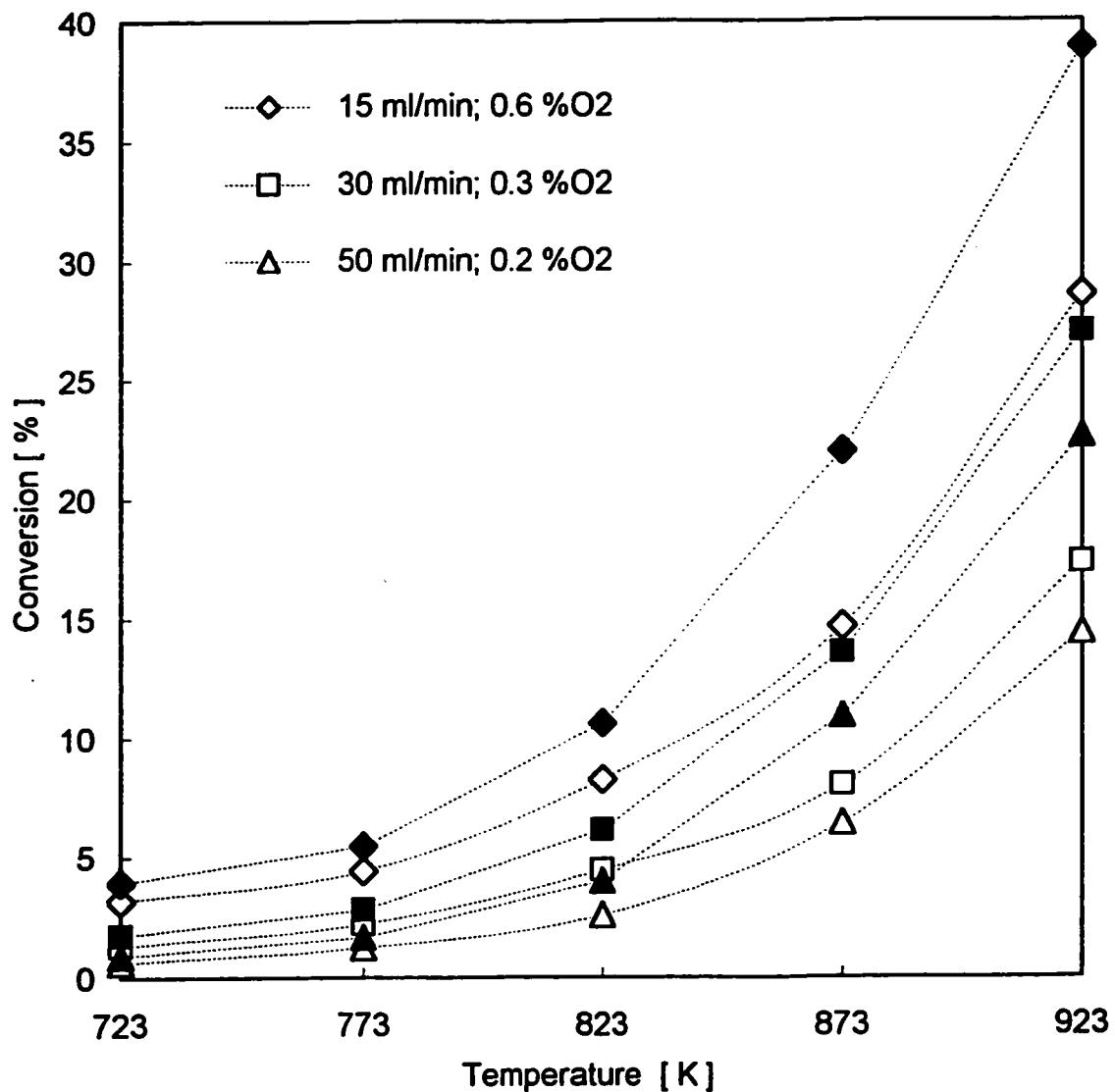


Figure 3.4 Conversion to nitrogen of 2 % nitric oxide in helium over 1 g LSMN-28 without (full symbols) and with (open symbols) oxygen added to the feed as a function of temperature

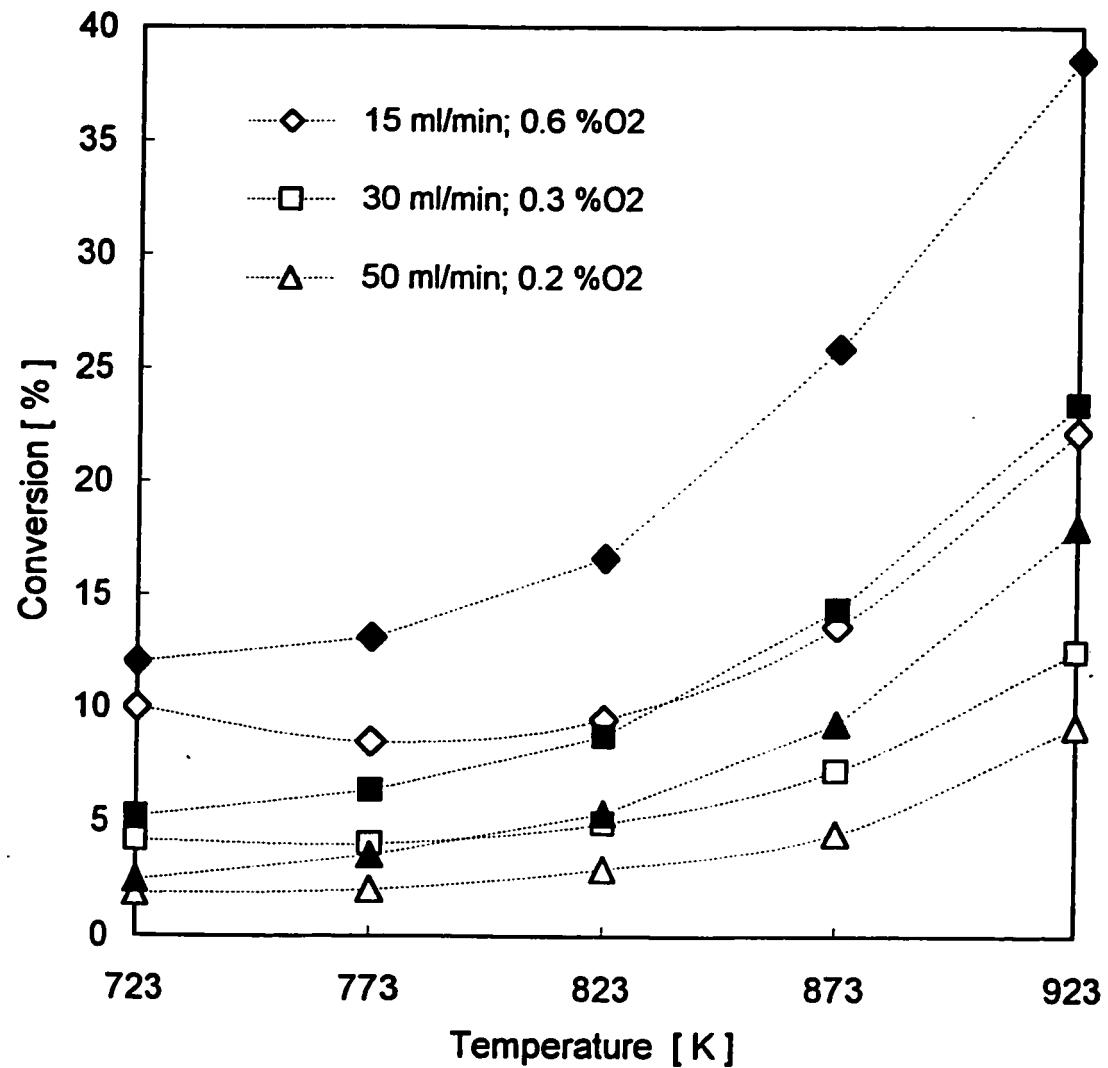


Figure 3.5 Conversion to nitrogen of 2 % nitric oxide in helium over LSNC without (full symbols) and with (open symbols) oxygen added to the feed as a function of temperature

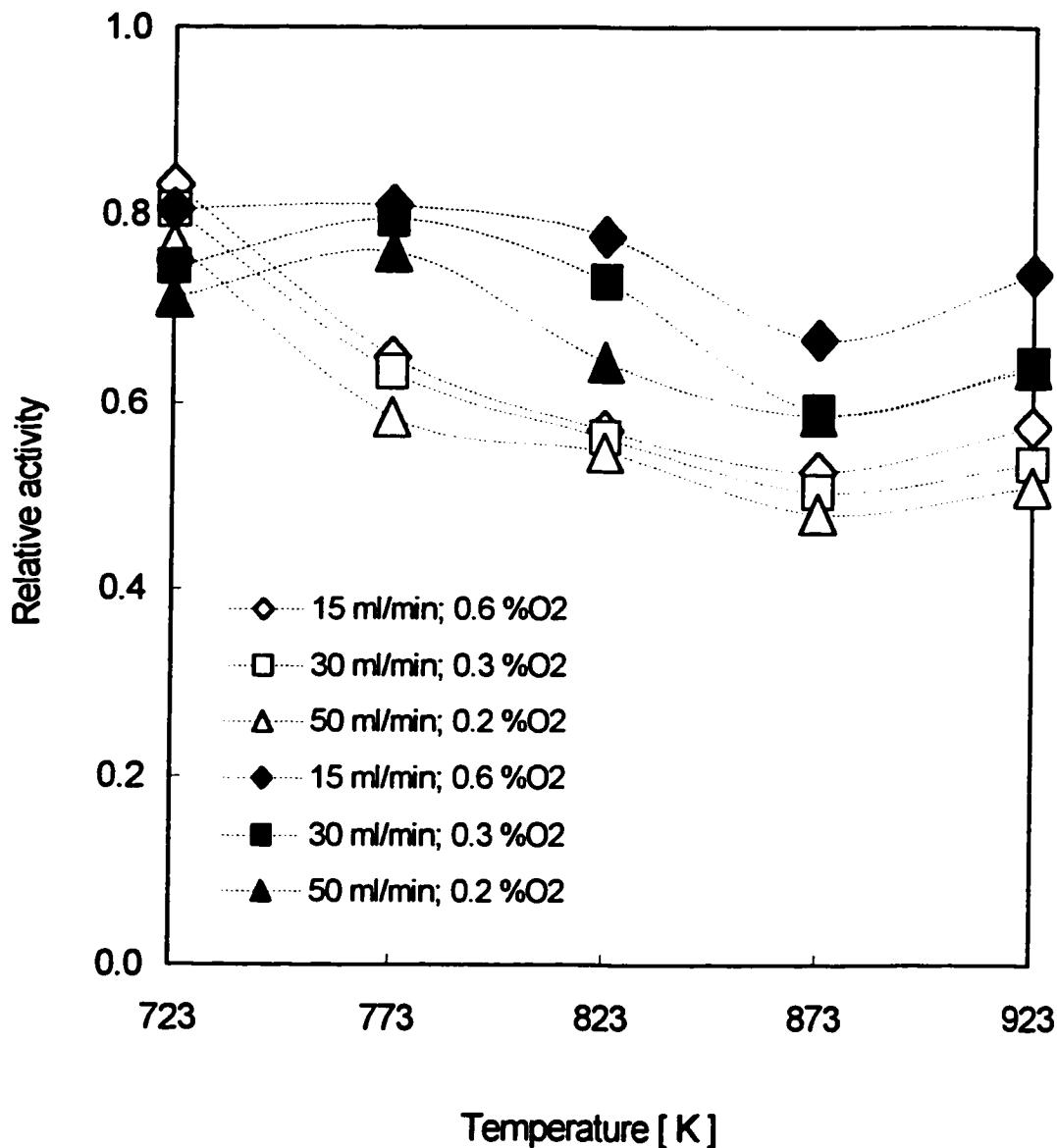


Figure 3. 6 Relative activity (x_{NO+O_2}/x_{NO}) of LSMN-28 (full symbols) and of LSNC (open symbols) perovskites in the decomposition of 2 % NO as a function of temperature; effect of flowrate and of O₂ concentration.

Note that in this case, the concentrations of added oxygen are of about the same order as those presumably produced by NO decomposition at the high temperatures. As can be seen for these two catalysts, oxygen, even at these low concentrations, has a similarly strong inhibiting effect as that observed for LSCuF with high concentrations, including its dependence on flowrate. Although in this case the dependence on flowrate is substantially less pronounced, particularly when considering the higher uncertainty on low temperature conversions, the trend remains undeniably the same : higher flowrate with lower oxygen concentration results in a stronger inhibition. Furthermore, in the case of LSMN-28 the pattern of variation of relative activity with temperature of the oxygen inhibiting effect closely resembles that for LSCuF (Fig. 3.3); it decreases slightly with temperature between 723 and 773 K, increases with temperature between 823 and 873 K and finally decreases again with temperature from 873 to 923 K. On the other hand, in the case of LSNC the oxygen inhibition increases continuously with temperature over the whole range between 723 and 873 K. Nevertheless, similarly as for the other two catalysts, above 873 K, the oxygen inhibition starts to decrease with temperature. It is in this temperature range of relatively high conversions, even for flowrates of 100 ml/min, where the three catalysts behave similarly.

Thus, the temperature range of 873 – 923 K, in which the activities are relatively high, was selected for more detailed kinetic study. Conversion data for different experimental conditions are given in Table 3.2.

Table 3.2: Effect of oxygen added to the feed on the NO conversion to nitrogen over three perovskites

[O ₂] %	Conversion of NO into N ₂ (%)									
	LSNC					LSMN-28				
	873 K	893 K	913 K	923 K	873 K	893 K	913 K	923 K	873 K	893 K
0	8.6	12.2	15.7	18.4	9.5	12.7	17.6	20.5	9.5	11.7
1	1.8	3.0	4.6	5.9	2.4	3.8	6.0	7.5	2.2	3.0
2	1.3	2.2	3.7	4.5	2.1	3.0	4.9	6.1	1.9	2.6
3	1.1	2.0	3.0	3.8	1.9	2.9	4.1	4.9	1.8	2.3
4	1.0	1.6	2.6	3.2	1.7	2.9	4.1	4.8	1.6	2.1
10	0.8	1.4	2.5	3.1	1.7	2.9	4.1	4.8	1.6	2.1
Q _{tot} = 50 ml/min; [NO] = 5 %										
0	5.7	7.6	9.5	12.3	5.9	8.4	12.2	14.4	6.3	7.1
0.5	1.7	2.5	3.4	4.4	1.9	2.9	4.7	5.6	2.0	2.3
1	1.0	1.4	2.5	3.8	1.3	2.0	3.4	4.9	1.2	1.4
2	0.6	1.1	1.8	2.5	1.2	1.9	3.2	3.8	1.1	1.3
3	0.5	0.9	1.4	2.1	1.2	1.7	2.5	3.1	1.0	1.2
4	0.4	0.6	1.2	1.8	1.2	1.7	2.5	3.1	0.9	1.2
10	0.2	0.5	1.1	1.6	1.2	1.7	2.5	3.1	0.9	1.2
Q _{tot} = 100 ml/min; [NO] = 5 %										
0	6.0	8.1	10.0	12.2	6.5	9.2	13.2	15.5	6.7	7.9
0.5	0.4	1.0	2.4	3.3	1.9	2.7	4.0	5.3	1.6	1.9
1	0.1	0.6	1.5	2.5	1.9	2.5	3.8	5.2	1.6	1.9
2	0.1	0.6	1.4	1.9	1.9	2.5	3.8	5.2	1.6	1.9
3	0.1	0.6	1.4	1.9	1.9	2.5	3.8	5.0	1.6	1.9
4	0.1	0.6	1.4	1.9	1.9	2.5	3.8	5.0	1.6	1.9
10	0.1	0.6	1.4	1.9	1.9	2.5	3.8	5.0	1.6	1.9
Q _{tot} = 100 ml/min; [NO] = 2 %										
0	6.0	8.1	10.0	12.2	6.5	9.2	13.2	15.5	6.7	7.9
0.5	0.4	1.0	2.4	3.3	1.9	2.7	4.0	5.3	1.6	1.9
1	0.1	0.6	1.5	2.5	1.9	2.5	3.8	5.2	1.6	1.9
2	0.1	0.6	1.4	1.9	1.9	2.5	3.8	5.2	1.6	1.9
3	0.1	0.6	1.4	1.9	1.9	2.5	3.8	5.0	1.6	1.9
4	0.1	0.6	1.4	1.9	1.9	2.5	3.8	5.0	1.6	1.9
10	0.1	0.6	1.4	1.9	1.9	2.5	3.8	5.0	1.6	1.9

For two temperatures of this region the influence on the nitric oxide decomposition (conversion to nitrogen) of oxygen added to the feed at different concentrations is shown in Figures 3.7-3.9 for the LSMN-28, LSNC and LSCuF respectively. While at the first sight the effect of oxygen on the conversion appears to be very similar for the three catalysts, on closer examination important differences become apparent. Of the three catalysts, it is the LSNC, which in terms of relative activity is the most affected by the added oxygen, particularly at 873 K. For example, at this temperature 1 % O₂ added to 2 % NO flowing at 100 ml/min reduces the conversion over LSNC to less than 2 % initial, whereas for LSMN-28 and LSCuF tested under the same conditions, the remaining activity is 29 and 24 % respectively. More than 3 % oxygen added to the feed (up to 10 %) did not cause a further significant decrease of activity. The observed saturation effect is most likely related to the equilibrium between gas phase concentration of oxygen and formation of some specific surface oxygen species. Comparatively strong oxygen inhibition and similar saturation effect was observed at 973 and 1073 K for other perovskites [9] or at 833, 853 and 873 K for Mn₂O₃ [22]. The weak oxygen inhibition observed for LSCuF and LSMN-28 at low temperatures (723 - 823 K) seems to be about the same order as that for Cu-ZSM-5 zeolites [13].

The most striking feature of the observed oxygen inhibition, regardless the temperature, is the fact, that it increases with flowrate (decreases with contact time), as indicated by the data in Table 3.2. For example, in the case of LSNC at 873 K, addition of 2 % oxygen to the feed decreases the activity by 85 % when the flowrate is 50 ml/min, and by 90 % when the flowrate is 100 ml/min. Similar is observed at other temperatures and oxygen concentrations and for other two catalysts. Actually, the same dependence on flowrate is illustrated in Figure 3.3. Although the concentration of oxygen was lower for higher flowrates, the relative activity decreased. This effect is apparent also in Figure 3.6. Such behavior indicates that the rate of oxygen desorption is not the slow process. On the contrary, the slow process must be the formation of the intermediate with the participation of some oxygen species.

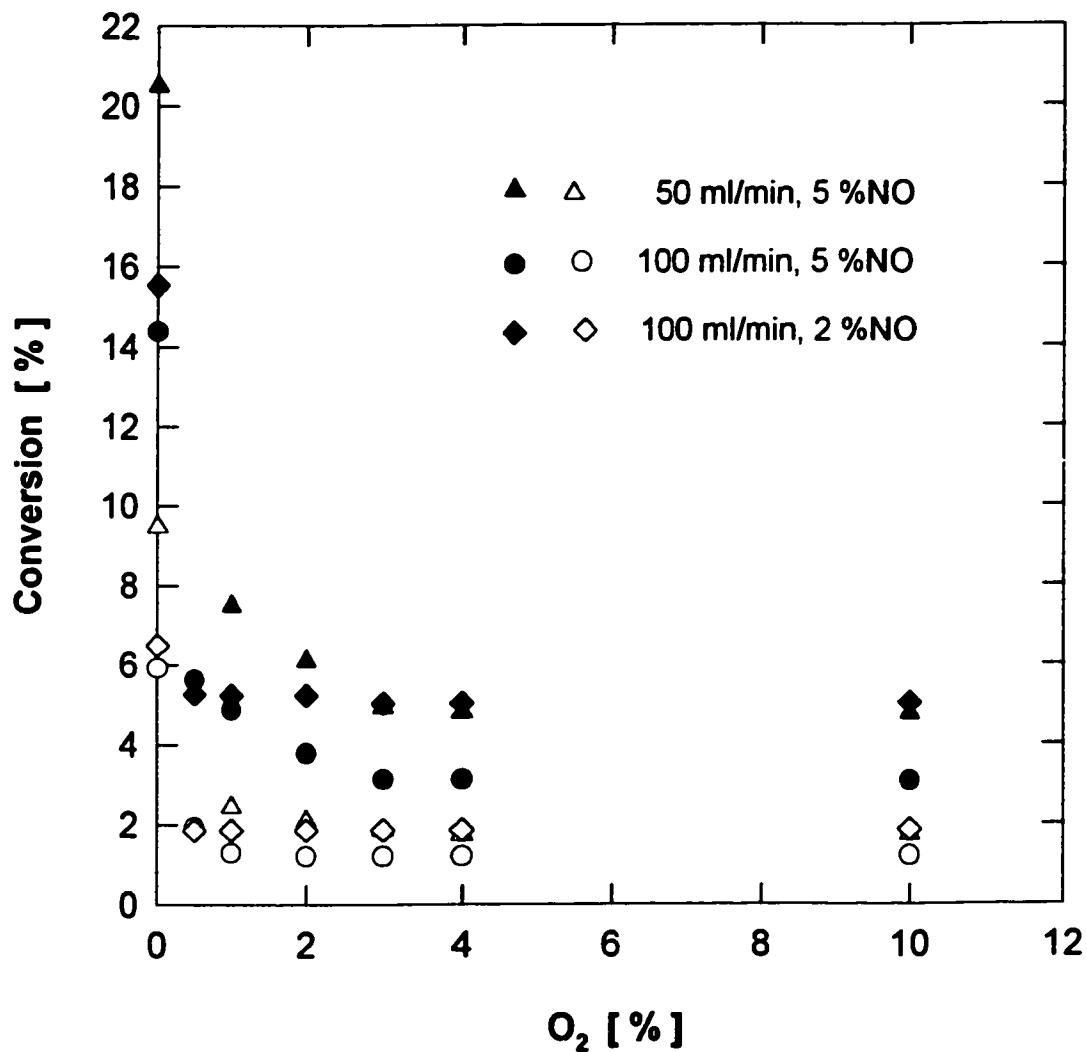


Figure 3.7 Influence of O_2 concentration in the feed on the conversion of nitric oxide over LSMN-28 perovskite at 873 K (open symbols) and 923 K (full symbols).

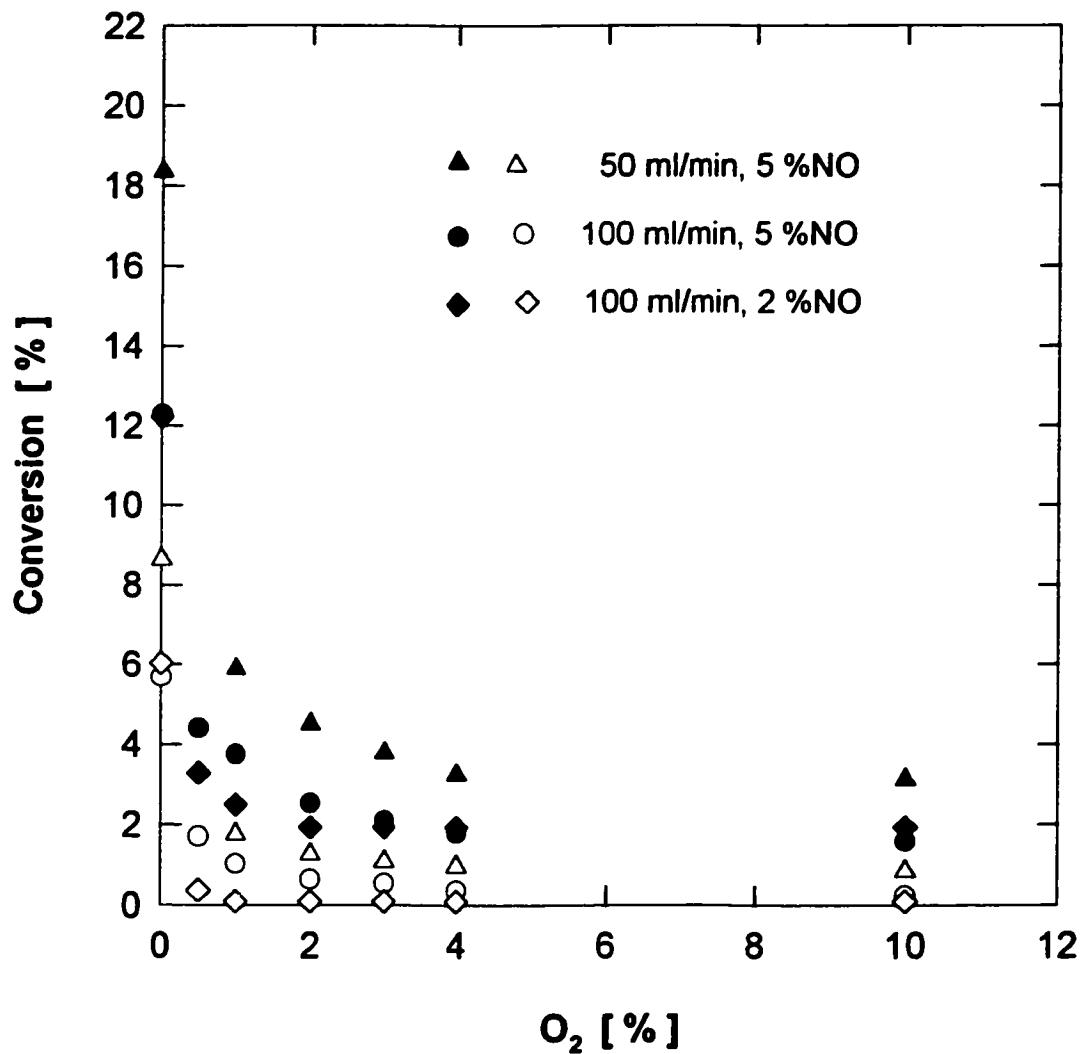


Figure 3.8 Influence of O_2 concentration in the feed on the conversion of nitric oxide over LSNC perovskite at 873 K (open symbols) and 923 K (full symbols).

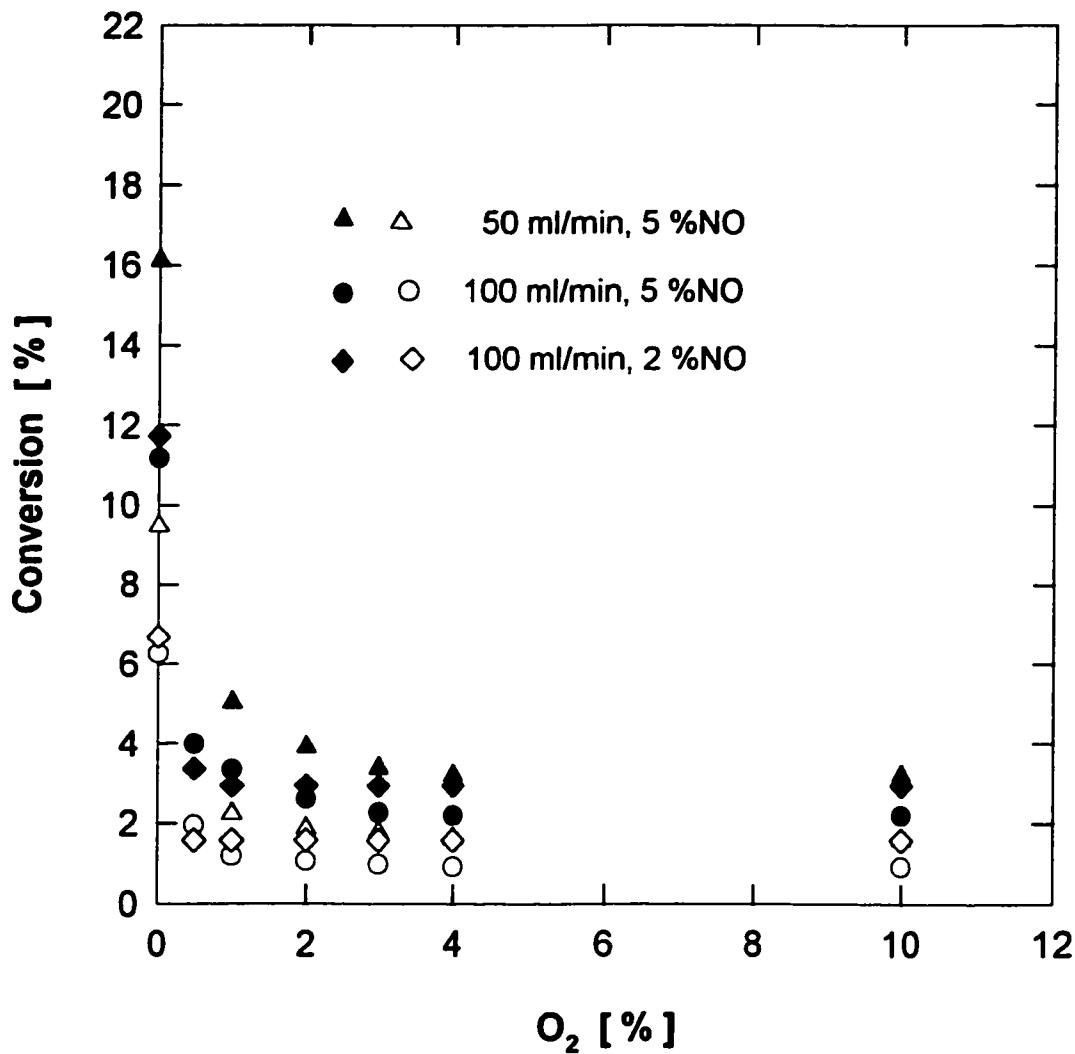


Figure 3.9 Influence of O_2 concentration in the feed on the conversion of nitric oxide over LSCuF perovskite at 873 K (open symbols) and 923 K (full symbols).

The unexpected variation of oxygen inhibition with temperature is most likely related to the relatively complex chemistry of oxygen and nitric oxide adsorption. On oxygen nonstoichiometric perovskite oxides, such as those studied in this work, depending on

temperature existence of various energetically different oxygen species is well known [23,24]. Oxygen adsorption may even proceed by an activated process. Furthermore, in these perovskites, oxygen mobility is relatively high and increases with temperature. The different surface oxygen species may serve (besides oxygen vacancies) as the active sites for NO adsorption, giving a variety of chemisorbed NO_x species of different structural characteristics and thermal stability [25-29]. Some of these might favor formation of dinitrogen (for example nitrito and chelated nitrite species), others will lead to the desorption of NO, or even NO_2 . Formation of particular species will further be complicated by the presence of oxygen, which may be expected to promote formation of unidentate and free nitrates, the species giving NO and NO_2 . These nitrate species, typically formed and stabilized on basic oxides, were observed at temperatures as high as 800 K over lanthana [29], and over several other materials such BaO/MgO [18], $\text{Na/Co}_3\text{O}_4$ [30] or $\text{YBa}_2\text{Cu}_3\text{O}_7$ [27]. Since the formation of free nitrates is likely an activated process, the observed variation of the inhibition effect with temperature is understandable.

3.5.3 Kinetics and Mechanism of NO decomposition

To rationalize the observed effects of oxygen added to the feed a new search for a suitable kinetic model was carried out. Similarly as in the previous case this was done by fitting, using a multiple regression analysis, the complete sets of data at individual temperatures to the integrated forms of kinetic equations. However, now P_{O_2} was assumed to correspond to the sum of $\text{P}_{\text{O}_2\text{-produced}}$ and $\text{P}_{\text{O}_2\text{-added}}$, when relevant. In principle, models derived previously (Table 3.1) would be expected to remain valid, at least up to a certain limit.

3.5.3.1 Low temperature range

Because of the complexity of the actual oxygen effect observed in the low temperature range (723 – 873 K) a systematic determination of kinetic parameters was not warranted. Nevertheless, the new conversion data for feeds with added oxygen allowed to test the empirical model III in Table 3.1 deduced from data for conversions without oxygen added to the feed over a wider range of data. The validity of this model was confirmed at individual temperatures. It should be pointed out that in this case the fitting did not allow an independent determination of the three kinetic parameters, but only their ratios. From the ratios of k_{II}/k_I (Table 3.3) we could deduce that for LSCuF and LSMn-28 the oxygen inhibition is more than an order of magnitude stronger than inhibition by NO, whereas in the case of LSNC the difference is only about fivefold.

Table 3.3 Ratios of kinetic constants k_{II}/k_I of model III (Table 3.1) for three perovskites at four temperatures

Catalyst	k_{II}/k_I			
	723 K	773 K	823 K	873 K
LSMN-28	28.3	26.4	-	-
LSNC	6.8	4.7	3.2	-
LSCuF	25.9	21.1	12.8	6.1

Validity of the model III involving oxygen not only as an inhibitor but also as a reactant could be explained in the following way. First of all, some specific surface oxygen species appears to play a role of an active site, on which adsorption of NO takes place. These oxygen sites are maintained by a relatively slow dissociative oxygen adsorption, hence the half order in oxygen. The most plausible template for the formation of dinitrogen seems a dimer-type intermediate such as $[N_2O_4]$ with an N-N bond produced

by adsorption of two NO molecules, successively or simultaneously, possibly starting with nitrito or chelated nitrite species. This reaction is apparently slow. However, at the same time parallel surface reactions to form different species, most likely unidentate and/or free nitrates, which will not favor decomposition into dinitrogen and oxygen but will rather give NO or NO₂, may also occur, especially when excess of oxygen is present. Such competing reactions would actually interfere with the decomposition; they would cause an inhibition. In fact, similar mechanism has previously been proposed for the kinetics of NO decomposition over Cu-ZSM-5 zeolites, over which, however, the population of the active oxygen species was considered as very high, independent of gas phase oxygen concentration [16]. Decomposition of NO at low temperature over copper chromite has also been assumed to proceed via surface oxygen and a dimer-type intermediate [31].

3.5.3.2 High temperature range (873 – 923 K)

As could have been expected, in the case of LSCuF the model I provided the best fit (Fig. 3.10), but only for temperatures between 893 and 923 K. For the other two catalysts, the model that gave the best fit to the data for oxygen free feeds, i.e. the model IV in Table 3.1, failed, resulting in a negative value of one of the parameters. More than a dozen of other plausible models were therefore tested in addition, but only the simplest, the model I ($r = k_{NO} \cdot P_{NO} / (1 + K \cdot P_{O_2})$), would provide an acceptable fit shown in Figures 3.11 and 3.12 for LSMN-28 and LSNC respectively. It has to be noted that for all three catalysts the models are valid only up to 2% added oxygen, reflecting the fact that higher oxygen concentrations caused little additional increase in the inhibition. This is apparently related by a surface saturation with oxygen.

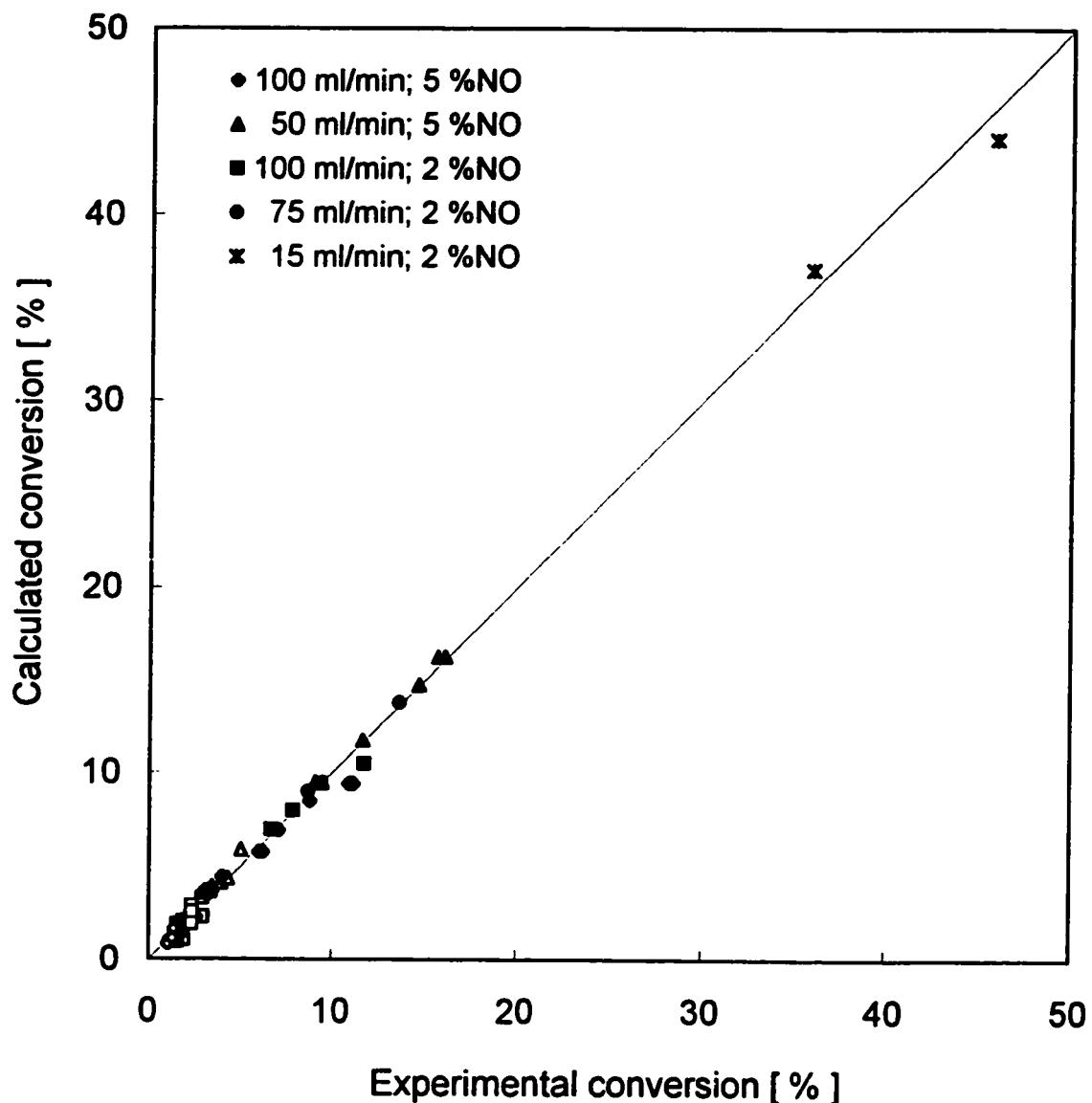


Figure 3.10 Predicted versus experimental conversion of nitric oxide to nitrogen over LSCuF perovskite ($r = k_{NO} \cdot P_{NO} / (1 + K \cdot P_{O_2})$); parameters given in Table 3.4 used in calculations; open symbols correspond to data obtained in the presence of oxygen added to the feed.

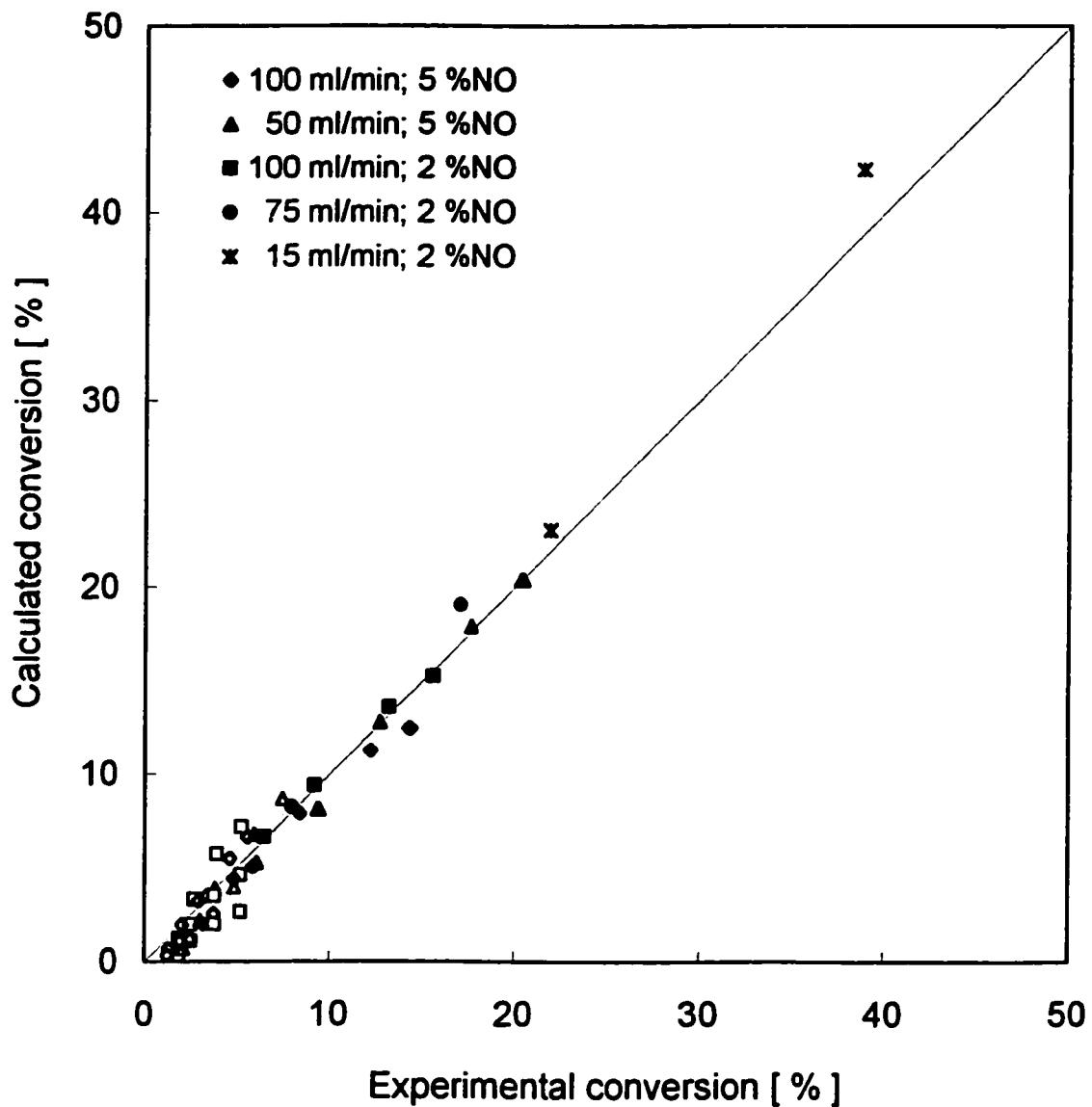


Figure 3.11 Predicted versus experimental conversion of nitric oxide to nitrogen over LSMN-28 perovskite ($r = k_{NO} \cdot P_{NO} / (1 + K \cdot P_{O_2})$); parameters given in Table 3.4 used in calculations; open symbols correspond to data obtained in the presence of oxygen added to the feed.

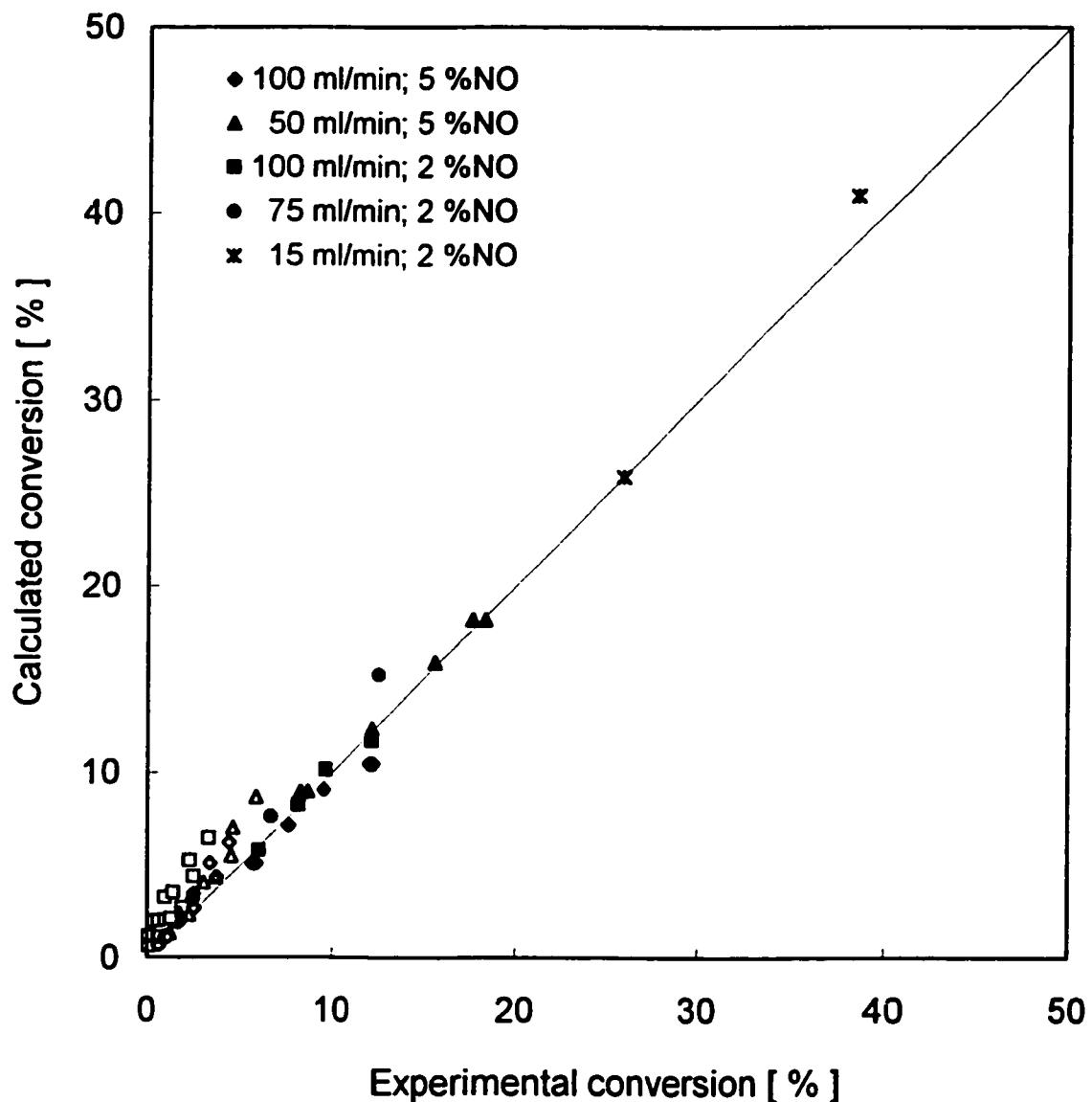


Figure 3.12 Predicted versus experimental conversion of nitric oxide to nitrogen over LSNC perovskite ($r = k_{NO} \cdot P_{NO} / (1 + K \cdot P_{O_2})$); parameters given in Table 3.4 used in calculations; open symbols correspond to data obtained in the presence of oxygen added to the feed.

Arrhenius plots of the two deduced parameters, k_{NO} and K , for the three catalysts are shown in Figure 3.13. Both parameters exhibit expected dependency on temperature.

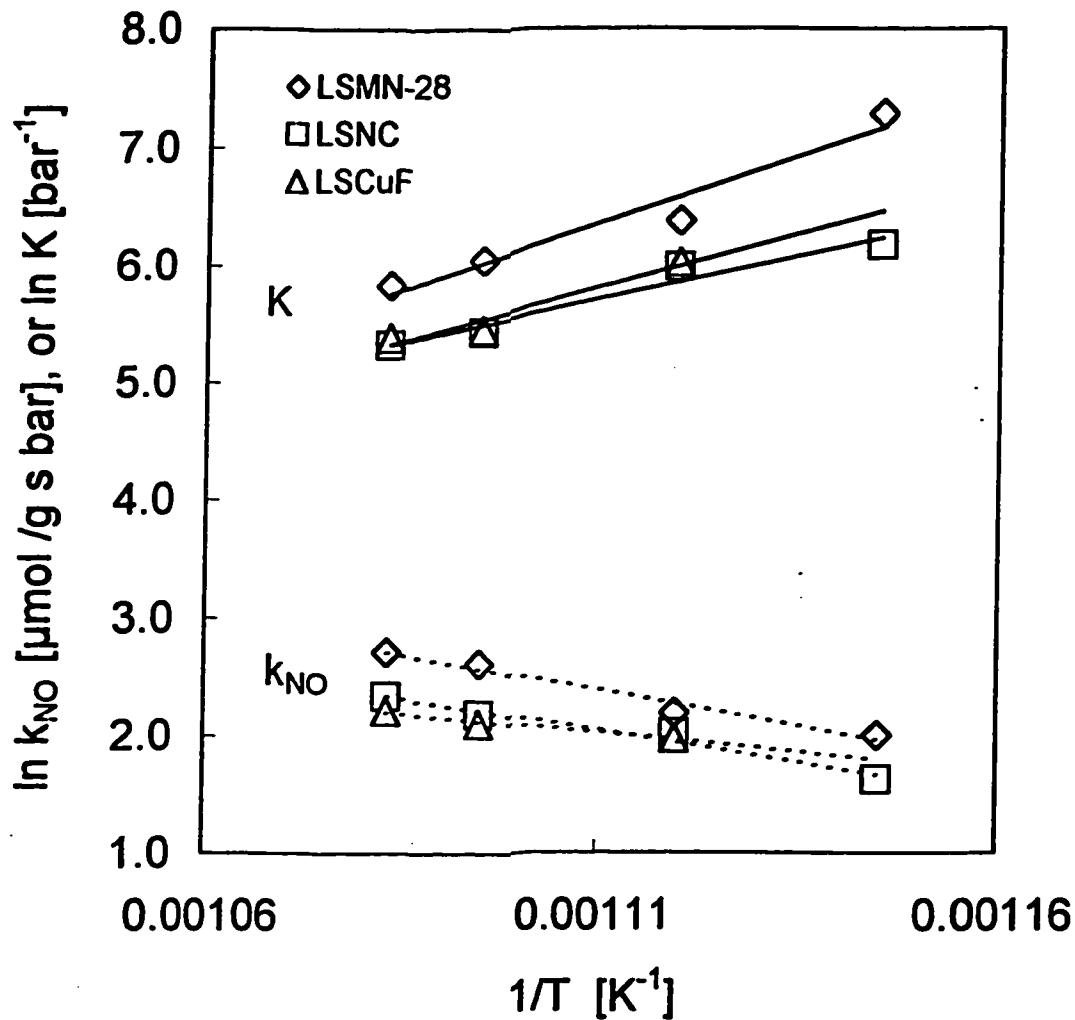


Figure 3.13 Arrhenius plot for k_{NO} (dotted line) and for K (full line) of the kinetic model
 $r = k_{NO} \cdot P_{NO} / (1 + K \cdot P_{O_2})$.

Both parameters exhibit expected dependency on temperature. The values of corresponding apparent activation energy, E_{app} , of pre-exponential factor A and of the enthalpy and entropy of oxygen adsorption ΔH_{ad} and ΔS_{ad} are given in Table 3.4.

Table 3.4 Parameters for the kinetic model: $r = k_{NO} \cdot P_{NO} / (1 + K \cdot P_{O_2})$

Composition	δ^a	SSA	E_{app}	$\ln A^b$	$-\Delta H_{ad}$	$-\Delta S_{ad}$
		m^2/g	kJ/mol	$\mu\text{mol/g}\cdot\text{s}\cdot\text{bar}$	kJ/mol	J/mol K
LSMN-28	0.065	12.7	102	16.0	188	156
LSNC	0.175	9.0	92	14.3	122	88
LSCuF	0.100	10.1	55	9.3	152	121

^a: oxygen vacancies based on Sr substitution

^b: $\ln A = \ln k_{NO} + E_{app}/RT$

In spite of the possibility that the adsorption constants may be interpreted in different ways, these values are in a reasonable agreement with some similar data available in literature. For example, for Mn_2O_3 Yamashita and Vannice [6] found a value of $-\Delta H_{ad}=146$ kJ/mol, whereas for Cu-ZSM-5 the calculated $-\Delta H_{ad}=108$ kJ/mol [13]. These values are somewhat higher than $-\Delta H_{ad}=73$ kJ/mol published by Amirmazmi et al., for Co_3O_4 [4]. Even though the exact interpretation of the deduced values of ΔH_{ad} is difficult, it is interesting to note their correlation with the formal value of nominal oxygen nonstoichiometry δ . The highest value of adsorption constant was obtained for LSMN-28, the composition having the lowest δ (0.065), while the lowest value was deduced for LSNC having the highest δ (0.175). This would be expected for the adsorption of oxygen since on perovskites with higher number of oxygen vacancies the oxygen adsorption is weaker.

The simple kinetic model deduced for the higher temperature range may be related to a mechanism conceptually similar to that outlined above for the low temperatures or previously for Cu-ZSM-5 [16]. At these higher temperatures the bulk oxygen mobility may be considered as sufficiently fast to maintain, by equilibration with the gas phase

oxygen a high population of reactive surface oxygen species, required for the formation of dinitrogen intermediate. Thus, above some low gas phase oxygen concentration the population of surface oxygen is no longer increased. At the same time, similarly as in the case of lower temperatures, at least two parallel reactions take place at the catalyst surface. The first reaction involves again adsorption of NO on some specific oxygen species to form an intermediate, possibly a dimer-type with an N-N bond and allowing an easy decomposition to dinitrogen. The second, inhibiting reaction involves formation of free nitrates which is increased in the presence of gas phase oxygen. The fast oxygen mobility would explain the first order dependence on oxygen in the inhibition term. Since the equilibrium constant to form the inhibiting nitrates decreases with temperature, the inhibition by oxygen also decreases. On the surface of the present perovskites, formation of LaONO_3 and $\text{Sr}(\text{NO}_3)_2$ stable to 848 and 908 K respectively [32] may be anticipated.

Overall, we may assume, that on perovskites, the nitric oxide decomposition takes place via some surface oxygen involving intermediate, while its inhibition is due to the formation, by an activated process, of unidentate and/or free nitrate species, giving no dinitrogen, but rather NO_2 (at lower temperatures) or NO (at higher temperatures). Depending on temperature influencing the stability of individual species, the surface equilibria and oxygen mobility the apparent kinetics may change.

3.6 Summary and Conclusions

Decomposition of nitric oxide over perovskites is evidently more complex than generally admitted. The complexity of nitric oxide decomposition is most likely general, not necessarily restricted to perovskites, but has apparently never been verified by studies covering sufficiently wide range of experimental conditions.

Depending on composition and on temperature, the overall kinetics may change substantially. Adsorbed oxygen, which may exist in a variety of forms, as well as its mobility, appears to play the central role in the mechanism. Two parallel reactions involving surface oxygen species, possibly different, may take place. One of these gives an intermediate consisting of an adsorbed dimer-type species with an N-N bond, which is easily decomposed to dinitrogen. The other reaction leads in the excess of oxygen to the formation of unidentate or free nitrate species, which can decompose only to NO_2 or NO . This reaction constitutes the inhibition. Nevertheless, in relation with the chemistry of oxygen and nitric oxide adsorption the degree of oxygen inhibition is very much dependent on temperature and the perovskite composition. Between 723 and 823 K it is rather weak and nearly constant (for LSCuF and LSMN-28), increasing fast with temperature between 823 and 873 K. For all three catalysts the inhibition is the strongest at 873 K and up to 923 K decreases with temperature. The observed oxygen inhibition is probably related to the formation of nitrate species, possibly unidentate and/or free nitrates, which cannot form an intermediate decomposing directly into dinitrogen (and oxygen).

Although between 873 and 923 K the inhibition of nitric oxide decomposition by oxygen at concentrations higher than 0.5 % can be described in terms of the adsorption constant using a simple model ($r = k_{\text{NO}} \cdot P_{\text{NO}} / (1 + K \cdot P_{\text{O}_2})$), the actual reaction mechanism may still involve some adsorbed oxygen species as the active site for the formation of intermediate.

Of the three perovskites studied, $\text{La}_{0.87}\text{Sr}_{0.13}\text{Mn}_{0.2}\text{Ni}_{0.8}\text{O}_{3-\delta}$ is the most active at the higher temperatures and over this composition the NO decomposition is the least affected (inhibited) by oxygen. On the other hand, $\text{La}_{0.8}\text{Sr}_{0.2}\text{Cu}_{0.15}\text{Fe}_{0.85}\text{O}_{3-\delta}$ is the most active at the lower temperatures, where the oxygen inhibition is relatively weak. Over $\text{La}_{0.66}\text{Sr}_{0.34}\text{Ni}_{0.3}\text{Co}_{0.7}\text{O}_{3-\delta}$ the oxygen inhibition is the strongest, regardless the temperature.

3.7 Acknowledgement

This work has been mainly supported by grants from Natural Sciences and Engineering Research Council of Canada.

3.8 References

- [1] O. Kubaschewski, C.B. Alcock and P.J. Spencer, in *Materials Thermochemistry*, 6th Ed., Pergamon Press, Oxford, 1993, Tables, p. 293.
- [2] J.W. Hightower and D.A. van Leirsburg, in R.L. Klimisch and J.G. Larson (Editors), *The Catalytic Chemistry of Nitrogen Oxides*, Plenum Press, New York, 1975, p. 63.
- [3] E.R.S. Winter, *J. Catal.*, 22 (1971) 158.
- [4] A. Amirmazmi, J.E. Benson and M. Boudart, *J. Catal.*, 30 (1973) 55.
- [5] M.A. Vannice, A.B. Walters and X. Zhang, *J. Catal.*, 159 (1996) 119.
- [6] T. Yamashita and A. Vannice, *J. Catal.*, 163 (1996) 158.
- [7] H. Hamada, Y. Kintaichi, M. Sasaki and T. Ito, *Chem. Lett.*, 7 (1990) 1069.
- [8] M. Iwamoto and H. Hamada, *Catal. Today*, 10 (1991) 57.
- [9] Y. Teraoka, T. Harada, H. Furukawa and S. Kagawa, *Stud. Surf. Sci. Catal.*, 75 (1993) 2649.
- [10] H. Yasuda, T. Nitadori, N. Mizuno and M. Misono, *Bull. Chem. Soc. Jpn.*, 66 (1993) 3492.
- [11] Z. Zhao, X. Yang and Y. Wu, *Appl. Catal. B: Environmental*, 8 (1996) 281.
- [12] R. Bontchev, K. Cheskova, D. Mehandjiev, J. Darriet, *React. Kinet. Catal. Lett.*, 63 (1996) 121.
- [13] Y. Li and W.K. Hall, *J. Catal.*, 129 (1991) 202.
- [14] Y. Yokomichi, T. Nakayama, O. Okada, Y. Yokoi, I. Takahashi, H. Uchida, H. Ishikawa, R. Yamaguchi, H. Matsui and T. Yamabe, *Catal. Today*, 29 (1996) 155.
- [15] M. Shelef, *Catal. Lett.*, 15 (1992) 305.

- [16] J. Valyon and W.K. Hall, *J. Phys. Chem.*, 97 (1993) 1204.
- [17] S. Xie, G. Mestl, M.P. Rosynek and J.H. Lunsford, *J. Am. Chem. Soc.*, 119 (1997) 10186.
- [18] G. Mestl, M.P. Rosynek and J.H. Lunsford, *J. Phys. Chem. B*, 101 (1997) 9329.
- [19] C. Tofan, D. Klvana and J. Kirchnerova, *Appl. Catal. A, General*, (2001) in print.
- [20] J. Kirchnerova and D. Klvana, *Solid State Ionics*, 123 (1999) 307.
- [21] H.S. Fogler, *Elements of Chemical Reaction Engineering*, Prentice Hall, Englewood Cliffs, N J, 1991.
- [22] T. Yamashita, A. Vanice, *Appl. Catal. B: Environmental*, 13 (1997) 141.
- [23] H. M. Zhang, Y. Shimizu, Y. Teraoka, N. Miura, N. Yamazoe, *J. Catal.*, 121 (1990) 432.
- [24] J.-P. Joly, D. Klvana and J. Kirchnerova, *React. Kinet. Catal. Lett.*, 68 (1999) 249.
- [25] G. Busca, V. Lorenzelli, *J. Catal.*, 72 (1981) 303.
- [26] M. C. Kung, H. H. Kung, *Catal. Rev.*, 27 (1985) 425.
- [27] J. Lin, A.T.S. Wee, K.L. Tan, K.G. Neoh and W.K. Teo, *Inorg. Chem.*, 32 (1993) 5522.
- [28] A. W. Aylor, S. C. Larsen, J. A. Reimer and A. T. Bell, *J. Catal.*, 157 (1995) 592.
- [29] S.-J. Huang, A.B. Walters and M.A. Vannice, *J. Catal.*, 192 (2000) 29.
- [30] P.W. Park, J.K. Kil, H.H. Kung and M.C. Kung, *Catal. Today*, 42 (1998) 51.
- [31] A. Lawson, *J. Catal.*, 29 (1972) 297.
- [32] C. C. Addison and N. Logan, in H .J. Emeléus and A.G. Sharpe (Editors), *Advances in Inorganic Chemistry and Radiochemistry*, Academic Press, New York and London, (1964), p.114.

CHAPITRE IV
DECOMPOSITION OF NITRIC OXIDE OVER PEROVSKITE OXIDE
CATALYSTS :EFFECT OF CO₂, H₂O AND CH₄

Reference :

C. Tofan, D. Klvana* et J. Kirchnerova (2001), Decomposition of Nitric Oxide over Perovskite Oxide Catalysts: Effect of CO₂, H₂O and CH₄, Applied Catalysis B : Environmental (accepted with corrections).

Keywords :

perovskite catalysts, direct nitric oxide decomposition, inhibition by carbon dioxide, inhibition by water, nitric oxide reduction by methane over perovskites

* Author for correspondence, e-mail address : danilo.klvana@courriel.polymtl.ca

4.1 Contexte*

Un effluent gazeux issu du processus de combustion a une composition généralement complexe. On y retrouve du dioxyde de carbone, de la vapeur d'eau et selon les conditions opératoires, de l'oxygène, des hydrocarbures imbrûlés, du monoxyde de carbone et des oxydes d'azote.

L'effet de l'oxygène sur la décomposition du NO a déjà été traité dans le chapitre précédent. On a considéré intéressant d'élargir l'étude en tentant de quantifier les effets des autres gaz (CO_2 , H_2O et CH_4) sur la décomposition du NO. Dans la littérature on n'a pas trouvé une telle étude pour le cas des catalyseurs de type pérovskite.

Le présent chapitre, qui est aussi sous la forme d'un article, montre que le dioxyde de carbone et la vapeur d'eau ont un effet inhibiteur sur la décomposition du NO, l'effet de l' H_2O étant moindre que celui du CO_2 . Les deux effets sont activés puisqu'ils augmentent avec la température. L'analyse cinétique des données a permis de dégager pour les trois catalyseurs testés les énergies apparentes d'inhibition du CO_2 et H_2O .

La présence d'un réducteur (CH_4) dans le mélange réactionnel a une influence positive sur la formation de l'azote, la conversion du NO en N_2 étant jusqu'à quatre fois plus grande en présence du CH_4 .

*ce texte n'est pas inclus dans l'article

4.2 Abstract

Direct nitric oxide decomposition over perovskites is fairly slow and complex, its mechanism changing dramatically with temperature. Previous kinetic study for three representative compositions ($\text{La}_{0.87}\text{Sr}_{0.13}\text{Mn}_{0.2}\text{Ni}_{0.8}\text{O}_{3-\delta}$, $\text{La}_{0.66}\text{Sr}_{0.34}\text{Ni}_{0.3}\text{Co}_{0.7}\text{O}_{3-\delta}$ and $\text{La}_{0.8}\text{Sr}_{0.2}\text{Cu}_{0.15}\text{Fe}_{0.85}\text{O}_{3-\delta}$) has shown that depending on the temperature range, inhibition effect of oxygen either increases or decreases with temperature. This paper concerns the effect of CO_2 , H_2O and CH_4 on the nitric oxide decomposition over the same perovskites studied at a steady state in a plug-flow reactor with 1 g catalyst and total flowrates of 50 or 100 ml/min of 2 or 5 %NO. The effect of carbon dioxide (0.5 – 10 %) was evaluated between 873 and 923 K, whereas that of H_2O vapor (1.6 or 2.5 %) from 723 to 923 K. Both CO_2 and H_2O inhibit the NO decomposition, but inhibition by CO_2 is considerably stronger. These effects are, over the three catalysts, increasing with temperature. Kinetic parameters for the inhibiting effects of CO_2 and H_2O over the three perovskites were determined. Addition of methane to the feed in the NO/ CH_4 ratio of four increases conversion of NO to N_2 about two to four times, depending on the initial NO concentration and on temperature. This, however, is still much too low for practical application. Furthermore, the rates of nitric oxide reduction by methane are substantially slower than that of methane oxidation in air. Thus, perovskites do not seem to be suitable for catalytic selective NO reduction with methane.

4.3 Introduction

Reduction of nitrogen oxides emissions, the most serious pollutants, which contribute to the increase of tropospheric ozone levels, acidification of environment and general damage to human health, has become one of the greatest challenges in environmental protection [1]. Canadian NO_x ($\text{NO} + \text{NO}_2$) emissions totaled about 2000 kt in 1995, which represented 9 % of the total NO_x emissions in North America. Canadian emissions are primarily associated with the transportation sector (about 59 %), with

industrial and non-industrial fuel combustion (about 28 %) and electrical power generation at about 12 % [2]. Similar situation exists in other industrial countries.

A practical NO abatement catalyst must show sustained activity in a rather large temperature range, with sudden temperature changes, generally in the presence of relatively high concentrations of gas-phase oxygen, water vapor and carbon dioxide. Depending on combustion conditions and on the type of fuel, the gas stream to be treated may also contain unburnt hydrocarbons, carbon monoxide, sulfur oxides, oxygenated hydrocarbons, particulates, and other by-products (Table 4.1). Moreover, the waste-gas streams must usually interact with catalyst at high flowrates. These conditions demand mechanically strong, shock-resistant, highly performing and sulfur poisoning resistant catalyst.

Table 4.1 Composition of exhaust gases from mobile and stationary sources

Source	T, K	[NO _x], %	[O ₂], %	Other
Diesel engine	473 - 673	0.002 – 0.07	5 - 10	CO _x (10%), H ₂ O (10%), HC(0.05-0.1%), particulates, SO _x (0.01-0.05)
Power plants	473 - 723	0.04 – 0.1	4 - 10	CO _x (5-7%), H ₂ O(10-15%), SO _x (0.001-0.3%)

For example, in the case of NO_x removal from effluents from diesel automotive engines (from 3 to below 0.6 g per mile) the estimated performance of reaction at 773 K is about 1.5×10^{-7} mol NO_x/m²·min, based on 4 kg catalyst with specific surface area of 150 m²/g (i.e. 0.375 μ mol/g·s). Among the numerous catalysts tested for direct NO decomposition into nitrogen and oxygen [3,4] the most active at 773 K and low flowrates (moderate) is Cu-ZSM-5 [5]. Ag/Co₃O₄ is 20 times slower [6], and other simple oxides 600 times (CuO) or more (Mn₂O₃, La₂O₃) [7,8]. At this temperature, the highest known activities of multi-metal perovskite oxides, which were for some time considered as having good potential [9,10], exhibit nearly 10 times lower activity than

$\text{Ag/Co}_3\text{O}_4$. Using the rate expression proposed for Cu-ZSM-5 catalysts by Li and Hall [5], the calculated rate of NO removal at 773 K, GHSV=50000 h^{-1} , $[\text{NO}] = 2500 \text{ ppm}$, and $[\text{O}_2] = 8 \%$ is approximately $0.05 \mu\text{mol/g}\cdot\text{s}$. This rate is lower by a factor of ten than the required rate for a small, mobile NO_x source. However, this conclusion is tentative because the literature contains practically no data on activity of the catalysts under practical conditions. Under real conditions the NO decomposition rates may be slower due to various inhibition effects of combustion products. Of course, such effects are expected to be function of catalyst composition. For example, in humid atmosphere the Cu-ZSM-5 are susceptible to dealumination, permanently losing their performance [11].

For simple oxides and for perovskites the influence of CO_2 and water vapor on NO decomposition is practically unknown, except for the work by Lawson who observed that water strongly inhibited NO decomposition over copper chromite [12]. Some limited data are available for the case of hydrocarbon combustion [13]. Furthermore, previous studies in our laboratories of methane combustion over $\text{La}_{0.65}\text{Sr}_{0.35}\text{Ni}_{0.3}\text{Co}_{0.7}\text{O}_3$ perovskite indicated that at temperatures above 820 K the reaction is noticeably inhibited by carbon dioxide, but not by water [14]. Combustion of propane proceeding at temperatures below 700 K was also inhibited, but to a considerably lower degree [15]. On the other hand, combustion of toluene at 600 K over a cordierite monolith supported $\text{La}_{0.65}\text{Sr}_{0.35}\text{Ni}_{0.29}\text{Co}_{0.69}\text{Fe}_{0.02}\text{O}_3$ perovskite was not inhibited measurably, even by large excess of carbon dioxide [16]. It was also observed that the deactivation of $\text{La}_{0.65}\text{Sr}_{0.35}\text{Ni}_{0.29}\text{Co}_{0.69}\text{Fe}_{0.02}\text{O}_3$ (14 wt% on silico-aluminate fibre) by 260 ppm methyl-mercaptan during methane combustion at 817 K slowed when 2 % H_2O was added [17], while carbon dioxide had nearly no effect, at least at lower temperature.

In spite of the low activities of perovskites in NO decomposition, with respect to practical needs [18,19], a study of the effect of CO_2 and H_2O on the NO decomposition into N_2 was considered worthwhile. Knowledge of their extent might be useful in understanding the complexity of the reactions involved in the NO decomposition.

This paper concerns the effect of CO₂ and H₂O on the direct nitric oxide decomposition over three perovskites: La_{0.87}Sr_{0.13}Mn_{0.2}Ni_{0.8}O_{3-δ} (LSMN-28), La_{0.66}Sr_{0.34}Ni_{0.3}Co_{0.7}O_{3-δ} (LSNC), and La_{0.8}Sr_{0.2}Cu_{0.15}Fe_{0.85}O_{3-δ} (LSCuF). Furthermore, since catalytic reduction of NO by using hydrocarbons, especially methane, represents an attractive alternative to NO_x removal [20], we have concluded the study by a brief complementary evaluation of the effect of methane on the rate of NO decomposition.

4.4 Experimental

The three perovskites were prepared by a method involving aqueous, highly homogeneous precursor slurry obtained by suspending lanthanum hydroxide in a solution of corresponding metal nitrates. The precursor slurry was dried under vacuum (freeze-dried), and then calcined in air under controlled conditions, typically 12 h at 863 K, followed by 4 h at 923 K. The obtained powders, particle size < 10 μm, were nearly phase pure and their specific surface area (SSA) determined by a single point method BET with nitrogen as an adsorbate was 12.7, 9.0, and 10.1 m²/g respectively for LSMN-28, LSNC and LSCuF. Details of preparation and characterization are presented elsewhere [18,21].

The experimental conditions under which we have studied the effect of different gases on nitric oxide decomposition were essentially the same as those used previously [18, 19]. Briefly, the activities were measured using a stainless steel U-shape reactor operating at a steady-state plug-flow mode. The total gas flow through catalyst bed was set to 50 or 100 ml/min using mass flow controllers (MKS and Brooks 580). The composition of the reaction gas was: NO (2 or 5 %) – O₂ (0-10 %) – CO₂ (0-10 %) – H₂O (0; 1.6; 2.5 %) – He (balance). H₂O was added to the feed by passing the flow of He through a saturator maintained at 298 K. The catalyst powder (1 g) was diluted by 7 ml pumice, particle size 350 - 416 μm, pre-calcined 8 h at 923 K. The temperature was varied stepwise between 723 and 923 K. Two K-type thermocouples inserted at the inlet

and outlet of the catalytic bed monitored the temperature. A gas chromatograph equipped with 5 Å molecular sieve column was used to quantify the N₂ present in the gas flow, first removing water by passing the effluents over a desiccant (Drierite) incorporated after the reactor. Before starting the evaluation the catalyst bed was purged several hours at 773 K by pure helium to remove adsorbed air and impurities. Between the experiments the reactor was cooled down to ambient temperature under a flow of helium. The experimental data were taken after 1 h on stream at each temperature, when the catalytic reaction practically reached steady-state conditions.

Catalytic activity in nitric oxide decomposition was evaluated in terms of the NO conversion into N₂, $x_{N_2} = 2[N_2]_{out} / [NO]_{in}$.

4.5 Results and discussion

4.5.1 Perovskites characteristics and their activity in NO decomposition

Our previous studies have indicated that activities of perovskite oxides in direct NO decomposition are in general rather low, falling within about the same order of magnitude. Nevertheless, some activity improvement can be obtained by judicious formulation of composition [9,18]. For three representative perovskites, which among a group of ten different compositions showed the best performance, La_{0.87}Sr_{0.13}Mn_{0.2}Ni_{0.8}O_{3-δ} (LSMN-28), La_{0.66}Sr_{0.34}Ni_{0.3}Co_{0.7}O_{3-δ} (LSNC) and La_{0.8}Sr_{0.2}Cu_{0.15}Fe_{0.85}O_{3-δ} (LSCuF), a complete kinetic study has been carried out. In the temperature range between 723 and 923 K a change of mechanism occurs. LSMN-28 showed the highest activity at high temperatures, while LSCuF was the most active at lower temperatures (723-823 K) [18]. The overall catalytic performance is particularly sensitive to the inhibition effect by oxygen and its very strong dependence on temperature, which are also a function of composition. The results have shown that the oxygen inhibition, which is strongest at about 853 K and then starts to decrease with

temperature, is in the temperature range of 873-923 K, best represented by a relatively simple model ($r = k_{NO} \cdot P_{NO} / (1 + K \cdot P_{O_2})$) [19]. The strongest oxygen inhibition was observed for LSNC, although over this perovskite the oxygen adsorption is the weakest. Figure 4.1 illustrates the activities of the three catalysts and Table 4.2 summarizes the characteristic kinetic data.

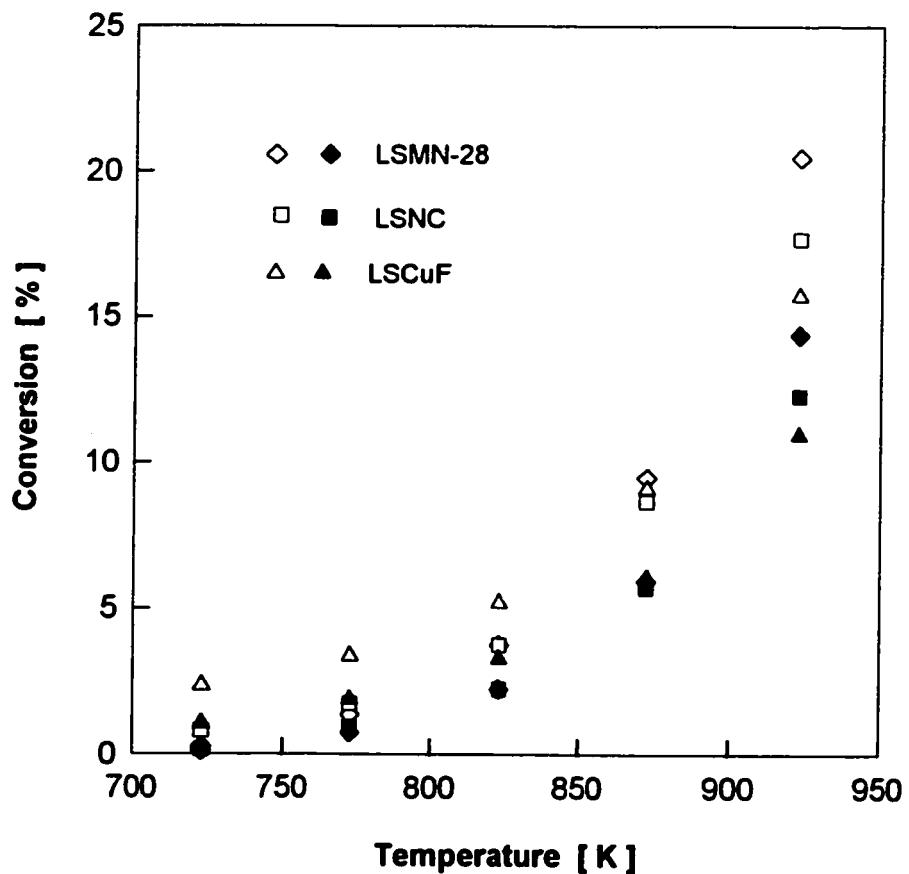


Figure 4.1 Conversion of 5 %NO to nitrogen over LSMN-28, LSNC and LSCuF perovskites (1 g) as a function of temperature; open symbols: 50 ml/min; full symbols: 100 ml/min.

Table 4.2 Parameters for the kinetic model: $r = k_{NO} \cdot P_{NO} / (1 + K \cdot P_{O_2})$, where
 $k_{NO} = A \cdot e^{(-E_{app}/RT)}$

Composition	δ^a	SSA	E_{app}	$\ln A$	ΔH_{ad}	ΔS_{ad}
		m^2/g	kJ/mol	$\mu\text{mol/g}\cdot\text{s}\cdot\text{bar}$	kJ/mol	J/mol K
LSMN-28	0.065	12.7	102	16.0	-188	-156
LSNC	0.175	9.0	92	14.3	-122	-88
LSCuF	0.100	10.1	55	9.3	-152	-121

^a: oxygen vacancies based on Sr substitution

4.5.2 Effect of carbon dioxide

Although unexpected, the effect of CO_2 added without addition of excess oxygen was found strongly inhibiting. Quantitative evaluation of this effect was therefore for practical reasons limited to upper temperature range (873-923 K), where the conversion of NO to N_2 was relatively high. It was for this temperature range for which the complete kinetics of direct NO decomposition was determined. As shown in Figures 4.2-4.4 for LSNM-28, LSNC and LSCuF respectively, for two temperatures of the studied range (873 and 923 K), addition of CO_2 to the feed significantly inhibits the NO decomposition and this effect increases with concentration increasing up to about 5 %.

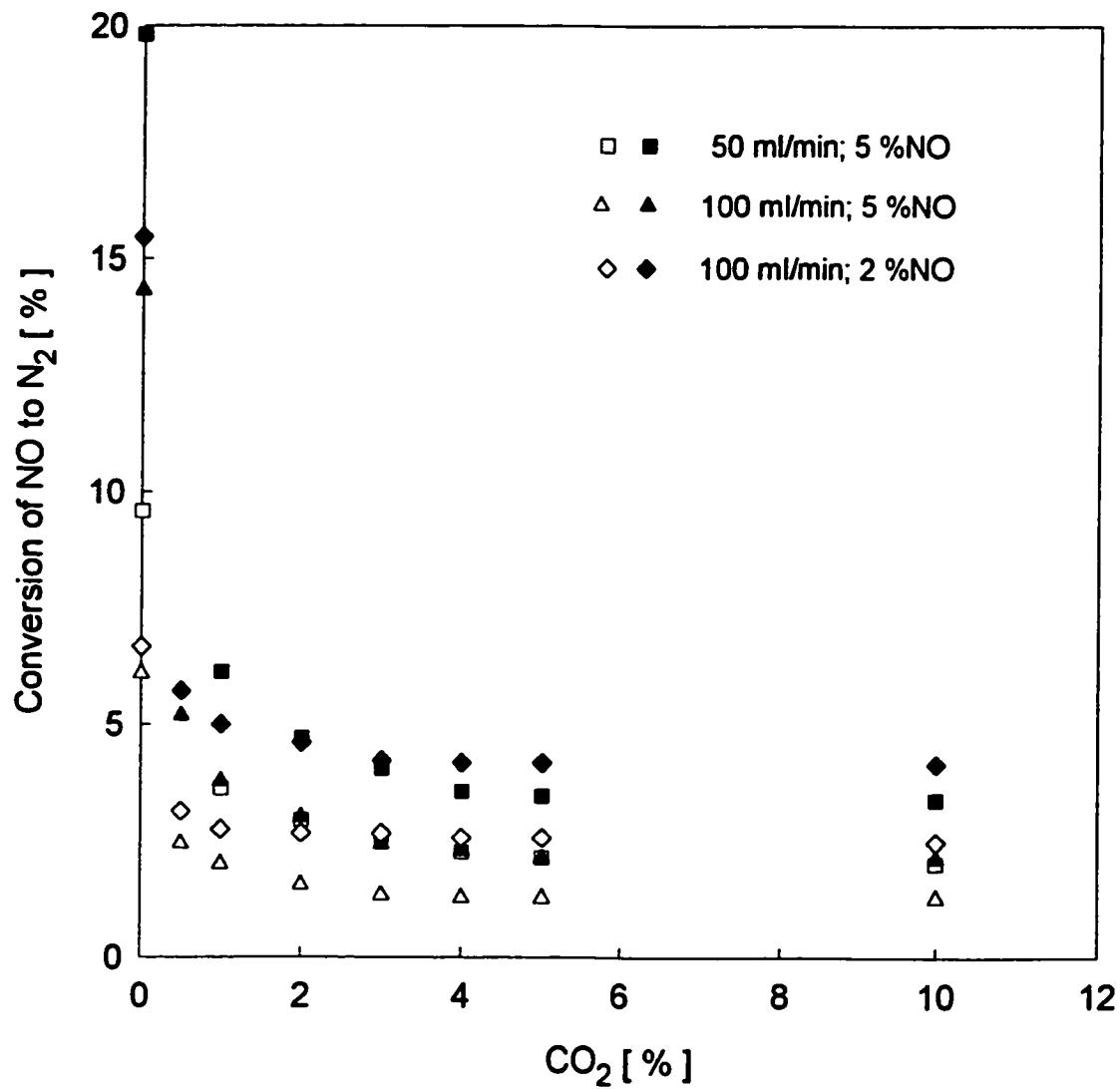


Figure 4.2 Effect of added CO_2 on direct NO decomposition to nitrogen over 1 g LSMN-28 perovskite at different flowrates and NO partial pressures at 873 K (open symbols) and 923 K (full symbols).

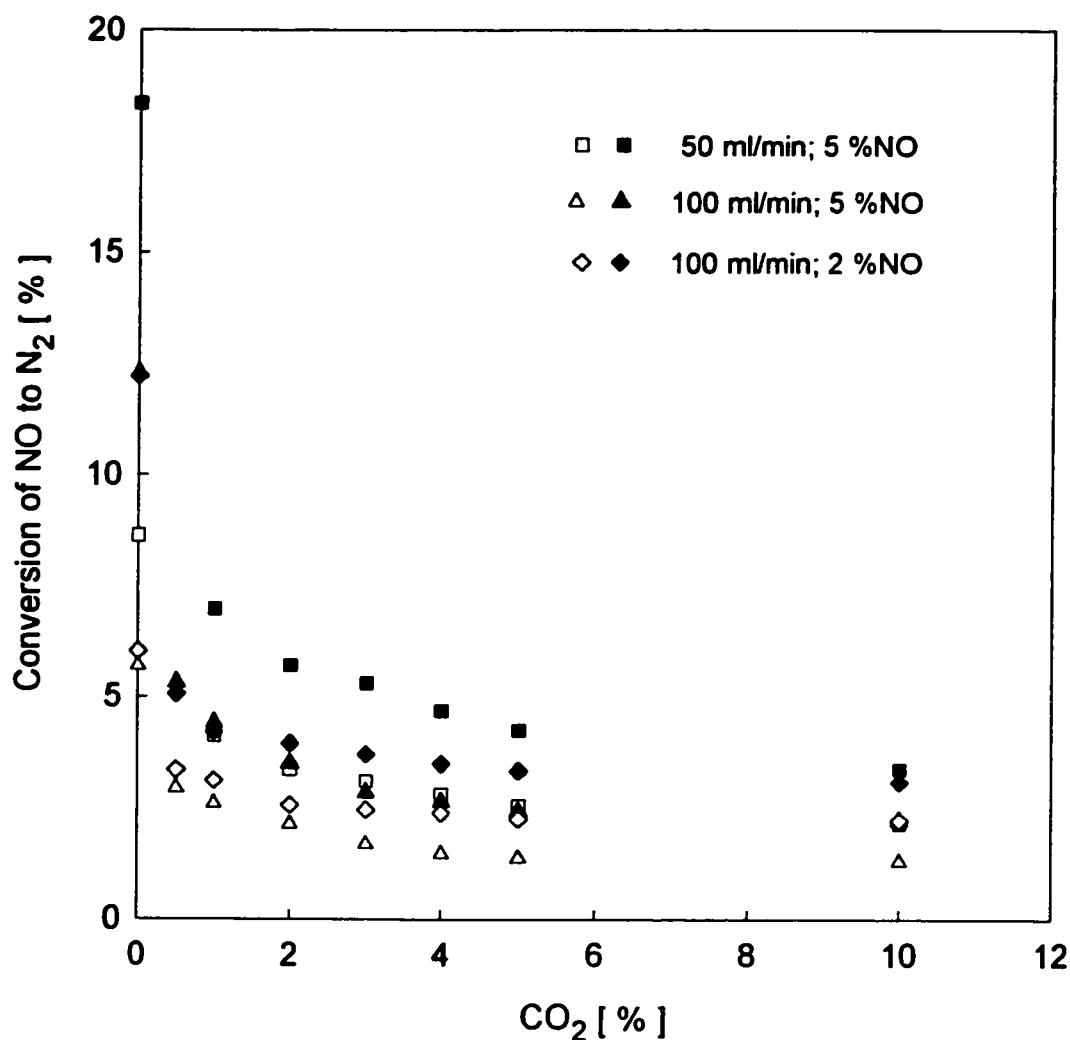


Figure 4.3 Effect of added CO_2 on direct NO decomposition to nitrogen over 1 g LSNC perovskite at different flowrates and NO partial pressures at 873 K (open symbols) and 923 K (full symbols).

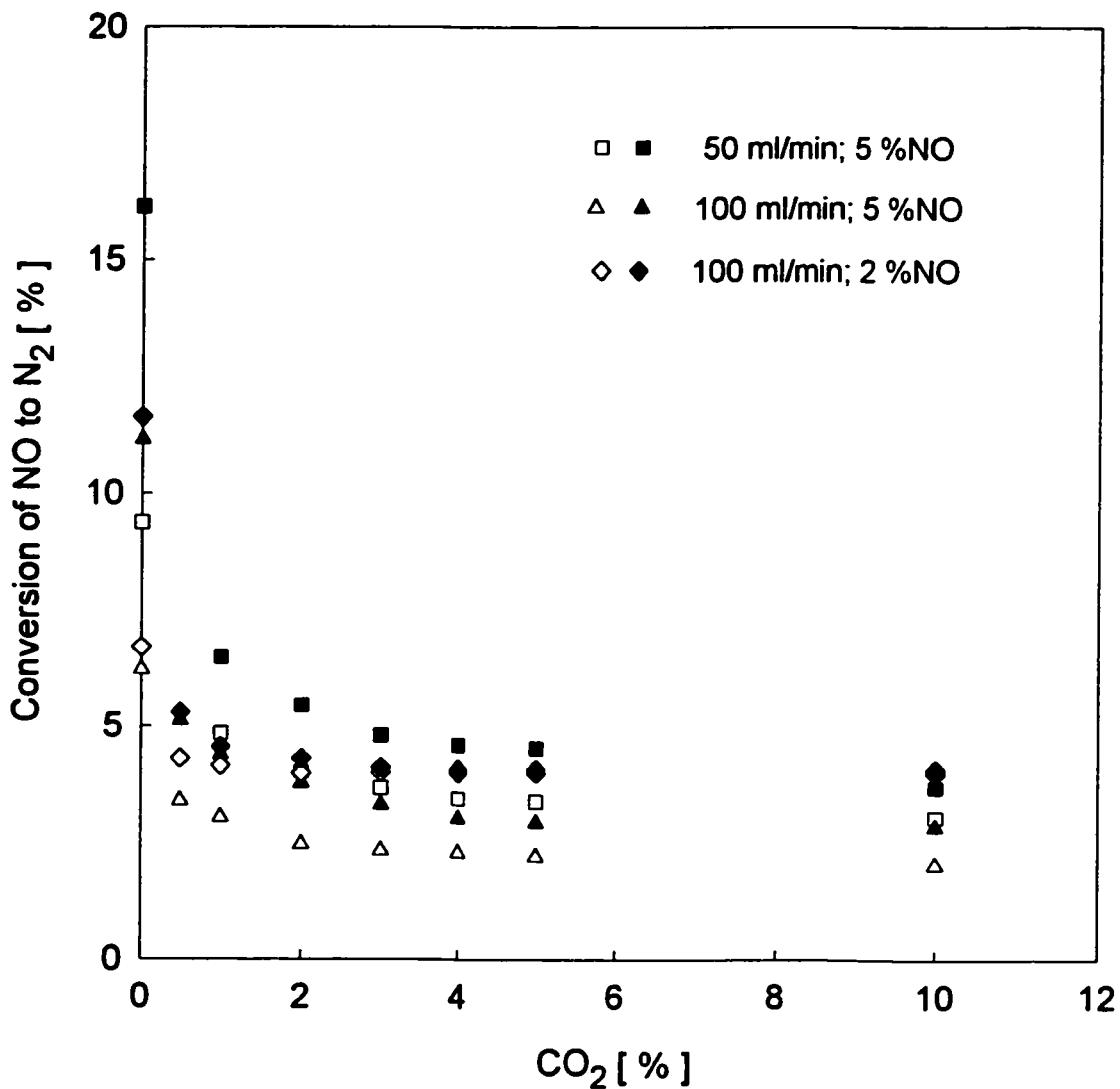


Figure 4.4 Effect of added CO₂ on direct NO decomposition to nitrogen over 1 g LSCuF perovskite at different flowrates and NO partial pressures at 873 K (open symbols) and 923 K (full symbols).

Higher CO₂ concentrations have nearly no additional effect, indicating some saturation effect. Similar saturation was observed for oxygen inhibition, which nevertheless, occurred at somehow lower concentrations. It should be noted, however, that this CO₂

inhibition effect is strictly reversible. On removing CO₂ from the feed, the original activity was always restored, even for the highest CO₂ concentrations. Very important feature of the CO₂ inhibition is the fact that in this temperature range, it increases with temperature. This contrasts the inhibition by oxygen, which in the same temperature range decreases as the temperature increases. Similarly contrasting is the dependence of CO₂ inhibition on flowrate and concentration of NO. While inhibition of oxygen decreases with decreasing flowrate, inhibition of CO₂ decreases with increasing flowrate and/or decreasing NO concentration. This inhibition might possibly result from an activated adsorption of some specific surface oxygen species, competing with the adsorption of NO to form the intermediate species leading to its decomposition. Indeed, on metal oxides and particularly on perovskites, CO₂ can adsorb via different species and mechanism [22]. Generally, in the low temperature range simple chemisorption, decreasing with temperature, occurs. Thus, propane combustion over LSNC at temperatures below 673 K was only weakly inhibited by CO₂, and the inhibition decreased with temperature [15], while combustion of toluene was at the same temperatures not inhibited [16]. In contrast, CO₂ inhibition of methane combustion over LSNC catalyst was at temperatures above 723 K somewhat stronger and was activated [14].

Although the CO₂ inhibition pattern of NO decomposition is more or less the same for all three perovskites, the overall effect is strongest and most dependent on temperature in the case of LSMN-28 and weakest for LSCuF. Indeed, in view of relative acidity of individual B-site ions, this trend would be expected. Judging from the stability of metal carbonates [23], the affinity of individual oxides for CO₂ adsorption, or their basicity, decreases in the following order: SrO > La₂O₃ > Mn₂O₃ > Ni₂O₃ > Co₂O₃ > CuO > Fe₂O₃.

Several different rate models were tested to find a simple kinetic equation that would take into account the inhibiting effect of carbon dioxide, covering only the

concentrations below the saturation effect, i.e. up to 2%. The linear regression analysis was used to fit the collected experimental data to integrated forms of individual kinetic equations. However, only the data directly related to the effect of CO₂ were used in this fitting. The following kinetic model provided a good fit of the data for all three perovskites tested:

$$r = \frac{k_{NO}P_{NO}}{1 + KP_{O_2} + k_{inhCO_2}P_{CO_2}}$$

Instead of imposing the previously obtained values for k_{NO} and K in the fitting, these values were also determined by the fitting. Arrhenius plots of k_{inhCO_2} for the three catalysts are shown in Figure 4.5, where they are compared with k_{inhH_2O} discussed in the next section.

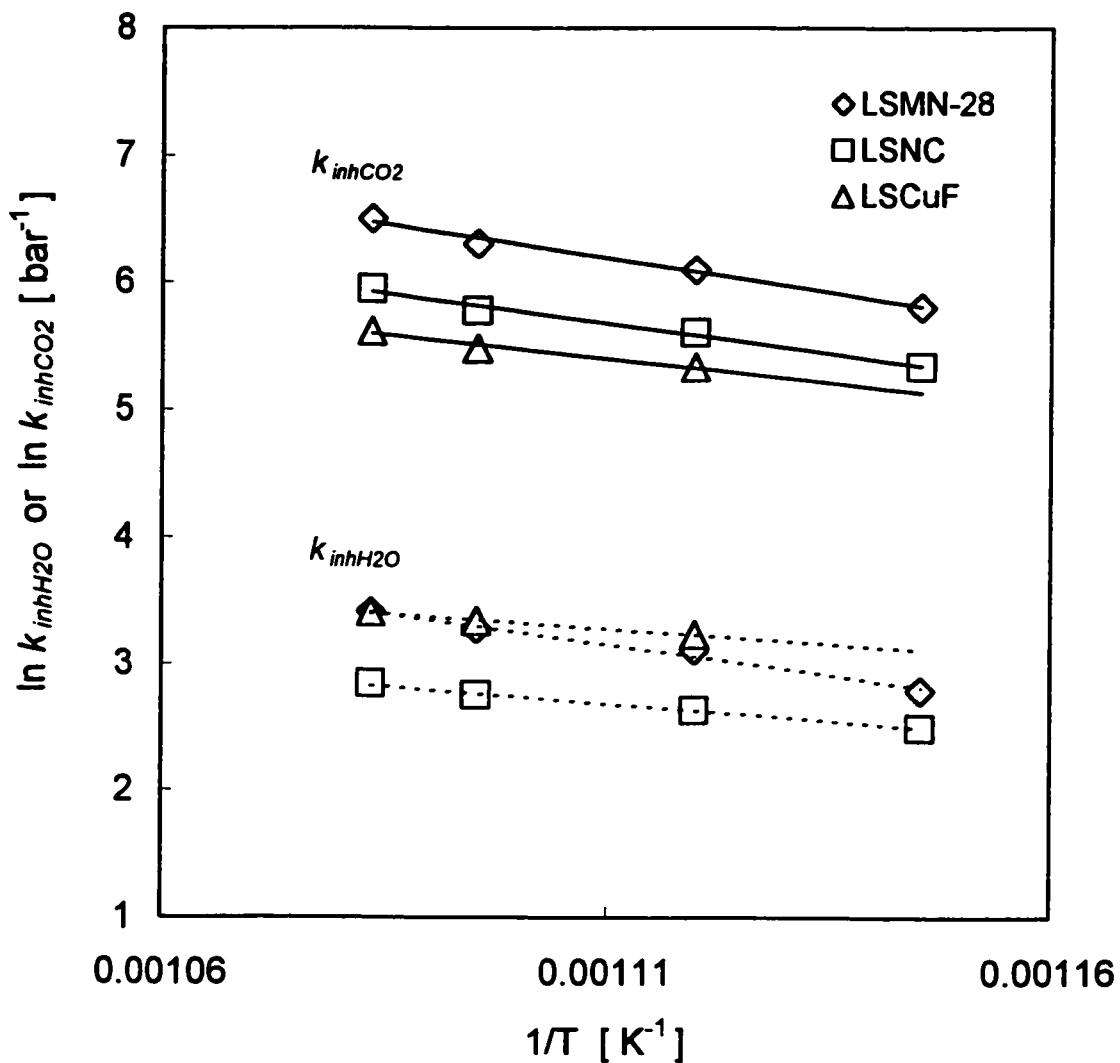


Figure 4.5 Arrhenius plots for the inhibition constants k_{inhCO_2} (full lines) and k_{inhH_2O} (dotted lines) of the kinetic models representing the inhibition of nitric oxide decomposition by CO_2 and H_2O over three perovskite catalysts.

The values of the corresponding apparent activation energy and of the pre-exponential factor are given in Table 4.3.

Table 4.3 Apparent activation energies and preexponential factors for the constants representing inhibition by CO_2 and H_2O of NO direct decomposition ($r = k_{\text{NO}} \cdot P_{\text{NO}} / (1 + K \cdot P_{\text{O}_2} + k_{\text{inh},j} P_j)$) over three perovskite catalysts

Perovskite	$(E_{\text{inh CO}_2})_{\text{app}}$ kJ/mol	$\ln A_{\text{inh CO}_2}^*$ bar ⁻¹	$(E_{\text{inh H}_2\text{O}})_{\text{app}}$ kJ/mol	$\ln A_{\text{inh H}_2\text{O}}^*$ bar ⁻¹
LSMN-28	89	18.1	81	14.0
LSNC	78	16.1	46	8.8
LSCuF	63	13.8	40	8.6

*: $\ln A_{\text{inh},j} = \ln k_{\text{inh},j} + (E_{\text{inh},j})_{\text{app}} / RT$; $j = \text{CO}_2$ or H_2O

Although the values of k_{NO} and K resulting from fitting this limited data set are slightly different from those based on fitting a larger set of data including those with added oxygen [19], within the error of their determination the agreement is very good. Indirectly, this gives more credibility to the model. As expected, the lowest carbon dioxide apparent inhibition energy was observed in the case of LSCuF.

4.5.3 Effect of water

Water vapor, invariably present in any combustion effluents in relatively large concentrations, adsorbs at low temperatures easily on all metal oxide catalysts, but the strength of the adsorption varies with the character of the oxide. This may affect various reactions, similarly as adsorption of carbon dioxide interferes in numerous processes. In fact, Lawson has observed a severe inhibition by water of NO decomposition over copper chromite [12]. For the present case of NO decomposition over LSMN-28, LSCN and LSCuF perovskites the inhibition by water is relatively weak in comparison with that of carbon dioxide and oxygen as shown for LSMN-28 in Figure 4.6, where the three effects are compared.

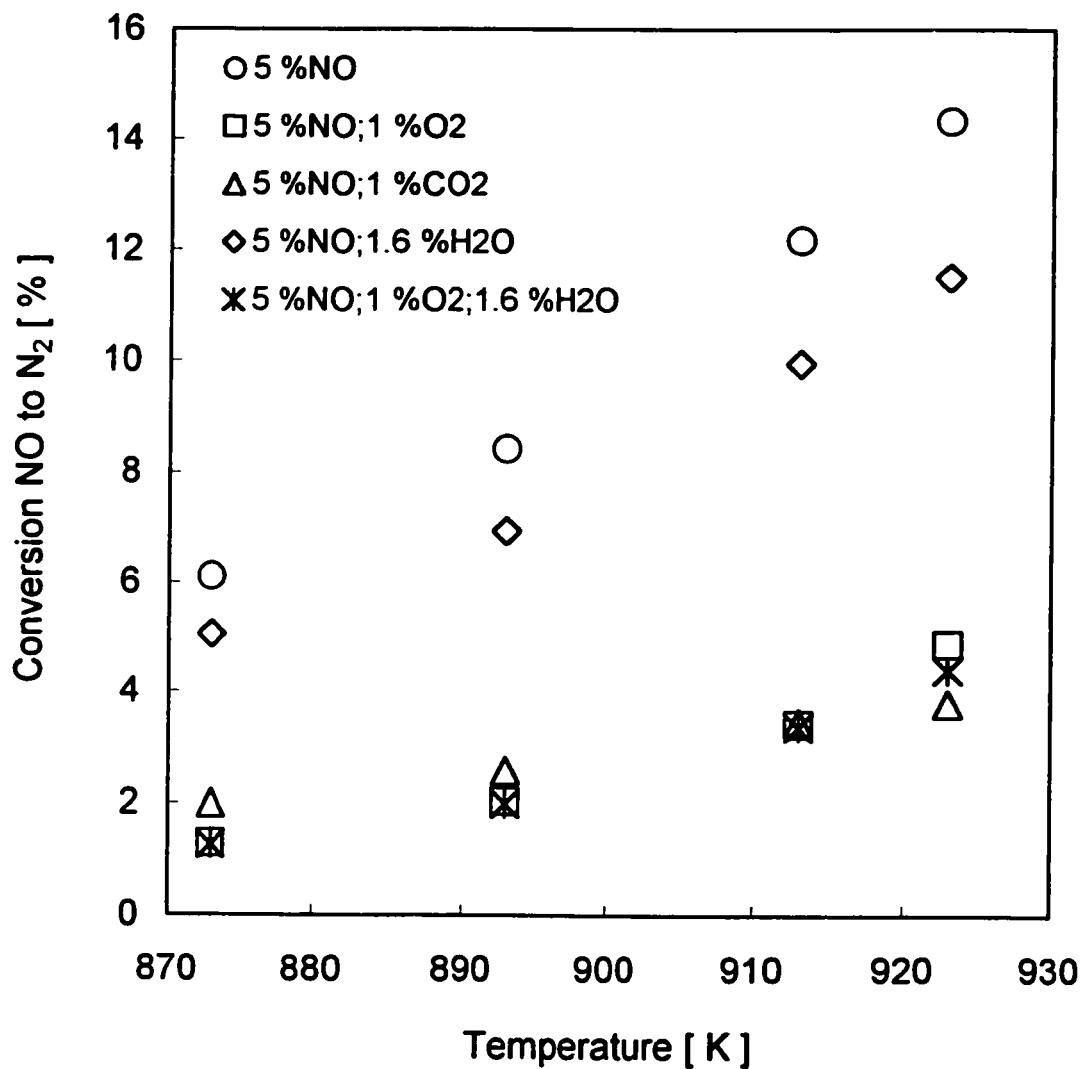


Figure 4.6 Effect of oxygen, carbon dioxide and water on direct NO decomposition to nitrogen over 1 g LSMN-28 perovskite; total flowrate 100 ml/min.

It was therefore possible to determine the extent of this water inhibition, which is reversible, similarly as is that of CO_2 , over a wider range of temperatures. Variation of the H_2O inhibition with temperature and other experimental conditions is illustrated in terms of relative activities in Figures 4.7 (for LSMN-28 and LSNC) and 4.8 (for LSCuF). The data in these figures indicate that the H_2O inhibition increases with temperature over the whole range studied. However, the effect is very weak up to about 823 K for all three perovskites. In the case of LSMN-28 and LSNC a sudden increase of H_2O inhibition is observed between 823 and 873 K, while between 873 K and 923 K the increase of this inhibition with temperature is again relatively slow. Furthermore, the sudden increase of H_2O inhibition is accompanied by a significant dependence on flowrate and NO concentration. At 723 and 773 K H_2O inhibition is more or less independent of flowrate and NO concentration. At 823 K, it is nearly independent of flowrate, but depends on concentration, being considerably stronger for 5% NO than for 2% NO. Between 873 and 923 K, for these two perovskites, water inhibition is the weakest at 50 ml/min and 2 % NO. In the case of LSCuF seems to proceed through a somehow different mechanism, similarly as in the case of oxygen inhibition [19]. Over this perovskite, H_2O inhibition seems to increase significantly only above 873 K, and the observed change with temperature depends again also on flowrate and NO concentration. For LSCuF the dependence on flowrate and NO concentration of the H_2O inhibition appears not only stronger than in the case of other two perovskites, but also its dependence on flowrate and NO concentration is different. Water inhibition is weaker at 100 ml/min than at 50 ml/min. In addition, at temperatures lower than 823 K the effect appears stronger for higher concentration of NO, whereas above 823 K, it is weaker at lower NO concentration. This contrasts not only the behavior of LSMN-28 and LSNC, but also the CO_2 inhibition. Overall, it is evident that the H_2O inhibition is activated and that a change in mechanism of its effect on NO decomposition is occurring at least once, at 873 K. Consequently, search of a kinetic model covering the H_2O inhibition was limited to the narrow temperature range of 873 to 923 K.

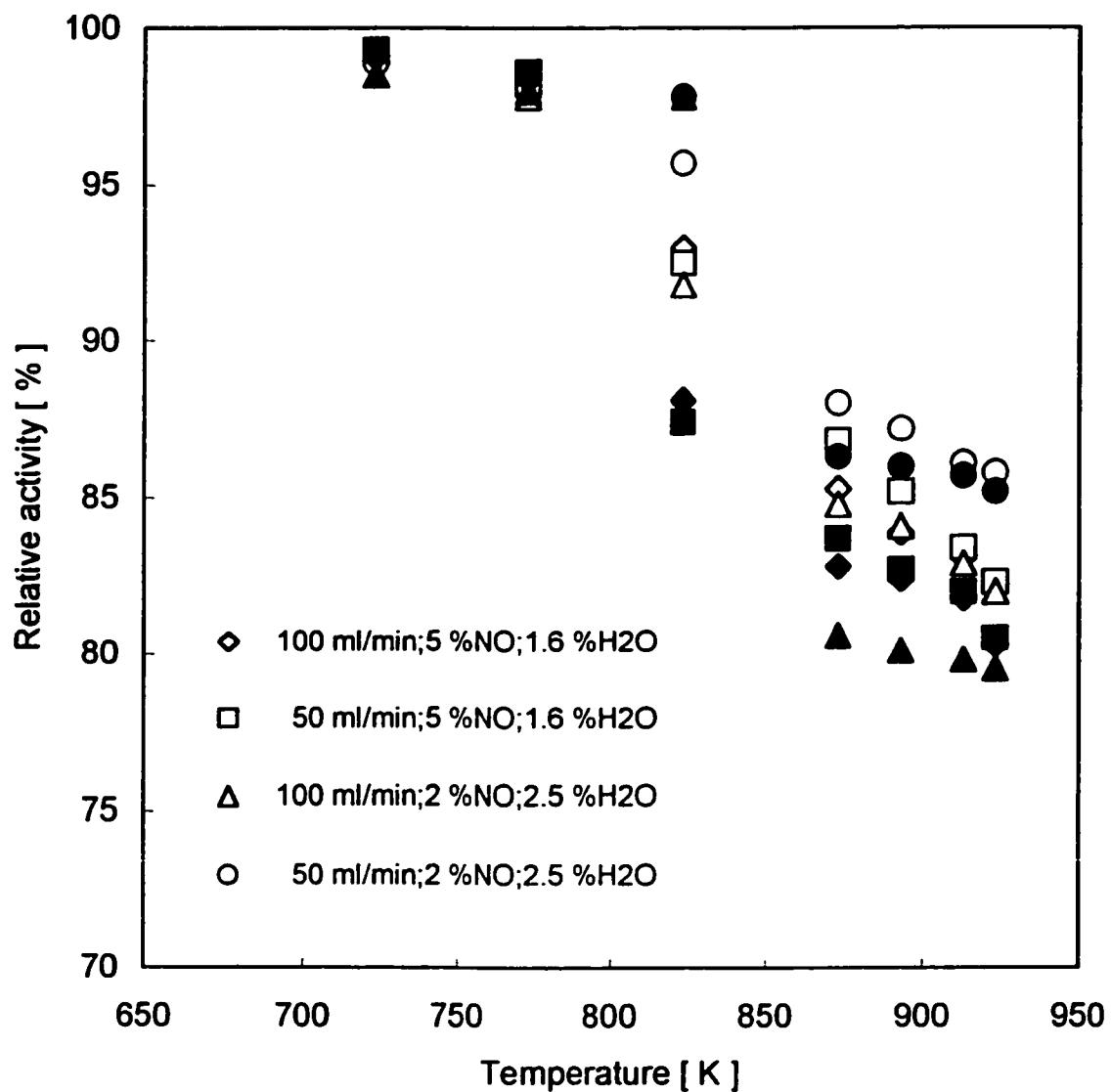


Figure 4.7 Relative activity of LSMN-28 (full symbols) and of LSNC (open symbols) perovskites in the direct decomposition of 2 or 5 % NO to nitrogen in the presence of water as a function of temperature.

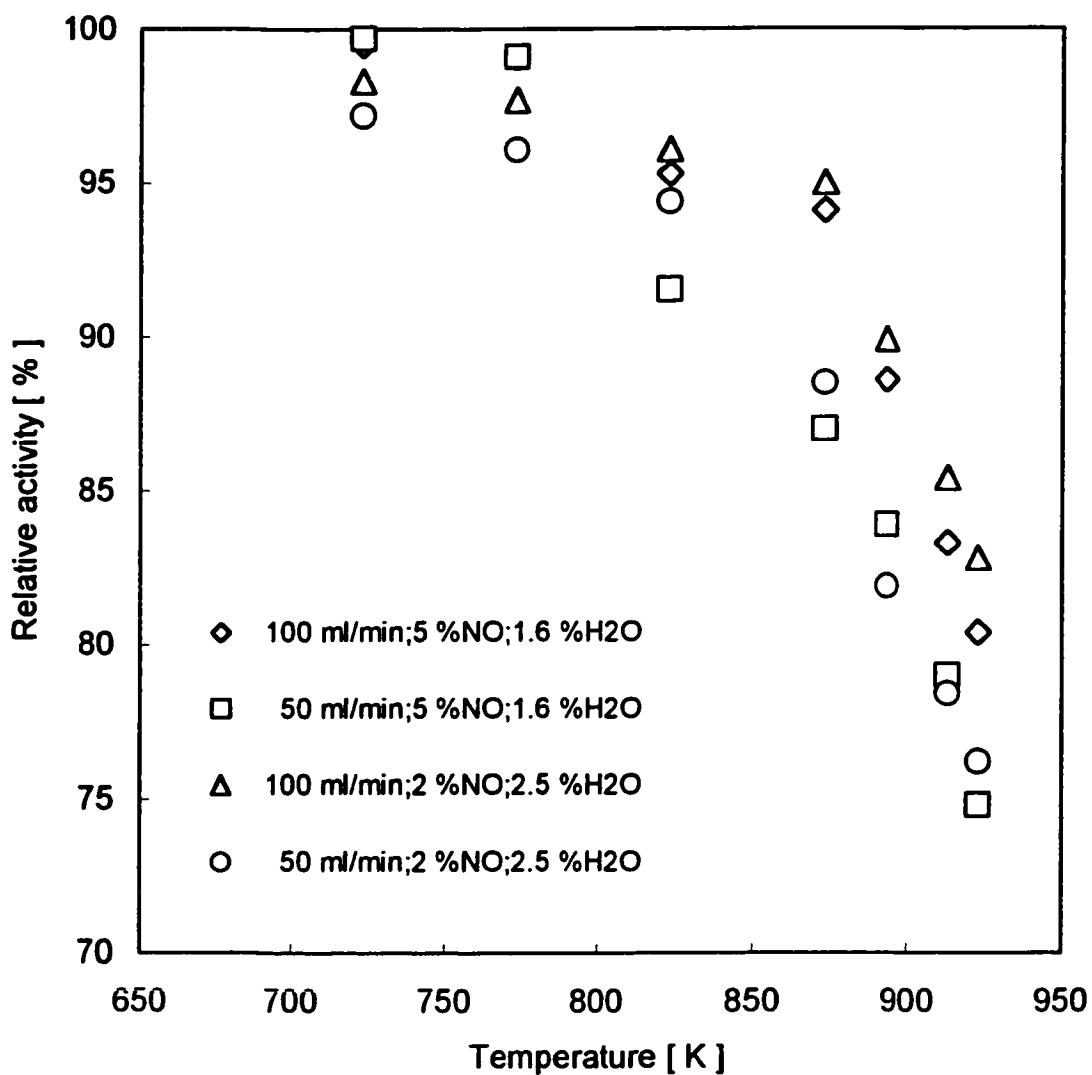


Figure 4.8 Relative activity of LSCuF perovskite in the direct decomposition of 2 or 5 % NO to nitrogen in the presence of water as a function of temperature.

In spite of apparent differences in the reaction mechanism for LSMN-28 and LSNC versus LSCuF, a single kinetic model mathematically similar to that found for carbon dioxide inhibition gave a satisfactory fit for the three perovskite compositions:

$$r = \frac{k_{NO} P_{NO}}{1 + KP_{O_2} + k_{inH_2O} P_{H_2O}}$$

Again, only conversion data directly related to water inhibition were included in the fitting procedure and all three parameters of the above equation were determined. The obtained values for k_{NO} and K are once more in a satisfactory agreement with those derived by using different sets of data, although the fit is not perfect. Arrhenius plots of $k_{inh\ H_2O}$ for the three perovskites are shown in Figure 4.5 and the corresponding values of the apparent activation energy for water inhibition and of pre-exponential factor are presented in Table 4.3. Similarly as in the case of carbon dioxide, the highest $(E_{inh\ H_2O})_{app}$ was found for LSMN-28, whereas the lowest value was obtained for LSCuF.

4.5.4 Effect of CH₄ on NO decomposition

Catalytic NO reduction using methane (in the presence of oxygen), represents an attractive alternative to NO_x removal [1,20] and satisfactory catalysts are actively searched in many laboratories. In view of low activities of perovskites in direct NO decomposition and knowing that the same perovskites exhibit a very good activity in total methane oxidation by oxygen [14], we have included a brief complementary evaluation of the effect of methane on the NO conversion.

For LSMN-28 and LSNC the experiments were carried out with stoichiometric mixtures (NO/CH₄ = 4) in helium and flowrates of 100 ml/min (2 %NO/0.5 %CH₄/He or 5 %NO/1.25 %CH₄/He) between 723 and 923 K. Activity of LSCuF was tested in total oxidation of 2.6 % methane by oxygen at two different concentrations (in air, by 5 % oxygen) and by 10% NO. The later experiments with LSCuF were carried out in a horizontal ceramic reactor with 0.5 g LSCuF, and at flowrates of 200 ml/min.

Figures 4.9 and 4.10 compare the activities of LSMN-28 and LSNC perovskites respectively in NO direct decomposition with those in NO reduction by methane.

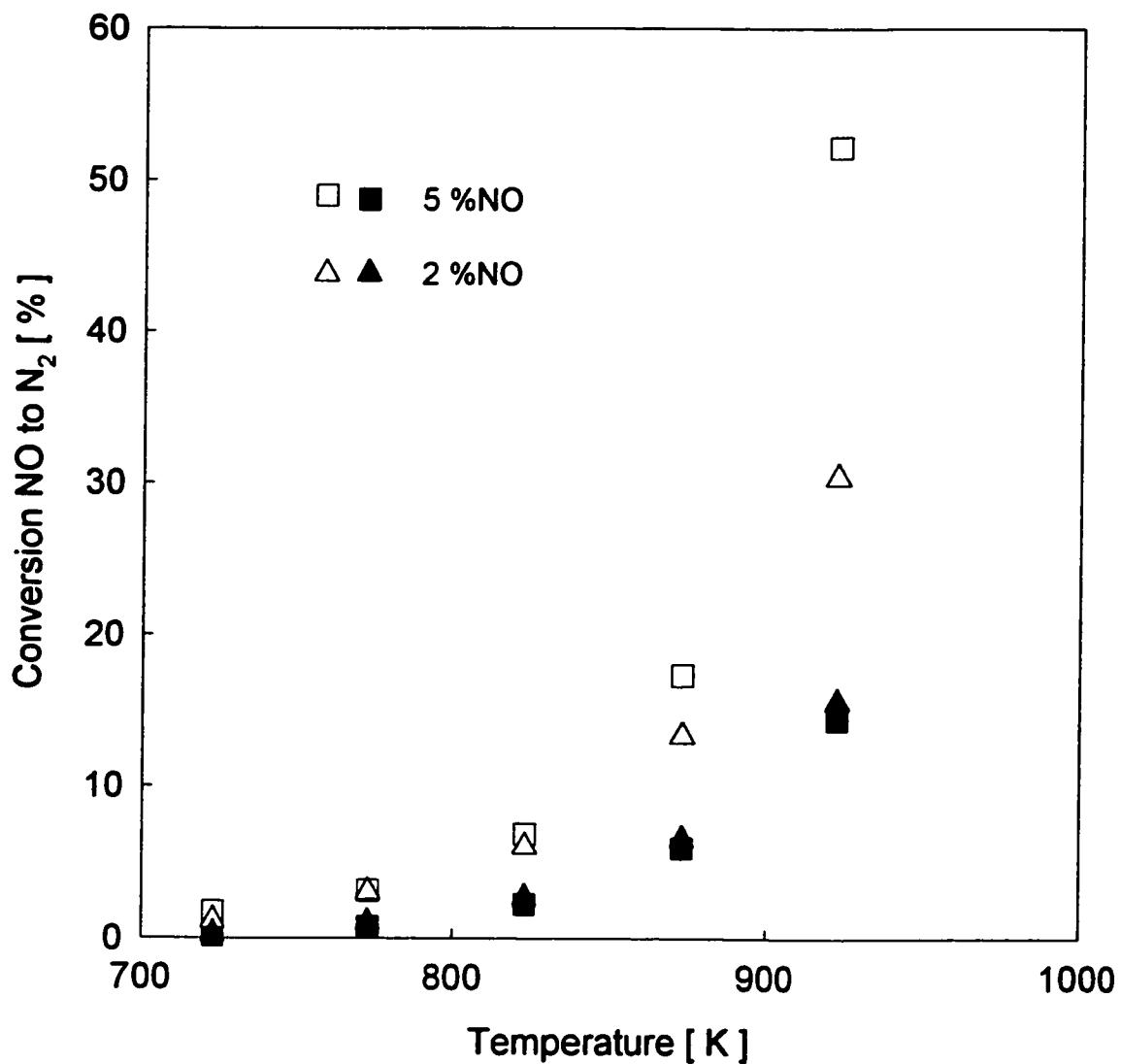


Figure 4.9 Effect of temperature on NO reduction by methane, $\text{NO/CH}_4 = 4$, (open symbols) and NO decomposition (full symbols) over LSMN-28 catalyst; total flowrate 100 ml/min.

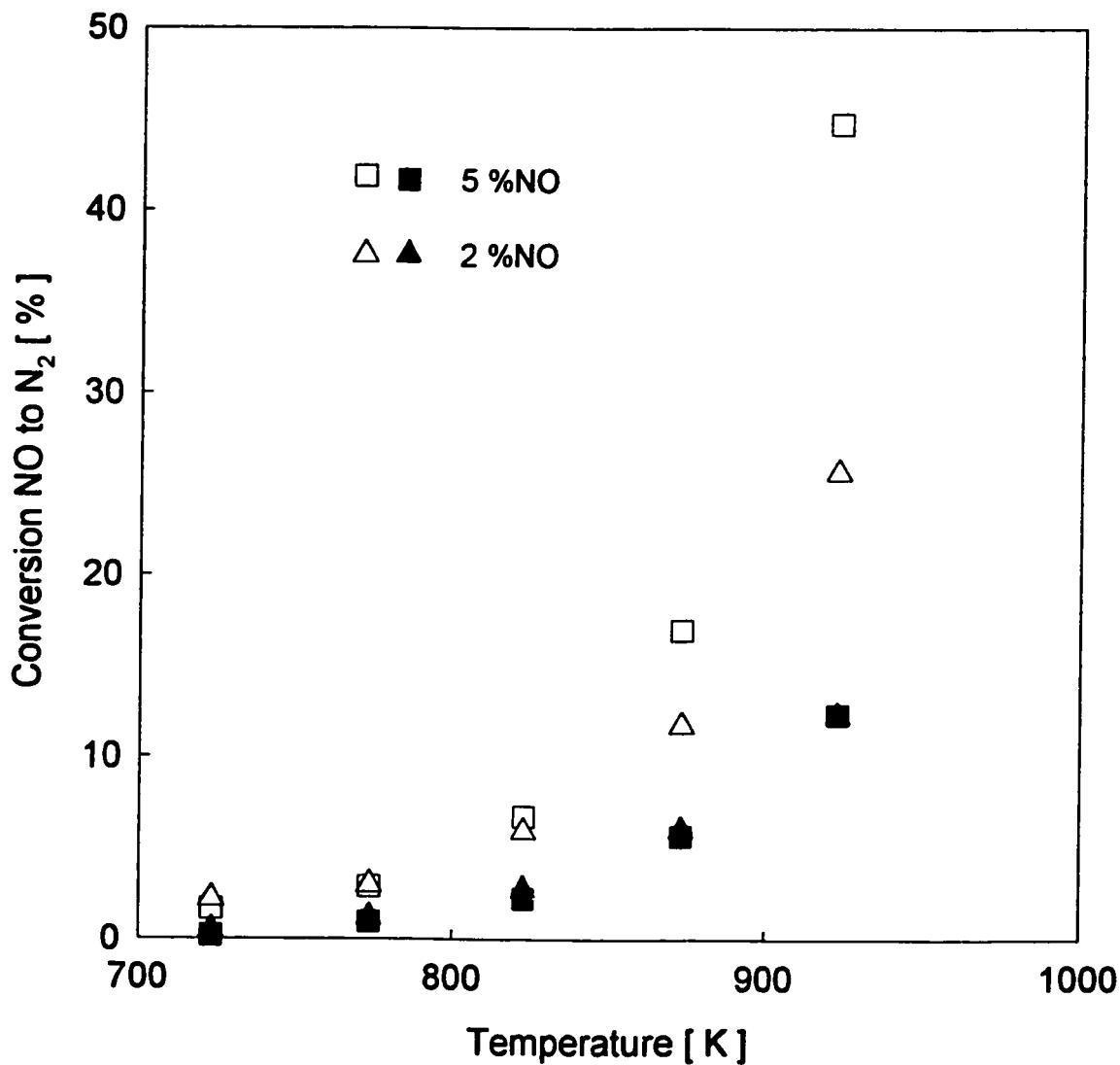


Figure 4.10 Effect of temperature on NO reduction by methane, $\text{NO}/\text{CH}_4 = 4$, (open symbols) and NO decomposition (full symbols) over LSNC catalyst; total flowrate 100 ml/min.

As shown in these figures, the conversion of NO to N₂ continuously increased with reaction temperature. In both cases addition of methane markedly increases the rate of nitrogen formation in a similar manner. The conversion of NO to N₂ in reduction reaction is two times higher than in direct decomposition with 2 % NO in the feed and 3 to 3.6 times higher with 5 % NO. However, these NO reduction rates are lower than could be expected on the basis of generally observed high activities of perovskites in oxidation reactions. For example, the estimated rates of nitrogen production over LSNC are 0.022 $\mu\text{mol N}_2/\text{g}\cdot\text{s}$ at 773 K and 0.19 $\mu\text{mol N}_2/\text{g}\cdot\text{s}$ at 923 K (100 ml/min; 2 % NO; 0.5 % CH₄; 1 g catalyst). These rates are only about twice as high as those reported by Huang et al. [24] for La₂O₃ for similar conditions (88 ml/min; 1.8 % NO; 0.45 % CH₄; 0.2 g catalyst). In addition, over La₂O₃, which by itself is a poor catalyst for methane oxidation by oxygen, as well as for direct NO decomposition, the rate of NO reduction by methane is significantly improved by the presence of oxygen [24,25]. Apparently, the presence of transition metals and the perovskite structure itself promote a too fast methane oxidation by oxygen, which interferes with the NO reduction. This is indirectly illustrated for the LSCuF perovskite in Figure 4.11 representing conversion of 2.6 % methane to CO₂ in three reaction mixtures as a function of temperature. The observed activity of LSCuF in CH₄/air combustion compares well with that of other highly active perovskites. In comparison, when NO is the oxidant, the rates of oxidation are about an order of magnitude lower. Furthermore, the lower apparent activation energy most likely reflects the strong inhibition effect of CO₂. These results strongly suggest that reduction of NO by methane over perovskites would not be selective and still remain too slow for practical application.

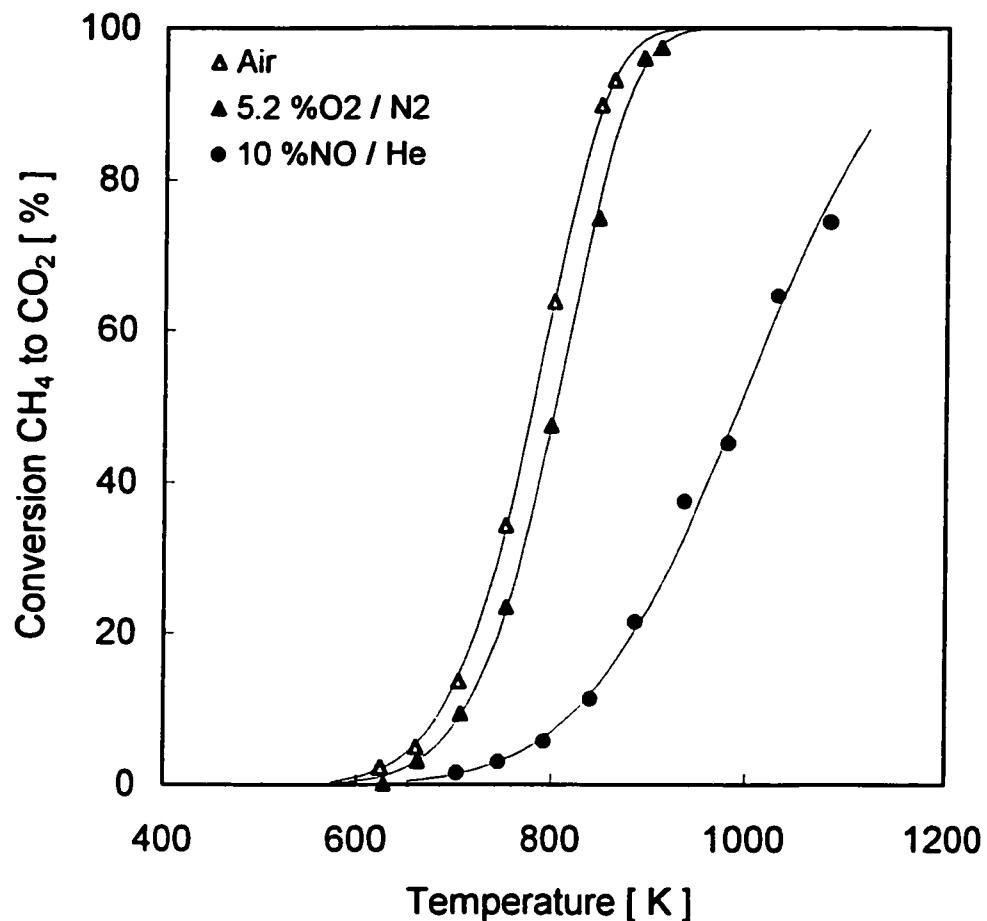


Figure 4.11 Oxidation of 2.6 % methane to carbon dioxide by oxygen and by nitric oxide over 0.5 g of $\text{La}_{0.8}\text{Sr}_{0.2}\text{Cu}_{0.15}\text{Fe}_{0.85}\text{O}_3$ perovskite powder ($< 10 \mu\text{m}$); plug-flow reactor, steady state conversions, feed flow 200 ml/min. The lines are calculated using following pseudo-first order constants: air: $E_{\text{app}} = 97 \text{ kJ/mol}$, $\ln A = 20.05 \mu\text{mol/g}\cdot\text{s}\cdot\text{bar}$; 5.2 %O₂/N₂: $E_{\text{app}} = 97 \text{ kJ/mol}$, $\ln A = 19.75 \mu\text{mol/g}\cdot\text{s}\cdot\text{bar}$; 10 % NO: $E_{\text{app}} = 76 \text{ kJ/mol}$, $\ln A = 14.65 \mu\text{mol/g}\cdot\text{s}\cdot\text{bar}$

4.6 Summary and conclusions

Catalytic activity of $\text{La}_{0.87}\text{Sr}_{0.13}\text{Mn}_{0.2}\text{Ni}_{0.8}\text{O}_{3-\delta}$ (LSMN-28), $\text{La}_{0.66}\text{Sr}_{0.34}\text{Ni}_{0.3}\text{Co}_{0.7}\text{O}_{3-\delta}$ (LSNC), and $\text{La}_{0.8}\text{Sr}_{0.2}\text{Cu}_{0.15}\text{Fe}_{0.85}\text{O}_{3-\delta}$ (LSCuF) perovskites in direct nitric oxide decomposition, which is relatively high in comparison with other oxide type catalysts, is strongly inhibited not only by oxygen, but also by carbon dioxide and to a lesser degree by water. At temperatures from 873 K to 923 K the inhibition effects of carbon dioxide and of water increase with temperatures, in contrast to the inhibition effect of oxygen, which in the same range decreases with temperature. The inhibition effect of carbon dioxide is the strongest for LSMN-28 and the weakest for LSCuF. The significantly weaker inhibition by water is for the three catalysts of about the same degree.

Methane accelerates significantly the rate of nitrogen formation, but not to a level required for any practical use. Furthermore, the rate of methane oxidation by nitric oxide is considerably slower than oxidation by oxygen. Thus, practical selective reduction of nitric oxide over perovskite catalysts by methane and most likely by other hydrocarbons, is unlikely to be achievable.

Overall, it may be concluded that transition metal based perovskites, which are characterized by high oxygen adsorption and relatively fast oxygen ion and electron conductivity and as a consequence exhibit very high activity in total (deep) oxidation reactions, are not necessarily good catalysts for nitric oxide decomposition or selective reduction (by methane).

4.7 Acknowledgement

This work has been mainly supported by grants from Natural Sciences and Engineering Research Council of Canada.

4.8 References

- [1] J.N. Armor, *Appl. Catal. B: Environmental*, 1(40 (1992) 221.
- [2] Environment Canada, *Canada's response to EPA Proposal on Transboundary Air Pollution*, March, 1998.
- [3] J. W. Hightower and D. A. van Leirsburg, in R. L. Klimisch and J. G. Larson (Editors), *The Catalytic Chemistry of Nitrogen Oxides*, Plenum Press, New York, 1975, p. 63.
- [4] V. I. Pârvulescu, P. Grange and B. Delmon, *Catal. Today*, 46 (1998) 233.
- [5] Y. Li and W. K. Hall, *J. Catal.*, 129 (1991) 202.
- [6] M. Iwamoto and H. Harada, *Catal. Today*, 10 (1991) 57.
- [7] X. Zhang, A. B. Walters and M. A. Vannice, *J. Catal.*, 155 (1995) 290.
- [8] T. Yamashita and M. A. Vannice, *J. Catal.*, 163 (1996) 158.
- [9] Y. Teraoka, T. Harada, H. Furukawa and S. Kagawa, *Stud. Surf. Sci. Catal.*, 75 (1993) 2649.
- [10] Y. Yokomichi, T. Nakayama, O. Okada, Y. Yokoi, I. Takahashi, H. Uchida, H. Ishikawa, R. Yamaguchi, H. Matsui and T. Yamabe, *Catal. Today*, 29 (1996) 155.
- [11] R. A. Grinsted, H. W. Jen, C. N. Montreuil, M. J. Rokosz and M. Shelef, *Zeolites*, 13 (1993) 602.
- [12] A. Lawson, *J. Catal.*, 24 (1972) 297.
- [13] G. I. Golodets, "Heterogeneous Catalytic Reactions Involving Molecular Oxygen", *Studies in Surface Science and Catalysis*, Vol. 15, Elsevier, Amsterdam (1983), p.437.
- [14] D. Klvana, J. Kirchnerova, P. Gauthier, J. Delval, J. Chaouki, *Can. J. Chem. Eng.*, 75 (1997) 509.
- [15] K. S. Song, D. Klvana and J. Kirchnerova, *Appl. Catal. A : General*, (2001) in print.
- [16] D. Klvana, S. Vantomme, J. Kirchnerova, J. Chaouki and S. Vigneron, *Proc. 1er Congrès International sur les nez électroniques et les composés odorants*, Paris, June 26-27, 1996.

- [17] D. Klvana, J. Delval, J. Kirchnerova and J. Chaouki, *Appl. Catal. A: General*, 165 (1997) 171.
- [18] C. Tofan, D. Klvana and J. Kirchnerova, *Appl. Catal., A, General*, (2001a) in print.
- [19] C. Tofan, D. Klvana and J. Kirchnerova, *Appl. Catal., A, General*, (2001b) in print.
- [20] Y. Li and J. N. Armor, *Appl. Catal. B: Environmental*, 1 (1992) L31.
- [21] J. Kirchnerova and D. Klvana, *Solid State Ionics*, 123 (1999) 307.
- [22] J. M. D. Tascon and G. L. Tejucá, *J. Chem. Soc., Faraday Trans. 1*, 77(3) (1981) 591.
- [23] Y. A. Chang, N. Ahmad, *Thermodynamic Data on Metal Carbonates and Related Oxides, Technology of Metallurgy Series*, New York, (1982).
- [24] S.-J. Huang, A. B. Walters, M. A. Vannice, *Appl. Catal. B: Environmental*, 17 (1998) 183.
- [25] M. D. Fokema, J. Y. Ying, *Appl. Catal. B: Environmental*, 18 (1999) 71.

DISCUSSION GÉNÉRALE

L'objectif des études qui forment cette thèse était d'évaluer les performances des pérovskites substituées $\text{La}_{1-x}\text{Sr}_x\text{B}_{1-y-z}\text{B}'_y\text{B}''_z\text{O}_{3-\delta}$ pour la décomposition directe du NO et de cerner les effets des divers paramètres réactionnels afin de contribuer à la compréhension de cette réaction complexe.

Les compositions des pérovskites ont été choisies de manière à remplir les exigences de base que doit avoir un catalyseur pour la décomposition du NO : bon conducteur électrique et ionique, favorisant la désorption de l'oxygène. Trois groupes de pérovskites ont été utilisés dans les études : le premier basé sur le cobalt comme principal élément actif, le second basé sur le nickel et le troisième ayant le cuivre comme élément actif. Le cuivre et le nickel ont été choisis pour leur propriété d'assurer une désorption facile et rapide de l'oxygène à basse température. Les autres ions dans les sites B ont été sélectionnés pour assurer une bonne stabilité de la structure pérovskite. Cette structure impose aussi les proportions entre les différents éléments utilisés. Par exemple, la pérovskite ayant une proportion trop élevée en cuivre dans sa composition ($\text{LaFe}_{0.34}\text{Cu}_{0.66}\text{O}_{3-\delta}$) n'a pu être obtenue à l'état pur. On peut supposer que cela est principalement du à l'inhabilité de la structure d'accorder un grand nombre de lacunes d'oxygène parce que seulement une fraction limitée des ions du cuivre et du fer peuvent accepter des valences supérieures à 2, respectivement à 3.

Les pérovskites sous forme de poudres ont été préparées par la méthode développée à l'École Polytechnique de Montréal par Dr. J. Kirchnerova et Prof. D. Klvana qui utilise comme précurseur une suspension homogène et réactive, obtenue à partir de l'hydroxyde de lanthane et d'une solution des nitrates des autres métaux, mélangés en proportions stœchiométriques. La suspension a été séchée par cryodessiccation et ensuite calcinée dans l'air, sous des conditions contrôlées. Cette méthode a permis

d'obtenir des échantillons ayant une structure pure de type pérovskite avec des surfaces spécifiques relativement grandes (9 à 22 m²/g).

Les performances des pérovskites pour la décomposition directe du NO ont été évaluées à l'aide de mesures cinétiques réalisées en régime permanent dans un réacteur tubulaire à écoulement piston. Les mesures ont été effectuées dans un large éventail de conditions expérimentales, en absence d'oxygène (Chapitre II), en présence d'oxygène (Chapitre III) et en présence d'anhydride carbonique et d'eau (Chapitre IV). Finalement, quelques tests en présence du méthane (Chapitre IV) ont été faits pour évaluer le potentiel des pérovskites comme catalyseurs pour la réduction du NO.

Le catalyseur (1g) a été dilué avec de la pierre ponce (7 mL) pour assurer une bonne perméabilité du lit. La pierre ponce présente une très faible activité pour la décomposition du NO. Dans la plupart des cas cette activité est négligeable par rapport à l'activité du catalyseur. Des corrections appropriées ont été apportées quand cela a été nécessaire. Ainsi, toutes les données prises en considération pour l'analyse des modèles représentent l'activité du catalyseur lui-même, et non du mélange catalyseur-pierre ponce. Des corrections pour les traces d'azote que l'on a trouvé dans l'alimentation du réacteur ont été aussi faites.

Une analyse diffusionnelle a été faite afin de s'assurer que la réaction n'est pas contrôlée par la diffusion externe ou interne au niveau du transfert de masse et de chaleur :

- Diffusion externe (critère de Mears) :

- critère pour transfert de masse :

$$\frac{r \rho_b R_o n}{k_c c_{NO}} < 0,15$$

- critère pour transfert de chaleur :

$$\frac{|\Delta H_r| r \rho_b R_o E}{h T^2 R} < 0,15$$

- Diffusion interne :

- critère pour transfert de masse (Wiesz-Prater) :

$$\frac{r \rho_p R_i^2}{D_e c_{NO}} = 1$$

- critère pour transfert de chaleur :

$$\frac{|\Delta H_R| r R_i^2}{\lambda T_s} < \frac{1}{\gamma}; \quad \gamma = E / RT$$

Puisque les critères ont été respectés pour toutes les conditions expérimentales, on a supposé qu'il n'y a pas des limitations diffusionnelles externes ou internes.

Une première analyse des données a été faite en supposant, pour la décomposition du NO en N₂, le modèle cinétique d'ordre 1, $r = k_{NO} P_{NO}$. Il est apparu que le modèle d'ordre 1 n'est pas adéquat, mais les déviations de ce modèle ont permis de déduire que l'oxygène produit par la décomposition du NO et le NO lui-même ont un effet inhibiteur sur la décomposition. Ainsi, pour l'analyse cinétique, on a choisi par la suite des modèles de type Langmuir-Hinshelwood qui prennent en considération soit seulement l'effet inhibiteur de l'oxygène, soit le double effet inhibiteur de l'oxygène et du NO :

$$r = k_{NO} P_{NO} / (1 + K_{O2} P_{O2}^m)$$

$$r = k_{NO} P_{NO}^n / (1 + K_{NO} P_{NO}^n + K_{O2} P_{O2}^m)$$

Il faut mentionner que pour tenir compte des possibilités d'adsorption du NO et de l'oxygène sur la surface du catalyseur, on a considéré seulement les ordres de réaction $n = 1$ et 2 par rapport au NO et $m = \frac{1}{2}$, 1 et 2 par rapport à l' O_2 .

Quelques travaux trouvés dans la littérature, concernant la décomposition du NO sur les oxydes simples ont montré l'existence de certaines espèces intermédiaires qui contiennent une liaison N-N dans leur structure. Une structure de ce type pourrait se former par adsorption successive ou simultanée des deux molécules de NO sur un même site actif. Dans le cas des pérovskites l'espèce intermédiaire pourrait prendre naissance sur différents types d'oxygène qui pourrait se former sur la surface du catalyseur. Les résultats obtenus dans cette étude indiquent aussi que, à des faibles concentrations, l'oxygène semble jouer un rôle de réactif. Ce rôle peut être expliqué par la participation de l'oxygène à la formation des espèces de type N_2O_3 ou N_2O_4 qui, en se décomposant vont libérer la molécule d'azote. Ainsi, en se basant sur les observations faites dans cette étude et sur des constatations faites pour d'autres systèmes catalytiques et en s'inspirant aussi du modèle proposé par Mars-van Krevelen pour la combustion, on a proposé un nouveau type de modèle pour la décomposition du NO :

$$r = \frac{k_{NO} P_{NO}^n P_{O_2}^m}{k_I P_{NO}^n + k_{II} P_{O_2}^m}$$

En absence d'oxygène dans l'alimentation, donc quand on considère uniquement l'oxygène produit par décomposition (calculé à partir de l'azote détecté dans l'effluent) ce modèle (avec $n=1$ et $m=\frac{1}{2}$ ou 1 , dépendement de la température) représente le mieux les données expérimentales pour la majorité des pérovskites testées.

En présence d'oxygène dans l'alimentation (on prend en considération l'oxygène ajouté et l'oxygène produit par la décomposition du NO) et à des bases températures (723-773 K pour LSMN-28, 723-823 K pour LSNC et 723-873 K pour LSCuF) le modèle proposé

dans l'étude en absence de l'oxygène dans l'alimentation ($r = \frac{k_{NO}P_{NO}P_{O_2}^{1/2}}{k_I P_{NO} + k_{II} P_{O_2}^{1/2}}$) reste valable. Dans ce cas les constantes cinétiques n'ont pas pu être déterminées individuellement, mais le rapport k_{II}/k_I montre que l'inhibition par l'oxygène est plus forte que l'inhibition par le NO.

À des hautes températures (873-923 K), en présence d'oxygène dans l'alimentation, un effet de saturation de la surface avec de l'oxygène semble se manifester. Pour des teneurs en oxygène qui ne dépassent pas 0,02 bar le seul modèle acceptable est :

$$r = \frac{k_{NO}P_{NO}}{1 + K_{O_2}P_{O_2}}$$

Les constantes cinétiques ont été déterminées pour les trois catalyseurs testés (LSMN-28, LSNC et LSCuF).

Les produits des combustion (CO_2 et H_2O) ont aussi un effet inhibiteur sur la décomposition du NO. Contrairement à l'effet de l'oxygène, les effets inhibiteurs de CO_2 et H_2O sont activés (l'inhibition augmente avec la température) sur tout le domaine des températures où l'étude a été faite (723-923 K pour H_2O et 873-923 K pour CO_2). Les données expérimentales ont montré que l'inhibition par CO_2 et H_2O dépend de la composition de la pérovskite. Cependant, elle peut être représentée par un modèle cinétique de même type :

$$r = \frac{k_{NO}P_{NO}}{1 + KP_{O_2} + k_{inhCO_2}P_{CO_2}} \text{ pour } CO_2 \quad (P_{CO_2} \leq 0,02 \text{ bar})$$

$$r = \frac{k_{NO}P_{NO}}{1 + KP_{O_2} + k_{inhH_2O}P_{H_2O}} \text{ pour } H_2O$$

Pour des concentrations similaires d'oxygène, CO_2 et H_2O , l'inhibition par l'oxygène est la plus forte, tandis que l'inhibition la plus faible est causée par H_2O . Tous les trois effets inhibiteurs, testés individuellement, sont réversibles.

Considérations sur le mécanisme de décomposition du NO

Le mécanisme de la réaction de décomposition du NO n'est pas encore complètement élucidé. Sur les pérovskites testées on a observé que l'oxygène peut se manifester non seulement comme inhibiteur (ce qui était déjà bien connu sur tous les catalyseurs) mais aussi comme "réactif", probablement en participant à la formations de sites actifs. Les études expérimentales ont aussi montré que pour une même concentration initiale en NO, l'inhibition par l'oxygène est plus faible quand le débit total est plus faible (donc quand le temps de contact est plus grand) ce qui indique que l'étape limitant de la décomposition n'est pas la désorption lente de l'oxygène adsorbé à la surface du catalyseur, mais plutôt l'étape de formation des espèces intermédiaires, étape à laquelle, dans cette étude, on suppose la participation de l'oxygène. On propose donc le mécanisme suivant pour la décomposition du NO en N_2 :

1) Adsorption du NO et formation des espèces intermédiaires

Dans le cas des catalyseurs de type pérovskite l'adsorption du NO peut se faire dans les lacunes d'oxygène, sur des cations, en formant des liaisons M-N-O, ou sur certaines espèces qui contient de l'oxygène, en formant des liaisons –O-N-O. Pour produire la molécule d'azote il faut cependant qu'une liaison N-N se forme. Cela pourrait se faire si deux molécules de NO s'adsorbent sur des paires des sites actifs voisins. Il y a aussi la possibilité de l'adsorption (successive ou simultanée) des deux molécules de NO sur un site unique formé par certaines espèces qui contiennent de l'oxygène. Il se formera alors une espèce intermédiaire de type "dimère", probablement N_2O_3 ou N_2O_4 . Cependant la formation des ces espèces qui englobe la liaison N-N pourrait se faire s'il n'y a pas des

empêchements stériques suite à l'adsorption de la première molécule de NO. Cette possibilité de formation des espèces de type "dimère" a été proposée pour les pérovskites dans la présente étude, en se basant sur le rôle de réactif de l'oxygène déduit à partir des observations expérimentales et elle est appuyée par l'équation cinétique proposée pour la décomposition du NO en absence de l'oxygène. Comme mentionnait dans le Chapitre III, les études faites par d'autres équipes sur les oxydes et zéolithes appuient cette présomption.

Il faut remarquer qu'il y a aussi un autre type d'intermédiaire qui pourrait se former par l'adsorption d'une seule molécule de NO sur des sites à caractère basique. Il s'agit des espèces de type nitrite ou nitrate. La présence de l'oxygène favorise la formation de ces intermédiaires.

2) Décomposition des espèces intermédiaires

Les espèces intermédiaires de type "dimère" pourraient, par leur décomposition, donner naissance à la molécule d'azote. Ainsi, les intermédiaires de ce type favoriseront la décomposition du NO.

Les espèces de type nitrite/nitrate auront plutôt tendance à se décomposer en NO ou NO₂. Par cette décomposition qui ne produit pas de N₂ on explique, dans cette étude, l'effet inhibiteur implicite de l'oxygène, et aussi du NO lui-même.

Dans le Chapitre II on présente deux variantes pour l'équation cinétique proposée pour la décomposition du NO en absence d'oxygène :

$$r = \frac{k_{NO} P_{NO} P_{O_2}^{1/2}}{k_I P_{NO} + k_{II} P_{O_2}^{1/2}} \quad \text{pour des basses températures}$$

$$r = \frac{k_{NO} P_{NO} P_{O_2}}{k_I P_{NO} + k_{II} P_{O_2}} \quad \text{pour des hautes températures}$$

Ce changement de l'ordre de réaction par rapport à l'oxygène peut être expliqué sur les catalyseurs de type pérovskite de manière suivante :

À des basses températures la formation des sites actifs à laquelle l'oxygène participe a lieu par l'adsorption dissociative lente de l'oxygène. Cela explique l'ordre $\frac{1}{2}$ par rapport à l'oxygène à ces températures. À des hautes températures la mobilité de l'oxygène de la structure est plus grande, ce qui explique la valeur 1 pour l'ordre de réaction par rapport à l'oxygène. Même si les équations cinétiques sont différentes le même mécanisme peut être envisagé : la décomposition du NO en N₂ se produit suite à la formation des intermédiaires de type N₂O₃ ou N₂O₄. L'inhibition, quant à elle, résulte de la formation de nitrites/nitrates qui au lieu de former N₂ par décomposition vont donner naissance à NO₂ (à des basses températures) ou NO (à des hautes températures).

CONCLUSIONS ET RECOMMANDATIONS

Les études qui font l'objet de cette thèse avaient comme objectif d'évaluer la possibilité d'utiliser des pérovskites de composition $\text{La}_{1-x}\text{Sr}_x\text{B}_{1-y-z}\text{B}'_y\text{B}''_z\text{O}_{3.8}$ pour la décomposition directe du NO et de cerner les effets des divers paramètres réactionnels sur la vitesse de réaction afin de contribuer à élucider le mécanisme de décomposition du NO en présence d'une surface catalytique.

À partir de l'ensemble des résultats obtenus on peut tirer les conclusions générales suivantes :

- La plupart des pérovskites testées ont une activité supérieure à celle obtenue pour des catalyseurs de type pérovskite dans d'autres laboratoires. Cependant, cette activité est encore beaucoup trop faible pour des applications pratiques, comme le montre la quantité irréaliste de pérovskite (8,6 t) qu'il faudrait pour traiter l'effluent d'un moteur diesel (voir ANNEXE 5);
- La composition des pérovskites a un effet important sur la cinétique de décomposition du NO. Les cations qui peuvent facilement changer d'état d'oxydation, comme le nickel et le cuivre semblent être la source de sites actifs pour l'adsorption du NO. La pérovskite LSCuF ($\text{La}_{0.8}\text{Sr}_{0.2}\text{Cu}_{0.15}\text{Fe}_{0.85}\text{O}_{3.8}$) est la plus active à base température ($T < 823$ K); quant à la pérovskite LSMN-28 ($\text{La}_{0.87}\text{Sr}_{0.13}\text{Mn}_{0.2}\text{Ni}_{0.8}\text{O}_{3.8}$) elle est la plus active à température élevée;
- La décomposition du NO sur la surface des pérovskites se déroule selon un mécanisme très complexe auquel participe probablement des produits intermédiaires formés sur des sites actifs spécifiques, dont l'apparition et la teneur dépend entre autre de la composition de la pérovskite et de la température. La surface spécifique (SSA), bien qu'importante, n'est pas un facteur déterminant.

À partir des données cinétiques obtenues en absence de l'oxygène ajouté au mélange réactionnel on peut tirer les conclusions suivantes :

- le NO lui-même, ainsi que l'oxygène produit par la réaction ont un effet inhibiteur sur la réaction;
- L'oxygène à faible concentration semble jouer aussi un rôle de réactif, en participant à la formation d'intermédiaires, probablement de type dimère, N_2O_3 ou N_2O_4 ;
- Le rôle inhibiteur du NO peut être attribué à la formation des nitrites ou nitrates à la surface catalytique, qui se désorbent par la suite sous forme de NO ou NO_2 ;
- La réaction de décomposition du NO, pour la majorité des pérovskites testées, peut être représentée adéquatement par le model cinétique ci-bas qui reflète bien l'effet des diverses espèces participant à la réaction :

$$r = \frac{k_{NO} P_{NO} P_{O_2}^m}{k_1 P_{NO} + k_2 P_{O_2}^m}, \quad m = \frac{1}{2}, \text{ pour basses } T; m = 1, \text{ pour hautes } T$$

À partir de l'étude cinétique complète, réalisée sur trois pérovskites représentatives ($La_{0,87}Sr_{0,13}Mn_{0,2}Ni_{0,8}O_{3-\delta}$, $La_{0,66}Sr_{0,34}Ni_{0,3}Co_{0,7}O_{3-\delta}$ et $La_{0,8}Sr_{0,2}Cu_{0,15}Fe_{0,85}O_{3-\delta}$) en présence d'oxygène ajouté à l'alimentation, on peut tirer les conclusions suivantes :

- L'oxygène a un effet inhibiteur qui dépend de la température, de la composition du catalyseur et du temps de contact. À basses températures, même à des temps de contact élevés, l'inhibition par l'oxygène est faible. L'inhibition croît cependant avec la température jusqu'à 873 K. Pour des températures plus élevées (873-923K), l'inhibition diminue avec la température;

- La décomposition du NO à des températures élevées et à des pressions $P_{O_2} \leq 0,02$ bar peut être représentée par le modèle cinétique:

$$r = \frac{k_{NO} P_{NO}}{1 + K_{O_2} P_{O_2}}$$

À partir de l'étude complémentaire réalisée avec les trois pérovskites en présence des produits de combustion, l'eau et l'anhydride carbonique, on peut tirer les conclusions suivantes :

- L'anhydride carbonique, et en moindre mesure, l'eau, ont un effet inhibiteur sur la réaction de décomposition du NO. Cependant, le degré d'inhibition dépend de la composition de la pérovskite;
- Dans le domaine des températures élevées, les inhibitions provoquées par CO_2 et H_2O augmentent avec la température, c.-à-d. sont activés ;
- L'effet inhibiteur du CO_2 sur la réaction de décomposition du NO dans le domaine $T = 873-923$ K et pour $P_{CO_2} \leq 0,02$ bar peut être représenté par le modèle cinétique :

$$r = \frac{k_{NO} P_{NO}}{1 + K_{O_2} P_{O_2} + k_{inhCO_2} P_{CO_2}}$$

- Pour le même domaine des températures l'effet inhibiteur de H_2O peut être représenté par un modèle cinétique similaire :

$$r = \frac{k_{NO} P_{NO}}{1 + K_{O_2} P_{O_2} + k_{inhH_2O} P_{H_2O}}$$

À partir des tests réalisés avec l'ajout du CH₄ dans l'alimentation on peut tirer les conclusions suivantes :

- Le CH₄ favorise la conversion du NO en N₂;
- La vitesse d'oxydation du CH₄ par NO est beaucoup moins élevée que la vitesse d'oxydation du CH₄ par O₂. Donc les pérovskites favorisent la combustion du CH₄ au détriment de la production du N₂ par la réduction sélective du NO;
- Les pérovskites La_{1-x}Sr_xB_{1-y}B'_yO_{3-δ} ne peuvent être utilisées comme catalyseur pour la réduction sélective du NO.

Pour donner plus de poids aux résultats et aux conclusions, qui dans certains cas reposent sur des présomptions, il serait souhaitable d'effectuer les études complémentaires suivantes :

- À l'aide de mesures cinétiques, réalisées en régime permanent et en régime transitoire, établir :
 - la concentration limite d'oxygène qui agit comme réactif;
 - la concentration de NO à laquelle l'inhibition de la réaction commence à se manifester;
- À l'aide d'expériences menées avec des produits marqués (isotopes) et des techniques telle la désorption programmée établir :
 - le type de produits intermédiaires qui participent à la réaction de décomposition du NO;
 - le type de sites actifs qui prennent part à la réaction de décomposition du NO et les conditions qui favorisent leur formation;
 - le type de sites actifs qui sont inhibés par O₂, CO₂, H₂O;

- À l'aide de mesures cinétiques avec un mélange réactionnel contenant en même temps NO, O₂, CO₂, H₂O vérifier, que les inhibitions individuelles déjà quantifiées agissent de façon cumulative et par conséquent le couplage des modèles cinétiques individuels dans un seul serait valable.

Finalement la conclusion que les pérovskites ne peuvent pas être utilisées comme catalyseurs pour la décomposition directe du NO ne devrait pas nuire au développement de leur potentiel dans d'autres domaines (combustion catalytique à haute température, piles à combustibles).

BIBLIOGRAPHIE

AMIRNAZMI, A., BENSON, J. E. et BOUDART, M. (1973) Oxygen inhibition in the decomposition of NO on metal oxides and platinum, J. Catal., 30, 55-65.

ANDERSON, H. U. et NASRALLAH, M. M. (1991) Characterization of oxides for low temperature solid oxide fuel cells, Annual Report, Contract No. 5090-260-2069, Gas Research Institute, Chicago, IL.

ARAI, H., YAMADA, T., EGUCHI, K. et SEIYAMA, T. (1986) Catalytic combustion of methane over various perovskite-type oxides, Appl. Catal., 26, 265-276.

ARAKAWA, T. et ADACHI, G. (1989) The direct reaction between nitric oxide and the superconductor $\text{YBa}_2\text{Cu}_3\text{O}_{7-\delta}$, Mat. Res. Bull., 24, 529-534.

ARMOR, J. N. (1992) Environmental catalysis, Appl. Catal. B : Environmental, 1 (4), 221-256.

ARMOR, J. N. (1994) Materials needs for catalysts to improve our environment, Chem. Mater., 6, 730-738.

ARMOR., J. N. et FARRIS, T. S. (1994) The unusual hydrothermal stability of Co-ZSM-5, Appl. Catal. B : Environmental, 4, L11-L17.

AYLOR, A. W., LARSEN, S. C., REIMER, J. A. et BELL, A. T. (1995) An infrared study of NO decomposition over Cu-ZSM-5, J. Catal., 157 (2), 592-602.

BIBLIOGRAPHIE

AMIRNAZMI, A., BENSON, J. E. et BOUDART, M. (1973) Oxygen inhibition in the decomposition of NO on metal oxides and platinum, J. Catal., 30, 55-65.

ANDERSON, H. U. et NASRALLAH, M. M. (1991) Characterization of oxides for low temperature solid oxide fuel cells, Annual Report, Contract No. 5090-260-2069, Gas Research Institute, Chicago, IL.

ARAI, H., YAMADA, T., EGUCHI, K. et SEIYAMA, T. (1986) Catalytic combustion of methane over various perovskite-type oxides, Appl. Catal., 26, 265-276.

ARAKAWA, T. et ADACHI, G. (1989) The direct reaction between nitric oxide and the superconductor $\text{YBa}_2\text{Cu}_3\text{O}_{7-\delta}$, Mat. Res. Bull., 24, 529-534.

ARMOR, J. N. (1992) Environmental catalysis, Appl. Catal. B : Environmental, 1 (4), 221-256.

ARMOR, J. N. (1994) Materials needs for catalysts to improve our environment, Chem. Mater., 6, 730-738.

ARMOR, J. N. et FARRIS, T. S. (1994) The unusual hydrothermal stability of Co-ZSM-5, Appl. Catal. B : Environmental, 4, L11-L17.

AYLOR, A. W., LARSEN, S. C., REIMER, J. A. et BELL, A. T. (1995) An infrared study of NO decomposition over Cu-ZSM-5, J. Catal., 157 (2), 592-602.

BATIOT-DUPEYRAT, C., MARTINEZ-ORTEGA, F., GANNE, M. et TATIBOUËT, J. M. (2001) Methane catalytic combustion on La-based perovskite type catalysts in high temperature isothermal conditions, Appl. Catal. A : General, **206**, 205-215.

BELESSI, V. C., COSTA, C. N., BAKAS, T. V., ANASTASIADOU, T., POMONIS, P. J. et EFSTATHIOU, A. M. (2000) Catalytic behavior of La-Sr-Ce-Fe-O mixed oxidic/perovskitic systems for the NO+CO and NO+CH₄+O₂ (lean-O₂) reactions, Catal. Today, **59**, 347-363.

BELL, A. T. (1997) Experimental and theoretical studies of NO decomposition and reduction over metal-exchanged ZSM-5, Catal. Today, **38**, 151-156.

BLAZOWSKI, W. S. et WALSH, D. E. (1975) Catalytic combustion : an important consideration for future applications, Comb. Sci. Technol., **10**, 233-244.

BLOMEN, L. J. M. J. et MUGERWA, M. N. (1993) Fuel Cell System, Plenum Press, New York.

BONTCHEV, R., CHESKOVA, K., MEHANDJIEV, D. et DARRIET, J. (1996) Nitric oxide decomposition over BaRu_xBi_{1-x}O₃ (x = 0.33, 0.50, 0.67, 1.00), React. Kinet. Catal. Lett., **63** (1), 121-127.

BURNETT, R. T., CAKMAK, S. et BROOK, J. R. (1998) The effect of urban ambient air pollution mix on daily mortality rates in 11 canadian cities, Can. J. Public Health, **89**, 142-150.

CAMPA, M. C., INDOVINA, V., MINELLI, G., MORETTI, G., PETTITI, I., PORTA, P. et RICCIO, A. (1993) The catalytic activity of Cu-ZSM-5 and Cu-Y zeolites in NO decomposition. Dependence on copper concentration, Catal. Lett., **23** (1-2), 141-149.

CENTI, G. et PERATHONER, S. (1995) Nature of active species in copper-based catalysts and their chemistry of transformation of nitrogen oxides, Appl. Catal. A : General, 132 (2), 179-259.

CHANG, Y. A. et AHMAD, N. (1982) Thermodynamic data on metal carbonates and related oxides, Technology of metallurgy series, New York.

CHANG, Y. -F. et McCARTY, J. G. (1997) Isotopic study of NO_x decomposition over Cu- or Co-exchanged ZSM-5 zeolite catalysts, J. Catal., 165 (1), 1-11.

CHAOUKI, J., GUY, C., SAPUNDZIEV, H., KUSOHORSKY, D. et KLVANA, D. (1994) Combustion of methane in a cyclic catalytic reactor, I&EC Research, 33 (12), 2957-2963.

CHEN, C. C., NASRALLAH, M. M. et ANDERSON, H. U. (1993) Synthesis and characterization of (CeO₂)_{0.8}(SmO_{1.5})_{0.2} thin film from polymeric precursors, J. Electrochem. Soc., 140 (12), 3555-3560.

CHIEN, M. W., PEARSON, I. M. et NOBE, K. (1975) Reduction and adsorption of nitric oxide on cobalt perovskite catalysts, Ind. Eng. Chem. Prod. Es. Dev., 14 (2), 131-134.

CHIRONNA, B. J. et ALTSCHULER, B. (1999) Chemical aspects of NO_x scrubbing, Pollut. Eng., April, 32-36.

CHOUDHARY, V. R. et RANE, V. H. (1991) Acidity/basicity of rare-earth oxides and their catalytic activity in oxidative coupling of methane to C₂-hydrocarbons, J. Catal., 130, 411-422.

CHUANG, S. S. C. et TAN, C. -D. (1997) Promotion of oxygen desorption on enhance direct NO decomposition over Tb-Pt/Al₂O₃ catalyst, J. Phys. Chem. B, 101 (15), 3000-3004.

CIAMBELLI, P., CIMINO, S., DE ROSSI, S., FATICANTI, M., LISI, L., MINELLI, G., PETTITI, I., PORTA, P., RUSSO, G. et TURCO, M. (2000) AMnO₃ (A = La, Nd, Sm) and Sm_{1-x}Sr_xMnO₃ perovskites as combustion catalysts: Structural, redox and catalytic properties, Appl. Catal. B: Environmental, 24 (3-4), 243-253.

COTTON, F. A. (1972) Advanced Inorganic Chemistry : a Comprehensive Text, 3rd Ed., Interscience Publishers, New York.

CURTIN, T., GRANGE, P. et DELMON, B. (1997) The direct decomposition of nitrogen monoxide, Catal. Today, 35, 121-127.

DALLA BETA, R. A. (1997) Catalytic combustion gas turbine systems : the preferred technology, Catal. Today, 35, 129-135.

DEGOBERT, P. (1992) Automobile et pollution, Éditions Technip, Paris.

DELL, R. M. et HOOPER, A. (1978) , Oxygen ion conductors, Solid Electrolytes – General Principles, Characterization, Materials, Applications, P. Hagenmuler, W. van Gool, Academic Press, New York, 291-312.

ENVIRONMENT CANADA (1998) Canada's response to EPA Proposal on transboundary air pollution, March.

FENG, M. et GOODENOUGH, J. B. (1994) A superior oxide-ion electrolyte, Eur. J. Solid State Inorg. Chem., 31 (7/8), 663-672.

FOGLER, H. S. (1991) Elements of chemical reaction engineering, Prentice Hall, Engelwood Cliffs, New Jersey.

FOKA, M., CHAOUKI, J., GUY, C. et KLVANA, D. (1994) Natural gas combustion of methane in a catalytic turbulent fluidized bed, Chem. Eng. Sci., **49**, 4639-4646.

FOKEMA, M. D. et YING, J. Y. (1999) The selective catalytic reduction of nitric oxide with methane over scandium oxide, yttrium oxide and lanthanum oxide, Appl. Catal. B: Environmental, **18**, 71-78.

FORNI, L., OLIVA, C., VATTI, F. P., KANDALA, M. A., EZERETS, A. M. et VISHNIAKOV, V. V. (1996) La-Ce-Co perovskites as catalysts for exhaust gas depollution, Appl. Catal. B: Environmental, **7(3-4)**, 269-284.

FRASER, J. M. et DANIELS, F. (1958) The heterogeneous decomposition of nitric oxide with oxide catalysts, J. Phys. Chem., **62**, 215-220.

FRITZ, A. et PITCHON, V. (1997) The current state of research on automotive lean NO_x catalysis, Appl. Catal. B: Environmental, **13**, 1-25.

GALASSO, F. S. (1969) Structure, Properties and Preparation of Perovskite-Type Compounds, Pergamon, Oxford.

GANDHI, H. S. et SHELEF, M. (1972) The adsorption of nitric oxide and carbon monoxide on nickel oxide, J. Catal., **24**, 241-249.

GANDHI, H. S. et SHELEF, M. (1973) The adsorption of nitric oxide on copper oxides, J. Catal., **28**, 241-249.

GARD, A. (1994) Specify better low NO_x burners for furnaces, Chem. Eng. Progress, **90** (1), 46-49.

GRINSTED, R. A., JEN, H. W., MONTREUIL, C. N., ROKOSZ, M. J. et SHELEF, M. (1993) The relation between deactivation of CuZSM-5 in the selective reduction of nitric oxide and dealumination of the zeolite, Zeolites, **13** (8), 602-606.

GOLODETS, G. I. (1983) Heterogenous catalytic reactions involving molecular oxygen, Studies in Surface Science and Catalysis, Vol. 15, Elsevier Science Publishers B. V., Amsterdam, 437-469.

GUILHAUME, N. et PRIMET, M. (1997) Three-way catalytic activity and oxygen storage capacity of perovskite LaMn_{0.976}Rh_{0.024}O_{3+δ}, J. Catal., **165**, 197-204.

GUNASEKARAN, N., SADDAWI, S. et CARBERRY, J. J. (1996) Effect of surface area on the oxidation of methane over solid oxide solution catalyst La_{0.8}Sr_{0.2}MnO₃, J. Catal., **159**, 107-111.

HALASZ, I., BRENNER, A., SHELEF, M. et Ng, K. Y. S. (1991) Decomposition of nitric oxide and its reduction by carbon monoxide over superconducting and related cuprate catalysts, Catal. Lett., **11** (3-6), 327-334.

HALASZ, I., BRENNER, A., SHELEF, M. et NG, K. Y. S. (1993) CO oxidation, NO decomposition and NO reduction on superconducting and related cuprates, Studies in Surface Science and Catalysis, Vol. 75 (New Frontiers in Catalysis, Pt. C), 2201-2204.

HALASZ, I., PAL-BORBELY, G. et BEYER, H. K. (1997) Decomposition of NO over Cu-ZSM-5 prepared by solid-state ion exchange, React. Kinet. Catal. Lett., **61** (1), 27-32.

HALL, W. K. et VALYON, J. (1992) Mechanism of nitric oxide decomposition over Cu-ZSM-5, Catal. Lett., **15** (3), 311-315.

HALLIOP, W., KIRCHNEROVA, J. et KARPINSKI, A. (2000) Bifunctional electrodes for electrically rechargeable Zn/air cells, 197th Meeting of the Electrochemical Society, Toronto, May 14-18.

HAMADA, H., KINTAICHI, Y., SASAKI, M. et ITO, T. (1990) Silver promoted oxide catalysts for direct decomposition of nitrogen monoxide, Chem. Lett., (7), 1069-1070.

HARTLEY, A., SAHIBZADA, M., WESTON, M., METCALFE, I. S. et MANTZAVINOS, D. (2000) $La_{0.6}Sr_{0.4}Co_{0.2}Fe_{0.8}O_3$ as the anode and cathode for intermediate temperature solid oxide fuel cells, Catal. Today, **55**, 197-204.

HAYASHI, H., INABA, H., MATSUYAMA, M., LAN, N. G., DOKIYA, M. et TAGAWA, H. (1999) Structural consideration of the ionic conductivity of perovskite-type oxides, Solid State Ionics, **122**, 1-15.

HAYES, R. E. et KOLACZKOWSKI, S. T. (1998) Introduction to catalytic combustion, Gordon and Breach Science Publishers.

HEADON, K., VAN DER LINDEN-DHONT, S., SEYEDYN-AZAD, F., MAO, W., ZHANG, D. -K., ZHAO, X. S. et LU, M. (1996) Decomposition of nitrogen oxides over zeolite-supported catalysts: effect of oxygen and methane, Sustainable Energy Environ. Technol., P. F. Greenfield, Singapore, 201-208.

HIGHTOWER, J. W. et van LEISBURG, D. A. (1975) Current status of the catalytic decomposition of NO. The Catalytic Chemistry of Nitrogen Oxides, R. L. Klimisch, J. G. Larson, Plenum Press, New York-London, 63-93.

HONG, S.-S., LEE, G.-D., PARK, J.-W., PARK, D.-W., CHO, M.-K. et OH, K.-J. (1997) Catalytic reduction of NO over perovskite-type catalysts, Korean J. Chem. Eng., 14(6), 491-497.

HUANG, K., LEE, H. Y. et GOODENOUGH, J. B. (1998) Sr- and Ni-doped LaCoO_3 and LaFeO_3 perovskites, new materials for solid-oxide fuel cells, J. Electrochem. Soc., 145, 3220-3227.

HUANG, P. -N. et PETRIC, A. (1996) Superior ion conductivity of lanthanum gallate doped with strontium and magnesium, J. Electrochem. Soc., 143 (5), 1644-1648.

HUANG, S. -J., WALTERS, A. B. et VANNICE, M. A. (1998) The adsorption and reaction of NO, CH_4 and O_2 on La_2O_3 and Sr-promoted La_2O_3 , Appl. Catal. B : Environmental, 17 (3), 183-193.

HUANG, S. -J., WALTERS, A. B. et VANNICE, M. A. (2000) Adsorption and decomposition of NO on lanthanum oxide, J. Catal., 192, 29-47.

HULGAARD, T. et DAM-JOHANSEN, K. (1993) Homogeneous nitrous oxide formation and destruction under combustion conditions, AIChE J., 39, 1342-1354.

IWAMOTO, M., (1991) Copper ion-exchanged zeolites as active catalysts for direct decomposition of nitrogen monoxide, Studies in Surface Science and Catalysis, Vol. 60 (Chem. Microporous Cryst.), 327-334.

IWAMOTO, M. (1994) Zeolites in environmental catalysis, Studies in Surface Science and Catalysis, Vol. 84 (Zeolites and Related Microporous Materials : State of the Art 1994), J. Weitkamp, H. G. Karge, H. Pfeifer, W. Holderich, Elsevier Science Publishers B. V., Amsterdam, 1395-1410.

IWAMOTO, M., (1996) Heterogenous catalysis for removal of NO in excess oxygen, Catal. Today, 29, 29-35.

IWAMOTO, M., YOKOO, S., SAKAI, K. et KAGAWA, S. (1981) Catalytic decomposition of nitric oxide over copper (II)-exchanged Y-type zeolites, J. Chem. Soc. Faraday Trans. I, 77, 1629-1638.

IWAMOTO, M., FURUKAWA, H. et KAGAWA, S. (1986) Catalytic decomposition of nitric monoxide over copper ion-exchanged zeolites, Studies in Surface Science and Catalysis, Vol. 28 (New Developments in Zeolite Science and Technology), Y. Murakami, A. Iijima, J. W. Ward, Elsevier Science Publishers B. V., Amsterdam, 943-949.

IWAMOTO, M. et HARADA, H. (1991) Removal of nitrogen monoxide from exhaust gases through novel catalytical processes, Catal. Today, 10 (1), 57-71.

IWAMOTO, M., MIZUNO, N., YAHIRO, H. (1991 a) Removal of nitrogen monoxide over copper ion-exchanged zeolite catalysts, Sekiyu Gakkaishi, 34 (5), 375-390.

IWAMOTO, M., MIZUNO, N., YAHIRO, H. et YOSHIOKA, T. (1991 b) Ion-exchange properties of copper with sodium on ZSM-5 zeolite and application of resulting Cu-ZSM-5 as nitric oxide decomposition catalyst, New Dev. Ion Exch., Proc. Int. Conf. Ion Exch., M. Abe, T. Kataoka, T. Suzuki, Kodansha: Tokyo, Japan, 407-412.

IWAMOTO, M., YAHIRO, H., TANDA, K., MIZUNO, N., MINE, Y. et KAGAWA, S. (1991 c) Removal of nitrogen monoxide through a novel catalytic process. 1. Decomposition on excessively copper ion exchanged ZSM-5 zeolites, J. Phys. Chem., 95 (9), 3727-3730.

JOLY, J. -P., KLVANA, D. et KIRCHNEROVA, J. (1999) TPD of oxygen from La-Sr-Ni-Co perovskite catalysts doped with Fe or Mn, React. Kinet. Catal. Lett., **68** (2), 249-255.

KAGAWA, S., OGAWA, H., FURUKAWA, H. et TERAOKA, Y. (1991) Cocation effect in catalytic property of copper ion-exchanged ZSM-5 zeolites for the direct decomposition of nitrogen monoxide, Chem. Lett., (3), 407-410.

KARPINSKI, A. P. et HALLIOP, W. (1997) Advanced Development program for lightweight, rechargeable, "AA" zinc-air battery, 5th Battery Exploratory Workshop, Burlington, VT, July 3.

KENDAL, K. R., NAVAS, C., THOMAS, J. K. et zur LOVE, H. -C. (1995) Recent developments in perovskite-based oxide ion conductors, Solid State Ionics, **82**, 215-223.

KIEßLING, D., SCHNEIDER, R., KRAAK, P., HAFTENDORN, M. et WENDT, G. (1998) Perovskite-type oxides – catalysts for the total oxidation of chlorinated hydrocarbons, Appl. Catal. B: Environmental, **19**, 143-151.

KIRCHNEROVA, J. (1999) Materials for catalytic gas combustion, Korean J. Chem. Eng., **16** (4), 427-433.

KIRCHNEROVA, J., HALLIOP, W. et KLVANA, D. (1999) Perovskite electrocatalysts for bifunctional oxygen electrodes for rechargeable Zn/air batteries, 3rd International Symposium on New Materials for Electrochemical Systems, Montreal, July 6-9.

KIRCHNEROVA, J. et KLVANA, D. (1994) Preparation and characterization of high surface perovskite electrocatalysts, Int. J. Hydrogen Energy, **19** (6), 501-506.

KIRCHNEROVA, J. et KLVANA, D. (1999) Synthesis and characterization of perovskite catalysts, Solid State Ionics, 123, 307-317.

KIRCHNEROVA, J. et KLVANA, D. (2000) Design criteria for high temperature combustion catalysts, Catal. Lett., 67, 175-185.

KIRCHNEROVA, J., KLVANA, D. et BOIVIN, I. (1998) Development of catalytic materials for high temperature combustion, Proceedings of the 1998 International Gas Research Conference, Vol. V, San Diego, 277-287.

KIRCHNEROVA, J., KLVANA, D., HINATSU, J., XIA, S., OLIVEIRA, J., ANANTARAMAN, A. et GOLEDZINOVSKA, M. (1995) New Ni-Co based perovskite as electrocatalysts in alkaline fuel cells, Proc. 1st Int. Symp. On New Materials for Fuel Cell Systems, O. Savadogo, P. R. Roberge et T. N. Veziroglu, Editions de École Polytechnique, Montréal, 190-200.

KIRCHNEROVA, J., VAILLANCOURT, J., KLVANA, D. et CHAOUKI, J. (1993) Evaluation of some cobalt and nickel based perovskites prepared by freeze-drying as combustion catalysts, Catal. Lett., 21 (1&2), 77-87.

KLVANA, D., CHAOUKI, J., GUY, C. et KIRCHNEROVA, J. (1996 a) Catalytic combustion : new catalysts for new technologies, Comb. Sci. Technol., 121 (1-6), 51-65.

KLVANA, D., DELVAL, J., KIRCHNEROVA, J. et CHAOUKI, J. (1997) Deactivation of fiber-supported $La_{0.65}Sr_{0.35}Ni_{0.29}Co_{0.69}Fe_{0.02}O_3$ catalyst by mercaptan during combustion of methane or natural gas, Appl. Catal. A : General, 165, 171-182.

KLVANA, D., KIRCHNEROVA, J., CHAOUKI, J., DELVAL, J. et YAICI, W. (1999)
a) Fiber supported perovskites for catalytic combustion of natural gas, Catal. Today, **47**, 115-121.

KLVANA, D., KIRCHNEROVA, J., GAUTHIER, P., DELVAL, J. et CHAOUKI, J. (1997) Preparation of supported $\text{La}_{0.66}\text{Sr}_{0.34}\text{Ni}_{0.3}\text{Co}_{0.7}\text{O}_3$ perovskite catalysts and their performance in methane and odorized natural gas combustion, Can. J. Chem. Eng., **75**, 509-519.

KLVANA, D., KIRCHNEROVA, J., TOFAN, C. (1999 b) Catalytic decomposition of nitric oxide by perovskites, Korean J. Chem. Eng., **16** (4), 470-477.

KLVANA, D., VAILLANCOURT, J., KIRCHNEROVA, J. et CHAOUKI, J. (1994) Combustion of methane over $\text{La}_{0.66}\text{Sr}_{0.34}\text{Ni}_{0.3}\text{Co}_{0.7}\text{O}_3$ and $\text{La}_{0.4}\text{Sr}_{0.6}\text{Fe}_{0.4}\text{Co}_{0.6}\text{O}_3$ prepared by freeze-drying, Appl. Catal. A : General, **109**, 181-193.

KLVANA, D., VANTOMME, S., KIRCHNEROVA, J. CHAOUKI, J. et VIGNERON, S. (1996 b) Oxydation catalytique du toluéne sur catalyseur perovskite, Proc. 1^{er} Congrès International sur le nez électroniques et les composés odorants, Paris, June, 26-27.

KOMATSU, T., NUNOKAWA, M., MOON, I. S., TAKAHARA, T., NAMBA, S. et YASHIMA, T. (1994) Kinetic studies of reduction of nitric oxide with ammonia on Cu^{2+} -exchanged zeolites, J. Catal., **148** (2), 427-437.

KORDESCH, K. et SIMADER, G. (1996) Fuel Cells and their Applications, VCH, Weinheim.

KUBASCHEWSKI, O., ALCKOCK, C. B. et SPENCER, P. J. (1993) Materials Thermochemistry, 6th Ed., Pergamon Press, Oxford.

KUCHEROV, A. V., GERLOCK, J. L., JEN, H. -W. et SHELEF, M. (1994) In-situ determination by ESR of the oxidation state of copper in Cu-ZSM-5 in flowing He and O₂ up to 500°C, J. Phys. Chem., **98** (18), 4892-4894.

KUEHN, E. (1994) Retrofit control technology reducing NO_x emissions, Power Eng., **98** (2), 23-28.

KUNG, H. H. (1989) Transition metal oxides: surface chemistry and catalysis, Studies in Surface Science and Catalysis, Vol. 45, Elsevier, New York, 162-166.

LADAVOS, A. K. et POMONIS, P. J. (1991) Comparative study of the solid-state and catalytic properties of La_{2-x}Sr_xNiO_{4.8} perovskites (x = 0.00-1.50) prepared by the nitrate and citrate methods, J. Chem. Soc. Faraday Trans., **87** (19), 3291-3297.

LARSSON, R. et JOHANSSON, L. Y. (1990) On the catalytic properties of mixed oxides for the electrochemical reduction of oxygen, J. Power Sources, **32**(3), 253-260.

LAWSON, A. (1972) A low temperature catalytic approach to NO_x control, J. Catal., **24**, 297-305.

LEE, J. H. et TRIMM, D. L. (1995) Catalytic combustion of methane, Fuel Process Technol., **42** (2&3), 339-359.

LI, Y. et ARMOR, J. N. (1992) Catalytic reduction of nitrogen oxides with methane in the presence of excess oxygen, Appl. Catal. B: Environmental, **1**, L31-L40.

LI, Y. et HALL, W. K. (1990) Stoichiometric catalytic decomposition of nitric oxide over Cu-ZSM-5 catalysts, J. Phys. Chem., **94** (16), 6145-6148.

LI, Y. et HALL, W. K. (1991) Catalytic decomposition of nitric oxide over Cu-zeolites, J. Catal., 129, 202-215.

LIBBY, W. F. (1971) Promising catalyst for auto exhaust, Science, 171 (3970), 499-500.

LIN, J., WEE, T. S., TAN, L. K., NEOH, K. G. et TEO, W. K. (1993) XPS/FTIR study of the interaction between nitric oxide and yttrium barium copper oxide ($YBa_2Cu_3O_7$), Inorg. Chem., 32 (24), 5522-5527.

LOMBARDO, E. A. et ULLA, M. A. (1998) Perovskite oxides in catalysis: past, present and future, Res. Chem. Intermed., 24 (5), 581-592.

MACHIDA, M., EGUCHI, K. et ARAI, H. (1987) High temperature catalytic combustion over cation-substituted barium hexaaluminates, Chem. Lett., (5), 767-770.

MACHIDA, M., EGUCHI, K. et ARAI, H. (1990) Effect of structural modification on the catalytic properties of Mn-substituted hexaaluminates, J. Catal., 123, 477-485.

MARTI, P. E., MACIEJEWSKI, M. et BAKER, A. (1994) Methane combustion over $La_{0.8}Sr_{0.2}MnO_{3+x}$ supported on MAI_2O_4 (M=Mg, Ni, Co) spinels, Appl. Catal. B : Environmental, 4, 225-235.

MEADOWCROFT, D. B. (1970) Low-cost oxygen electrode material, Nature, 226 (5248), 847-848.

MESTL, G., ROSYNEK, M. P. et LUNSFORD, J. H. (1997 a) Decomposition of nitric oxide over barium oxide supported on magnesium oxide. 2. In situ Raman characterization of phase present during the catalytic reaction, J. Phys. Chem. B, 101 (45), 9321-9328.

MESTL, G., ROSYNEK, M. P. et LUNSFORD, J. H. (1997 b) Decomposition of nitric oxide over barium oxide supported on magnesium oxide. 3. In situ Raman characterization of the role of oxygen, J. Phys. Chem. B, 101 (45), 9329-9334.

MESTL, G., ROSYNEK, M. P. et LUNSFORD, J. H. (1998) Decomposition of nitric oxide over barium oxide supported on magnesium oxide. 3. In situ Raman characterization of oxide phase transitions and peroxide species by ¹⁸O-labeling, J. Phys. Chem. B, 102 (1), 154-161.

METCALFE, I. S. et BAKER, R. T. (1996) Temperature programmed investigation of La(Ca)CrO₃ anode for the oxidation of methane in solid oxide fuel cells, Catal. Today, 27, 285-288.

MEUBUS, P. (1977) Catalytic decomposition of nitric oxide in the presence of alkaline earth oxides, J. Electrochem. Soc., 124 (1), 49-58.

MINH, N. Q. (1995) Ceramic fuel cells, J. Am. Ceram. Soc., 76 (3), 563-588.

OGATA, A., OBUCHI, A., MIZUNO, K., OHI, A. et OHUCHI, H. (1993) Active sites and redox properties of supported palladium catalysts for nitric oxide direct decomposition, J. Catal., 144 (2), 452-459.

OTTO, K. et SHELEF, M. (1969) Adsorption of nitric oxide on chromia supported on alumina, J. Catal., 14 (3), 226-237.

OTTO, K. et SHELEF, M. (1970) The adsorption of nitric oxide on iron oxides, J. Catal., 18, 184-192.

PARK, P. W., KIL, J. K. KUNG, H. H., KUNG, M. C. (1998) NO decomposition over sodium-promoted cobalt oxide, Catal. Today, 42, 51-60.

PARRAVANO, G. (1952) Ferroelectric transition and heterogeneous catalysis, J. Chem. Phys., 20, 342-343.

PARRAVANO, G. (1953) Catalytic activity of lanthanum and strontium manganite, J. Am. Chem. Soc., 75, 1497-1498.

PÂRVULESCU, V. I., GRANGE, P. et DELMON, B. (1998 a) Catalytic removal of NO, Catal. Today, 46, 233-316.

PÂRVULESCU, V. I., OELKER, P., GRANGE, P. et DELMON, B. (1998 b) NO decomposition over bicomponent Cu-Sm-ZSM-5 zeolites, Appl. Catal. B : Environmental, 16, 1-17.

PFEFFERLE, L. D. et PFEFFERLE, W. C. (1987) Catalysis in combustion, Catal. Rev. -Sci. Eng., 26 (2&3), 219-267.

PIRONE, R., GARUFI, E. et SANTAGATA, F. (1996) Effect of copper content on the activity of Cu-ZSM-5 zeolites at high Si/Al ratio towards NO decomposition, IChemE Res. Event, Eur. Young Res. Chem. Eng., 2, 594-596.

PONCE, S., PENA, M. A. et FIERRO, J. L. G. (2000) Surface properties and catalytic performance in methane combustion of Sr-substituted lanthanum manganites, Appl. Catal. B : Environmental, 24, 193-205.

PRASAD, R., KENNEDY, L. A., et RUCKENSTEIN, E. (1984) Catalytic combustion, Catal. Rev. -Sci. Eng., 26(1), 1-57.

- RADTKE, F., KOEPPEL, R. A. et BAIKER, A. (1995) Formation of hydrogen cyanide over Cu/ZSM-5 catalyst used for the removal of nitrogen oxides from exhaust of lean-burn engines, Environ. Sci. Technol., **29** (10), 2703-2705.
- REHSPRINGER, J. L., POIX, P., KADDOURI, A., ANDRIAMASINORO, D. et KIENNEMANN, A. (1991) Methane oxidative coupling by definite compounds (perovskite, cubic or monoclinic structure) obtained by low temperature processes, Catal. Lett., **10**, 111-120.
- ROBERTS, G. L. (2000) A review of mixed-transition metal oxides as bifunctional electrodes, Rev. Process. Chem. Eng., **3**(2), 151-174.
- SAINT-JUST, J. et der KINDEREN, J. (1996) Catalytic combustion : from reaction mechanism to commercial applications, Catal. Today, **29** (1-4), 387-395.
- SALAMA, T. M., SHIDO, T., OHNISHI, R. et ICHIKAWA, M. (1994) Low-temperature catalytic decomposition of NO over excess-loading gold (I) in NaY zeolite, J. Chem. Soc., Chem. Commun., **24**, 2749-2750.
- SAMMELS, A. F., COOK, R. L., WHITE, J. H., OSBORN, J. J. et MACDUFF, R. C. (1992) Rational selection of advanced solid electrolytes for intermediate temperature fuel cells, Solid State Ionics, **52**, 111-123.
- SARACCO, G., CERRI, I., SPECCHIA, V. et ACCORNERO, R. (1999 a) Catalytic pre-mixed fibre burners, Chem. Eng. Sci., **54** (15), 3599-3608.
- SARACCO, G., GEOBALDO, F. et BALDI, G. (1999 b) Methane combustion on Mg-doped LaMnO₃ perovskite catalysts, Appl. Catal. B.: Environmental, **20** (4), 277-288.

- SCHWAB, G.-M., STAEGER, R. et von BAUMBACH, H. H. (1933) The effect of metallic oxides in decomposing nitric oxide and their place in the periodic table, Z. Physik. Chem. B, 21, 65-83.
- SEIYAMA, T. (1993) Total oxidation of hydrocarbons on perovskite oxides, Chem. Ind., Vol. 50 (Properties and Applications of Perovskite-Type Oxides), L. G. Tejuda, J. L. G. Fierro, Marcel Dekker, New York, 215-234.
- SEKIZAWA, K., WIDJAJA, H., MAEDA, S., OZAWA, Y. et EGUCHI, K. (2000) Low temperature oxidation of methane over Pd catalyst supported on metal oxides, Catalysis Today, 59, 69-74.
- SHELEF, M., OTTO, K. et GANDHI, H. (1969) Heterogenous decomposition of nitric oxide on supported catalysts, Atmos. Environ., 3 (2), 107-122.
- SHELEF, M. (1992) On the mechanism of nitric oxide decomposition over Cu-ZSM-5, Catal. Lett., 15 (3), 305-310.
- SHELEF, M. (1995) Selective catalytic reduction of NO_x with N-free reductants, Chem. Rev., 95, 209-225.
- SHIMADA, H., MIYAMA, S. et KURODA, H. (1988) Decomposition of nitric oxide over Y-Ba-Cu-O mixed oxide catalysts, Chem. Lett., (10), 1797-1800.
- SINQUIN, G., HINDERMANN, J. P., PETIT, C. et KIENNEMANN, A. (1999) Perovskites as polyvalent catalysts for total destruction of C₁, C₂ aromatic chlorinated volatile organic compounds, Catal. Today, 54, 107-118.

SONG, K. S., KLVANA, D. et KIRCHNEROVA, J. (2001) Kinetics of propane combustion over $\text{La}_{0.66}\text{Sr}_{0.34}\text{Ni}_{0.3}\text{Co}_{0.7}\text{O}_3$ perovskite, Appl. Catal. A : General, in print.

STEPHAN, K., HACKENBERGER, M., KIESSLING, D. et WENDT, G. (1999) Supported perovskite-type oxide catalysts for the total oxidation of chlorinated hydrocarbons, Catal. Today, **54**, 23-30.

STOJANOVIC, M., HAVERKAMP, R. G., MIMS, C. A., MOUDALLALAND, H. et JACOBSON, A. J. (1997) Synthesis and characterization of $\text{LaCr}_{1-x}\text{Ni}_x\text{O}_3$ perovskite oxide catalysts, J. Catal., **165**, 315-323.

TABATA, K. (1988) Decomposition of nitric oxide by barium yttrium copper oxyde ($\text{Ba}_2\text{YCu}_3\text{O}_{7-\delta}$), J. Mater. Sci. Lett., **7**(2), 147-148.

TABATA, K., FUKUDA, H., KOHAKI, S., MIZUNO, N. et MISONO, M. (1988) Uptake of nitric oxide gas by yttrium, barium, copper oxide ($\text{YBa}_2\text{Cu}_3\text{O}_{7-\delta}$), Chem. Lett., **(5)**, 799-802.

TABATA, K. et MISONO, M. (1990) Elimination of pollutant gases – oxidation of CO, reduction and decomposition of NO, Catal. Today, **8**, 249-261.

TASCON, J. M. D. et TEJUCA, G. L. (1981) Adsorption of carbon dioxide on the perovskite-type oxide lanthanum cobaltate, J. Chem. Soc., Faraday Trans.1, **77** (3), 591-602.

TEJUCA, L. G., FIERRO, J. L. G. et TASCON, J. M. D. (1989) Structure and reactivity of perovskite-type oxides, Advances in Catalysis, Vol. 36, D. D. Eley, H. Pines, P. B. Weisz, Academic Press, New York, 237-328.

TEJUCA, L. G. et FIERRO, J. L. G. (1993) Properties and Applications of Perovskite-Type Oxides, Marcel Dekker, New York.

TERAOKA, Y., FUKUDA, H. et KAGAWA, S. (1990) Catalytic activity of perovskite-type oxides for the direct decomposition of nitrogen monoxide, Chem. Lett., (1), 1-4.

TERAOKA, Y., HARADA, T., FURUKAWA, H. and KAGAWA, S. (1993) Catalytic property of perovskite-type oxides for the direct decomposition of nitric oxide, Studies in Surface Science and Catalysis, Vol. 75 (New Frontiers in Catalysis, Pt. C), 2649-2652.

TERAOKA, Y., ZHANG, H. M., OKAMOTO, K. et YAMAZOE, N. (1988) Mixed ionic-electronic conductivity of lanthanum strontium cobalt iron oxide ($La_{1-x}Sr_xCo_1-yFe_yO_{3-\delta}$) perovskite-type oxides, Mater. Res. Bull., 23 (1), 51-58.

TOFAN, C., KLVANA, D. et KIRCHNEROVA, J. (2001a) Direct decomposition of nitric oxide over perovskite-type oxide catalysts, Appl. Catal. A: General, sous presse.

TOFAN, C., KLVANA, D. et KIRCHNEROVA, J. (2001b) Kinetics of Direct Decomposition of Nitric Oxide over Three Perovskite Catalysts, Appl. Catal. A: General, sous presse.

TOFAN, C., KLVANA, D. et KIRCHNEROVA, J. (2001c) Decomposition of Nitric Oxide over Perovskite Oxide Catalysts: Effect of CO_2 , H_2O and CH_4 , Appl. Catal. B: Environmental, accepté avec corrections.

TRIMM, D. L. (1983) Catalytic combustion (review), Appl. Catal., 7 (3), 249-282.

TSAI, C.-Y., DIXON, A. G., MOSER, W. R. et MA, Y. H. (1997) Dense perovskite membrane reactors for partial oxidation of methane to syngas, AIChE Journal, 43(11A), 2741-2750.

TWU, J. et GALLAGHER, P. K. (1993) Preparation of bulk and supported perovskites, Chem. Ind., Vol. 50 (Properties and Applications of Perovskite-Type Oxides), L. G. Tejaca, J. L. G. Fierro, Marcel Dekker, New York, 1-24.

VALYON, J. et HALL, W. K. (1993 a) Studies of the desorption of oxygen from Cu-zeolites during NO decomposition, J. Catal., 143, 520-532.

VALYON, J. et HALL, W. K. (1993 b) Studies of the surface species formed from NO on copper zeolites, J. Phys. Chem., 97 (6), 1204-1212.

VANNICE, M. A., WALTERS, A. B. et ZHANG, X. (1996) The kinetics of NO_x decomposition and NO reduction by CH₄ over La₂O₃ and Sr/La₂O₃, J. Catal., 159 (1), 119-126.

VARGA, J., FUDALA, A., HALASZ, J., SCHOBEL, G. et KIRICSI, I. (1995) ZSM-5 zeolites modified by solid-state ion-exchange for NO decomposition, Studies in Surface Science and Catalysis, Vol. 94 (Catalysis by Microporous Materials), 665-672.

VISWANATHAN, B. (1992) Carbon monoxide oxidation and nitric oxide reduction on perovskite oxides, Catal. Rev.-Sci. Eng., 34(4), 337-354.

VOORHOEVE, R. J. H. (1977) Perovskite-related oxides as oxidation-reduction catalysts, Advanced Materials in Catalysis, J. J. Burton, R. L. Garten, Academic Press, New York, 129-180.

VOORHOEVE, R. J. H., REMEIKA, J. P. et TRIMBLE, L. E. (1975) Nitric oxide and perovskite-type catalysts: solid state and catalytic chemistry, The Catalytic Chemistry of Nitrogen Oxides, R. L. Klimisch, J. G. Larson, Plenum Press, New York-London, 215-231.

WAN, L. (1993) Poisoning of perovskite oxides by sulphur dioxide, Chem. Ind., Vol 50 (Properties and Applications of Perovskite-Type Oxides), G. L. Tejua, J. L. G. Fierro, Marcel Dekker, New York, 145-170.

WARNATZ, J., MAAS, U. et DIBBLE, R. W. (1996) Combustion : physical and chemical fundamentals, modelling and simulation, experiments, pollutant formation, Springer-Verlag Berlin, Heidelberg, New York, 219-231.

WINDAWI, H. et CHU, W. (1996) Control VOCs via catalytic oxidation, Chem. Eng. Progress, March, 37-41.

WINTER, E. R. S. (1971) The catalytic decomposition of nitric oxide by metallic oxides, J. Catal., 22, 158-170.

XIE, S., MESTL, G. ROSYNEK, M. P. et LUNSFORD, J. H. (1997) Decomposition of nitric oxide over barium oxide supported on magnesium oxide. 1. Catalytic results and in situ Raman spectroscopic evidence for a barium-nitro intermediate, J. Am. Chem. Soc., 119 (42), 10186-10191.

XU, S. J. et THOMSON, W. J. (1997) Perovskite-type oxide membranes for the oxidative coupling of methane, AIChE Journal, 43 (11A), 2731-2740.

XU, S. J. et THOMSON, W. J. (1998) Stability of $\text{La}_{0.6}\text{Sr}_{0.4}\text{Co}_{0.2}\text{Fe}_{0.8}\text{O}_{3-\delta}$ perovskite membranes in reducing and nonreducing environments, Ind. Eng. Chem. Res., **37**, 1290-1299.

YAMASHITA, T. et VANNICE, A. (1996) NO decomposition over Mn_2O_3 and Mn_3O_4 , J. Catal., **163 (1)**, 158-168.

YAMASHITA, T. et VANNICE, A. (1997) Temperature-programmed desorption of NO adsorbed on Mn_2O_3 and Mn_3O_4 , Appl. Catal. B : Environmental, **13 (2)**, 141-155.

YAO, H. C. et SHELEF, M. (1974) Nitric oxide and carbon monoxide chemisorption on cobalt-containing spinels, J. Phys. Chem. **78 (24)**, 2490-2496.

YASUDA, H., MIZUNO, N. et MISONO, M. (1990) Role of valency of copper in the direct decomposition of nitrogen monoxide over well characterized $\text{La}_{2-x}\text{A}'_x\text{Cu}_{1-y}\text{B}'_y\text{O}_4$, J. Chem. Soc., Chem. Commun., **16**, 1094-1096.

YASUDA, H., NITADORI, T., MIZUNO, N. et MISONO, M. (1993) Catalytic decomposition of nitrogen monoxide over valency-controlled La_2CuO_4 -based mixed oxides, Bull. Chem. Soc. Jpn., **66 (11)**, 3492-3502.

YOKOMICHI, Y., NAKAYAMA, T., OKADA, O., YOKOI, Y., TAKAHASHI, I., UCHIDA, H., ISHIKAWA, H., YAMAGUCHI, R., MATSUI, H. et YAMABE, T. (1996) Fundamental study on the NO_x direct decomposition catalysts, Catal. Today, **29**, 155-160.

YUR'EVA, T. M., POPOVSKII, V. V. et BORESKOV, G. K. (1965) Catalytic activity of metal oxides of the IVth period of the periodic system with respect to oxidation reactions. II. Decomposition of nitric oxide, Kinetika i Kataliz, **6 (6)**, 1041-1045.

ZERNIKE, J. (1967) Catalytic combustion and its limit. Commemorating the discovery of this phenomenon 150 years ago, Chem. Weekbl., 63, 321-325.

ZHANG, H. M., SHIMIZU, Y., TERAOKA, Y., MIURA, N. et YAMAZOE, N. (1990) Oxygen sorption and catalytic properties of lanthanum strontium cobalt iron oxide $La_1-xSr_xCo_{1-y}Fe_yO_3$ Perovskite-type oxides, J. Catal., 121 (2), 432-440.

ZHANG, X, WALTERS, A. B. et VANNICE, A. (1994 a) NO_x decomposition and reduction by methane over La_2O_3 , Appl. Catal. B : Environmental, 4, 237-256.

ZHANG, X, WALTERS, A. B. et VANNICE, A. (1995 a) NO adsorption, decomposition and reduction by methane over rare earth oxides, J. Catal., 155, 290-302.

ZHANG, Y. et FLYTZANI-STEPHANOPOULOS, M. (1994 b) Catalytic decomposition of nitric oxide over promoted copper-ion-exchanged ZSM-5 zeolites, ACS Symp. Ser., 552, 7-21.

ZHANG, Y., SUN, T., SAROFIM, A. F. et FLYTZANI-STEPHANOPOULOS, M. (1995 b) Decomposition of NO over metal-modified Cu-ZSM-5 catalysts, ACS Symp. Ser., 587, 133-146.

ZHANG, Y. et FLYTZANI-STEPHANOPOULOS, M. (1996) Hydrothermal stability of cerium modified Cu-ZSM-5 catalyst for nitric oxide decomposition, J. Catal., 164 (1), 131-145.

ZHAO, Z., YANG, X. et WU, Y. (1996) Comparative study of nickel-based perovskite-like mixed oxide catalysts for direct decomposition of NO, Appl. Catal. B : Environmental, 8 (3), 281-297.

ZWINKELS, M. F. M., JÄRÄS, S. G. et MENON, P. G. (1993) Catalytic materials for high-temperature combustion, Catal. Rev. -Sci. Eng., 35 (3), 319-358.

ANNEXE 1
Caractéristiques physiques d'oxydes d'azote

Tableau A1.1 Caractéristiques physiques du monoxyde, dioxyde, trioxyde, tetraoxyde et protoxyde d'azote

Caractéristique	NO	NO₂	N₂O₃	N₂O₄	N₂O
Massé molaire g/mole	30,01	46,01	76,01	92,02	44,01
Densité relative (air = 1)	1,04	1,58		3,2	1,53
Massé spécifique g/mL	1,27 à -150,2 °C			1,5 à 21 °C	1,97 à 25 °C
Point d'ébullition °C	-151,8	21,5	3,5 (décomposition)	21,2	-88,5
Point de fusion °C	-163,6	-9,3	-100	-11,2	-91,0
Couleur	-	rouge- marron	bleu (liquide et solide)	-	-

ANNEXE 2

Montage expérimental

Les tests d'activité, ainsi que l'étude cinétique ont été réalisés à l'aide du montage présenté à la figure A 2.1.

Les réactions chimiques ont lieu dans un réacteur tubulaire en acier inoxydable en forme de U ayant un diamètre intérieur de 0.7 cm et une longueur de 30 cm. Le lit catalytique est de 10 mL. Pour assurer une bonne perméabilité du lit catalytique, ainsi qu'une opération isotherme du réacteur, le catalyseur (1 g) a été dilué avec 7 mL d'inerte (pierre ponce).

Le réacteur est placé dans un four isolé avec de la laine minérale. Le four est formé par un récipient métallique cylindrique dans lequel se trouve un élément chauffant, également de forme cylindrique qui est séparé du réacteur par un écran métallique. Ce dernier permet une meilleure répartition de la chaleur autour du réacteur. Un agitateur est placé dans le four, sous le réacteur, afin d'assurer une bonne uniformisation de la température par une circulation forcée de l'air autour du réacteur.

Un manomètre à mercure placé à l'entrée du réacteur permet de connaître la perte de charge dans le réacteur. Deux thermocouples de type K sont placés dans le lit catalytique à l'entrée et à la sortie pour mesurer la température.

L'alimentation du réacteur avec les différents gaz (NO, He, O₂, CO₂ et CH₄) est faite par l'intermédiaire de débitmètres massiques MKS ou Brooks, calibrés, reliés à un ordinateur. Ce dernier permet de régler les débits de chacun des gaz. L'eau est ajoutée au mélange réactionnel en faisant passer l'hélium par un saturateur maintenu à une température constante (298 K dans cette étude).

À la sortie du réacteur le mélange gazeux est acheminé vers le système d'analyse constitué d'un spectromètre IR à transformée de Fourier (Bomen Inc.) et d'un chromatographe (Perkin-Elmer Sigma 300 Gas Chromatograph).

Le spectromètre IR est muni d'une cellule d'un volume de 1 L et d'un détecteur MCT (mercure-cadmium-tellure). Il a été utilisé spécialement pour détecter l'éventuelle présence du N₂O. La calibration du spectromètre a été faite pour des mélanges avec une concentration en N₂O entre 0,0103 % et 1,03 % obtenus par dilution avec de l'hélium d'un mélange standard de 1,03 %N₂O dans azote. Les régions IR utilisées pour la calibration sont : 589,7-587,3 cm⁻¹, 2271,0-2135,0 cm⁻¹, 2622,0-2500,4 cm⁻¹ et 3531,9-3423,9 cm⁻¹.

Le chromatographe utilise un détecteur à conductibilité thermique. Les températures du four, détecteur et injecteur sont respectivement 373, 353 et 373 K. La vitesse du gaz porteur (hélium) est de 30 mL/min. Le chromatographe est muni d'une colonne à tamis moléculaire 5Å et permet la détection de l'O₂, N₂ et NO. Les temps de rétention sont 4,4 min pour O₂, 6,2 min pour N₂, et 9,4 min pour NO. Cependant, à cause de la forme du pic du NO et à cause des réactions qui peuvent avoir lieu dans la partie située entre le réacteur et le chromatographe entre NO et O₂ déjà présent ou formé lors de la réaction, seul l'azote a été quantifié. La courbe de calibration de l'azote a été établie à partir d'un mélange standard de 0,976 %N₂ dans He.

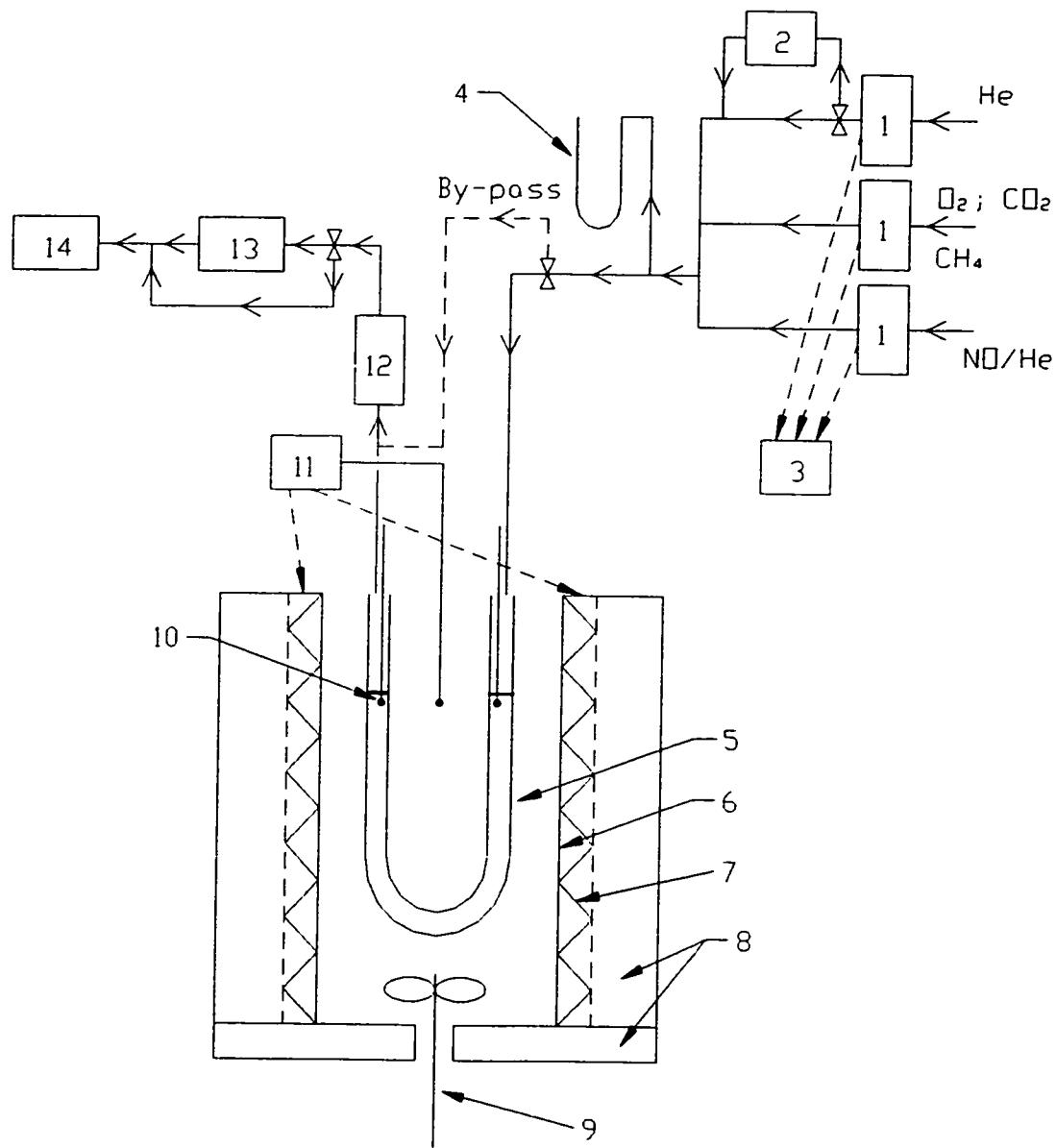


Figure A2.1 Montage expérimental

1- débitmètres massiques; 2- saturateur; 3- contrôleur de débit; 4- manomètre; 5- réacteur; 6- écran métallique; 7- éléments chauffants; 8- isolant; 9- agitateur; 10- thermocouples; 11- contrôleur de température; 12- dessicant; 13- spectromètre; 14- chromatographe G-L.

ANNEXE 3**Perovskites in Environmental and Related Catalysis : their Potentiel and Limitations****Reference :**

J. Kirchnerova, C. Tofan et D. Klvana (2000) Perovskites in Environmental and Related Catalysis : their Potentiel and Limitations, presented by C. Tofan at 50th Canadian Chemical Engineering Conference, Montréal.

Air pollution is a continuous problem. The most serious pollutants, nitrogen oxides, originate in high temperature processes, on which depends much of our heat and energy supply. With constantly growing energy consumption the demands for the development of efficient nitric oxide removal technologies and cleaner alternatives to energy production where fossil fuels, particularly natural gas, remain a highly economical source, are getting more and more urgent. Catalysis plays an important role not only in the area of NO_x removal, but it is also at the center of more efficient and cleaner energy production alternatives such as catalytic combustion or fuel cells. In all these areas economical, highly performing catalysts are need. Among the variety of available materials, perovskites, especially those represented by $\text{La}_{1-x}\text{Sr}_x\text{MO}_3$, attract for their excellent catalytic properties a lot of attention and some may become industrially important. This paper represents an overview of a current status of perovskite oxides in relation to their potential use in environmental catalysis.

La pollution atmosphérique est un problème majeur. Les polluants les plus nocifs, les oxydes d'azote (NO_x), sont générés par la combustion à haute température. Avec l'augmentation de la consommation d'énergie il devient de plus en plus nécessaire de développer non seulement des technologies efficaces d'abattement des NO_x , mais aussi des technologies plus propres pour la génération d'énergie à partir de combustibles fossiles. Le gaz naturel représente une source importante et économique. Puisque la catalyse est indispensable dans les deux domaines, on a besoin de catalyseurs très performants et peu coûteux. Parmi les matériaux disponibles, les pérovskites, particulièrement celles représentées par $\text{La}_{1-x}\text{Sr}_x\text{MO}_3$, semblent attirer beaucoup l'attention à cause de leurs excellentes propriétés catalytiques. Certaines pourraient trouver des applications industrielles. Cet article présent une aperçue de l'état actuel de la recherche sur les pérovskites, leur potentiel et leurs limitations comme catalyseurs environnementaux.

Our constantly growing consumption of energy and of material goods is inevitably associated with potential growth of pollution. Appropriate measures have to be therefore taken to prevent its escalation and continuous development of environmentally friendly technologies is required. This awareness is not new; it dates back several decades. Progress has been made, but much remains to be done.

Among the multitude of undesirable and often harmful pollutants that require efficient control such as toxic gases, wide range of volatile organic compounds and organic and inorganic particulates, nitrogen oxides are the most serious. Their abatement represents since several decades a continuous challenge. Nitric oxide, the direct precursor of highly noxious nitrogen dioxide, is generated in all high temperature combustion processes using air as an oxidant. These processes supply most of our current energy needs and they are even part of the arsenal of different clean-up technologies. When the fuel, such as biomass, contains organic, easily oxidizable nitrogen, the amount of combustion generated nitrogen oxides is considerably higher. In a number of places there are currently economically driven incentives to include biomass as a source of energy, because it is renewable.

To succeed globally in the abatement of combustion generated pollutants, variety of approaches (*strategies*) is possible and should be developed. These include more efficient and less polluting use of fuels by improved burners and precise control of the fuel/air ratio (Gard, 1994; Kuehn, 1994) as well as reliable and effective clean-up technologies. Longer-term strategies include development of alternative ultra-low or zero NO_x technologies such as catalytic combustion and fuel cells, particularly those based on solid oxide electrolytes. Most of the required technologies rely on highly active catalysts. Thus, successful development and implementation of any of these environmentally friendly technologies is directly dependent on the availability of highly performing economically acceptable catalytic materials. These materials are expected to be thermally stable, robust and durable to withstand the severe conditions of their

operation: high temperatures, high space velocities, sudden temperature changes, and corrosive atmosphere of combustion products. They also have to be very active, when handling, for example, low pollutant concentrations in an excess of combustion products.

At present majority of the clean or clean-up catalytic technologies is dominated by platinum and by other noble metals, especially palladium and rhodium. However, because of their high cost, limited long-term availability and other specific factors, for example significant volatility at elevated temperatures, much effort is spent to develop alternative catalysts. Variety of materials is being investigated, but one larger family of catalysts, perovskite-type mixed oxides, has received a lot of attention. As will become clear, by their very nature perovskites, especially those represented by $\text{La}_{1-x}\text{Sr}_x\text{MO}_3$ (where M stands for Co, Ni, Mn, Fe, Cu or their combination), could be considered as almost universal catalysts for a number of oxygen involving reactions.

Why perovskites?

Perovskite oxides, usually represented by a simple formula ABO_3 , are characterized by a unique crystal structure in which the larger, body centered cation A ($r_A > 0.09$ nm) is twelve fold coordinated by oxygen, whereas the smaller B cation ($r_B > 0.05$ nm), located at the corners of the cube is octahedrally coordinated by six oxygen ions. The radii of admissible A and B cations and of oxygen ion, r_A , r_B and r_O respectively, are related to the structural tolerance factor $t = (r_A + r_O) / ((r_B + r_O) \cdot 2^{0.5})$ within the range of 0.75 to 1.0. This structure permits to accommodate a wide variety of metal ions of different valences and also has an unusual capacity to accept a number of different types of defects. This structure, unlike any other, gives rise to many technologically important properties such as high electronic and ionic conductivity and excellent capacity for reversible oxygen sorption, which are equally important in heterogeneous catalysis. Especially invaluable is the ability of the structure to stabilize mixed-valence, as well as

unusual valence states of useful catalytically active metals such as cobalt, manganese, nickel, iron, and titanium.

Although the technologically interesting properties of many perovskites have been known for decades (Galasso, 1969), their potential in catalysis has been recognized only rather recently. Perovskites have been suggested as catalysts thirty years ago for the very same reason they continue to command attention: search for a suitable low cost replacement of expensive platinum in the area of environmental catalysis. In 1970 Meadowcroft reported a high activity of lanthanum cobaltite in oxygen reduction in alkaline solution. His report prompted Libby (1971) to propose the same material as an auto exhaust catalyst. While until now Libby's suggestion proved to be far fetched, it had sparked an intensive research and interest around the world. This interest was further boosted by the discovery of "high" temperature superconductivity of $\text{YBa}_2\text{Cu}_3\text{O}_{7-\delta}$ (Tejucá et al., 1989) and seems to continue as attested by a relatively large number of different articles published over the last years, although only few can be considered as truly innovative. Variety of different perovskite compositions has been evaluated in numerous reactions, including those in reduction atmospheres and dozens of patents on their potential applications and/or preparations were issued. While no perovskite catalyst has found yet an industrial application, these studies have largely contributed to a better understanding of many oxidation reactions. After thirty years in vogue, it is perhaps time to ask again where is the true practical potential of these fascinating materials. In this paper we present an overview of a current status of lanthanum-strontium-transition metal-based perovskite oxides in relation to their potential use in environmental catalysis. Some of the examples are supplemented by our own data, for which the experimental details are given in specific sections.

Perovskites Preparation Techniques

Efficient and reliable synthesis of a fine homogeneous powder with a well defined morphology is the first important step towards successful application of any given perovskite composition, be it as a supported catalyst or as a bulk (catalytic) ceramic. While a given composition dictates its intrinsic properties, the overall (catalytic) performance is strongly dependent also on the catalyst morphology and therefore on the preparation process. The challenge is to prepare a phase homogeneous material having a highly defective surface with a large number of active sites. Several satisfactory techniques are available, most of them using dissolved precursors as a starting point (Tejucá et al., 1989; Twu and Gallagher, 1993). Initial solution, which provides the best homogeneity of precursors, is then processed by a variety of techniques, including spray-freezing/freeze-drying, complexation, precipitation, or explosion, each of which is followed by calcination (heat treatment) to form the desired perovskite phase. Table A3.1 summarizes the available methods and their characteristics. Actually, the solution-based methods differ in a way of processing the solution before the final step of perovskite formation. The key to success in obtaining a fine-grained homogeneous material is to maintain the homogeneity through the whole preparation process, in particular during the calcination. The choice of appropriate calcination conditions, i.e. temperature and time, which depend on several factors such as the final perovskite composition, the nature of the precursor, the nature of the complexing or precipitating agent is very important. Care has to be taken to avoid any local sintering and to minimize formation of stable, in most cases undesirable, intermediate phases. Solution spray-freezing/freeze-drying appears to be the best method, but it is relatively long (the solvent removal is very slow and costly) and requires reliable freeze-drying equipment. As such this method is poorly suited for low cost large-scale production. Other methods do not rely on freeze-drying, but necessitate large quantities of either complexing or precipitation agents. These have to be removed during calcination often requiring higher

temperatures and result in high volume of fume gases, increase the cost of precursor materials and the risk of contamination.

Table A3.1 Comparison of Available Methods for Preparation of Perovskite Powders

Method	Advantages	Disadvantages
Ceramic	Simplicity, low cost No additives Minimum fumes	Poor homogeneity Low precursor reactivity → High calcination temperatures Low SSA
Co-precipitation	Good homogeneity Good precursor reactivity Intermediate calcination temperatures Relatively high SSA	Additives needed High volume fumes/ or washing Risk of contamination
Sol-gel	Very good homogeneity Good precursor reactivity Intermediate calcination temperatures Very high SSA	Additives needed High volume fumes Risk of contamination
Complexation	Very good homogeneity Good precursor reactivity Intermediate calcination temperatures Relatively high SSA	Additives needed High volume fumes Risk of contamination
Explosion	Excellent homogeneity Good precursor reactivity Intermediate calcination temperatures High SSA	Additives needed, careful control Very high volume fumes Risk of contamination Risk of run-off
Solution spray-freezing/freeze-drying	No additives Excellent homogeneity High precursor reactivity → Lowest calcination temperatures High SSA	Slow drying / control needed Specialized equipment required
Aqueous slurry using lanthanum hydroxide	No additives Good homogeneity High precursor reactivity → Lowest calcination temperatures Lowest volume of fumes High SSA	No disadvantages with respect to other methods

To circumvent these inconveniences a new method has recently been developed (Kirchnerova and Klvana, 1999). This method uses reactive highly homogeneous slurry of lanthanum hydroxide in a solution of remaining metal nitrates and partially precipitated metal hydroxides as the starting precursor. Although freeze-drying has so far been used for water removal, other drying techniques, particularly spray-drying are potentially suitable. Laboratory tests have shown that simple drying at ambient conditions (in a fume hood) leads to comparable results. Table A3.2 provides examples of perovskite compositions successfully prepared in this laboratory.

Table A3.2: Selected Perovskites Prepared By a New Method

(Kirchnerova and Klvana, 1999)

Composition	Calcination ^a		SSA m ² /g	Practical Applications Examples
	K	h		
$\text{La}_{0.66}\text{Sr}_{0.34}\text{Ni}_{0.3}\text{Co}_{0.7}\text{O}_3$	893	4	10	AFC ; Cat. Comb. T<1000 K
$\text{La}_{0.66}\text{Sr}_{0.34}\text{Ni}_{0.29}\text{Co}_{0.69}\text{Fe}_{0.02}\text{O}_3$	893	4	10	AFC ; Cat. Comb. T<1000 K
$\text{La}_{0.8}\text{Sr}_{0.2}\text{MnO}_3$	893	4	12	SOFC, cathode Cat. Comb. T<1000 K
$\text{La}_{0.7}\text{Sr}_{0.3}\text{Mn}_{0.3}\text{Ni}_{0.7}\text{O}_3$	893	4	10	AFC
$\text{La}_{0.8}\text{Sr}_{0.2}\text{Cu}_{0.15}\text{Fe}_{0.85}\text{O}_3$	925	4	12	Cat. Comb. T<1100 K
$\text{La}_{0.66}\text{Sr}_{0.34}\text{Ni}_{0.2}\text{Fe}_{0.8}\text{O}_3$	1150	16	5.7	SOFC, cathode Cat. Comb. T<1150 K
$\text{La}_{0.9}\text{Sr}_{0.1}\text{Al}_{0.85}\text{Co}_{0.15}\text{O}_3$	1000	12	17	Cat. Comb. T<1250 K
$\text{La}_{0.9}\text{Sr}_{0.1}\text{Al}_{0.87}\text{Fe}_{0.13}\text{O}_3$	1300	30	4	Cat. Comb. T<1550 K
$\text{La}_{0.9}\text{Sr}_{0.1}\text{Cr}_{0.95}\text{Y}_{0.05}\text{O}_3$	1150	12	1.6	SOFC interconnects
$\text{YBa}_2\text{Cu}_3\text{O}_{7-\delta}$	1120	10	1.1	Superconductors, catalysts

^a: following the initial calcination 12 h at 865 ± 5 K

Perovskites as Combustion Catalysts

Catalytic combustion is one of the most environmentally acceptable means to produce heat or energy from fuels such as natural gas or other hydrocarbons, while keeping the NO_x emissions at the minimum. The key to this process is an efficient catalyst, which assures, over its surface, a self-propagating combustion of nonstoichiometric, fuel lean mixtures. The leaner the mixture, the lower the temperature of the system. At the same time, the lower temperature means less NO_x formed. Below about 1273 K acceptable (negligible) levels of NO_x are generated. The virtues of catalytic combustion have been known and reasonably well understood for decades and several technologies were developed (Zernike, 1967; Pfefferle and Pfefferle, 1987; Chaouki et al., 1994; Foka et al., 1994; Saint-Just and der Kinderen, 1996; Dalla Betta, 1997; Hayes and Kolaczkowski, 1998). However, lack of suitable economical catalysts has hindered their wider acceptance. Most of the existing technologies use noble metal catalysts, mainly platinum and palladium (Lee and Trimm, 1995), which are exceptionally active and can, especially platinum, tolerate relatively high concentrations of sulphur oxides. Nevertheless, platinum is expensive and the temperature of its operation is limited to about 1200 K. Several transition metal oxides exhibit a good catalytic activity in total oxidation of methane, which is the most difficult hydrocarbon to activate. Particularly active in most of the oxygen involving reactions is Co_3O_4 (Golodets, 1983). The activity of other transition metal oxides decreases in the following order: $\text{Co}_3\text{O}_4 > \text{MnO}_2 > \text{NiO} \geq \text{CuO} > \text{Cr}_2\text{O}_3 \geq \text{Fe}_2\text{O}_3$. These materials are inexpensive and can easily be prepared with sufficiently high specific areas. As such, individually or in combination, they are used in a number of processes. However, their thermal stability is poor, making their applications in catalytic combustion limited. In contrast, the thermal stability of the corresponding perovskites LaMO_3 ($\text{M} = \text{Co, Mn, Ni, Fe or Cr}$) is substantially improved. The catalytic activity of these simple (binary) perovskites, most of which are nearly stoichiometric in oxygen, is also relatively good, following about the same order as that of the parent transition metal oxides (Tejuca et al., 1989) and can be largely improved by

a variety of substitutions on both the A site and the B site. Such substitutions permit to control oxygen stoichiometry and may induce or stabilize otherwise unstable metal ions, such as trivalent nickel or even copper. Because of their higher oxygen mobility and higher capacity for reversible oxygen sorption, oxygen non-stoichiometric perovskites ($\text{A}_{1-x}\text{A}'_x\text{BO}_{3-\delta}$) are typically more active than their parent transition metal oxide (Arai et al., 1986; Kirchnerova et al., 1993; Batiot-Dupeyrat et al., 2001).

In view of their high catalytic activity in total oxidation (combustion) of a multitude of organic compounds (Seiyama, 1993), several perovskites containing base metals would appear as the prime candidates for a variety of catalytic combustion technologies (Chaouki et al., 1994; Foka et al., 1994; Klvana et al., 1996a,b; Saracco et al., 1999a,b; Kirchnerova, 1999, Song et al., 2001). In several aspects, particularly due to an excellent selectivity toward the complete oxidation of methane, i.e. selectivity to carbon dioxide formation even in oxygen deficient atmosphere (Choudhary and Rane, 1991; Rehspringer et al., 1991; Klvana et al., 1997), some perovskites may appear to be comparable or even superior to platinum. Nevertheless, perovskites are a priori susceptible to poisoning by sulphur oxides (Wan, 1993) to the extent which depends on their particular composition, even though some may tolerate very low sulphur levels such as in odorized natural gas (Klvana et al., 1997, 1999a). The degree and rate of sulphur oxide poisoning will also depend on the temperature of operation, and is expected to decrease at temperatures above 1070 K. For temperatures below 1070 K, the most active are cobalt-based perovskites (Arai et al., 1986; Kirchnerova et al., 1993). Especially active as low temperature combustion catalyst is the composition $\text{La}_{0.66}\text{Sr}_{0.34}\text{Ni}_{0.3}\text{Co}_{0.7}\text{O}_3$ (LSNC) (Klvana et al., 1994; Klvana et al. 1997, Song et al., 2001), which was originally developed for oxygen evolution in alkaline media (Kirchnerova and Klvana, 1994). The excellent catalytic activity of LSNC is most likely related to its high electronic as well as ionic conductivity (Huang et al., 1998). Nevertheless, for their higher thermal stability strontium substituted lanthanum manganites $\text{La}_{1-x}\text{Sr}_x\text{MnO}_3$ with $x \leq 0.2$ seem to be preferred in many laboratories (Arai et al., 1986; Marti et al., 1994;

Gunasekaran et al., 1996; Saracco et al., 1999a,b; Ponce et al., 2000). Yet, although LaFeO_3 shows comparatively low activity, substitution by strontium, such as in $\text{La}_{0.8}\text{Sr}_{0.2}\text{FeO}_3$ results in a marked activity enhancement and would therefore deserve more attention (Batiot-Dupeyrat et al., 2001). However, while the temperature range of their potential applications is extended, even these perovskites will not withstand longer operation above 1270 K. A suitable material for high temperature catalytic combustion has been searched actively for several decades (Blazowski and Walsh, 1975; Zwinkels et al., 1993; Dalla Betta, 1997), and in the mid nineteen eighties a new type of catalysts, transition metal (manganese) substituted hexaaluminates which exhibit good catalytic activity and high thermal stability have been developed (Machida et al., 1987). However, these materials having a β -alumina structure (Machida et al., 1990) and exhibiting a two-dimensional coefficient of thermal expansion suffer from poor resistance to thermal shock and are therefore unsuitable for fabrication of bulk monoliths. Materials exhibiting an isosteric expansion, for example perovskites, should be preferable. Indeed, it was shown recently, that by doping refractory perovskites such as LaAlO_3 or SrTiO_3 with a transition metal of low volatility, particularly with iron, a catalyst with acceptable activity and with very good thermal stability could be obtained (Kirchnerova et al., 1998; Kirchnerova and Klvana, 2000). These perovskite-type catalysts also exhibit a better selectivity than hexaaluminates to complete oxidation. While their long-term durability, the upper temperature limit of operation and their sensitivity to poisoning at high operation temperatures remains to be determined, these materials hold a good promise.

Catalytic combustion plays also an important role in the abatement of a variety of volatile organic compounds from different industrial effluents (Windawi and Chu, 1996). In these technologies, several perovskite catalysts might prove to be very useful for a number of specific applications, provided no sulphur is present (Kvana et al., 1996b). This area is probably under-explored and would deserve more innovative work with respect to optimization of composition towards specific needs. On the other hand,

transition metal based perovskites seem unlikely to be suitable for combustion of chlorinated compounds, because of their potential interaction with hydrogen chloride resulting formed during their combustion. In fact use of several perovskites has been investigated even for total oxidation of chlorinated hydrocarbons. Although some were shown as very active (Kießling et al., 1998; Stephan et al., 1999; Sinquin et al., 1999), their resistance to poisoning by the produced chlorine or hydrochloric acid was poor.

Perovskites in Fuel Cells

Fuel cell is a device, which directly converts available free energy of fuel “combustion” into electricity. In contrast to gas phase combustion, the two reactants (fuel and oxygen) must react separated by an electrolyte transporting one of the reactants in form of an ion. Electrons passed externally release the energy and no NO_x are generated. Fuel cells of very wide range of capacities can be constructed, from mW to MW.

The crucial material dictating the rest of the components and the cell design is the electrolyte. Based on the electrolyte, which also dictates the temperature of operation, different technologies have been developed over the years (Blomen and Mugerwa, 1993; Kordesch and Simader, 1996), each finding its specific niche of applications. Two of these, i.e. alkaline fuel cells (AFC) using concentrated solution of potassium hydroxide, and solid oxide fuel cells (SOFC) at present using yttria stabilized zirconia, can make a direct use of perovskite catalyst as part of the cathode. In fact for SOFC operating at temperatures above 1200 K, perovskites are indispensable and as outlined below, in the future SOFC designs perovskites may play far more important role.

Alkaline Fuel Cells

Characterized by low cost and versatility, AFC systems are particularly suitable for small power units and were before the advent of polymer electrolyte based cells favored

for transportation. Although the interest in these systems faded, their potential remains (Kordesch and Simader, 1996). Similarly as other fuel cells, for their good performance AFC depend on a highly active electrically conducting catalyst for oxygen reduction (cathode). However, in contrast to those based on acidic electrolytes, AFC's do not rely on platinum. Although AFC's typically employ silver or cobalt based spinels as the preferred catalyst, since the Meadowcroft's suggestion in 1970, cobalt and nickel based perovskites have been shown in several laboratories as very active (Tejucá et al., 1989; Larsson and Johansson, 1990). One of the best performing perovskites for oxygen reduction is $\text{La}_{0.66}\text{Sr}_{0.34}\text{Ni}_{0.3}\text{Co}_{0.7}\text{O}_3$ (Kirchnerova et al., 1995), which is not only highly active, but also is a very good electrical conductor. Fine perovskite powders are especially suitable for bifunctional oxygen electrodes of Zn/air rechargeable batteries, for which their application has been explored for more than twenty years (Roberts, 2000). A series of specially formulated perovskite powders prepared in this laboratory by the new, above described method (Kirchnerova and Klvana, 1999) has also been tested successfully in production of oxygen electrodes for zinc/air rechargeable batteries (Karpinski and Halliop, 1997; Kirchnerova et al., 1999; Halliop et al., 2000).

Solid Oxide Fuel Cells

SOFC seem to be the only area where perovskite, namely $\text{La}_{1-x}\text{Sr}_x\text{MnO}_3$, currently represents the best available material for the cathode. In fact there is a good chance that an all perovskite SOFC will be developed in a near future.

SOFC have been under development for nearly fifty years, and some of the technologies are well mature. In spite of different designs, all of them use thin zirconia electrolyte membranes, nickel/zirconia cermet (composite ceramic) as the anode, $\text{La}_{1-x}\text{Sr}_x\text{MnO}_3$ cathodes, and $\text{La}_{1-x}\text{Sr}_x\text{CrO}_3$ interconnects (Minh, 1995). This choice of component materials represents a far from ideal compromise between availability and actual requirements. Stabilized zirconia has for a long time been known as the best suitable

solid electrolyte, but to obtain acceptable ionic conductivity high operation temperatures and small thickness are required. Among available materials, only perovskites are chemically stable while exhibiting high enough electronic and ionic (O^{2-}) conductivity to be used as cathode. Although cobaltites are much better conductors than manganites, they are chemically and mechanically incompatible with zirconia. Ni/zirconia cermet is the answer to the poor stability of perovskites in reducing anode atmosphere.

Nevertheless, over the last decade there is a great incentive to develop better-suited materials, from the electrolyte to the other components. The effort in several laboratories seems to bring some fruits. Interestingly, most attention is focused on perovskites (Sammells et al., 1992; Kendal et al., 1995; Hayashi et al., 1999). Apparently based on the high mixed ionic-electronic conductivity of $La_{1-x}Sr_xCo_{1-y}Fe_yO_{3-\delta}$ (LSCF) reported in 1988 by Teraoka et al., and subsequently shown excellent oxygen sorption and catalytic properties by the same group (Zhang et al., 1990), $La_{0.6}Sr_{0.4}Co_{0.2}Fe_{0.8}O_3$ has been studied as a better cathode material (Anderson and Nasrallah, 1991; Chen et al., 1993), specifically for intermediate temperature (800 – 1000 K) fuel cells. This material attracts further interest as oxygen permeating membrane to be potentially used for oxidative coupling of methane (Xu and Thomson, 1997) or for production of syngas by methane oxidation (Tsai et al., 1997). Other very promising perovskite compositions, specifically strontium and nickel substituted $LaCoO_3$ and $LaFeO_3$, have been recently studied (Huang et al., 1998). These perovskites are better conductors than $La_{1-x}Sr_xMnO_3$ and their coefficient of thermal expansion would be acceptable for zirconia.

In 1994, Feng and Goodenough have found a new perovskite-type electrolyte, which exhibits significantly higher conductivity than zirconia and would allow lower operation temperatures. The composition of this new material, $La_{1-x}Sr_xGa_{1-y}Mg_yO_3$ where optimum value of x is 0.2 and of y 0.1 or 0.15 depending on temperature (Huang and Petric, 1996), would possibly also allow the use of better cathode and anode materials such as nickel

substituted cobaltites or ferrites. Although gallium is expensive, considering the small thickness of the electrolyte membrane needed, this new electrolyte might eventually find acceptance.

Since current state of art SOFC systems do not permit perovskites as anodes, but rely on Ni-cermet, natural gas has to be reformed to avoid anode poisoning by coking. Development of electrolytes assuring high oxygen flux and of perovskites exhibiting higher mixed conductivity and better compatibility with the electrolyte might open a way for using the same material for both cathode and anode (Hartley et al., 2000). Oxide based anode would possibly allow a direct use of natural gas improving thereby the overall efficiency. Indeed, should a given material prove to be suitable for operation as an oxygen membrane in partial oxidation of methane, or of other hydrocarbons, it should in principle be also suitable as an anode. The challenge is to formulate a composition, which will be chemically and thermally stable, catalytically active for methane oxidation, good mixed conductor and mechanically compatible with the electrolyte. The LSCF system seems to have properties very close to the need (Xu and Thomson, 1998). Other perovskite systems based on chromium for potential use as anode material have been studied, but have not shown the expected performance (Metcalfe and Baker, 1996; Stojanovic et al., 1997). Improvement in stability of LSCF system ($\text{La}_{0.6}\text{Sr}_{0.4}\text{Co}_{0.2}\text{Fe}_{0.8}\text{O}_3$) might be obtained by further decreasing the content of strontium, and/or by doping with a third transition metal. It has been our experience, supported by ample literature data, that optimum oxygen deficiency δ referred to strontium substitution is about 0.17, i.e. strontium substitution $x = 0.34$.

Perovskites in Nitrogen Oxides Removal

Removal of nitric oxides from combustion effluents remains a great challenge, in spite of different strategies available and in spite of all progress in this important area of environmental catalysis so far achieved (Pârvulescu et al., 1998). Catalytic direct

decomposition and reduction are two areas of nitric oxides destruction, in which perovskites have historically attracted a lot of attention (Voorhoeve et al., 1975; Tejuca et al., 1989) but failed to be useful for practical applications. Although over the last years interest in finding some suitable perovskite composition(s) even for these applications has been revived, in spite of previous failures, as will be shown, it is unlikely, that this effort will bring some fruits.

Direct Nitric Oxide Decomposition

In principle, thermodynamically feasible direct decomposition represents the best means of nitric oxide removal. However, this reaction is so slow that it requires either a highly active catalyst, or an external energy source for activation. Catalytic decomposition of nitric oxide has been studied for nearly a century and dozens of materials have been evaluated (Hightower and van Leirsburg, 1975, Iwamoto, 1991). Of these numerous materials, the best activity was observed over platinum, Co_3O_4 , some perovskites, and especially over copper substituted zeolites. Nevertheless, even copper zeolites, which at 773 K are about two orders of magnitude more active than the other active materials and were for more than a decade considered as highly promising, are inadequate for practical needs.

The early studies of catalytic properties of perovskites, concerning mainly lanthanum substituted manganites and cobaltites (Voorhoeve et al., 1975; Chien et al., 1975), have indicated that when tested under conditions approaching those realistic for practical applications these materials are inactive, in spite of their excellent activity in carbon monoxide and hydrocarbon oxidation. Furthermore, because of their easy poisoning by sulphur oxides, perovskites were deemed impractical as automotive catalysts. Yet, new wave of interest in perovskites as nitric oxide decomposition catalysts ensued after the discovery of "high temperature" superconductors at the end of nineteen eighties and some, when tested under rather low flowrates, were considered as promising (Tabata et

al., 1988; Teraoka et al., 1990; Ladavos and Pomonis, 1991; Teraoka et al., 1993; Yasuda et al., 1990; Yasuda et al., 1993), although other highly sintered (SSA < 1 m²/g) perovskites evaluated under reasonable flowrates were again found inactive (Halasz et al., 1991).

Being motivated by high activity of some of the perovskites developed for methane combustion, we have also undertaken a study of direct nitric oxide decomposition over perovskites selecting the compositions in which cobalt, nickel and copper were considered as the main, activity bearing sites (Klvana et al, 1999b; Tofan et al., 2001). This comparative study, in which a steady state activity of ten different multi-component perovskite compositions, mostly prepared with SSA between 9 to 22 m²/g, has been evaluated, was carried out under a wide range of experimental conditions in a plug-flow reactor using 1 g fine perovskite powder (Tofan, 2001). The results of this study have in part confirmed some of the earlier work, but also new important information has been obtained. The decomposition was found far more complex than generally admitted, being strongly inhibited not only by oxygen but also by nitric oxide itself, apparently through competing oxidation reactions of the surface bound species. Yet, analysis of conversion data, obtained when no oxygen was added to the feed, has indicated that a model involving oxygen not only as inhibitor, but also as reactant, can best describe kinetics of nitric oxide decomposition. This seemingly contradictory result suggests that the decomposition proceeds via some oxygen involving intermediate such as O-N-NO₂ or (NO₂)₂. Depending on temperature, the decomposition seems to follow at least two different mechanisms, probably in relation with the availability of different types of oxygen species (Zhang et al., 1990; Joly et al., 1999). While some effects of composition and of SSA were clearly evident as shown for example by the data in Table A3.3, the activities of the new perovskites fall within the same order of magnitude. Although the activities of the new perovskites are higher than those of individual component metal oxides, suggesting that the perovskite structure has some beneficial effect, they fall short of practical needs by at least three orders of magnitude.

Table A3.3 Apparent Kinetic Parameters of the Pseudo-First Order Rate Model for Nitric Oxide Decomposition over Several Perovskite Catalysts

CATALYST	I.D.	δ^*	SSA	E_{app}^a	E_{app}^b	k_{1-723}^c	k_{1-923}^d
				m ² /g	kJ/mol	kJ/mol	μmol/gsbar
$\text{La}_{0.66}\text{Sr}_{0.34}\text{Ni}_{0.3}\text{Co}_{0.7}\text{O}_{3-\delta}$	LSNC	0.17	9.0	60	105	1.32	9.8
$\text{La}_{0.66}\text{Sr}_{0.34}\text{Ni}_{0.29}\text{Co}_{0.69}\text{Fe}_{0.02}\text{O}_{3-\delta}$	LSNCF	0.17	10.5	55 ^e	108	2.25 ^e	9.1
$\text{La}_{0.6}\text{Sr}_{0.34}\text{Ag}_{0.06}\text{Ni}_{0.4}\text{Co}_{0.6}\text{O}_{3-\delta}$	LSANC	0.23	10.0	79	109	0.68	8.9
$\text{La}_{0.4}\text{Sr}_{0.6}\text{Mn}_{0.4}\text{Ni}_{0.6}\text{O}_{3-\delta}$	LSMN-46	< 0.3	16.0	65	108	1.50	9.4
$\text{La}_{0.7}\text{Sr}_{0.3}\text{Mn}_{0.3}\text{Ni}_{0.7}\text{O}_{3-\delta}$	LSMN-37	0.15	9.8	45 ^f	87	2.36 ^f	6.5
$\text{La}_{0.87}\text{Sr}_{0.13}\text{Mn}_{0.2}\text{Ni}_{0.8}\text{O}_{3-\delta}$	LSMN-28	> 0.065	12.7	94	119	0.41	11.3
$\text{La}_{0.95}\text{Sr}_{0.05}\text{Mn}_{0.13}\text{Ni}_{0.87}\text{O}_{3-\delta}$	LSMN-19	> 0.025	10.5	65	103	0.79	10.3
$\text{La}_{0.8}\text{Sr}_{0.2}\text{Cu}_{0.15}\text{Fe}_{0.85}\text{O}_{3-\delta}$	LSCuF	< 0.175	10.1	40	75	2.61	8.8
$\text{La}_{0.8}\text{Sr}_{0.2}\text{Cu}_{0.15}\text{Al}_{0.85}\text{O}_{3-\delta}$	LSCuA	0.175	21.8	28	82	1.93	4.0
$\text{La}_{0.66}\text{Sr}_{0.34}\text{Ti}_{0.66}\text{Cu}_{0.34}\text{O}_{3-\delta}$	LSCuT	0.01	1.1	0.6	40	1.95	0.2
$\text{La}_2\text{CuO}_3/\text{CuO/LaFeO}_3$	LFCu	-	8.6	56 ^g	76	1.00 ^g	4.6

^a : estimate based on Sr (and Cu when applicable) substitution

^b : apparent activation energy derived by regression from high temperature values of k_1 (pseudo-first order constant) obtained from conversion data for 15 mL/min, 2 vol% NO, 1 g catalyst

^c : apparent activation energy derived by regression from high temperature values of k_1 obtained from conversion data for 100 mL/min, 5 vol% NO, 1 g catalyst,

^d : the highest values of k_1 at 723 K (from data for 15 mL/min, 2 vol% NO, 1 g catalyst)

^e : the highest values of k_1 at 923 K (from data for 100 mL/min, 5 vol% NO, 1 g catalyst)

^f : for 5 vol% NO, 50 mL/min, 1.5 g catalyst

^g : for 5 vol% NO, 30 mL/min, 1 g catalyst

^g : for 5 vol% NO, 50 mL/min, 1 g catalyst

This low activity is further reduced by the presence of water and especially of carbon dioxide, as illustrated for the case of $\text{La}_{0.8}\text{Sr}_{0.2}\text{Cu}_{0.15}\text{Fe}_{0.85}\text{O}_3$ (LSCuF) perovskite in Figure A3.1, where the inhibition by water and carbon dioxide is compared with the

very strong inhibition by oxygen. Of the eleven compositions tested, LSCuF perovskite can be consider as the overall best performing. Thus, overall performance in direct nitric oxide decomposition of this perovskite is rather poor, similarly as that of most of other metal oxides.

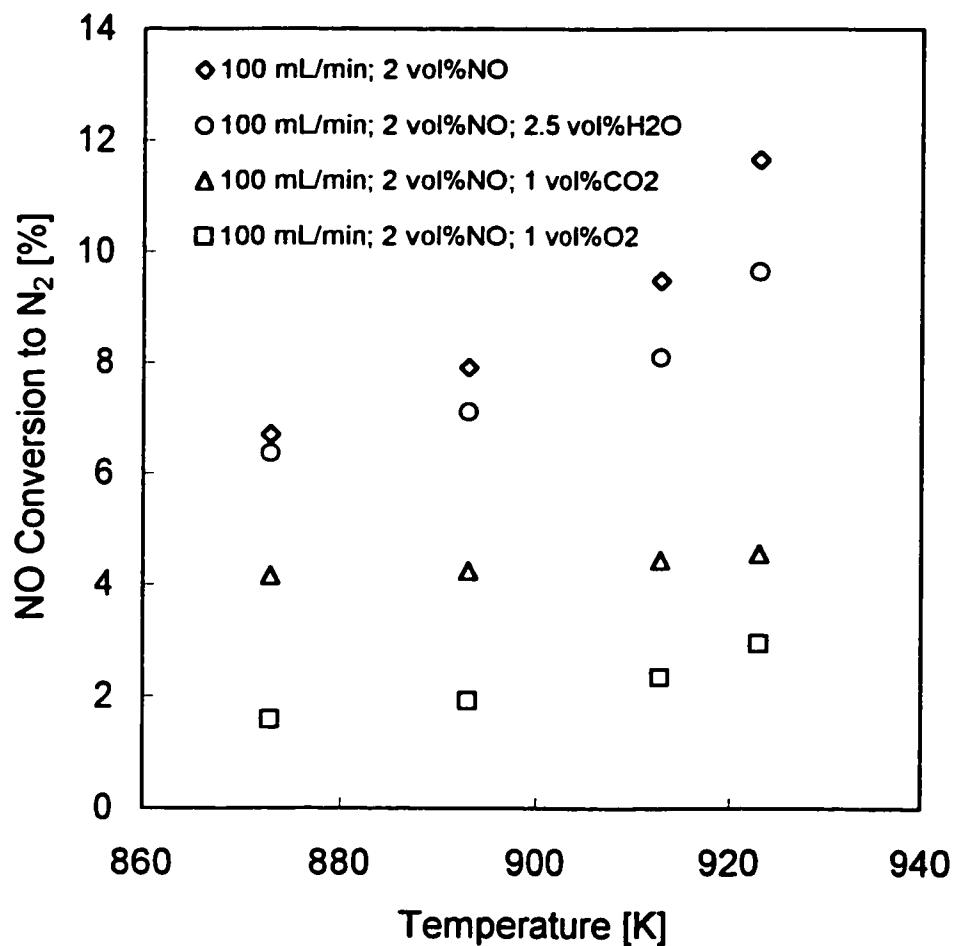


Figure A3.1 Effect of water, of carbon dioxide and of oxygen on the decomposition of nitric oxide over 1 g of $\text{La}_{0.8}\text{Sr}_{0.2}\text{Cu}_{0.15}\text{Fe}_{0.85}\text{O}_3$ perovskite powder ($< 10 \mu\text{m}$) diluted by 7 mL of precalcined inert pumice particles (350-416 μm); plug-flow reactor, steady state conversions.

Catalytic Reduction of Nitrogen Oxides

Failure to find suitable catalyst for direct nitric oxide decomposition had necessitated the development of alternative NO_x destructive ways, such as three-way automotive catalytic systems (Fritz and Pitchon, 1997) and selective catalytic reduction, SCR, (Li and Armor, 1992; Shelef, 1995; Pârvulescu et al., 1998), which are currently the only available industrial processes. Three-way catalysis, at present relying on noble metals, takes advantage of a unique composition of automotive effluents and necessitates a fine-tuning of fuel/air ratio, because it is ineffective in the presence of excess oxygen. The available selective catalytic reduction systems developed for stationary emission sources employ ammonia as reducing agent and vanadia/titania or zeolite catalysts. Neither of the processes represents an ideal solution to the problem and further developments are required (Armor, 1994). The most urgent need seems to be development of de- NO_x catalyst efficient in the presence of oxygen, required for lean-burn engine technology and for diesel engines. Lean-burn engine technology would represent an improvement of fuel economy. While the current SCR technologies are effective, use of ammonia as reductant is costly and represents some hazards due to its possible slips. Its replacement by more practical and benign reductants, such as light hydrocarbons, would represent an important improvement. Indeed, this area of catalysis is currently very active and again, perovskites are enjoying a lot of interest both for automotive three-way catalytic activity (Viswanathan, 1992; Forni et al., 1996; Guilhaume and Primet, 1997), and for SCR (Hong et al., 1997; Belessi et al., 2000 and references therein). Nevertheless, although perovskites would a priory appear attractive, because of their generally high activity in oxidation reactions by oxygen, it may be difficult to find a composition over which the reduction of nitric oxides would be selective. So far, most of the studies in this area indicate that either the activity of transition metal based perovskites is too low for practical application (Forni et al., 1996; Fritz and Pitchon, 1997), or the reduction is nonselective. When oxygen is present in the effluents, the reductant, whether carbon monoxide or hydrocarbon, is oxidized before nitric oxide is reduced. This is well

illustrated by our own steady-state experimental data, obtained in a plug-flow type alumina ceramic reactor and shown in Figure A3.2.

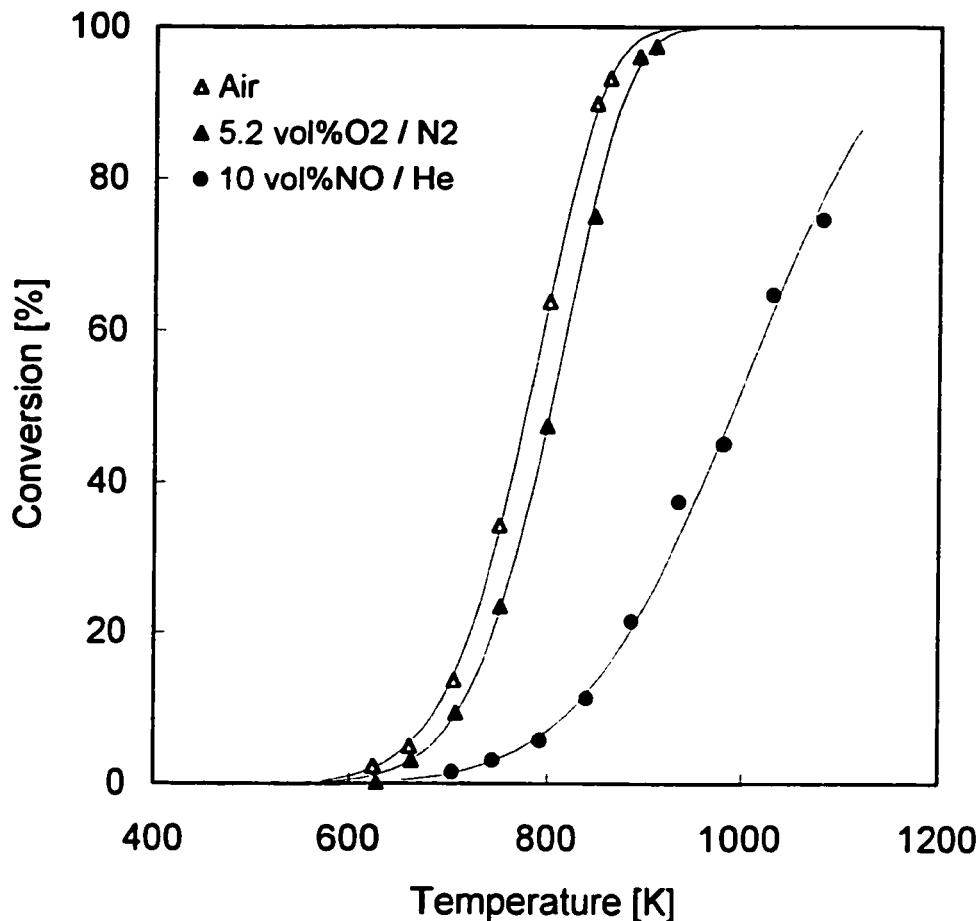


Figure A3.2 Oxidation of 2.6 vol% methane to carbon dioxide by oxygen and by nitric oxide over 0.5 g of $\text{La}_{0.8}\text{Sr}_{0.2}\text{Cu}_{0.15}\text{Fe}_{0.85}\text{O}_3$ perovskite powder ($< 10 \mu\text{m}$) diluted by 10 mL of precalcined inert pumice particles (350-416 μm); plug-flow reactor, steady state conversions, feed flow 200 mL/min. The lines are calculated using following pseudo-first order constants: air: $E_{\text{app}} = 97 \text{ kJ/mol}$, $\ln A = 20.05 \mu\text{mol/g}\cdot\text{s}\cdot\text{bar}$; 5.2 vol%O₂/N₂: $E_{\text{app}} = 97 \text{ kJ/mol}$, $\ln A = 19.75 \mu\text{mol/g}\cdot\text{s}\cdot\text{bar}$; 10 vol% NO: $E_{\text{app}} = 76 \text{ kJ/mol}$, $\ln A = 14.65 \mu\text{mol/g}\cdot\text{s}\cdot\text{bar}$.

This figure compares oxidation of methane by different oxygen concentrations with that by nitric oxide over LSCuF perovskite. As evident, methane is oxidized substantially faster by oxygen than by nitric oxide. It may also be noted that the lower apparent activation energy for the latter reaction most likely reflects the strong inhibition by carbon dioxide. Not surprisingly, the NO_x reduction in the presence of oxygen by methane is not selective. Thus, the discussed perovskites appear to be inadequate also for this application.

Summary and Conclusions

As a family, La_{1-x}Sr_xMO₃ (where M stands for Co, Ni, Mn, Fe, Cu, Cr or their combination) perovskites are not only highly interesting materials, but also a number of them might in a near future become important as commercial catalysts or catalytically active ceramics for use in the field of environmental protection. Indeed, some of them are already indispensable for SOFC. Other important areas of potential applications are catalytic combustion of sulphur free or very low sulphur content streams, high temperature catalytic combustion, alkaline fuel cell systems and oxygen permeable membranes. To fully exploit their potential, innovative approaches for formulating new highly performing (perovskite) compositions for specific applications are needed.

While in some of these areas perovskites may compete with platinum, it would be unrealistic to expect that they can be tailored to any requirement. For example, they remain unsuitable for treating effluents containing sulphur in significant concentrations and are also unlikely to be useful for combustion of chlorinated hydrocarbons. Perovskites are not sufficiently active, and therefore unsuitable, for direct decomposition of nitric oxide, nor most likely for selective nitric oxide reduction.

Still, studies of perovskites as model compounds for various catalytic reactions remain useful, provided new information is being sought.

Acknowledgment

Based on research carried out over several years this work has in part been supported by several sources: Natural Sciences and Engineering Research Council of Canada, Hydrogen Industry Council, Gaz Métropolitain, Natural Gas Technology Center, Gaz de France, Ministère de l'Énergie et des Ressources du Québec.

References

- Anderson, H. U. and M. M. Nasrallah, "Characterization of Oxides for Low Temperature Solid Oxide Fuel Cells", Annual Report, Contract No. 5090-260-2069, Gas Research Institute, Chicago, IL, 1991.
- Arai, H., T. Yamada, K. Eguchi and T. Seiyama, "Catalytic Combustion of Methane over Various Perovskite-Type Oxides", *Appl. Catal.*, **26**, 265-276 (1986).
- Armor, J. N., "Materials Needs for Catalysts to Improve our Environment", *Chem. Mater.* **6**, 730-738 (1994).
- Belessi, V. C., C. N. Costa, T. V. Bakas, T. Anastasiadou, P. J. Pomonis, A. M. Efstatthiou, "Catalytic Behavior of La-Sr-Ce-Fe-O mixed oxidic/perovskitic systems for the NO+CO and NO+CH₄+O₂ (lean-O₂) Reactions", *Catal. Today*, **59**, 347-363 (2000).
- Batiot-Dupeyrat, C., F. Martinez-Ortega, M. Ganne and J. M. Tatibouët, "Methane Catalytic Combustion on La-Based Perovskite Type Catalysts in High Temperature Isothermal Conditions", *Appl. Catal. A: General*, **206**, 205-215 (2001).
- Blazowski, W. S. and D. E. Walsh, "Catalytic Combustion: An Important Consideration for Future Applications", *Comb. Sci. Technol.*, **10**, 233-244 (1975).

Blomen, L. J. M. J. and M. N. Mugerwa, Eds., **Fuel Cell Systems**, Plenum Press, New York, 1993.

Chaouki, J., C. Guy, H. Sapundziev, D. Kusohorsky and D. Klvana, "Combustion of Methane in a Cyclic Catalytic Reactor", **I&EC Research**, **33**(12), 2957-2963 (1994).

Chen, C. C., M. M. Nasrallah and H. U. Anderson, "Synthesis and Characterization of $(CeO_2)_{0.8}(SmO_{1.5})_{0.2}$ thin Film from Polymeric Precursors", **J. Electrochem. Soc.**, **140**(12), 3555-3560 (1993).

Chien, M. W., I. M. Pearson and K. Nobe, "Reduction and Adsorption of Nitric Oxide on Cobalt Perovskite Catalysts", **Ind. Eng. Chem. Prod. Res. Dev.**, **14**(2), 131-134 (1975).

Choudhary, V. R. and V. H. Rane, "Acidity/Basicity of Rare-Earth Oxides and their Catalytic Activity in Oxidative Coupling of Methane to C₂-Hydrocarbons", **J. Catal.**, **130**, 411-422 (1991).

Dalla Betta, R. A., "Catalytic Combustion Gas Turbine Systems: the Preferred Technology", **Catal. Today**, **35**, 129-135 (1997).

Feng, M. and J. B. Goodenough, "A Superior Oxide -Ion Electrolyte", **Eur. J. Solid State Inorg. Chem.**, **31**(7/8), 663-672 (1994).

Foka, M., J. Chaouki, C. Guy and D. Klvana, "Natural Gas Combustion of Methane in a Catalytic Turbulent Fluidized Bed", **Chem. Eng. Sci.**, **49**, 4639-4646 (1994).

Forni, L., C. Oliva, F. P. Vatti, M. A. Kandala, A. M. Ezerets and V. V. Vishniakov, "La-Ce-Co Perovskites as Catalysts for Exhaust Gas Depollution", *Appl. Catal. B: Environmental*, **7**(3-4), 269-284 (1996).

Fritz, A. and V. Pitchon, "The Current State of Research on Automotive Lean NO_x Catalysis", *Appl. Catal. B: Environmental*, **13**, 1-25 (1997).

Galasso, F. S., "Structure, Properties and Preparation of Perovskite-Type Compounds", Pergamon, Oxford, 1969.

Gard, A., "Specify Better Low NO_x Burners for Furnaces", *Chem. Eng. Progress*, **90**(1), 46-49 (1994).

Golodets, G. I., "Heterogeneous Catalytic Reactions Involving Molecular Oxygen", *Studies in Surface Science and Catalysis*, Vol. 15, Elsevier, Amsterdam (1983), pp.437-469.

Guilhaume, N. and M. Primet, "Three-Way Catalytic Activity and Oxygen Storage Capacity of Perovskite LaMn_{0.976}Rh_{0.024}O_{3+δ}", *J. Catal.*, **165**, 197-204 (1997).

Gunasekaran N., S. Saddawi and J. J. Carberry, "Effect of Surface Area on the Oxidation of Methane over Solid Oxide Solution Catalyst La_{0.8}Sr_{0.2}MnO₃", *J. Catal.*, **159**, 107-111 (1996).

Halasz, I., A. Brenner, M. Shelef and K. Y. S. Ng, "Decomposition of Nitric Oxide and its Reduction by Carbon Monoxide over Superconducting and Related Cuprate Catalysts", *Catal. Lett.*, **11**(3-6), 327-334 (1991).

Halllop, W., J. Kirchnerova and A. Karpinski, "Bifunctional Electrodes for Electrically Rechargeable Zn/Air Cells", 197th Meeting of the Electrochemical Society, Toronto, May 14-18, 2000.

Hartley, A., M. Sahibzada, M. Weston, I. S. Metcalfe and D. Mantzavinos, "La_{0.6}Sr_{0.4}Co_{0.2}Fe_{0.8}O₃ as the Anode and Cathode for Intermediate Temperature Solid Oxide Fuel Cells", *Catal. Today*, **55**, 197-204 (2000).

Hayashi, H., H. Inaba, M. Matsuyama, N. G. Lan, M. Dokiya and H. Tagawa, "Structural Consideration of the Ionic Conductivity of Perovskite-Type Oxides", *Solid State Ionics*, **122**, 1-15 (1999).

Hayes, R. E. and S. T. Kolaczkowski, "Introduction to Catalytic Combustion", Gordon and Breach Science Publishers, 1998.

Hightower, J. W. and D. A. van Leirsburg, "Current Status of the Catalytic Decomposition of NO", in "The Catalytic Chemistry of Nitrogen Oxides", R. L. Klimisch and J. G. Larson, Eds., Plenum Press, New York, (1975), pp.63-93.

Hong, S.-S., G.-D. Lee, J.-W. Park, D.-W. Park, M.-K. Cho, K.-J. Oh, "Catalytic Reduction of NO over Perovskite-Type Catalysts", *Korean J. Chem. Eng.*, **14**(6), 491-497 (1997).

Huang, P.-n. and A. Petric, "Superior Ion Conductivity of Lanthanum Gallate Doped with Strontium and Magnesium", *J. Electrochem. Soc.*, **143**(5), 1644-1648 (1996).

Huang, K., H. Y. Lee and J. B. Goodenough, "Sr- and Ni-Doped LaCoO₃ and LaFeO₃ Perovskites, New Materials for Solid-Oxide Fuel Cells", *J. Electrochem. Soc.*, **145**, 3220-3227 (1998).

Iwamoto, M., "Copper Ion-Exchanged Zeolites as Active Catalysts for Direct Decomposition of Nitrogen Monoxide", *Stud. Surf. Sci. Catal.*, (Chem. Microporous Cryst.), **60**, 327-334 (1991).

Joly, J. P., D. Klvana and J. Kirchnerova, "TPD of Oxygen from La-Sr-Ni-Co Perovskite Catalysts Doped with Fe or Mn", *React. Kinet. Catal. Lett.*, **68**(2), 249-255 (1999).

Karpinski, A. P. and W. Halliop, "Advanced Development Program for Lightweight, Rechargeable, "AA" Zinc-Air Battery", *5th Battery Exploratory Workshop*, Burlington, VT, July 3, 1997.

Kendal, K. R., C. Navas, J. K. Thomas and H-C. zur Loya, "Recent Developments in Perovskite-Based Oxide Ion Conductors", *Solid State Ionics*, **82**, 215-223 (1995).

Kirchnerova, J., J. Vaillancourt, D. Klvana and J. Chaouki, "Evaluation of Some Cobalt and Nickel Based Perovskites Prepared by Freeze-Drying as Combustion Catalysts", *Catal. Lett.*, **21**, 77-87 (1993).

Kirchnerova, J. and D. Klvana, "Preparation and Characterization of High Surface Perovskite Electrocatalysts", *Int. J. Hydrogen Energy*, **19**(6), 501-506 (1994).

Kirchnerova, J., D. Klvana, J. Hinatsu, S. Xia, J. Oliveira, A. Anantaraman and M. Goledzinovska, "New Ni-Co Based Perovskite as Electrocatalysts in Alkaline Fuel Cells", in *Proc. 1st Int. Symp. on New Materials for Fuel Cell Systems*, O. Savadogo, P.R. Roberge and T.N. Veziroglu, Eds., Editions de École Polytechnique, Montréal, July 1995, pp.190-200.

Kirchnerova, J., D. Klvana and I. Boivin, "Development of Catalytic Materials for High Temperature Combustion", Proceedings of the 1998 International Gas Research Conference, San Diego, Nov. 1998, Vol. V, pp.277-287.

Kirchnerova, J., "Materials for Catalytic Gas Combustion", Korean J. Chem. Eng., **16**(4), 427-433 (1999).

Kirchnerova, J. and D. Klvana, "Synthesis and Characterization of Perovskite Catalysts", Solid State Ionics, **123**, 307-317 (1999).

Kirchnerova, J., W. Halliop and D. Klvana, "Perovskite Electrocatalysts for Bifunctional Oxygen Electrodes for Rechargeable Zn/Air Batteries", 3rd International Symposium on New Materials for Electrochemical Systems, Montreal, July 6-9, 1999.

Kirchnerova, J. and D. Klvana, "Design Criteria for High Temperature Combustion Catalysts", Catal. Lett., **67**, 175-185 (2000).

Kießling, D., R. Schneider, P. Kraak, M. Haftendorn, G. Wendt, "Perovskite-Type Oxides – Catalysts for the Total Oxidation of Chlorinated Hydrocarbons", Appl. Catal. B: Environmental, **19**, 143-151 (1998).

Klvana, D., J. Vaillancourt, J. Kirchnerova and J. Chaouki, "Combustion of Methane over $\text{La}_{0.66}\text{Sr}_{0.34}\text{Ni}_{0.3}\text{Co}_{0.7}\text{O}_3$ and $\text{La}_{0.4}\text{Sr}_{0.6}\text{Fe}_{0.4}\text{Co}_{0.6}\text{O}_3$ Prepared by Freeze-Drying", Appl. Catal. A: General, **109**, 181-193 (1994).

Klvana, D., J. Chaouki, C. Guy and J. Kirchnerova, "Catalytic Combustion: New Catalysts for New Technologies", Comb. Sci. Technol., **121**(1-6), 51-65 (1996a).

Klvana, D., S. Vantomme, J. Kirchnerova, J. Chaouki and S. Vigneron, "Oxydation catalytique du toluéne sur catalyseur perovskite", Proc. 1er Congrès International sur les nez électroniques et les composés odorants, Paris, June 26-27, 1996b.

Klvana, D., J. Kirchnerova, P. Gauthier, J. Delval and J. Chaouki, "Preparation of Supported $\text{La}_{0.66}\text{Sr}_{0.34}\text{Ni}_{0.3}\text{Co}_{0.7}\text{O}_3$ Perovskite Catalysts and their Performance in Methane and Odorized Natural Gas Combustion", Can. J. Chem. Eng., **75**, 509-519 (1997).

Klvana, D., J. Kirchnerova, J. Chaouki, J. Delval and W. Yaici, "Fiber Supported Perovskites for Catalytic Combustion of Natural Gas", Catal. Today, **47**, 115-121 (1999a).

Klvana, D., J. Kirchnerova and C. Tofan, "Catalytic Decomposition of Nitric Oxide by Perovskites", Korean J. Chem Eng., **16**(4), 470-477 (1999b).

Kordesch, K. and G. Simader, "Fuel Cells and their Applications", VCH, Weinheim, 1996.

Kuehn, E., ed., "Retrofit Control Technology Reducing NO_x Emissions", Power Eng., **98**(2), 23-28 (1994).

Ladavos, A. K. and P. J. Pomonis, "Comparative Study of the Solid-State and Catalytic Properties of $\text{La}_{2-x}\text{Sr}_x\text{NiO}_{4-\delta}$ Perovskites ($x = 0.00-1.50$) Prepared by the Nitrate and Citrate Methods", J. Chem. Soc. Faraday Trans., **87**(19), 3291-3297 (1991).

Larsson, R. and L. Y. Johansson, "On the Catalytic Properties of Mixed Oxides for the Electrochemical Reduction of Oxygen", J. Power Sources, **32**(3), 253-260 (1990).

Lee J. H. and D. L. Trimm, "Catalytic Combustion of Methane", Fuel Process Technol., **42**(2&3), 339-359 (1995).

Li, Y. and J. N. Armor, "Catalytic Reduction of Nitrogen Oxides with Methane in the Presence of Excess Oxygen", *Appl. Catal. B: Environmental*, **1**, L31-L40 (1992).

Libby, W. F., "Promising Catalyst for Autoexhaust", *Science*, **171**(3970), 499-500 (1971).

Machida, M., K. Eguchi and H. Arai, "High Temperature Catalytic Combustion over Cation-Substituted Barium Hexaaluminates", *Chem. Lett.*, (5), 767-770 (1987).

Machida, M., K. Eguchi and H. Arai, "Effect of Structural Modification on the Catalytic Properties of Mn-Substituted Hexaaluminates", *J. Catal.*, **123**, 477-485 (1990).

Marti, P. E., M. Maciejewski and A. Baker, "Methane Combustion over $\text{La}_{0.8}\text{Sr}_{0.2}\text{MnO}_{3+x}$ Supported on MAl_2O_4 (M = Mg, Ni, Co) Spinels", *Appl. Catal. B: Environmental*, **4**, 225-235 (1994).

Meadowcroft, D. B., "Low-Cost Oxygen Electrode Material", *Nature*, **226**, 847-848 (1970).

Metcalfe, I. S. and R. T. Baker, "Temperature Programmed Investigation of $\text{La}(\text{Ca})\text{CrO}_3$ Anode for the Oxidation of Methane in Solid Oxide Fuel Cells", *Catal. Today*, **27**, 285-288 (1996).

Minh, N. Q., "Ceramic Fuel Cells", *J. Am. Ceram. Soc.*, **76**(3), 563-588 (1995).

Pârvulescu, V. I., P. Grange and B. Delmon, "Catalytic Removal of NO", *Catal. Today*, **46**, 233-316 (1998).

Pfefferle, L. D. and W. C. Pfefferle, "Catalysis in Combustion", *Catal. Rev. -Sci. Eng.*, **26**(2&3), 219-267 (1987).

Ponce S., M. A. Peña and J. L. G. Fierro, "Surface Properties and Catalytic Performance in Methane Combustion of Sr-Substituted Lanthanum Manganites", *Appl. Catal. B: Environmental*, **24**, 193-205 (2000).

Rehspringer, J. L., P. Poix, A. Kaddouri, D. Andriamasinoro and A. Kiennemann, "Methane Oxidative Coupling by Definite Compounds (Perovskite, Cubic or Monoclinic Structure) Obtained by Low Temperature Processes", *Catal. Lett.*, **10**, 111-120 (1991).

Roberts, G. L., "A Review of Mixed-Transition Metal Oxides as Bifunctional Electrodes", *Rev. Process. Chem. Eng.*, **3**(2), 151-174 (2000).

Saint-Just, J. and J. der Kinderen, "Catalytic Combustion: from Reaction Mechanism to Commercial Applications", *Catal. Today*, **29**(1-4), 387-395 (1996).

Sammells, A. F., R. L. Cook, J. H. White, J. J. Osborn and R. C. MacDuff, "Rational Selection of Advanced Solid Electrolytes for Intermediate Temperature Fuel Cells", *Solid State Ionics*, **52**, 111-123 (1992).

Saracco, G., I. Cerri, V. Specchia and R. Accornero, "Catalytic Pre-Mixed Fibre Burners", *Chem. Eng. Sci.*, **54**(15), 3599-3608 (1999a).

Saracco, G., F. Geobaldo and G. Baldi, "Methane Combustion on Mg-Doped LaMnO₃ Perovskite Catalysts", *Appl. Catal. B: Environmental*, **20**(4), 277-288 (1999b).

Seiyama T., "Total Oxidation of Hydrocarbons on Perovskite Oxides", in "Properties and Applications of Perovskite-Type Oxides", L. G. Tejuga and J. L. G. Fierro, Eds., Chem. Ind., Vol. 50, Marcel Dekker, New York (1993) pp. 215-234.

Shelef, M., "Selective Catalytic Reduction of NO_x with N-Free Reductants", Chem. Rev., **95**, 209- 235 (1995).

Sinquin, G., J. P. Hindermann, C. Petit and A. Kiennemann, "Perovskites as Polyvalent Catalysts for Total Destruction of C₁, C₂ Aromatic Chlorinated Volatile Organic Compounds", Catal. Today, **54**, 107-118 (1999).

Song, K. S., D. Klvana and J. Kirchnerova, "Kinetics of Propane Combustion over La_{0.66}Sr_{0.34}Ni_{0.3}Co_{0.7}O₃ Perovskite", Appl. Catal. A: General, in print, (2001).

Stephan, K., M. Hackenberger, D. Kiessling and G. Wendt, "Supported Perovskite-Type Oxide Catalysts for the Total Oxidation of Chlorinated Hydrocarbons", Catal. Today, **54**, 23-30 (1999).

Stojanovic, M., R. G. Haverkamp, C. A. Mims, H. Moudallaland and A. J. Jacobson, "Synthesis and Characterization of LaCr_{1-x}Ni_xO₃ Perovskite Oxide Catalysts", J. Catal., **165**, 315-323 (1997).

Tabata, K., H. Fukuda, S. Kohiki, N. Mizuno and M. Misono, "Uptake of Nitric Oxide Gas by Yttrium, Barium, Copper Oxide (YBa₂Cu₃O_{7-δ})", Chem. Lett., (5), 799-802 (1988).

Tejuga, L. G., J. L. G. Fierro and J. M. D. Tascon, "Structure and Reactivity of Perovskite-Type Oxides", in Advances in Catalysis, D. D. Eley, H. Pines and P. B. Weisz, Eds., Academic Press, New York **36**, 237-328, (1989).

Teraoka, Y., H. M. Zhang, K. Okamoto and N. Yamazoe, "Mixed Ionic-Electronic Conductivity of Lanthanum Strontium Cobalt Iron Oxide ($\text{La}_{1-x}\text{Sr}_x\text{Co}_{1-y}\text{Fe}_y\text{O}_{3-\delta}$) Perovskite-Type Oxides", *Mater. Res. Bull.*, **23**(1), 51-58 (1988).

Teraoka, Y., H. Fukuda and S. Kagawa, "Catalytic Activity of Perovskite-Type Oxides for the Direct Decomposition of Nitrogen Monoxide", *Chem. Lett.*, (1), 1-4 (1990).

Teraoka, Y., T. Harada, H. Furukawa and S. Kagawa, "Catalytic Property of Perovskite-Type Oxides for the Direct Decomposition of Nitric Oxide", *Stud. Surf. Sci. Catal.*, **75** (New Frontiers in Catalysis, Pt. C), 2649-2652 (1993).

Tofan, C., D. Klvana and J. Kirchnerova, "Direct Decomposition of Nitric Oxide over Perovskite-Type Catalysts, Part I : Activity when no Oxygen is Added to the Feed", *Appl. Catal. A: General*, (in print), 2001.

Tofan, C., PhD Theses, Ecole Polytechnique, Montreal, 2001.

Tsai, C-Y, A. G. Dixon, W. R. Moser and Y. H. Ma, "Dense Perovskite Membrane Reactors for Partial Oxidation of Methane to Syngas", *AIChE Journal*, **43**(11A), 2741-2750 (1997).

Twu, J. and P. K. Gallagher, "Preparation of Bulk and Supported Perovskites", in "Properties and Applications of Perovskite-Type Oxides", Tejuca, L. G. and J. L. G. Fierro, Eds., Marcel Dekker, New York (1993), pp.1-24.

Viswanathan, B., "Carbon Monoxide Oxidation and Nitric Oxide Reduction on Perovskite Oxides", *Catal. Rev.-Sci. Eng.*, **34**(4) 337-354 (1992).

Voorhoeve, R. J. H., J. P. Remeika and L. E. Trimble, "Nitric Oxide and Perovskite-Type Catalysts: Solid State and Catalytic Chemistry", in "The Catalytic Chemistry of Nitrogen Oxides", R. L. Klimisch and J. G. Larson, Eds., Plenum Press, New York-London, 215-233 (1975).

Wan, L. "Poisoning of Perovskite Oxides by Sulfur Dioxide", in Tejuca, L. G. and J. L. G. Fierro, Eds., "Properties and Applications of Perovskite-Type Oxides", Marcel Dekker, New York (1993) pp.145-170.

Windawi, H. and Chu, W., "Control VOCs via Catalytic Oxidation", Chem. Eng. Progress, March, 37-41 (1996).

Xu, S. J. and W. J. Thomson, "Perovskite-Type Oxide Membranes for the Oxidative Coupling of Methane", AIChE Journal, 43(11A), 2731-2740 (1997).

Xu, S. J. and W. J. Thomson, "Stability of $\text{La}_{0.6}\text{Sr}_{0.4}\text{Co}_{0.2}\text{Fe}_{0.8}\text{O}_{3-\delta}$ Perovskite Membranes in Reducing and Nonreducing Environments", Ind. Eng. Chem. Res., 37, 1290-1299 (1998).

Yasuda, H., N. Mizuno and M. Misono, "Role of Valency of Copper in the Direct Decomposition of Nitrogen Monoxide over Well Characterized $\text{La}_{2-x}\text{A}'_x\text{Cu}_{1-y}\text{B}'_y\text{O}_4$ ", J. Chem. Soc., Chem. Commun., 16, 1094-1096 (1990).

Yasuda, H., T. Nitadori, N. Mizuno and M. Misono, "Catalytic Decomposition of Nitrogen Monoxide over Valency-Controlled $\text{La}_2\text{CuO}_{4-\delta}$ Based Mixed Oxides", Bull. Chem. Soc. Jpn., 66(11), 3492-3502 (1993).

Zhang, H. M., Y. Shimizu, Y. Teraoka, N. Miura and N. Yamazoe, "Oxygen Sorption and Catalytic Properties of Lanthanum Strontium Cobalt Iron Oxide $\text{La}_{1-x}\text{Sr}_x\text{Co}_{1-y}\text{Fe}_y\text{O}_3$ Perovskite-Type Oxides", J. Catal., 121(2), 432-440 (1990).

Zernike, J., "Catalytic Combustion and its Limit. Commemorating the Discovery of this Phenomenon 150 Years ago", *Chem. Weekbl.*, **63**, 321-325 (1967).

Zwinkels, M. F. M., S. G. Järäs and P. G. Menon, "Catalytic Materials for High-Temperature Combustion", *Catal. Rev.-Sci. Eng.*, **35**(3), 319-358 (1993).

ANNEXE 4**Évaluation des modèles cinétiques**

La fraction molaire de N₂ dans les gaz à la sortie du réacteur (x) est calculée en fonction des concentrations du N₂ à la sortie ([N₂]_S) et du NO à l'entrée ([NO]_E) du réacteur :

$$x = \frac{2[N_2]_S}{[NO]_E}$$

Dans tous les cas quand l'oxygène n'était pas ajouté dans l'alimentation (l'étude de la décomposition en absence de l'oxygène et l'étude de la décomposition en présence de CO₂ et H₂O), sa pression partielle a été calculée en fonction du NO qui s'est transformé en azote :

$$P_{O_2,S} = \frac{1}{2} x P_{NO,E}$$

Pour l'étude faite en présence d'oxygène dans l'alimentation, la pression partielle de O₂ est la somme de la pression partielle initiale de l'oxygène et de la pression partielle de l'oxygène formé par la décomposition du NO :

$$P_{O_2,S} = P_{O_2,E} + \frac{1}{2} x P_{NO,E}$$

L'analyse a été faite pour chaque température à laquelle les données ont été collectées. Étant donné le caractère des données expérimentales collectées (mode intégral), la démarche pour la validation d'un modèle a été la suivante (on utilise comme exemple le modèle IV.6 (Chapitre II), $r = \frac{k_{NO} P_{NO} P_{O_2}}{k_I P_{NO} + k_{II} P_{O_2}}$) :

Pour le réacteur à écoulement piston :

$$W = F_A^0 \int_0^x \frac{dx}{-r_A}$$

Alors,

$$\frac{1}{r} = \frac{k_I}{k_{NO}} \frac{P_{NO}}{P_{NO}P_{O_2}} + \frac{k_{II}}{k_{NO}} \frac{P_{O_2}}{P_{NO}P_{O_2}} = \frac{k_I}{k_{NO}} \frac{1}{P_{O_2}} + \frac{k_{II}}{k_{NO}} \frac{1}{P_{NO}}$$

$$\frac{1}{r} = \frac{k_I}{k_{NO}} \left[\frac{1}{\frac{1}{2} P_{NO}^0 x} \right] + \frac{k_{II}}{k_{NO}} \frac{1}{P_{NO}^0 (1-x)}$$

$$\frac{W}{F_{NO}^0} P_{NO}^0 = \frac{1}{2} \frac{k_I}{k_{NO}} \int_0^x \frac{1}{x} dx + \frac{k_{II}}{k_{NO}} \int_0^x \frac{1}{1-x} dx$$

$$\frac{W}{F_{NO}^0} P_{NO}^0 = \frac{1}{2} \frac{k_I}{k_{NO}} \ln x + \frac{k_{II}}{k_{NO}} [-\ln(1-x)]$$

À partir de cette équation on a défini la fonction qui a été analysée par régression linéaire :

$$Y = f(X_1, X_2)$$

$$\text{où } Y = \frac{W}{F_{NO}^0} P_{NO}^0 ; X_1 = \ln x ; X_2 = -\ln(1-x)$$

L'intervalle de confiance pour l'analyse de régression a été de 95 %.

Le degré de validité du modèle a été déterminé par une analyse statistique. Si le modèle a été validé, on a déterminé les paramètres cinétiques inconnus. Dans le cas de cet exemple on ne peut pas déterminer les paramètres individuels (2 équations avec 3 inconnues : k_{NO} , k_I et k_{II}), mais on a pu déterminer les rapports k_I/k_{NO} et k_{II}/k_{NO} .

Dans le cas où l'oxygène est présent dans l'alimentation, l'équation à analyser par régression linéaire a été obtenue de la manière suivante :

$$\frac{1}{r} = \frac{k_I}{k_{NO}} \frac{1}{\left[\frac{1}{2} P_{NO}^0 x + P_{O_2}^0 \right]} + \frac{k_{II}}{k_{NO}} \frac{1}{P_{NO}^0 (1-x)}$$

$$\frac{W}{F_{NO}^0} P_{NO}^0 = 2 \frac{k_I}{k_{NO}} \left[\ln \left(x + \frac{2P_{O_2}^0}{P_{NO}^0} \right) \right] + \frac{k_{II}}{k_{NO}} \left[-\ln(1-x) \right]$$

$$Y = f(X_1, X_2)$$

$$\text{où } Y = \frac{W}{F_{NO}^0} P_{NO}^0; \quad X_1 = \ln \left(x + \frac{2P_{O_2}^0}{P_{NO}^0} \right); \quad X_2 = -\ln(1-x)$$

ANNEXE 5

Calcul d'un réacteur hypothétique pour la décomposition directe du NO

Un effluent d'un moteur diesel d'une voiture économique a la composition suivante :

O ₂ : 5-15 %	CO : 100-800 ppm
N ₂ : 70-80 %	SO ₂ : 40-200 ppm
CO ₂ : 2-12 %	H ₂ : 30-300 ppm
H ₂ O : 1,8-10 %	HC : 20-100 ppm (équivalent CH ₄)
NO _x : 30-600 ppm	particules : 0,04-0,1 g/m ³

Les débits de gaz sont très fluctuants en fonction des accélérations et décélérations et varient entre 10 et 150 m³/h (c.n.). En utilisant comme catalyseur la pérovskite La_{0,87}Sr_{0,13}Mn_{0,2}Ni_{0,8}O_{3-δ} (SSA = 12,7 m²/g) et en supposant un réacteur à écoulement piston, une température constante T = 873 K et un débit initial de NO, F_{NO}⁰ = 744 µmol/s on détermine la masse de catalyseur nécessaire pour une conversion du NO en N₂ de 75 %. On considère que seule la réaction de décomposition directe du NO a lieu (NO → ½ N₂ + ½ O₂). On a observé que les effets inhibiteurs du O₂ et CO₂ plafonnent aux concentrations de 2 %. Pour le calcul on a donc supposé que le gaz a la composition suivante : 0,06 %NO, 2 %O₂, 2 %CO₂, 2 %H₂O (N₂ balance).

La masse de catalyseur (W) nécessaire pour une réaction A → B qui se déroule dans un réacteur à écoulement piston :

$$W = F_A^0 \int_0^x \frac{dx}{-r_A}$$

On suppose l'équation de vitesse suivante* :

$$r(x) = \frac{k_{NO}P_{NO}}{1 + K_{O_2}P_{O_2} + k_{inhCO_2}P_{CO_2} + k_{inhH_2O}P_{H_2O}}$$

$$r(x) = \frac{k_{NO}P_{NO}^0(1-x)}{1 + K_{O_2}\left(\frac{1}{2}P_{NO}^0x + P_{O_2}\right) + k_{inhCO_2}P_{CO_2} + k_{inhH_2O}P_{H_2O}}$$

$$k_{NO} = 7,2 \text{ } \mu\text{mol/g s bar}$$

$$P_{NO}^0 = 0,0006 \text{ bar}$$

$$K_{O_2} = 1400 \text{ bar}^{-1}$$

$$P_{O_2} = 0,02 \text{ bar}$$

$$k_{inh.CO_2} = 333 \text{ bar}^{-1}$$

$$P_{CO_2} = 0,02 \text{ bar}$$

$$k_{inh.H_2O} = 16,2 \text{ bar}^{-1}$$

$$P_{H_2O} = 0,02 \text{ bar}$$

$$\frac{1}{r} = \frac{1}{k_{NO}P_{NO}^0(1-x)} + \frac{\frac{1}{2}K_{O_2}x}{k_{NO}(1-x)} + \frac{K_{O_2}P_{O_2}}{k_{NO}P_{NO}^0(1-x)} + \frac{k_{inhCO_2}P_{CO_2}}{k_{NO}P_{NO}^0(1-x)} + \frac{k_{inhH_2O}P_{H_2O}}{k_{NO}P_{NO}^0(1-x)}$$

$$\int_0^x \frac{1}{r} dx = \left(\frac{1}{k_{NO}P_{NO}^0} + \frac{K_{O_2}P_{O_2}}{k_{NO}P_{NO}^0} + \frac{k_{inhCO_2}P_{CO_2}}{k_{NO}P_{NO}^0} + \frac{k_{inhH_2O}P_{H_2O}}{k_{NO}P_{NO}^0} \right) \int_0^x \frac{1}{1-x} dx + \frac{1}{2} \frac{K_{O_2}}{k_{NO}} \int_0^x \frac{x}{1-x} dx$$

$$\int_0^x \frac{1}{1-x} dx = -\ln(1-x)$$

$$\int_0^x \frac{x}{1-x} dx = -x - \ln(1-x)$$

Pour $x = 0,75$ on obtient $W = 8,6 \text{ t}$

*Remarque :

On a utilisé un modèle cumulant tous les effets inhibiteurs.